The University Of Sheffield.

Biofilm development and management in aircraft fuel systems

By:

Alexander Edward McFarlane

A thesis submitted in partial fulfilment of the requirements
for the degree of Doctor of Philosophy

The University of Sheffield
Faculty of Science
Department of Animal and Plant Sciences

Submission Date
22nd September 2016

For

Joyce, William, Audrey and Thomas

Table of Contents

Abstract

Microbial contamination of jet fuel systems is a well-documented phenomenon. However, the introduction of novels fuels and materials will change these environments and hence the microbial communities that develop within them. This thesis explores the potential impact of introducing novel fuels and construction materials into the jet fuel supply chain on microbial communities, biofilm development and function with the aim of developing an understanding of the underpinning biological, chemical and physical processes. Our work has focused on a) characterising the microbial communities present within conventional aircraft fuel systems and their role in biofilm development and fuel degradation and b) the effect of introducing alternative fuels and new construction materials on these processes.

Using a range of molecular genetic techniques, we have characterised microbial communities found in diverse conventional fuel systems. Communities within jet fuel systems were found to be more diverse than previously documented and traditional indicator species were not always detected in field samples. We use novel, multifactorial laboratory microcosm experiments, varying parameters such as microbial community structure, fuel type and surface composition, to enhance our understanding of this problem. Our data show that varying fuel type strongly influenced microbial growth rate and cell attachment of industry-standard isolates, as well as the community structure of complex mixed communities. Varying material composition, including the addition of chromate-leaching paint, had little effect on community structure. Instead the biggest driver for change in these systems was the location of the biofilm - either the fuel or water phase. Overall, this research helps to elucidate understanding of the principles that govern biofilm formation in jet fuel systems, pre-empting future operational problems following the introduction of alternative fuels and materials.

Declaration

No portion of the work referred to in this thesis has been submitted in support of an application for another degree or qualification at this or any other university or institute of learning.

Nomenclature

°	Degrees
°C	Degrees Celsius
µl	Microliters
µm	Micrometres
µM	Micromolar
3D	Three dimentional
amp^{100}	Ampicillin 100 µg
ASTM	The American Society of the International Association for Testing and Materials
ATCC	American Type Culture Collection
ATP	Adenosine triphosphate
BH	Bushnell-Haas
bp	Base pairs
Bray Curtis	A statistic used to quantify the compositional dissimilarity between two points
BSA	Bovine Serum Albumin
BTL	Biomass to Liquid
CE	Capillary electrophoresis
CH_3	Methyl group
Cl	Chlorine
cm	Centimetres
CO	Carbon monoxide
CoQ	Certificate of quality
CSLM	Confocal scanning laser microscopy
CTAB	Cetyl trimethylammonium bromide
CTL	Coal to Liquid
C_x	Normal alkane of X length
dATP	Deoxyadenosine triphosphate
DCM	Dichloromethane
dCTP	Deoxycytidine triphosphate
DEF STAN	Defence standard
DGGE	Denaturing gradient gel electrophoresis
dGTP	Deoxyguanosine triphosphate
DiEGME	Diethylene glycol monomethyl ether
DMF	Dimethylformamide
DNA	Deoxyribonucleic acid
dNTP	Nucleoside triphosphate
dsDNA	Double stranded deoxyribonucleic acid
dTTP	Deoxythymidine triphosphate
EB	Elution buffer
EDTA	Ethylenediaminetetraacetic acid
EGME	Ethylene glycol monomethyl ether
ELISA	enzyme-linked immunosorbent assay
EPS	Extracellular polymeric substance

et al.	And others
FAE	Fatty acid esters
FAEE	Fatty acid ethyl esters
FAME	Fatty acid methyl esters
FDR	False discovery rate
Fe_2O_3	Iron oxide
Fe_3O_4	Magnetite
FSII	Fuel system icing inhibitor
FT	Fischer-Tropsch synthesis
fwhm	Full width at half maximum
g	Gravity
g	Grams
GC	Gas chromatography
GC-FAME	Gas chromatography - Fatty acid methyl esters
GC-MS	Gas chromatography - Mass spectrometer
GCxGC	Two dimensional gas chromatography
GTL	Gas to Liquid
H_2	Hydrogen
H_2S	Hydrogen sulphide
HDPE	High density polyethylene
HiFi	High fidelity
HRJ	Hydro-treated renewable jet fuel
IATA	International Air Transport Association
ITS	Inter transcribed spacer
JP	Jet propellant
kPa	kilopascal
kV	Kilovolts
L	Litres
LB	Luria-Bertani
M	Moles
m	Metres
maxEE	Maximum expected error
MEA	Malt extract agar
MEB	Malt extract broth
mg	Milligram
$MgCl_2$	Magnesium chloride
MIC	Microbially induced corrosion
ml	Millilitres
mm	Millimetres
mM	Millimoles
MS	Mass spectrometer
NaCl	Sodium chloride
ng	Nanograms
NGS	Next generation sequencing
NIH	National Institute of Health

NIST	The National Institute of Standards and Technology
nm	Nanometres
nM	Nanomoles
OD^{600}	Optical density at 600 nanometres
OTU	Operational taxonomic unit
PCoA	Principle coordinate analysis
PCR	Polymerase chain reaction
pH	A numeric scale used to specify the acidity or basicity of an aqueous solution
ppm	Parts per million
psi	Pounds per square inch
PTFE	Polytetrafluoroethylene
p-value	The probability of obtaining a result equal to or more than what was observed
Q10	One in ten errors
Q20	One in one hundred errors
Q30	One in one thousand errors
QIIME	Quantitative insights into microbial ecology
qPCR	Quantitative real time polymerase chain reaction
Q-TOF	Quadrupole time-of-flight
q-value	p-value corrected for false discovery rate
r^2	The measure of how close the data are to the fitted regression line
rDNA	Ribosomal deoxyribonucleic acid
RDP	Ribosomal Database Project
rpm	Revolutions per minute
rRNA	Ribosomal ribonucleic acid
SDS	Sodium dodecyl sulphate
SEM	Scanning electron microscope
SET	Sucrose, EDTA, Tris-HCl
sp.	Species (singular)
SPK	Synthetic paraffinic kerosene
spp.	Species (plural)
SRB	Sulphur reducing bacteria
TE	Tris, EDTA
TGAC	The Genome Analysis Centre
TP	Time point
TriEGME	Triethylene glycol monomethyl ether
Tris-HCl	Tris-Hydrochloride
TS-1	Russian Federation Standard jet fuel
TSA	Tryptone-Soya agar
TSB	Tryptone-Soya broth
U	Units
UK	United Kingdom
UniFrac	A distance metric used for comparing biological communities
US	United States
USA	United States of America
USAF	United States Air Force
UV/Vis	Ultra violate / Visible

v	Volume
V	Volts
v/m	Volume / Mass
v/v	Volume / Volume
w/v	weight / volume
x	Times
X-gal	5-bromo-4-chloro-3-indolyl-β-D-galactopyranoside
XTL	Undefined feedstock to Liquid
YM	Yeast-malt
α	Alpha
β	Beta
γ	Gamma
δ	Delta
λ	Lambda

List of Figures

List of Tables

Presentations, publications, awards and future grants

Presentations

The 14th international symposium on stability, handing and use of liquid fuels (IASH). October 4th to 8th 2015 (Charleston, South Carolina).

The 7th European Aeronautics Days (Aerodays) 2015. October 20th to 23rd (London, England).

Publications

McFarlane, A. E., Thornton, S. F. and Rolfe, S. A. (2015). How will novel fuels and materials impact microbial contamination in aircraft fuel systems? *International Association for Stability, Handling and Liquid Fuels (IASH)*. Charleston, South Carolina.

See Appendix A for further information.

Awards

Awarded the Dr. John Bacha Scholarship at IASH 2015.

Awarded the European young researcher award at Aerodays 2015.

Future grants

The research undertaken in this project has been further sponsored by Airbus S.A.S and Innospec Ltd.

Acknowledgements

At the end of this four year journey, I would like to acknowledge the many people have helped me. It strikes me just how lucky and extremely privileged I have been to have had such fantastic support. I would like to start by thanking everyone who has made this thesis possible. In particular I would like to extend a special thank you to my supervisors Dr. Steve Rolfe and Prof. Steve Thornton. Your academic guidance, encouragement and mentoring has allowed me to grow as a research scientist. I could not have done this without you and I look forward to working with both of you in the future.

To my parents Elaine and Mac and my sister Malena. Words cannot express how grateful I am to you and for all the sacrifices you have made over the years. Until a few years ago I never thought this would be possible. You have always believed in me, helped me cope with dyslexia, and kept pushing me forward through my struggles with ME. Hopefully this goes some way to showing that there is more than just the tip to the iceberg.

To Sandra, Vince, Helen and Jess, the influence you had during my formative years has helped shape who I am as a person and over the years you have continued to help and support me in everything that I have done. Thank you.

Throughout my adult life I have been extremely fortunate to have some great people in my life, particularly my best friends Morgan, Richard, Simon and Tom. The last four years have been a roller-coaster, but you've always been there to support me, particularly with your fantastic scientific hypotheses after a beer or two. I couldn't ask for better friends. Jam curry!

Lochy, you have been a great friend and invaluable sounding board over the last few years. You have always been there, offering me a friendly ear and some sound advice whenever I needed it. Thank you for everything. Sanctuary wouldn't be the same without you.

Throughout my working career I have had the opportunity to work with some amazing people, many of whom have had a lasting impact. Firstly, I would like to thank my industry supervisors, Paul Bogers and Joanna Bauldreay. Paul, without you none of this would be possible, thank you for giving me to opportunity to reach my potential. Joanna, you have continually taught and mentored me over my time at Shell and university. I wouldn't be in the position I am now without your support. I would also like to thank my other colleagues from Shell, in particular Phil Rugen, Steve Threadgold and Dave Owen. Over the years your advice and friendship has been invaluable.

This experience as a PhD student would not have been possible without my course and lab mates. You all deserve a special thank you. You have supported me, kept me going when I was down, always been up for a Friday night pint and even come back to work at 2 am help me. To Nichola Austen, Sam Amsbury, Alice Baillie, Emily Beardon, Despina Berdeni, Colin Bonnington, James Bradley, Andrea Bragg, Laura Brooks, Will Buswell, Luke Cartwright, Debbie Coldwell, Anne Cotton, Leo Furci, Jason Griffiths, Petra Hedbavna, Kayleigh Kerins, Eric Kuria, Joanna Landymore, Ana Lopez, Richard Louden, Andy McNally, Alexis Moschopoulos, Steve Muddimer Catherine Preece, Roland Schwarzenbacher, Jody Smith, David Pardo, Sarah Sommer, Marion Tout, Julia Van Campen, Nichola White, Alex Williams, Matt Wilson, Steph Wood, Mustafa Yassin and Peijin Zhang, thank you.

I would also like to thank Despina Berdeni, Simon Blakey, James P. Berry, Paul Blackbourn, Anne Cotton, Andrew Fairburn, Petra Hedbavna, Chris Hill, Gabriella Kakonyi, Maggie Killion, Katherine Fish, Ana Lopez, David Pardo, Darren Robinson, Jody Smith, Sarah Sommer, Joost Stassen, Simon Thorpe, Heather Walker and Mustafa Yassin for providing invaluable advice and assistance with many of the technical aspects of this thesis and to everyone who donated samples to this project who wished to remain anonymous.

Finally, I would like to extend a special thank you to Nichola White. You have worked tirelessly in the background sorting a million and one things out during my PhD. Thank you for everything, none of our lab would be able to achieve our PhDs without your efforts.

The work presented within this thesis was sponsored by Shell Research Ltd.

Chapter One

Life in the wing: An introduction to microbial contamination of aircraft fuel systems

1. General introduction

1.1 Microbial contamination: The problem

Since the 1960s, uncontrolled biodeterioration has been widely reported as a problem throughout the petrochemical industry, costing billions of dollars every year[1] (Balster *et al*. 2006; Raikos *et al*. 2011). Jet fuels (and middle distillates[2] in general) are particularly susceptible to microbial degradation. This is due to the abundance of low molecular weight aliphatic hydrocarbons (~C_{10} to C_{16}), which microorganisms preferentially break down when compared to larger, more complex molecules (>C_{20}) (Brown *et al*. 2010). However, this is likely to change in the future due to the introduction of alternative fuels.

Jet fuel systems contain all of the chemical and physiological requirements for microorganisms to proliferate: water, essential trace nutrients (provided by additives), an energy source (from the hydrocarbon), temperatures in the mid-range (most hydrocarbon utilising microorganisms are mesophiles) and oxygen (Brown *et al.* 2010). Of these chemical and physiological requirements, water is the most important as it is essential for active growth[3]. Water is used by cells to dissolve chemicals and carry solutes into the cell via transport mechanisms. Water also acts as a solvent for the cells biochemical reactions and as a medium to eliminate soluble waste (Mara & Horan 2003).

Water may enter a fuel system in a number of different ways. Finely dispersed droplets of water (<40 µm) may contaminate jet fuels during fuel handling and storage activities, water vapour may enter from the atmosphere (particularly in geographic areas of high humidity) or rain water may enter into leaky tanks (Brown *et al*. 2010). Once associated with the fuel, water can exist in three states, dissolved, free water in suspension and free settled water.

The ability of a fuel to keep water in solution is mainly temperature dependent. As temperature decreases, the availability of free water increases, which can result in a fuel

[1] Contamination of hydrocarbon fuels by bacteria and fungi is a serious and costly problem. These microorganisms have the potential to cause problems within the supply chain such as a) biofilm formation, b) production of biosurfactants, c) fuel deterioration and d) corrosion, resulting in increased maintenance and replacement costs, as well as potential filter blocking (Denaro *et al*. 2005; White *et al*. 2011).

[2] Middle distillates are a class of hydrocarbons comprising of kerosene, jet fuel, diesel and residual heating oils, which boil between approximately 175-370 °C. Middle distillates have a variable composition, but generally comprise of linear and branched chain aliphatic hydrocarbons, cycloparaffins and aromatics in approximately the C_{10}-C_{20} range (Nessel *et al*. 1999).

[3] Some bacterial species are able to form endospores when starved of nutrients under certain conditions. Endospores are dormant forms, with clear structural and biochemical differences compared to active cells, allowing the species to survive under extreme conditions, until the environment become more favourable (Piggot & Coote 1976).

water haze. This free water begins to coalesce on the inner surface of the tank and/or sink to the bottom, where a fuel-water interface is formed (Passman 2003; Smith 1991). This process is known as fuel-water shedding and is particularly prevalent in areas with a large diurnal temperature variation.

Microbes require bioavailable (i.e. free) water to proliferate (Passman 2003), with around 1 % required for substantial growth (Gaylarde *et al*. 1999). The formation of a fuel-water interface facilitates growth, which in turn can lead to accumulation of biomass, fuel/additive degradation, corrosion and production of metabolic by-products, which prevent filter coalescers[4] removing free water (White *et al*. 2011). These factors contribute to increased maintenance costs and in the worst case can lead to aircraft disasters. For example, in 1958 a US Air Force (USAF) Boeing B-52 bomber crashed due to in-line fuel filter plugging (or blocking due to biomass) (Rauch *et al*. 2006). Two years later, problems with wing tank corrosion and fuel gauge malfunctions were noted in civil aircraft, sparking a global survey of jet fuel supply and distribution systems. *Hormoconis resinae* was prevalent in 90 % of fuel systems and new housekeeping practices based around the removal of free water from storage tanks were implemented immediately (Graef 2003; McFarlane 2009).

Environmental conditions dictate whether microorganisms are planktonic or sessile. The latter attach to fuel system substrata e.g. tank walls, by producing extracellular polymeric substances (EPS) and begin to replicate. As replication advances, a biofilm of primary microorganisms and EPS begins to form over the substrate, heterogeneously at first until a confluent blanket is formed. Eventually the mature biofilm begins encapsulating planktonic microorganisms and suspended particulates, forming a complex community (Denyer *et al*. 1993; Kobrin 1993; Srivastava *et al*. 2006). Encapsulated microorganisms begin to affect the surrounding environment (Denyer *et al*. 1993) by releasing metabolites into the fuel layer and degrading the fuel/additives. Fuel degradation is complex, involving a consortium of different microorganisms (both aerobic and anaerobic). Many microorganisms utilise the degradation products produced in the initial oxidation process, forming amines, mercaptans, volatile fatty acids and hydrogen (anaerobes) (Ray & Bhunia 2013; Franke-Whittle *et al.* 2014) or carbon dioxide and water (aerobes), contributing to operational problems, such as filter plugging and corrosion. Here changes in a) the type and concentration of ions, b) pH values and c) oxidation-reduction potential occurs (Videla & Herrera 2005), resulting in pitting due

[4] A coalescer is a filter element, which removes free water by causing fine water droplet to coalesce on the filter's surface and then separate out of the fuel by gravity (Rugen *et al*. 2007).

to the production of corrosive metabolic by-products, creation of anaerobic niches and cathodic depolarization (Srivastava *et al*. 2006).

The availability of trace elements, in particular nitrogen and phosphorus (provided by additives[5]), is often a limiting factor in the growth of microorganisms within fuel systems (Das & Chandran 2011). Additive usage is dependent on crude source, refinery process, country of origin and civil/military application (Auffret *et al*. 2009; McNamara *et al*. 2005; Nicolau *et al*. 2008; Rand 2003).

At the fuel/water interface microorganisms can produce biosurfactants, which lower the interfacial surface tension of the fuel, allowing a stable suspension of microorganisms, water and debris to be produced (Anon. 2015). Therefore microorganisms suspended in contaminated fuel will not settle out in accordance with Stoke's Law[6]; coalescers/filter water separators can be compromised potentially allowing contaminants to be loaded onto an aircraft (Anon. 2009; Passman 2003). Microbial problems can be minimised by tightly controlled facility designs, handling procedures and housekeeping measures (Anon. 2015).

However, these procedures may need to be reviewed in future as, due to environmental pressures new synthetic[7] and hydroprocessed renewable[8] jet fuels are being introduced. These modern fuels contain only paraffinic hydrocarbons with no aromatic or sulphur compounds (Stratton *et al*. 2011) and it is to be expected that the introduction of these fuels will cause changes in community structure, function and dynamics, potentially introducing new risks in the jet fuel supply chain and providing the justification for this research. The following literature review outlines the existing knowledge of microbial contamination of jet fuels and jet fuel systems.

[5] Broadly they can be broken down into the following categories: Engine performance (metal deactivator additive (e.g. N,N'disalicylidene-1,2-propanediamine) and lubricity improver additive such as Hitec 580), fuel handling (static dissipator additive e.g. Stadis® 450), fuel stability (antioxidants e.g. 2,6-ditertiary-butyl-phenol) and contamination control (fuel system icing inhibitor (FSII) e.g. Diethylene Glycol Monomethyl Ether (DiEGME)) (Anon. 2011b) and are added for a variety of reasons, the most important of which is safety, e.g. conductivity improvers minimise risk of electrostatic charge build and explosion.

[6] Stoke's law determines the terminal velocity or settling velocity of spherical particles falling under the force of gravity in a fluid (Van Loon & Duffy 2005).

[7] Synthetic paraffinic kerosene (SPK) is an alternative fuel created by the gasification of coal, natural gas or biomass to form synthesis gas, which is processed and upgraded using Fischer-Tropsch (FT) synthesis (Stratton *et al*. 2011).

[8] Hydro-processed renewable jet fuel is an alternative fuel created by hydro-processing renewable oils, such as those created from jatropha, camelina and algae (Stratton *et al*. 2011).

1.2 Microorganism within fuel systems

Microorganisms can be classified into archaea, bacteria, fungi (yeasts and moulds), viruses, protozoa and algae. Ubiquitous in the environment, they are commonly found in the air, soil, water (Passman 2003; Raikos *et al*. 2012). It is widely documented that bacteria, yeasts and moulds (filamentous fungi), such as *Hormoconis resinae* (Guiamet & Gaylarde 1996), can survive in hydrocarbon fuels/water (Balster *et al*. 2006; Brown *et al*. 2010; Gaylarde *et al*. 1999; Raikos *et al*. 2011; Rauch *et al*. 2006; White *et al*. 2011; Young *et al*. 2001). However, viruses[9], protozoa and algae are rarely found in middle distillate fuels and are not discussed further (Passman 2003).

Bacteria are very diverse, with millions of species thought to exist globally (Dykhuizen 1998). This is in part due to the ability of bacteria ability to exchange genetic information via mobile genetic elements such as conjugative plasmids (Ghigo 2001), transposons (Pray 2008) and bacteriophages (Hendrix 2002) as well as their extremely rapid growth rate, which increases the potential for mutational change. They can be obligately aerobic (require oxygen), anaerobic (require the absence of oxygen) or facultative[10] (can live in the presence or absence of oxygen) (Passman 2003), have a rigid cell wall, and are either spherical, rod-like or spiral in shape, ranging from 1-5 μm in size (Ackerman & Dunk-Richards 1991; Toole & Toole 1995).

Bacteria, such as *Bacillus licheniformis* (Rauch *et al*. 2006), produce biosurfactants, which stabilise water in fuel (Van Hamme *et al*. 2006) and EPS, which allows them to attach to surfaces to form a biofilm and help protect them from desiccation (Passman 2003; Vuong *et al*. 2004). Biofilms often have a lower sensitivity to treatment by chemical biocides (Guiamet & Gaylarde 1996) and provide ideal environments for sulphur reducing bacteria[11] (SRB) to grow as anaerobic conditions are often present (Denyer *et al*. 1993), resulting in corrosion and sulphide souring of fuel products (Gibson 1990; Videla & Herrera 2005).

Certain bacteria, such as *Bacillus spp.* and *Clostridium spp.* (Piggot & Coote 1976), also produce endospores in response to adverse changes in the environment. The process of spore formation is complex, but basically involves replication of cell genetic material

[9] At present viruses are not documented to play a significant role in fuel system microbiology. However, much like ocean environments, it is possible that viruses could have a significant effect on microbial communities in jet fuel e.g. effects on nutrient cycling (Suttle 2005).

[10] Facultative microorganisms fill an important niche in a biofilm, utilising oxygen and therefore creating anoxic conditions, which are favourable for obligate anaerobe to survive (Passman 2003).

[11] For example, *Arthrobacter spp.* produce metabolites that are known to support SRB (Rauch *et al*. 2006).

followed by the laying down of a tough outer coat which is highly resistant to extreme temperature and deficiencies in water, nutrients and air. The spores will lie dormant and only germinate when environmental conditions become more conducive to the growth of vegetative cells, facilitating the spread of contamination through distribution systems (Yousefi Kebria *et al*. 2009).

Yeasts (such as *Yarrowia lipolytica* (Passman 2003)) are unicellular, spherical or ovoid in shape and have a cell wall made up of glucan and/or mannan. They reproduce by budding (Dujon 2010), are aerobic and have a preference of mildly acidic conditions (pH 5) (Passman 2003). Some yeasts can produce extracellular capsules consisting of mucopolysaccharide that helps to protect them against chemical attack.

Moulds (such as *Hormoconis resinae* (Haggett & Morchat 1992)) are bounded by a well-defined, multi-layered cell wall composed of chitin. They typically exhibit branched growth or mycelia made up of individual filaments called hyphae, which form an entangled mass (Harding *et al*. 2009), and are thought to be responsible for filter blockage problems (Sutherland 2004). Moulds reproduce via spores produced by specialised hyphae, which disperse and germinate to produce new growth masses. Fungal spores are fundamentally different in function to bacterial spores[12]. However, a few resting spores can be produced within hyphae that are able to withstand adverse growth conditions or survive a period of dormancy. These resting spores are analogous to bacterial spore production. Generally growth is confined to the edges of the biomass, as nutrients are unable to diffuse to the centre as size increases (Denyer *et al*. 1993). Moulds are also aerobic and prefer mildly acidic conditions (pH 5) (Passman 2003).

1.3 Biofilms

Typically microorganisms are thought of as planktonic; free-floating microorganisms growing independently from one another. However, when introduced to a surface or interface, microorganisms begin to accumulate, amalgamating into complex communities known as biofilms. The term “biofilm” was first coined by Costerton *et al*. (1978), and can be defined as a community of microorganisms in which cells that are embedded within a self-produced matrix of water and biopolymers, adhere to each other and/or to a surface.

[12] The function of fungal spores is reproductive, whereas bacterial spores are resistance structures used to survive unfavourable conditions.

In 1940, whilst studying the metabolic activity of marine microorganisms, Heukelekian and Heller found that bacteria were able to proliferate in oligotrophic systems by utilising micronutrients which were too dilute for their planktonic counterparts (Heukelekian & Heller 1940). Later that decade, ZoBell discovered that the majority of marine bacteria are sessile, either growing exclusively or preferentially on surfaces to concentrate nutrients around the attached bacteria (ZoBell 1943). These early studies set the foundation for research in microbial biofilms. However, it is only in recent decades, since the discovery that the majority of naturally-occurring microorganisms are sessile (O`Toole *et al*. 2000) that a concerted effort has been undertaken to understand this phenomenon.

Both single- and multi-species biofilms have been documented in a range of different environments and surfaces, dating further back than the 1930s (Angst 1923). In most natural environments, multi-species biofilms are common place, with the most notable exception being in the medical field, where single-species biofilms are observed in a variety of infections and on medical surfaces (Adal & Farr 1996). Despite this, most studies have been undertaken on single-species biofilms, predominantly: *Pseudomonas aeruginosa*, *Pseudomonas fluorescens*, *Escherichia coli* and *Vibrio cholerae*, have been used (O`Toole *et al*. 2000).

1.3.1 Biofilm composition

Cells within a biofilm are physiologically distinct from planktonic cells of the same species, specifically altering their genetic pathways to trigger biofilm development. Biofilms are formed by producing a nutrient-rich matrix, known as EPS. The composition of EPS varies greatly between biofilms and has historically been difficult to analyse, due to the large range of biopolymers within the EPS matrix (Flemming *et al*. 2007; Karatan & Watnick 2009). However, it is composed largely of extracellular DNA, proteins and polysaccharides, which comprises over 90 % of the total biomass within a biofilm (Andrews *et al*. 2010). These three components play a key role in the aggregation, cohesion and adhesion of biofilms. However, these EPS components also confer a number of other benefits to the cells encapsulated within. Polysaccharides and proteins form a barrier, offering the cells a resistance to antimicrobial agents and biocides, specific and nonspecific host defences during infection, as well as shielding the cells from predation by protozoa.

Hydrophilic polysaccharides retain water within the biofilm, creating a hydrated microenvironment within the biofilm, offering protection against environmental stresses such as desiccation in arid environments. Charged polysaccharides and proteins facilitate the

sorption of organic and inorganic compounds into the biofilms, accumulating nutrients from the environment providing carbon, nitrogen and phosphorus-containing compounds, which can be utilised by the biofilm community. Extra-cellular DNA provides a foundation for extra-cellular communication and the exchange of genetic information (horizontal gene transfer) (Flemming & Wingender 2010). These EPS matrices are so successful that it is estimated that over 99 % of all life may exist within a biofilm (Vu *et al*. 2009).

1.3.2 Biofilm formation

Biofilm formation is triggered when bacteria sense a change in environmental conditions, transitioning from planktonic to sessile life. These triggers usually include changes in temperature, nutrient or oxygen levels and pH, varying greatly between species (O`Toole *et al*. 2000). For example, *P. aeruginosa* and *P. fluorescens* form biofilms under most conditions, whereas some *E. coli* strains require oligotrophic conditions and *Vibrio cholerae* will only form biofilms in eutrophic conditions, when there is an abundance of amino acids (Dewanti & Wong 1995; O'Toole & Kolter 1998; Pratt & Kolter 1998; Watnick *et al*. 1999). This complexity in trigger conditions can be attributed to the fact that microorganisms have multiple genetic pathways that control this behaviour (O`Toole *et al*. 2000).

Once triggered, cells begin to swarm, mobilising together using their flagella, through Brownian motion or chemotactic processes to move towards the surface. It has been observed that *P. aeruginosa* swim along the surface, until they sense an appropriate location before making contact. At present, not much is known about how bacteria sense surfaces, but chemical stimuli like nutrient availability/polysaccharide sensing and physical stimuli using type-IV pili and flagella are thought to play a key role (O'Toole & Wong 2016). Once contact has been made, cells begin to form a monolayer across the surface. At this point, the cells are not stationary but use a twitching motion and type-IV pili to facilitate movement across the surface. It is thought that this twitching motion is a community behaviour, as it is most frequently noticed when cells are in contact with one another (Semmler *et al*. 1999). At this stage, biofilm formation is dynamic, held in place via weak Van de Waals forces. Micro-colonies form and move across the surface, even returning to a planktonic state. They must overcome electrostatic repulsion, depending on the charge of both the surface and the cell, before finally settling on the surface.

Surface characteristics play an important role in the initial attachment of microorganisms. Increases in surface roughness enhance microbial attachment, as they increase the overall surface area and reduce the shear force on the cells during attachment, which is critical in

areas with high flow rates e.g. water pipes. Hydrophobicity and electrostatic interactions will also influence the ability of cells to attach (Renner & Weibel 2011).

Once settled the monolayer of cells begins to exude EPS, permanently anchoring the cell to the surface. At this stage the attachment is irreversible, and is known as primary adhesion or locking. Cells then begin to adapt to life in a biofilm. Clustered together, they increase the synthesis of EPS, and begin to repress the production of cellular appendages, such as flagella, to produce a more stable sessile colony.

Cells then begin to replicate, and a confluent blanket of primary microorganisms and EPS begins to form over the substrate in micro-colonies. The bacteria become encapsulated within the EPS, forming a barrier between the cells and the environment. As the community grows, quorum sensing[13] regulates cell functions, the acquisition of nutrients, and metabolite production, until a mature biofilm is formed (Harmsen *et al*. 2010). As biofilms mature, the accumulation of cells and EPS leads to the formation of 3D structures. The biofilm begins encapsulating planktonic microorganisms and suspended particulates, forming a complex community (Denyer *et al*. 1993; Kobrin 1993; Srivastava *et al*. 2006), which affect the surrounding environment (Denyer *et al*. 1993). Once fully mature, cells begin to detach from the biofilm, and disperse within the environment. These new colonies adsorb onto new surfaces, forming biofilms in new environments (Renner & Weibel 2011).

Usually, the detachment of a biofilm happens when an environment ceases to support the community. This may be due to depleted nutrients or an excess of waste (though starvation is typically cited as the main cause of detachment). Cells in the outer layers of the biofilm transition back to planktonic life, switching on genes required for planktonic life. These signals require more research before they are fully understood (O`Toole *et al*. 2000).

1.3.3 Biofilms in aircraft

The protective nature of biofilms hold particular relevance in relation to biofilms found within aircraft wing tanks. The jet fuels found within these tanks are a rich carbon source, for microorganisms that are able to utilise it as an energy source. However, fuels are highly toxic (particularly short-chain length hydrocarbons), and any microorganism utilising this carbon source must be able to withstand exposure.

[13] Quorum sensing is a form of chemical communication between bacteria. A central process in biofilm formation, cells use quorum sensing to query their environment (Renner & Weibel 2011).

Additionally jet fuel systems are exposed to an extreme range of temperature during flight. During flight, bulk fuel temperatures are required to be 3 °C higher than the maximum freeze point of the fuel (Zabarnick & Ervin 2010); -47 °C for Jet A-1. However, the extremities of the tank (where the microbial communities are typically found) are subjected to the harshest conditions. In these areas it is conceivable temperatures could range between +40 °C and -50 °C, between take-off and landing. This extreme temperature fluctuation causes any free water to go through freeze-thaw cycles, restricting its bioavailability.

These temperature fluctuations not only exert an extreme selection pressure, but affect the ability of microorganisms to metabolise hydrocarbons. At low temperatures, the viscosity of jet fuel increases, and the volatilisation of short chain alkanes is decreased. This coupled with slower metabolic processes at low temperatures, restricts the availability of the hydrocarbons as an energy source. It has been observed that rates of hydrocarbon degradation decrease with decreasing temperature; it is thought to be directly linked to decreased rates of enzymatic activity (Leahy & Colwell 1990). Conversely, higher temperatures (30 to 40 °C) increase the rates of hydrocarbon metabolism. However, it also increases the membrane toxicity of hydrocarbons, making them more toxic (Boethling & Alexander 1979).

During flight, the air space in wing tanks is rendered inert, by pumping nitrogen into the tanks to prevent the fuel from igniting. This creates a nitrogen-rich atmosphere, restricting the level of available oxygen to around 12 %. However, oxygen gradients are common place within biofilms, so it is unlikely that this will have an impact on the microbial communities, as oxygen levels are still relatively high, though it is a possible selection pressure. Due to this extreme environment, it is likely that biofilms play a key role in the ability of microorganisms to survive within these systems.

1.4 Microbial populations in aviation fuels

Although the Polymerase Chain Reaction (PCR) and next generation sequencing have made culture-independent analysis of microbial community composition routine, the aviation industry has been relatively conservative when analysing microbial communities; isolation and culture-based techniques are commonly used to identify bacterial communities within aviation fuel (Dolan 2002; McNamara *et al*. 2005; Rauch *et al*. 2006; Swift 1988). However, it is well documented that a high percentage of environmental microorganisms are uncultivable (Brown *et al*. 2010). Despite this limitation, very few studies have been

undertaken using culture-independent molecular techniques to characterise microbial populations in aviation fuels.

Denaro *et al*. (2005) undertook a comparative study of culture-dependent and culture-independent methods. Microorganisms from each sample were cultured both on agar and directly lysed (eliminating microbial cultivation). Their analysis identified the presence of 36 microbial species, including 28 that were previously undocumented in aviation fuels. Of these species, 61.9 % were only identifiable using culture-independent methods (33.3 % by both culture-dependent and culture-independent methods, 4.8 % by culture-dependent methods only) (Denaro *et al*. 2005); confirming that there are many uncultivable species thriving in jet fuel systems (Amann *et al*. 1995; Hugenholtz & Pace 1996).

In 2006 Rauch *et al*. undertook a study that analysed 36 samples from aircraft wing tanks, ground storage tanks and fuel distribution systems, from 11 geographically separate areas. Samples were cultured, cloned and identified using capillary DNA sequencing and gas chromatography of fatty acid methyl esters (GC-FAME), identifying a total of 17 microbial species (predominantly Gram positive aerobes and facultative anaerobes), 4 of which were previously undocumented in aviation fuels (Rauch *et al*. 2006).

In 2007, Vangsness *et al*. studied the effect of Diethylene glycol monomethyl ether (DiEGME) on microbial contamination in 93 aviation fuel samples. Adenosine triphosphate (ATP) photometry was the primary method used to characterise bioburden in this study. However, the same culture-independent techniques used by Denaro *et al*. (2005) were also used to characterise these samples. This analysis concluded that although each sampling site may have some unique consortia, that majority of fuel systems appear to be dominated by the same types of species (Vangsness *et al*. 2007).

In 2010, Brown *et al*. used samples of Jet A (8 samples), Jet Propellant (JP) 8 (17 samples) taken from aircraft and JP-8 samples (22 samples) taken from ground storage tanks to create a genetic library, which was used to compare bacterial communities between the continental USA and outside of the continental USA. They observed similar species to the previous studies, however on average Jet A had a lower bacterial diversity than JP-8, and was dominated by different species (Brown *et al*. 2010). This indicates that fuel type and treatment (additivation), have an influence of microbial communities.

Outside of the USA, Raikos *et al*. (2011) took 33 samples of JP-8 from 6 geographically separated airports in Greece. They cultured the samples and identified the isolates using PCR

primer sets designed to identify bacteria, archaea and fungi. The study identified two types of bacteria (*Agrobacterium tumefaciens* and *Staphylococcus epidermidis*), one of which (*Agrobacterium tumefaciens*) had not been isolated from fuel samples previously. Neither archaea nor fungi were detected in this study.

The microorganisms discovered in aviation fuels have been compiled below (see Table 1.1 and Table 1.2). They show that in aviation fuels there are a higher number of prokaryotic taxa compared to eukaryotic taxa (Raikos *et al*. 2011) and of these the bacteria Actinobacteria, Firmicutes and Proteobacteria are the most commonly described (76.6 %). When using both culture-dependent and culture-independent techniques the orders Actinomycetales (20.8 %), Enterobacteriales (13.0 %), Burkholderiales (10.4 %) and Rhizobiales (6.5 %) occur most frequently. However, several of these studies have not looked for eukaryotes, which may introduce a bias. Eukaryotes make up the remaining identified species (20.8 %) and they are dominated by Ascomycota, of which Eurotiomycetes (5.6 %) are the most prevalent.

However, it should be noted that these studies have primarily been undertaken by the USAF, and as such the most commonly studied aviation fuel is JP-8 (military grade jet fuel), as opposed to Jet A or Jet A-1 (commercial jet fuel). Though the base molecules of these fuels are similar, JP-8 contains fuel system icing inhibitor (FSII) (typically diethylene glycol monomethyl ether) to prevent ice crystals forming during flight[14]. FSII has been documented as having biostatic properties, with concentrations of >15 % (v/v) needing to be maintained in the aqueous phase of fuel tanks to control/eliminate microbial growth (Balster *et al*. 2009). However, this is a somewhat controversial area and there is some debate about its biostatic properties.

The initial study into the biocidal properties of FSII was done by Hettige & Sheridan (1989), who were unable to detect any antimicrobial affects when DiEGME was compared with a series of biocides; a result that Westbrook (2000) also concluded in JP-8. Geiss & Frazier (2001) then went on to conclude that DiEGME actually has a nutritive effect on microbial growth. Hill *et al*. (2005) reported DiEGME had a biocidal effect on a mixed community after

[14] Ethylene glycol monomethyl ether (EGME) was used in military fuels (JP-4) as a fuel system icing inhibitor up to the early 1980s, when it was replaced by diethylene glycol monomethyl ether (DiEGME) (in JP-4 and JP-8) because of concerns with the flash point of the fuel. In recent years triethylene glycol monomethyl ether (TriEGME) has begun being used (JP-8) because it is less toxic than its predecessors (Balster *et al*. 2009). Therefore depending on the age of the study in question different icing inhibitors were being used.

prolonged exposure (10-17 days at 10-12 % (v/v)). However, they noted that after repeat exposure the population's resistance increased, and therefore concluded that DiEGME's biocidal properties are most likely due to its hygroscopic properties rather than any toxicity effects. This area was again revisited by Balster *et al*. (2009) after aircraft wing tank coating failures (Zabarnick *et al*. 2007). They concluded that toxic effects were inoculum dependent, when tested against American Type Culture Collection (ATCC) pure cultures and field samples (15 to >60 % (v/v)), and that although TriEGME performed better than DiEGME, it was still unable to completely inhibit growth at 60 % (v/v). From these studies it can be seen that FSIIs have a variable effect on microbes and it is likely to have an impact on community dynamics. It is therefore to be expected that microbial communities differ in fuel containing FSII versus those not containing FSII (Passman 2013).

Other studies have also been done on middle distillate fuels, predominantly diesels and biodiesels, such as that by Lee *et al*. (2010), Cyplik *et al*. (2011) and Bücker *et al*. (2014), after initially being reviewed by Gaylarde *et al*. (1999), who compiled a list of 125 organisms isolated from fuel samples. Additionally, White *et al*. (2011) undertook a study primarily on marine and automotive diesels (though some kerosene was included) that showed that the bacterial genera *Pseudomonas*, *Burkholderia* and *Bacillus* were most prevalent in contaminated diesel fuel when using culture-dependent techniques, whereas culture-independent techniques (pyrosequencing of 16S rRNA genes) showed that *Marinobacter*, *Achromobacter*, *Burkholderia* and *Halomonas* were prevalent. They also used denaturing gradient gel electrophoresis (DGGE) to show that introducing bio-components into fuel blends, caused variation in microbial communities (White *et al*. 2011). These studies have not examined aviation fuels and so have not been reviewed further.

Table 1.1 – Prokaryotic contaminants identified from aviation fuel. Table based on Rauch *et al*. (2006). Microorganisms identified using culture-dependent analysis have been denoted with a ● symbol, microorganisms identified using culture-independent analysis have been denoted with a ○ symbol. Where both types of analysis have been used both symbols are used. Microorganisms have arranged by Class. (Bakanauskas 1958; Hazzard 1961; Gandee & Reed 1964; Finefrock & London 1966; Weisburg *et al*. 1991; Ferrari *et al*. 1998; Gaylarde et al. 1999; Dolan 2002; Shelton *et al*. 2002; Denaro 2005; Rauch *et al*. 2006; Brown *et al*. 2010; Raikos *et al*. 2011; White *et al*. 2011).

Prokaryotes	JP-4	JP-8	Jet A	Jet A-1	Kerosene
Actinobacteria					
Arthrobacter sp.		○		●	
Brachybacterium sp.					●
Brevibacterium ammoniagenes	●			●	
Brevibacterium epidermidis		○			
Corynebacterium sp.		●			
Curtobacterium sp.			●		
Dietzia sp.		○			
Kocuria rhizophilia		○			
Leucobacter komagatae		○			
Microbacterium oleovorans			●		
Micrococcus luteus		●			
Micrococcus sp.	●	○	●	●	
Mycobacterium mucogenicum			○		
Propionibacterium acnes			●		
Rhodococcus equi			●○		
Rhodococcus opacus			○		
Rhodococcus sp.		●	●○		
Rothia amarae			●		
Rothia mucilaginosa			○		
Streptomyces sp.			●	●	
Alphaproteobacteria					
Agrobacterium tumefaciens		●			
Bradyrhizobium sp.			○		
Brevundimonas vesicularis		○			
Caulobacter vibroides			○		
Methylobacterium sp.		●	●		
Phyllobacterium mysinacearum			●		

Prokaryotes	JP-4	JP-8	Jet A	Jet A-1	Kerosene
Rhizobium sp.			●○		
Sphingomonas sp.		○			●
Bacilli					
Bacillus acidocaldarius	●	●○	●	●	
Bacillus cereus		●○			
Bacillus lentimorbus		●○			
Bacillus licheniformis		●○			
Bacillus megaterium		●○			
Bacillus pasteurii					
Bacillus pumilus		●○			
Bacillus sp.	●	●○	●○	●	
Bacillus subtilis					
Granulicatella sp.			○		
Lactococcus lactis			○		
Staphylococcus aurens		○			
Staphylococcus cohnii		○			
Staphylococcus epidermidis		○			
Staphylococcus sp.		●○	○		
Staphylococcus warneri		○			
Streptococcus sp.		○			
Betaproteobacteria					
Acidovorax sp.			○		
Alcaligenes paradoxus		○			
Alcaligenes sp.		○	●		
Alcaligenes xylosoxidans		○			
Aquabacterium sp.			○		
Aquasprillum metamorphum			○		
Burkholderia sp.			●○		
Diaphorobacter nitroreducens			○		
Herbaspirillum frisingense			●		
Hydrogenophilus sp.		●			
Pandoraea sp.			●		
Ralstonia sp.			○		
Clostridia					
Clostridium sardiniense			●○		

Prokaryotes	JP-4	JP-8	Jet A	Jet A-1	Kerosene
Deltaproteobacteria					
Desulfovibrio sp.	●		●	●	
Wolinella succinogenes			○		
Flavobacteriia					
Chryseobacterium sp.		●			
Flavobacteriaceae					○
Flavobacterium (microbacterium)	●		●	●	
Flavobacterium diffusum	●		●	●	
Gammaproteobacteria					
Acinetobacter calcoacetius			●	●	
Acinetobacter cerificans			●	●	
Actinomadura yumanensis		●			
Aerobacter aerogenes	●		●	●	
Aeromonas sp.			●	●	
Enterobacter cloacae			●	●	
Enterobacter (Pantoea)			●	●	
Escherichia sp.	●				
Ewingella americana			●		
Haemophilus Parainfluenzae			○		
Pantoea ananatis		○			
Photorhabdus luminescens			○		
Pseudomonas aeruginosa	●	●	●	●	
Pseudomonas sp.	●	●	●	●	●○
Rahnella aquatilis			●○		
Serratia marcescens			●	●	
Serratia odorifera			●	●	
Shigella sp.		●			
Xenorhabdus nematophilus		●			
Nitrospirae					
Nitrospira sp.		●			
Other					
Streptophyta sp.		●			

Table 1.2 – Eukaryotic contaminants identified from aviation fuel. Table based on Rauch *et al*. (2006). Microorganisms identified using culture-dependent analysis have been denoted with a ● symbol, microorganisms identified using culture-independent analysis have been denoted with a ○ symbol. Where both types of analysis have been used both symbols are used. Microorganisms have arranged by Class.

Eukaryotes	JP-4	JP-8	Jet A	Jet A-1	Kerosene
Chaetothyriomycetes					
Rhinocladiella sp.				●	
Dothideomycetes					
Aureobasidium pullulans	●	●		●	
Helminthosporium sp.	●			●	
Eurothiomycetes					
Aspergillus sp.	●		●	●	
Aspergillus niger	●		●	●	
Aspergillus fumigatus	●		●	●	
Exophiala jeanselmei		●			
Paecilomyces sp.	●		●	●	
Paecilomyces variotii	●		●	●	
Penicillium corylophilum	●		●	●	
Penicillium sp.	●		●	●	
Phialophora sp.			●	●	
Incertae sedis					
Hormoconis (Cladosporium or	●	●	●	●	
Other					
Discophaerina fagi		●			
Tothersrichoderma sp.			●	●	
Tothersrichoderma viride			●	●	
Trichosporium sp.				●	
Saccharomycetes					
Candida famata			●	●	
Candida lipolytica			●	●	
Candida sp.			●	●	

Eukaryotes	JP-4	JP-8	Jet A	Jet A-1	Kerosene
Sordariomycetes					
Acremonium sp.			●	●	
Acremonium strictum			●	●	
Fusarium moniliforme			●	●	
Fusarium sp.			●	●	
Urediniomycetes					
Rhodotorula sp.			●	●	

1.5 Factors contributing to the contamination of aircraft fuel systems

1.5.1 Fuel systems

After distillation, jet fuels are sterile due to the extreme manufacturing temperatures and pressures. The fuel is then transferred into a holding tank where it is sub-sampled and analysed, batched as a finished product and a certificate of quality (CoQ) issued. This is the first time the fuel is potentially exposed to microbial contamination. After the CoQ has been issued, the fuel is available for release into the fuel distribution system by a number of transport routes such as pipelines, road trucks, rail cars, river barges and sea tankers. These are generally non-dedicated, allowing for cross contamination of jet fuel with other products e.g. biodiesel, as well as introducing further contaminants, such as free water and particulates. The fuel will eventually reach another storage tank (either at an airport or an intermediate terminal) and go into a dedicated distribution system (airports) or a second transportation method (intermediate terminal). After arrival at an airport, the fuel is allowed to settle, reanalysed and loaded onto a plane using either 1) a hydrant servicer/dispensing vehicle, 2) a cart connected to an underground hydrant system, or 3) a refuelling tanker via a gantry or loading rack (see Figure 1.1) (Rugen *et al*. 2007).

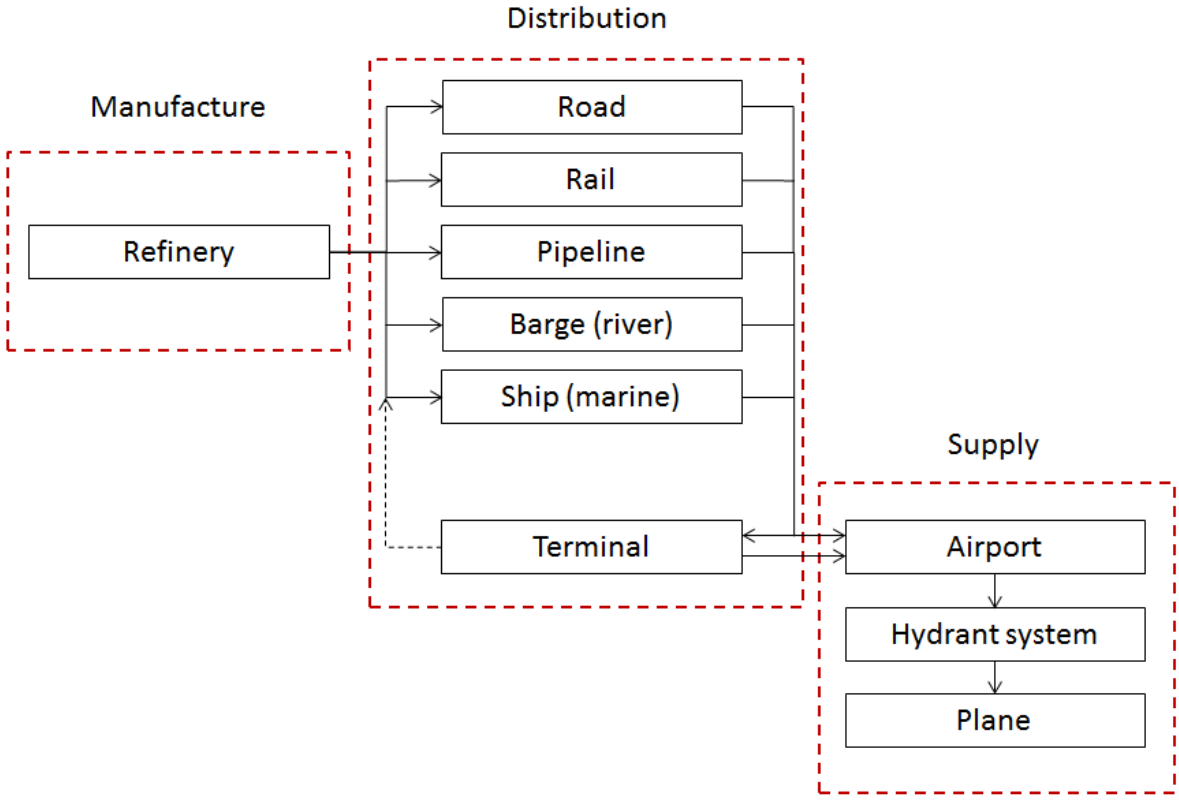

Figure 1.1 – Generic aviation fuel supply chain (Rugen *et al*. 2007)

1.5.2 Water

Water is the most critical component for microbial proliferation in fuel systems (Passman 2013), and is carefully controlled. Water vapour enters a fuel system through natural gas exchange and rain water ingress. Once associated with the fuel, water is dissolved up to about 60 ppm at 25 °C in jet fuels, depending on the natural surfactant levels (see Figure 1.2), which can be altered by the activity of microorganisms (Brown *et al*. 2010; Muriel *et al*. 1996). Water can also become emulsified as a dispersion of small, suspended water droplets. If the fuel is not surfactant laden, these droplets will coalesce and settle out onto the tank surfaces, forming a fuel/water interface, which provides a microbial substrate (Rugen *et al*. 2007). At the low temperatures experienced during flight, suspended or settled free water can form ice crystals, which can disrupt unheated fuel system filters causing fuel starvation to engines and consequent combustion problems (Murray *et al*. 2011; Zherebtsov & Peganova 2012).

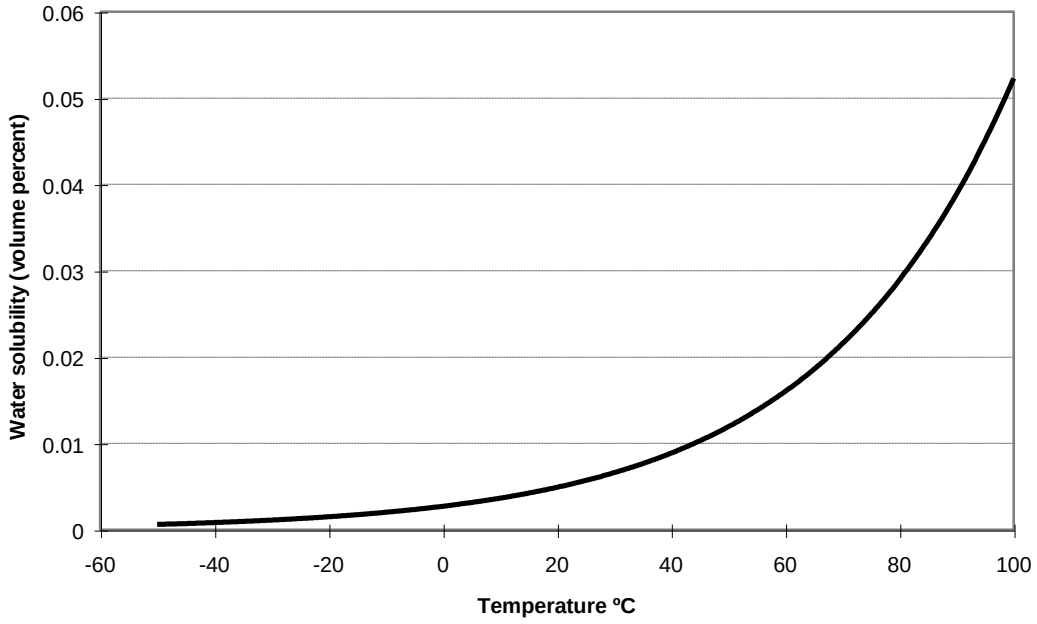

Figure 1.2 – Water solubility in jet fuel (Anon. 1988)

1.5.3 Particulates

As little as 1 mg of particulates per 100 ml of fuel can cause filtration problems (Gaylarde *et al*. 1999). Particulate contamination can occur as airborne dusts, product carryover from ships, and salts from refinery salt driers or marine distribution. However, the most common form is rust (Fe_2O_3 and Fe_3O_4), from the degradation of distribution equipment and tanks (Rugen *et al*. 2007). It has been noted by Videla (1989) that presence Fe_3O_4 (magnetite) stimulates the corrosion of mild steel in a saline medium (Denyer *et al*. 1993). The area of (inorganic) jet fuel filtration has been well studied (Bhan *et al*. 1988; Clark *et al*. 2011; Hazlett 1969) and is not covered here. Biofilm development encapsulates inorganic particles and planktonic microorganisms, which then influence its physical properties and community dynamics (Denyer *et al*. 1993; Passman 2003).

1.5.4 Cross contamination

In recent years the transportation of jet fuel through non-dedicated distribution routes has caused problems with the cross contamination of fuel products, most notably due to biodiesel (Baker 2012). Since biodiesel and jet fuel share the same distribution routes, fatty acid methyl esters (FAME) has begun to act as a jet fuel contaminant. There are two main issues with this, 1) FAME is surface active, sticking to surfaces and increasing the risk of cross contamination and 2) FAME is a non-hydrocarbon fuel component and the jet fuel specification states that only hydrocarbon components or approved additives are allowed. This issue is hotly debated within the aviation industry: at present the specification allows

for 100 ppm of FAME in jet fuel and the fuel is considered off specification and unfit for use on board aircraft if this level is exceeded (Anon. 2008; Anon. 2011b). A study by (Hill 2011) evaluated the effect of trace amounts of FAME (in jet fuel) on the growth of microorganisms. He concluded that (100 ppm) FAME did increase marginally the susceptibility of jet fuel to microbial growth. However, the study did not take into account any long term implications of FAME accumulation on metallic surfaces (Hill 2011).

1.5.5 Surfaces and substrates

As fuel travels through the supply chain, it comes into contact with a variety of substrates, such as mild and stainless steel, aluminium alloys (in particular 2024 and 7075-T6) and modern composite carbon fibres reinforced with epoxy resin. These surfaces are often coated with polyurethane lacquers or epoxy linings or protected by a leaching and anodising process (aluminium alloys), and have historically included chromates, which are suspected to have a biocidal effect within a fuel system. Both the physical and chemical properties of these surfaces will have an impact on potential biofilm formation, as an increase in surface roughness increases the initial surface adhesion and subsequent colonisation, as well as nutrients provided by the surfaces themselves (Percival *et al*. 1999). Most microorganisms can attach to surfaces; the rate of attachment and strength of the interaction reflect an interplay between microbial and substrate surface characteristics (Kobrin 1993).

1.5.6 Fuel tanks

Aircraft fuel tanks are a particularly harsh environment; fuels can be nutrient deficient[15] (Gaylarde *et al*. 1999), temperatures can go as low as -44 °C[16] (Zabarnick & Ervin 2010), causing all available free water to freeze, and constant agitation during refuelling can make it more difficult for biofilms to adhere to surfaces, increasing the risk of microorganisms sloughing off and blocking filters (Alnnasouri *et al*. 2011). These conditions make an aircraft fuel tank one of the harshest and most variable environments for microorganisms to survive in the supply chain. Despite this, contamination of jet fuel systems by microorganisms continues to be a problem within the aviation industry and the introduction of novel components is likely to alter the existing ecosystem.

[15] Fuels will provide varied nutrients depending on source refinery, process, additive content etc.
[16] Currently aircraft are limited to operation 3°C above the freeze point of the fuel specification being used e.g. -40 °C for Jet A, -47 °C for Jet A-1 etc. (Zabarnick & Ervin 2010).

1.5.7 Nutrients

Jet fuels still contain relatively high quantities of sulphur species compared to other fuel types[17] (Anon. 2011b). There is some debate as to whether the sulphur content of fuel acts as a nutrient source or as a toxin. Gaylarde *et al*. (1999) suggest that at low levels sulphur can enhance microbial activity while McNamara (2000) reported that a sulphur level of 0.2 % in fuel inhibits microbial growth. However, a further source advised that at 0.2 % sulphur acts as a nutrient source (Anon. 2000). It is likely that these opposing stand points depend on the bioavailability of the sulphur species. Hill (2011) postulates that mercaptan oxidation (Merox) treated jet fuel is more susceptible to growth than hydro-treated because it contributes essential nutrients like sulphur and nitrogen, which would otherwise be growth limiting (see Section 1.6). Therefore we can hypothesise the low sulphur alternative fuels may be growth inhibitory.

Oxygen is normally abundant in fuel tanks, due to the continual replenishment as tanks are refilled. The limiting factor for growth is probably the availability of other nutrients, particularly phosphorus, which is usually present at <1 ppm in fuels. Nitrogen and iron may also be important limiting nutrients. However, fuel additives and contaminants regularly contains these, therefore removing one of the limiting factors for the growth of microorganisms (Gaylarde *et al*. 1999).

Microbial survival is dependent on the procurement of water and chemical elements for the synthesis of cellular material (Passman 2003). Microorganisms must also have an energy generating system, consisting of an electron donor and a terminal electron acceptor in order to metabolise these elements. This electron transfer is undertaken via a redox reaction (the loss of an electron from one substance (oxidation) and added to another (reduction). Aerobes use oxygen as the terminal electron acceptor (i.e. it is reduced) to oxidise glucose and produce energy, whilst anaerobes replace oxygen with a variety of compounds such as nitrate and sulphate in the electron transport chain (Hutchins 1991). An alternative to anaerobic respiration is fermentation, which replaces the electron transport chain observed in aerobic and anaerobic respiration with the glycolysis of glucose to produce pyruvate and ATP.

[17] For example the specification for Jet A-1 (DEF STAN 91-91) allows a total sulphur content 3000 ppm (Anon. 2011b), as opposed to sulphur free diesel (EN 590), which allows for a total sulphur content of 10 ppm (Anon. 2009).

1.5.8 Environment

Microorganisms have the ability to adapt to a wide range of environments and may be categorised by their response to temperature: thermophiles (30 to 80 °C), mesophiles (10 to 45 °C) and psychrophiles (-8 to 37 °C) (Wilkinson 1975; Madigan & Marrs 1997; Toole & Toole 1995). Bacteria have also adapted to extremes of pH, acidophiles favour habitats of pH <5 and alkaliphiles pH >8 (Passman 2003). Microbes associated with middle distillates can tolerate pH ranges ~4 to 9 and temperatures 18 °C to 35 °C; they are predominantly mesophilic. Growth can, however, occur over range 5 °C to 80 °C and some microbes found in the fuel systems of supersonic aircraft are thermophiles (Neihof 1988).

1.6 Kerosene and jet fuels

1.6.1 Conventional fuels

Crude oil is composed of varied aliphatic, aromatic and heterocyclic compounds (Gaylarde *et al*. 1999). It is distilled to produce petroleum fractions such as jet fuel, which has carbon chain lengths of approximately C_{10}-C_{16} (Gaylarde *et al*. 1999) and a boiling range between 130 and 300 °C[18] (Anon. 2011b; Song 2003). Jet fuels comprise of saturated[19] and unsaturated[20] hydrocarbons, as well as hetero-atomic species (e.g. sulphur, nitrogen and oxygen compounds), other complex species and additives. The exact ratio of chemical species within a given fuel is governed by the crude oil used and the operational and production constraints at the point of manufacture[21] (Gaylarde *et al*. 1999; Tissot & Welte 1984).

Due to extreme operating conditions, jet fuel specifications are the most demanding in the petroleum industry. The fuel must be able to ignite readily and burn consistently, whilst being thermally stable (Pande *et al*. 2001) and have good cold flow properties at low temperatures[22] (Gaylarde *et al*. 1999; Zabarnicm & Ervin 2010). The main grades are Jet A,

[18] The maximum temperature allowed in the DEF STAN 91-91 (issue 7) jet fuel specification is 300 °C, though the final boiling point of most jet fuels is typically much lower than this (Anon. 2011b).

[19] Saturated hydrocarbons are hydrocarbons containing only a single bond between carbon atoms. Each carbon atom is also bonded to as many hydrogen atoms as possible. In jet fuels these usually comprise of normal and iso-paraffins, as well as naphthenes (Housecroft & Constable 2002).

[20] Unsaturated hydrocarbons are hydrocarbons that contain one or more carbon-carbon double bonds and broadly comprise of olefins, aromatics (up to 25 %) and naphtheno aromatics (Anon. 2011b; Housecroft & Constable 2002).

[21] For example the refinery process used will have a large impact on the final product i.e. a Merox-treated fuel will contain more sulphur species than a hydrocracked fuel (Anon. 2011b).

[22] Jet fuel must have a low vapour pressure and freeze point, whilst still being able to flow (i.e. have a low viscosity) at low temperatures (Gaylarde *et al*. 1999).

Jet A-1, Jet B, TS-1, (commercial), JP-4, JP-5 and JP-8 (military); each has a separate specification (Bacha *et al*. 2000).

1.6.2 Refinery processes

Crude is converted into refinery streams by hydrogenation, distillation, extraction, reformation, cracking and blending (Babich & Moulijn 2003). Refinery processes such as Merox-treatment, hydro-treatment and hydro-cracking are used to produce a finished jet fuel; process choice impacts on molecule type (particularly sulphur). This is important for the growth of microorganisms, as nutrient levels will vary by treatment method. For example, a study by Hill (2011) showed that Merox-treated jet fuel was more susceptible to microbial degradation than hydro-treated jet fuel.

Merox-treatment converts mercaptans into disulphides, using a proprietary catalytic chemical process. The process requires an alkaline environment (provided by sodium hydroxide (NaOH)) and a strong caustic (typically hydrochloric (HCl) or hydrofluoric acid (HF)). Jet fuel is introduced into a vessel containing the caustic wash, where the sodium hydroxide and hydrogen sulphide (H_2S) (present in the jet fuel) react to produce sodium hydrosulphide (NaHS) and water (H_2O). The resulting products are then transferred into the Merox reactor, where mercaptan oxidation takes place ($4RSH + O_2 \rightarrow 2RSSR + 2H_2O$). The Merox-treated jet fuel is then allowed to settle, splitting the remaining hydrophilic caustic solution from the hydrophobic jet fuel; a process known as sweetening. The sweetened jet fuel in then water washed, to remove any remaining hydrophilic compounds, salt dried to remove the water and finally clay treated to remove particulates as well as any unwanted hydrophobic compounds. Merox-treatment reduces the disulphide level, however relative to other jet fuel processing methods the overall the reduction in sulphur species (or other heteroatoms) is relatively small. Hydro-treatment uses hydrogen and an alumina based catalyst impregnated with cobalt and molybdenum to remove sulphur and is the preferred method for producing jet fuel. The jet fuel feed stock is preheated and enriched with hydrogen-rich gas where it is vaporised and passed through the catalyst before entering the reactor, which produces hydrogen sulphide. The fuel is then cooled and the liquid fuel separated from the hydrogen-rich gas and hydrogen sulphide and then distilled to produce the finished product. Hydrocracking[23] can also be used to remove sulphur by hydrogen addition to produce hydrogen sulphide. Hydro-treated/hydro-cracked fuels have to be

[23] Hydrocracked components are defined as petroleum derived hydrocarbons that have been subjected to a hydrogen partial pressure of greater than 7000 kPa (70 bar or 1015 psi) during manufacture (Anon. 2011b).

augmented with either a higher sulphur fuel or a lubricity additive to improve the lubricity of the finished fuel (Ebbinghaus & Wiesen 2001).

1.6.3 Jet fuel additives

There are four main groups: engine performance, fuel handling, fuel stability and contamination control. They can be added at the refinery during distribution or when the fuel leaves the terminal.

1.6.3.1 Engine performance

Lubricity improvers contain polar groups that form a surface film on contact with metal; fatty acids and esters are typically used (Margaroni 1998; Rand 2003). Their microbial degradation potentially removes their lubricating properties, which is potentially hazardous to aircraft operations (Hill 2003). A study by the US Navy in 2012 showed a linoleic acid based lubricity improver to be at risk of degradation by microorganisms, causing reduced fuel lubricity (Stamper *et al*. 2012).

1.6.3.2 Fuel handling

Conductivity improvers are a blend of aromatics, sulphonic acid and polymers (sulphur and nitrogen based), used to help dissipate electrical charge build up and prevent explosion (Anon. 2011b). Icing inhibitors (diethylene monoglycol ether) prevent free water forming ice crystals at low temperatures (Zabarnick *et al*. 2010) and also have biostatic properties. Leak detectors (naphthalimide (Cavestri & Kalley 1999)) are used to detect and locate leaks in fuel systems (Anon. 2011b).

1.6.3.3 Fuel stability

These include antioxidants and metal deactivators. Antioxidants are phenols, which interrupt reactions between oxygen and free radicals in fuel, helping to prevent particulates, gums and solid deposits forming (Zabarnick 1998). Trace metals such as copper, cadmium, cobalt, iron and zinc catalyse oxidation reactions involved in fuel instability (Anon. 2011b). Metal deactivators (N,N'-disalicylidene 1,2-propanediamine) chelate these metals nullifying their catalytic effect, as well as preventing particulate contamination forming aggregates (Waynick 2001).

1.6.3.4 Contamination control

Biocides are used to kill microorganisms and are mainly non-oxidising, composed of aldehydes, amines, halogenated compounds and sulphur compounds. Finally, corrosion

inhibitors[24] are surfactants and attach to metal surfaces to form a barrier between the metal and corrosive agents (Bacha *et al*. 2007).

1.7 Alternative fuels

The aviation industry is inherently conservative and therefore has been slow to embrace a greener future (Kivits *et al*. 2010). However, with environmental pressures increasing and the gap between product supply and demand growing, alternative fuels are being explored to improve fuel efficiency and offer greater energy security (Daggett *et al*. 2006). (This follows the precedent for automotive fuels where ethanol in gasoline and FAME in diesel are already being used (Anon. 2011a; Anon. 2011c)). Viable, replacement options such as fatty acid esters (FAEs) synthetic paraffinic kerosene's (SPKs) and hydro-treated renewable jet fuels (HRJs) are currently under evaluation (Anon. 2012b; Corporan *et al*. 2011; Kinder 2010; Shonnard *et al*. 2010).

1.7.1 Fatty acid esters

FAEs are long chain fatty acid esters, obtained by the transesterification of triglyceride fat groups into base oils. The final composition of these esters is dependent on the original feed stock, and transesterification process (utilising methanol will produce FAME, ethanol fatty ethyl esters (FAEE), and is a comparatively cheap way of converting large, branched molecules into smaller straight chained molecules. Base feed stocks are typically sourced from plant or animal materials, such as jatropha seeds, having moved away from feed stocks that compete with food sources (see Figure 1.3) (Blakey *et al*. 2011).

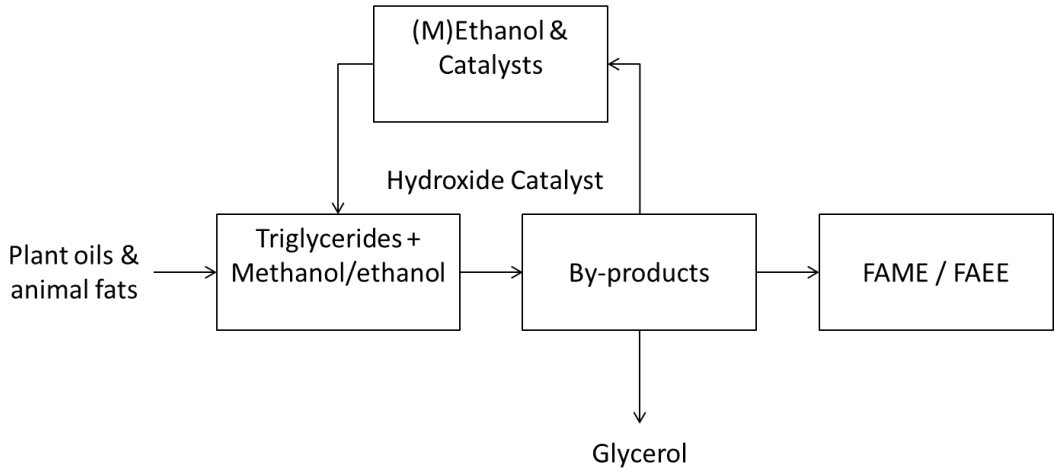

Figure 1.3 – Transesterification process (Blakey *et al*. 2011)

[24] Corrosion inhibitors and lubricity improvers have the same chemistry.

1.7.2 Synthetic paraffinic kerosene

SPK's are obtained from three main non-petroleum feed stocks: Coal (CTL), gas (GTL) and biomass (BTL). They are converted into hydrocarbons via a Fischer-Tropsch (FT) synthesis where syngas (H_2 and CO) produced from the feedstocks, is polymerised (in the presence of a heterogeneous catalyst) to produce paraffins, olefins, oxygenates and water and then hydro-treated to remove sulphur (see Figure 1.4) (Kinder 2010; Rafiq 2012).

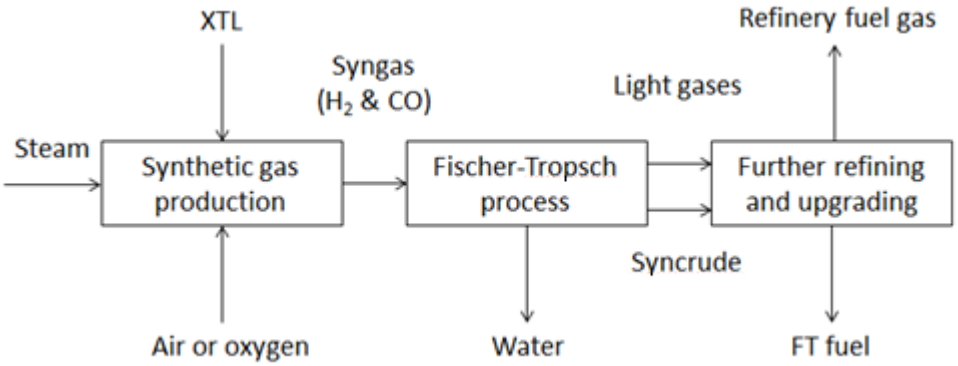

Figure 1.4 – Outline of the conversation XTL via the FT process and its resulting products (Thomsik 2008)**.**

1.7.3 Hydro-treated renewable jet fuel

HRJ feedstocks are composed of fatty acids and fatty acid methyl esters. They are primarily glycerol with an oxygen functional group at one end and an aliphatic hydrocarbon chain (with varying double bonds) at the other. Most exist as either triglycerides, diglycerides or monoglycerides bound together (where appropriate) by esters, as well as free fatty acids by carboxylic acid groups. These are then broken down using hydro-treatment (see Section 1.6). This removes the double bonds, ester and carboxylic acid groups to leave n-paraffins, which can be fractionated and used as a component in jet fuels (see Figure 1.5) (Kinder 2010).

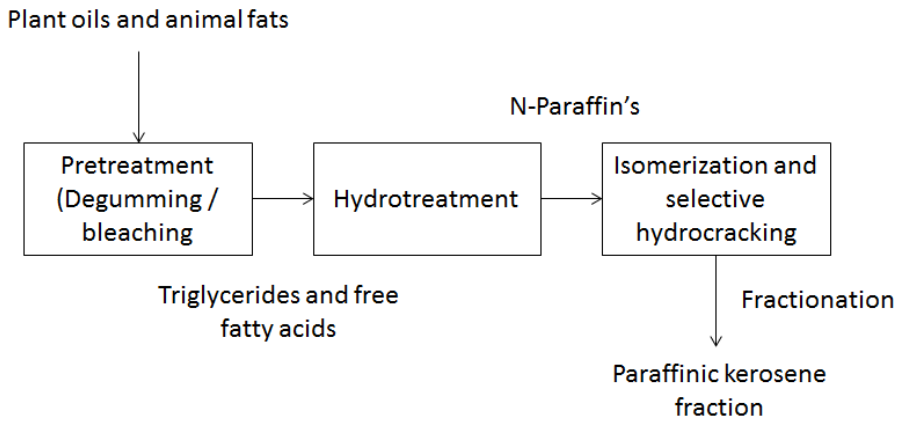

Figure 1.5 – Outline of the conversation of fatty acids to n-paraffin's via hydro-treatment (Kinder 2010)**.**

1.7.4 A brief history of the use of alternative fuels in aviation

Since 2007 a number of test flights have been undertaken using alternative fuels. The first of these was undertaken by USAF, in August 2007, where a B-52 trialled 50:50 blends of synthetic fuels (S-8 and later GTL kerosene) and JP-8 preforming emissions testing. However, the readiness of gas derived fuels in a commercial environment was initially demonstrated by Airbus, Rolls Royce and Shell, by undertaking the first test flight of an Airbus A380, from the UK to France on a 37.4 % (v/v) blend of synthetic fuel (ensuring the minimum density requirement was met). Later that year, Virgin Atlantic undertook the first commercial flight on a biomass derived synthetic fuel (20 % (v/v) coconut and babassu palm oil). Due to the public backlash of utilising a food source as a feed stock for jet fuel, Air New Zealand selected jatropha seeds (a high oil content inedible seed), to produce a drop-in HRJ. In 2008 they flew a Boeing 747-400 on a 50:50 blend of this HRJ and conventional jet fuel between Auckland and Wellington (New Zealand), showing a potential fuel burn save of 1.2 % and demonstrating that HRJ could be used as a drop-in replacement for jet fuel. Following suit, Continental Airlines flew the first aircraft on fuel derived from algae in January 2009 from Houston, where a Boeing 737-800 was powered using a mixture of 47.5 % jatropha and 2.5 % algae derived fuels mixed with conventional jet fuel. Later that month Japan Airlines also flew one engine on a Boeing 747-300 out of Tokyo, on a blend of algae derived fuel (42 % camelina, 8 % jatropha and <0.5 % algae), further highlighting its feasibility. On 13th October 2009, following the certification of the fuel, Qatar Airways in conjunction with Shell Research flew the first commercial flight using GTL kerosene, from London to Doha (Blakey *et al*. 2011). Since 2009, a new specification (ASTM D7566) has been introduced, that allows up to 50 % synthetic jet fuel to be blended with conventional jet fuel (Kinder 2010), a land

mark that will undoubtedly have an effect on the microbial communities within jet fuel systems.

1.8 Synthesis

The aviation industry is changing. Novel construction components and alternative fuels are being introduced, providing benefits compared to their traditional counterparts. However, these changes will alter existing ecosystems present in the jet fuel supply chain and it has already been noted that community dynamics are shifting from a fungal dominated community to a bacterial one (Raikos *et al*. 2011). Though their detection is partly due to advances in molecular techniques, this would indicate that alternative fuel may have a larger impact on bacterial rather than fungal communities.

The reduction in components/compounds with documented anti-microbial effects, such as copper (alloyed in aluminium used in aircraft wing tanks) (Percival *et al*. 1999) and sulphur species (Gaylarde *et al*. 1999) is likely to allow microorganisms to proliferate more freely. Also, a) the increase in free water partitioning out of fuels due to lower density XTLs, b) additional nutrient availability from FAME (due to increasing use of non-dedicated supply) and c) increased additive usage may provide better nutrient sources (Brown *et al*. 2010).

Microorganisms preferentially breakdown straight chain paraffins over more complex aromatics, so a shift in fuel composition increasing paraffins and decreasing aromatics will make hydrocarbon degradation simpler (Brown *et al*. 2010). This compositional change will also reduce the availability of sulphur and nitrogen based terminal electron acceptors making it harder for microorganisms utilising them to compete.

Therefore we are able to hypothesise that the introduction of new components, compounds and fuels will alter the existing community dynamics and create a more favourable environment for some microorganisms to survive. For example, a recent study in the US has identified a dominance of *Acetobacter spp.* utilising ethanol and converting it into acetic acid, which is causing corrosion problems (Anon. 2012a).

1.9 Overall aims and objectives

The overall hypothesis underlying this thesis is that the introduction of novel fuels and materials into the aviation industry will lead to changes in microbial community structure and function, posing new challenges in the biodegradation of fuels, corrosion of surfaces and biofouling. Therefore a programme of work has been undertaken with the aim of exploring the microbial communities that exist in current, conventional aircraft fuel systems and investigating the impact that introducing alternative fuels and novel materials has on these communities. Both planktonic and attached (biofilm) communities are investigated with the aim of identifying biological, chemical and physical processes that underlie these changes.

Samples of contaminated fuel and water (field samples) have been characterised and both pure cultures of known fuel degraders and complex communities isolated from the fuel supply chain have been examined. Laboratory studies used microcosms, as they provided a useful system with which to explore how changes in the fuels and surfaces influenced community dynamics. Over the course of this research programme, the following areas are explored:

Chapter 2: What is the diversity of microbial contamination in existing jet fuel systems?

To date, little research has examined microbial communities in conventional civilian aviation fuel systems with the majority of studies using culture-based methods.

Hypotheses: 1) Culture-independent analysis will identify a greater diversity of organisms in aviation fuel systems than have been found by previous culture-dependent studies. 2) Introducing contaminated samples into microcosms will allow complex microbial communities to develop, suitable for further study.

Aims: 1) To characterise the microbial communities found in jet fuel systems from field samples using both culture-dependent and culture-independent methods and relate these results to operational activities and the existing literature. 2) To develop appropriate methodologies for analysing microbial communities from both the field and microcosms.

Objectives:

1. Obtain contaminated fuel and water samples from various civil aviation fuel systems.
2. Develop methodologies for extracting representative DNA samples for high-throughput sequencing from complex communities (prokaryotic and eukaryotic).

3. Use culture-independent high-throughput gene sequencing to investigate the diversity of microbial communities in jet fuel systems.

4. Develop laboratory-based microcosms for growing mixed microbial communities and examine how nutrient media affect their growth.

5. To isolate in pure-culture and characterise community members for further analysis in the laboratory.

This chapter aims to provide a deeper understanding of the diversity of microbial communities found within civil aviation fuel systems and forms the basis to understand how the introduction of alternative fuels and novel materials may impact these communities.

Chapter 3: How will novel fuels impact microbial contamination in jet fuel systems?

Hypothesis: Changing fuel type (i.e. varying the available hydrocarbon composition from ring structures to straight chains) will affect the ability of microorganisms to utilise alternative fuels as a carbon source and therefore changes in community composition will occur when alternative fuels are compared to conventional fuels.

Existing industry tests for microbial contamination use a few organisms as standards that have been identified as able to utilise jet fuel for growth.

Aims: 1) To understand how fuel types affect the growth and metabolism of industry-standard isolates and field isolates from chapter 2. 2) To examine the impact of changing fuel type on the growth and composition of complex communities.

Objectives:

1. Analyse the effect of alternative fuels on the growth of single isolates, both industry standard and field isolates, compared to conventional jet fuels.

2. Analyse the effect of alternative fuels on the growth and composition of complex communities, compared to conventional jet fuels.

This chapter aims to develop a greater understanding of how the introduction of alternative fuels will impact the microbial communities in aircraft fuel systems. This is important as changing communities may reduce the effectiveness of existing tests for microbial contamination and influence problems associated with microbial growth (e.g. increased corrosion or filter plugging) that may arise from the introduction of these fuels.

Chapter 4: How will novel surfaces impact microbial contamination in jet fuel systems?

Hypotheses: 1) Microbial communities will differ in the planktonic and sessile phases 2) Altering surface composition will influence the structure of microbial communities that attach to these surfaces.

Aims: To understand the impact of changing experimental properties on the growth and structure of complex microbial communities, by varying a) surface type (aluminium, epoxy, chromate leaching), and b) fuel type. Planktonic and sessile communities are compared.

Objectives:

1. Establish microcosms containing complex microbial communities
2. Examine how altering surface composition influences these communities
3. Examine how the planktonic and sessile communities differ in these systems

Ultimately this chapter will provide a greater understanding of how the introduction of novel surface materials will impact the microbial communities in jet fuel systems.

The results from these experiments are synthesised to develop an understanding of the factors that control microbial diversity and abundance in different stages of the fuel supply chain and how these will alter as a consequence of the increased use of alternative fuels and novel materials. In the longer term, the knowledge gained in this study may be used to develop management strategies aimed at limiting the problems associated with microbial growth and investigate novel (non-biocide) management/mitigation strategies.

Chapter Two

What is the diversity of microbial contamination in jet fuel systems?

2.1 Introduction

One hundred and twenty years ago, Miyoshi (1895) documented the first case of microbial growth on n-alkanes. Since then microbial contamination has become a widespread problem in the petrochemical industry, estimated to cost billions of dollars a year (Balster *et al*. 2006; Raikos *et al*. 2011). Temperature fluctuations cause dissolved water to separate from the bulk fuel creating surface-fuel-water interfaces. Microorganisms grow at these interfaces, utilising the fuel as a carbon source by secreting emulsifiers, such as rhamnolipids, to increase hydrocarbon solubility. Microorganisms also secrete biosurfactants, creating a suspension of microdroplets within the fuel. In 2014, Meckenstock *et al*. found that microorganisms grow within these suspended microdroplets, creating another previously undocumented interface. These systems provide not only an excellent carbon source, but also contain essential trace nutrients (typically from additives), such as nitrogen and phosphorus, creating an ideal environment for microbial growth (Ruiz *et al*. 2015).

In jet fuel systems microbial contamination is particularly problematic and results in three main issues: a) microbiologically influenced corrosion (MIC) (Little & Lee 2013), b) microbial fouling (Hill & Hill 2008) and c) microbial spoilage (Smith 1988). Issues associated with microbial fouling are due predominantly to the formation of biofilms on system surfaces, resulting in filter plugging and inaccurate tank gauge readings (Passman 2013; Williams & Lugg 1980). Such microbial problems have been directly attributed to causing aircraft disasters since the 1950s (Rauch *et al*. 2006; Yemashova *et al*. 2007; Zabarnick *et al*. 2011).

Historically, these incidences have piqued the interest of the USAF, which has undertaken the majority of the research profiling microbial communities in jet fuel systems. In 2005, Denaro *et al*. used both culture-dependent and culture-independent[25] analyses to identify 36 operational taxonomic units (OTUs). Rauch *et al.* (2006) reviewed the literature (from 1958 onwards), citing 37 previously discovered microbial taxa (21 prokaryotes, 16 eukaryotes) and identified 5 new species. Brown *et al.* extended this work in 2010, obtaining 16S rRNA gene sequences from contaminated water samples by direct PCR and cloning them. Sequences from the clone libraries were compared against the Ribosomal Database Project (RDP) database, identifying 803 sequences in the JP-8[26] sample set. However, taxonomic

[25] This was achieved by directly amplifying the contaminated water using PCR, and ligating the PCR amplicons in a vector, amplifying them in clones and sequencing the 16S and 18S rRNA.
[26] JP-8 is a military grade jet fuel with similar bulk properties to Jet A and Jet A-1. However additive packages vary considerably from commercial jet fuel.

diversity was not assigned and these sequences were not unique, with the two most abundant microorganisms accounting for ~12 % of the sequences.

Other studies (Dolan 2002; Ferrari *et al*. 1998; McNamara *et al*. 2005; Swift 1988) used only culture-dependent methods with associated limitations; significantly that many environmental microorganisms are likely to be uncultivable. Bias was therefore introduced into these data sets by underestimating the true diversity of the microbial community (Amann *et al*. 1995; Brock 1987; Brown *et al*. 2010; Staley 1985).

To enumerate microorganisms in the fuel phase where microbial densities are typically low, another common practice is to incubate the fuel over a nutrient-rich mineral medium, (typically Bushnell-Haas medium), in place of the environmental water found in tanks. This creates an artificially eutrophic system, ensuring that microorganisms within these systems have no growth limitations beyond their ability to utilise the fuel as a carbon source. However, this also introduces biases, selecting for microorganisms that grow best at high nutrient levels. To the author's knowledge, no studies have been undertaken on the effect of Bushnell-Haas mineral medium on microbial communities found within jet fuel systems.

The aim of this study is to use culture-independent analyses to characterise microbial communities typically found in jet fuel systems. Specific genes (16S rRNA and Internal Transcribed Spacer (ITS)) were amplified using PCR to identify prokaryotic and eukaryotic microorganisms from microbial communities sampled from 11 different sites across Europe and the Middle East, as well as providing information on the relative abundance of these taxa. Members of these communities have also been examined using culture-dependent methods and comparisons made between the two techniques. Additionally, communities have been used as inocula in a series of microcosm-based experiments to understand the impact of using microcosms and nutrient-rich mineral media on species diversity. This study expands our knowledge of microbial community dynamics in jet fuel systems and challenges the *status quo* on how to best analyse these communities.

2.1.1 Chapter aims and objectives

The aim of this chapter is to characterise the microbial communities present within typical aircraft distribution supply chains by employing culture-dependent and culture-independent techniques. Samples were taken from a variety of geographical locations, from both aircraft and ground storage tanks.

The objectives of this chapter are:

a) To culture and isolate representative microorganisms (both prokaryotes and eukaryotes) for future studies;
b) To understand the diversity of microbial communities in jet fuel systems and identify the dominant microorganisms;
c) To compare field samples with a variety of microcosm treatments, such as the use of nutrient media, to understand the effect microcosms have on microbial populations;
d) To compare field samples taken from different environments (aircraft vs. terrestrial storage tanks) to understand the differences in these communities.
e) Relate this information to the source material, to further understand how the use of culture-dependent analyses and high-nutrient environments have influenced the understanding of microbial communities within jet fuel systems.

2.2 Materials and methods

2.2.1 Sampling

Thirty three commercial jet fuel samples, 30 conventional (from 10 different European airports and refineries) and 3 alternative (2 European and 1 from the Middle East; synthetic kerosene) (see Figure 2.6 for countries of origin) were taken from aircraft wing tanks, ground storage tanks and hydrant systems. These environmental fuel/water field samples were collected into 1L sterile, high-density polyethylene (HDPE) bottles. They were packaged and shipped (at ambient temperature) to the University of Sheffield for microbial contamination analyses. Samples were usually received into the laboratory within 3 days of collection and processed for both DNA extraction and/or used as an inoculum for microcosms within 48 hours of arrival. Where samples contained an aqueous phase, 10 ml of sample was withdrawn using a 4-inch disposable sterile needle and 10 ml syringe and passed through a sterile 0.22 µm nitrocellulose syringe filter (Merck Millipore, USA) to capture any organisms present. Filters were then frozen at -20 °C prior to DNA extraction.

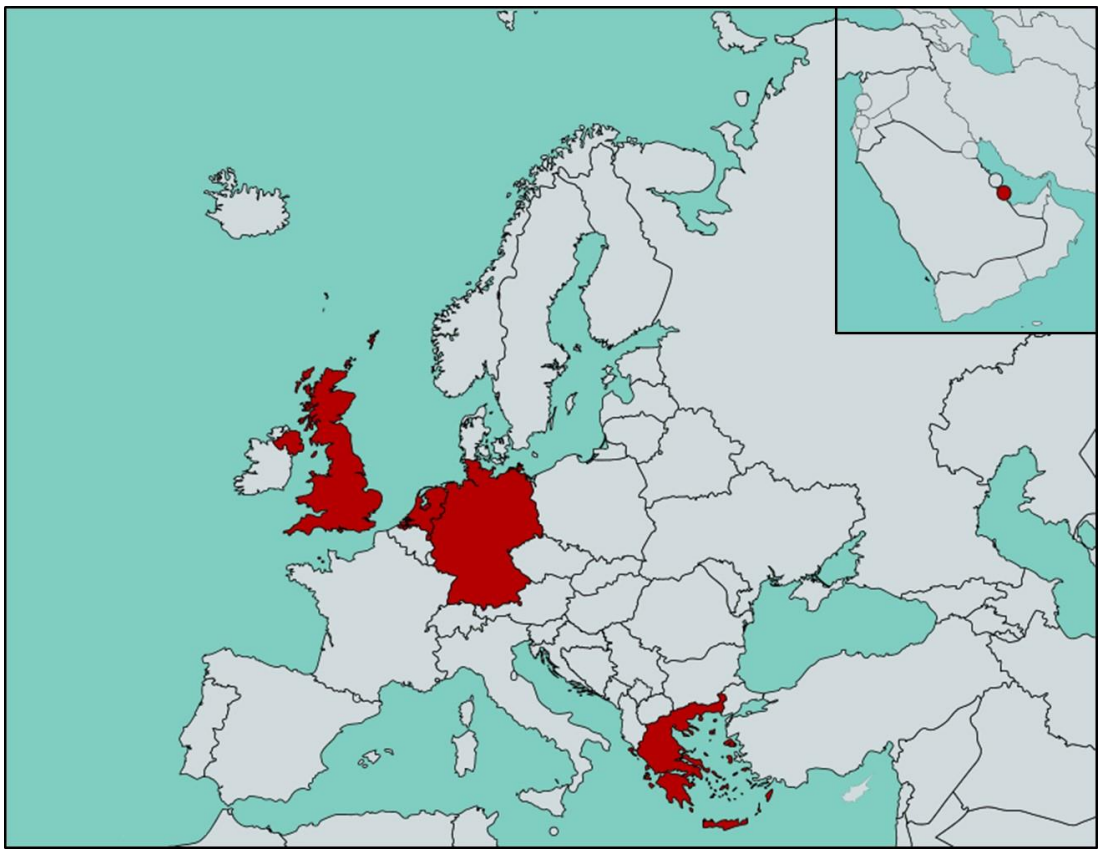

Figure 2.6 – Sample location map. Countries where samples were taken are highlighted in red (Giannekas 2016).

2.2.2 Microcosm set-up

Microcosms were set up in two ways, using either contaminated water or contaminated jet fuel taken from the field samples. Where contaminated water was present, 1 ml was used as an inoculum in microcosms containing 100 ml of Merox-treated Jet A-1 and 100 ml of Bushnell-Haas nutrient medium (Sigma-Aldrich, UK). For samples of jet fuel, 100 ml was overlaid over either 100 ml Bushnell-Haas nutrient medium or 100 ml of distilled water. Both types of microcosm were set up in 500 ml Duran® bottles (Fisher Scientific, UK). Prior to the addition of fuel, systems were sterilised using a Prestige Medical bench top autoclave (Prestige Medical, UK). Merox-treated Jet A-1 was sterilised by passing the fuel through a 0.22 µm nitrocellulose filter paper (Merck Millipore, USA). Microcosms were then left to incubate for 90 days at 25 °C in a water bath (Grant Instruments, UK) and subsequently used in culture-independent microbial community analysis (see Appendix B).

2.2.3 Culture-dependent analysis

2.2.3.1 Isolation of biofilm forming microorganisms

One millilitre of contaminated water was removed from the field samples into a 1.5 ml Eppendorf tube, using a 4-inch sterile needle and 1 ml sterile syringe. Ten microlitre aliquots were then pipetted onto both a Tryptone-Soya (TSA)[27] agar plate and a Malt extract (MEA)[28] (Anon. 2005) agar plate, spread out and incubated for up to 5 days at 25 °C. Samples were checked daily and individual colonies picked using a sterile 10 µl loop, streaked onto fresh agar plates and allowed to grow for a further 3 days at 25 °C. Once individual colonies were visible, their morphologies were recorded and then, using a sterile tooth pick, used to inoculate a 5 ml liquid broth of either TSB or MEB, corresponding to their parent plate. The liquid cultures were placed in an IKA Vibrax VXR basic shaker (IKA Works GmbH & Co. KG, USA), at ~1000 rpm and incubated at 25 °C for up to 5 days, until turbid. After the incubation period, 700 µl of the liquid culture was mixed with 300 µl of 50 % (v/v) sterile glycerol in a 2 ml sterile cryogenic vial (Greiner bio-one, Germany), mixed using a Top Mix FB15024 vortex mixer (Fisher Scientific, UK) for 5 seconds and stored at -80 °C, as glycerol stocks. An aliquot of the remaining liquid culture (1.8 ml) was pipetted into a sterile 2 ml collection tube and centrifuged at 10,000 x *g* for 30 seconds, using an Eppendorf 5417C microcentrifuge (Eppendorf AG, Germany). The supernatant was then removed and the bacterial pellet suspended in 1 ml of a sterile 0.15 M sodium chloride solution and mixed in a vortex mixer

[27] 15 g/L Tryptone, 5 g/L Soya Peptone, 5 g/L Sodium Chloride and 15 g/L Agar, pH 7.3 ± 0.3
[28] 30 g/L Malt Extract, 5 g/L Mycological Peptone and 15 g/L Agar, pH 5.4 ± 0.2

for 5 seconds. The pellets were again centrifuged at 10,000 x *g* for 30 seconds, the supernatant removed and the bacterial pellets stored at -20 °C prior to DNA extraction.

2.2.3.2 DNA extraction and quantification from isolated prokaryotic microorganisms

One hundred and fifty microliters of sorbitol buffer[29], was added to the tube containing the bacterial pellets, along with 3 x 3 mm sterile tungsten beads. Microorganisms were then ground in a SPEX Centriprep 8000M Mixer/Mill (Glen Creston, UK) for 5 minutes. Fifty units of lyticase (Sigma-Aldrich, UK) were then added and the samples incubated at 30 °C for 30 minutes in a water bath. DNA extractions were performed using an UltraClean® Microbial DNA Isolation kit (MO BIO Laboratories, USA), according to the manufacturer's instructions[30].

2.2.3.3 PCR amplification and purification of 5.8S and 16S rRNA genes

One microliter of isolated DNA was used as a template in 50 µl PCR[31] reactions. The reactions contained 2.5 U *Taq* DNA polymerase, 1x ammonium reaction buffer, 2.5 mM magnesium chloride, 0.2 µM of each dNTP (dATP, dCTP, dGTP and dTTP), 0.2 µM of either 799F (5'-AACMGGATTAGATACCCKG-3') (Chelius & Triplett 2001) and 1193R (5'-ACGTCATCCCCACCTTCC-3') primers (Bodenhausen *et al*. 2013) (16S rRNA gene; prokaryotes), or ITS3 (5'-GCATCGATGAAGAACGCAGC-3') and ITS4 (5'-TCCTCCGCTTATTGATATGC-3') (White *et al*. 1990) (ITS and 5.8S rRNA gene; eukaryotes) and the remaining volume made up with nuclease-free water. A 'no template' control (nuclease-free water) was also included with every batch of PCR reactions prepared. PCR amplification used the following conditions: 94°C for 5 minute initial denaturation; 30 cycles of denaturing at 94 °C for 30 seconds, annealing at 58 °C for 30 seconds and elongating at 72 °C for 30 seconds; and a final elongation of 72 °C for 5 minutes. Product size was then checked by gel electrophoresis in a 1 % (w/v) agarose gel and 0.001 % of a 10 mg/ml ethidium bromide solution (Sigma-Aldrich, UK). Products were electrophoresed for 45 minutes and the voltage varied depending on the size of the gel. This was done by increasing the voltage by 6 V per centimeter of the gel i.e. a 10 cm gel would have 60 V applied to it, compared to a 20 cm which would have 120 V applied to it. The amplicons were compared with Hyperladder I (Bioline, UK). Amplicons of the correct size were purified using a QIAquick® PCR purification

[29] 1 M Sorbitol, 500 mM EDTA (pH 8), 10 mM 2-mercaptoethanol.

[30] It was necessary to modify the lysis stage of manufacturer's instructions, with a more aggressive mechanical lysis of the cells as well as a pre-treating with lyticase. Without these steps inconsistent DNA yields were obtained from stock centre isolates, representative of a range of microorganisms found in jet fuel systems. The ability to extract DNA representatively is critical to the use of next generation sequencing for characterising microbial communities, as unrepresentative extraction will introduce biases into the dataset.

[31] All PCR components were supplied by Bioline (Bioline Reagents Ltd., UK) and the primers by Invitrogen (Life Technologies Corporation, UK).

kit (QIAGENE, Netherlands), as per the manufacturer's instruction, eluted in a 10 mM Tris-HCl (pH 8.5) buffer (EB buffer) and checked again by gel electrophoresis, as above. Products were stored at -20 °C.

2.2.3.4 Transformation and cloning of PCR amplicons into DH5-α competent cells

Ligation reactions[32] were set up using 25 ng of the purified PCR amplicons, 5 µl of ligation buffer, 1 µl of pGEM®-T Easy Vector, 1 µl of DNA ligase and made up to 10 µl using nuclease-free water. A positive control and negative control (nuclease-free water) were also prepared for each set of ligation reactions. Samples were incubated overnight at 4 °C.

After incubation, 2 µl of the ligation reaction was mixed with 50 µl of DH5-α competent cells (Invitrogen, USA) in a 1.5 ml microcentrifuge tube. pUC19 vector was used as a control. Samples were incubated on ice for 20 minutes, heat shocked at 42 °C for 45 to 50 seconds in a water bath and then incubated on ice for 2 minutes. Nine hundred and fifty microliters of pre-warmed (37 °C) Luria Bertani (LB) broth[33], containing 100 µg/L Ampicillin (amp^{100}) was added to the competent cells, mixed gently, placed in a shaker at 150 rpm and incubated at 37 °C for 1.5 hours. Two hundred microliters of the liquid cultures were then pipetted onto duplicate LB amp^{100} agar plates[34], spread out and allowed to dry. Once dry, the cultures were incubated for 20 hours at 37 °C.

Six individual white colonies were picked (where possible 3 from each plate), using a sterile 10 µl loop, streaked onto fresh LB amp^{100} agar plates and incubated for 20 hours at 37 °C. An individual colony from each plate was picked, (using a sterile tooth pick) and used to inoculate a 5 ml LB broth. The liquid cultures were then placed in a shaker, at 1000 rpm and incubated at 37 °C for 20 hours until turbid. Glycerol stocks were prepared (as above). An aliquot of the remaining liquid culture (1.8 ml) was pipetted into a sterile 2 ml collection tube and centrifuged at 6,800 x *g* for 3 minutes. The supernatant was then removed and the bacterial pellet suspended in 1 ml 0.15 M NaCl. The pellets were again centrifuged at 6,800 x *g* for 3 minutes, the supernatant removed and the bacterial pellets stored at -20 °C.

[32] All ligation reaction components were supplied by Promega (Promega Corporation, USA) and the DH5-α competent cell by Invitrogen (Life Technologies Corporation, UK).
[33] 10 g/L Tryptone, 5 g/L Yeast extract and 5 g/L sodium chloride.
[34] These plates had 70 µl of a (50 µl) Dimethylformamide (DMF): (20 µl) 5-bromo-4-chloro-3-indolyl-β-D-galactopyranoside (X-Gal) solution spread on top.

2.2.3.5 Extraction of isolated plasmid DNA

Plasmid DNA was extracted using a QIAquick® Miniprep kit (QIAGENE, Netherlands), as per the manufacturer's instruction, eluted in a 10 mM Tris-HCl (pH 8.5) buffer (EB buffer). Products were then stored at -20 °C before sequencing or digestion.

2.2.3.6 Restriction enzyme digestion of isolated plasmid DNA

Two microliters of isolated plasmid DNA was used as a template for two separate restriction enzyme digests (per sample). The DNA was added directly to a mixture containing 0.5 µl either EcoR1 or Rsa1[35], 1.5 µl of the appropriate restriction buffer, 0.15 µl acetylated BSA and 10.85 µl of nuclease-free water. The mixture was incubated at 37 °C for 60 minutes and the digests checked by electrophoresis.

2.2.3.7 Sequencing of isolated microorganisms

Three hundred and five samples of isolated plasmid DNA were sent to the Core Genomics Facility (University of Sheffield, UK) for sequencing, using an Applied Biosystems 3730 DNA analyser (Life Technologies Corporation, UK). These represented a range of colonies isolated from different field samples in Section 2.2.3.1. Isolated plasmid DNA was sequenced using the T7 forward promoter primer (5'-TAATACGACTCACTATAG-3'). Once sequencing was completed, raw data was analysed using Chromas Lite (Technelysium Pty Ltd., Australia), converted into .FASTA file format and uploaded to Ribosomal Database Project (RDP) (Michigan State University, USA) for prokaryotes and the Internal Transcribed Spacer 2 Ribosomal RNA Database (ITS 2) (University of Wurzburg, Germany) for eukaryotes and the closest matching organism identified. A species name was only given if ≥99% sequence identity was achieved.

[35] All restriction enzyme components were supplied by New England Biolabs (New England Biolabs® Inc., UK).

2.2.4 Culture-independent analysis and metagenomics

2.2.4.1 Quantitative real time PCR (qPCR)

2.2.4.1.1 Production of standards

Pseudomonas putida (ATCC 700007) and *Candida tropicalis* (ATCC 48138) were grown on Luria-Bertani[36] (LB) agar and yeast-malt[37] (YM) agar respectively, for 24 hours at 25 °C. Once single colonies were observed, duplicate colonies were picked from each plate, (with a sterile tooth pick) and used to inoculate a 5 ml liquid broth; either LB broth or YM broth respectively. Liquid cultures were then placed in a shaker and incubated for 24 hours at 25 °C. An aliquot (1.8 ml) of each liquid culture was then transferred to a 2 ml sterile microcentrifuge tube and the DNA extracted using an UltraClean® Microbial DNA Isolation kit (MO BIO Laboratories, USA) following the manufacturer's instructions.

The extracted DNA was quantified using Quant-iT™ PicoGreen® dsDNA reagent (Molecular Probes, Inc., USA). A standard curve (0 to 200 ng/µl) was prepared by dilution of the 100 µg/ml λ DNA standard provided with the kit. TE buffer (10 mM Tris-HCl, 1 mM EDTA, pH 7.5) was filtered through a 0.2 µm polyethersulfone syringe filter (Sartorious Stedim Biotech, France) to remove particulates. A 200-fold dilution of PicoGreen was prepared in the TE buffer. Samples and standards were aliquoted into a black 96 well microplate (Sterilin Ltd., UK); each well contained 98 µl of the TE buffer, 100 µl of the PicoGreen working solution and 2 µl of DNA. Samples were incubated for 5 minutes in the dark at ambient temperature before measuring the fluorescence (excitation at 485 nm, emission at 545 nm) with a FluoStar Optima spectrophotometer (BMG Labtech, USA). The concentration of the extracted DNA was determined by comparison with the standard (see Figure 2.7) (Andrews *et al*. 2010).

[36] 10 g/L Tryptone, 5 g/L Yeast extract, 5 g/L Sodium chloride, 15 g/L Agar.
[37] 3 g/L Yeast extract, 3 g/L Malt extract, 5 g/L Mycological peptone, 10 g/L Dextrose, 15 g/L Agar.

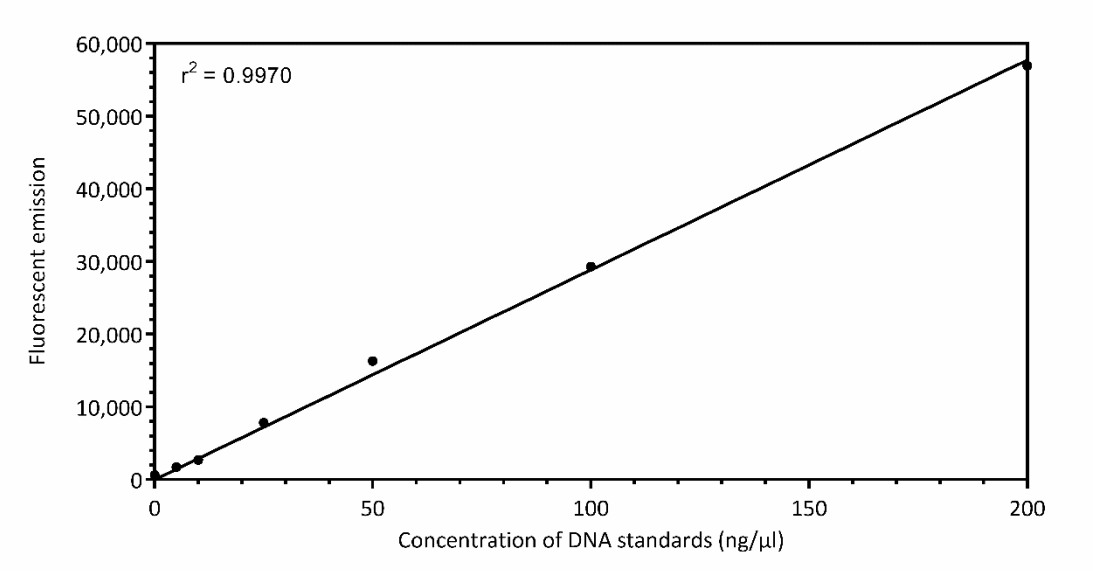

Figure 2.7 – Standard curve produced from the fluorescent emission of DNA standards.

Escherichia coli standards were produced from the DNA sodium salt (Sigma-Aldrich, UK). The DNA (0.25 U[38]) was suspended in 200 µl TE buffer (10 mM Tris-HCl, 1 mM EDTA, pH 7.5) and quantified in a Lambda 40 UV/Vis spectrophotometer (Perkin Elmer Instruments, USA)[39]. A serial dilution was performed to produce standards ranging from 0 to 50 ng/µl.

2.2.4.1.2 Quantitative PCR

Quantitative PCR (qPCR) was performed in two stages. Initial analysis was performed using the *P. putida* and *C. tropicalis* DNA standards. Standards containing 50, 25, 12.5, 5, 2.5 and 0 ng/µl of DNA from both organisms were analysed, as well as mixed samples containing 25:25, 2.5:2.5, 25:1.25 and 1.25:25 ng/µl DNA (*P. putida* : *C. tropicalis*). Subsequent analysis used the *E. coli* (50, 25, 10, 5 and 0 ng/µl) and *C. tropicalis* (50, 25, 12.5, 5, 0 ng/µl) standards as well as DNA extracted from the field samples. Reactions contained 5 µl SYBR Green PCR kit master mix[40] (QIAGEN, Netherlands), 1 µl of 2.5 µM of each 799F (5'-AACMGGATTAGATACCCKG-3') (Chelius & Triplett 2001) and 1193R (5'-ACGTCATCCCCACCTTCC-3') (Bodenhausen *et al*. 2013) or ITS3 (5'-GCATCGATGAAGAACGCAGC-3') and ITS4 (5'-TCCTCCGCTTATTGATATGC-3') primers (White *et al*. 1990), 2 µl of the target DNA and the volume made up to 10 µl with nuclease-free

[38] One unit of DNA is equivalent to an absorbance of 1.0 at 260 nm in 1 ml of 1 mM Tris-HCl (pH 7.5), with 1mM NaCl and 1 mM EDTA.

[39] Concentration = (A_{260} – A_{320}) x dilution factor x 50, where A_{260} is the absorbance at 260 nm, A_{320} is the absorbance at 320 nm and 50 µg/ml is the quantity of pure dsDNA at an A_{260} of 1.0 (A_{260} of 1.0 = 50 µg/ml).

[40] SYBR Green PCR kit master mix contains HotStartTaq *Plus* DNA Polymerase, Rotor-Gene SYBR Green PCR Buffer and SYBR Green I dye (Anon. 2016b).

water. Standards were prepared in triplicate. For the first experiment, both primer sets were used on all of the samples to check for cross amplification. On subsequent runs, the *E. coli* DNA standards and the field samples were amplified with 799F and 1193R and the *C. tropicalis* DNA standards and the field samples were amplified with ITS3 and ITS4. A negative control (nuclease-free water) was performed in each experiment. PCR amplifications were performed with a Rotor-Gene Q (QIAGENE, Netherlands) real-time PCR cycler according to manufacturer's instructions. Amplification conditions were: 95 °C for 5 minute initial denaturation; 45 cycles of denaturing at 95 °C for 30 seconds, annealing at 58 °C for 30 seconds and elongating at 60 °C for 30 seconds. Values were multiplied by 5000 to give the amount of DNA per litre of sample received and then corrected to give *P. putida* or *C. tropicalis* genome equivalents. Genome sizes were obtained from GenBank and were 5.96 Mbp and 14.46 Mbp respectively. The *P. putida* genome contains 7 copies of the 16S rRNA gene and the *C. tropicalis* genome contains 3 ITS regions hence values reported as genome equivalents can be converted into amplicon equivalents by multiplication by these values.

2.2.4.2 Illumina sequencing

2.2.4.2.1 DNA extraction and quantification from microbial communities

Ten ml of the aqueous phase was withdrawn from the microcosms using a 4-inch disposable sterile needle and 10 ml syringe and passed through a sterile 0.22 µm nitrocellulose syringe filter (Merck Millipore, USA) to capture any organisms present. Filters were then frozen at -20 °C prior to DNA extraction. Filters from both the field samples (see Section 2.2.1) and the microcosms were introduced into a 1.5 ml microcentrifuge tube and the DNA extracted as outlined in Section 2.2.3.2.

2.2.4.2.2 Amplification PCR

Two microliters of isolated DNA were used as a template in 20 µl PCR reactions. The reactions contained 0.4 units KAPA HiFi HotStart DNA Polymerase, 4 µl of 5x KAPA HiFi Fidelity buffer, 25 mM $MgCl_2$, 10 µM of each dNTP (dATP, dCTP, dGTP and dTTP), 10 µM of either 799F (5'-AACMGGATTAGATACCCKG-3') (Chelius & Triplett 2001) and 1193R (5'-ACGTCATCCCCACCTTCC-3') primers (Bodenhausen *et al*. 2013) (16S rRNA gene; prokaryotes), or ITS3 (5'-GCATCGATGAAGAACGCAGC-3') and ITS4 (5'-TCCTCCGCTTATTGATATGC-3') (White *et al*. 1990) (ITS and 5.8S rRNA gene; eukaryotes) and with overhang adapters attached. The remaining volume was made up with nuclease-free water and each reaction ran in triplicate. A negative control (nuclease-free water) was also added to every PCR mix prepared. The PCR amplification was performed on a Life-ECO thermal cycler (Bioer Technology Co., China) with the following conditions: 95 °C for 3 minute

initial denaturation; 25 cycles of denaturing at 95 °C for 30 seconds, annealing at 58 °C for 30 seconds and elongating at 72 °C for 30 seconds; and a final elongation of 72 °C for 5 minutes. Products were checked by electrophoresis on a 1 % agarose gel.

2.2.4.2.3 PCR cleanup (AMPure XP beads)

PCR products were purified using AMPure XP beads (Beckman Coulter Inc., USA). Triplicate PCR reactions were pooled and 25 µl of the pooled sample transferred into a 96-well reaction plate. AMPure XP beads were mixed and 20 µl added to each reaction[41]. Samples were incubated at room temperature for 5 minutes and then for a further 2 minutes on an Agencourt SPRI Super Magnet Plate (Beckman Coulter Inc., USA). The beads were washed twice with 200 µl of freshly prepared 80 % (v/v) ethanol solution and allowed to air dry for 15 minutes. The beads were then suspended in 60 µl of 10 mM Tris (pH 8.5) buffer and incubated at room temperature for 2 minutes. Samples were then placed on the Magnet Plate and incubated until the supernatant had cleared. Fifty microliters of the supernatant were transferred to a 96-well reaction plate and stored at -20 °C.

2.2.4.2.4 Indexing PCR

Five microliters of isolated DNA solution were used as a template in 50 µl PCR reactions. The reactions contained 1 unit KAPA HiFi HotStart DNA Polymerase, 10 µl of 5x KAPA HiFi Fidelity buffer, 25 mM $MgCl_2$, 10 µM of each dNTP (dATP, dCTP, dGTP and dTTP), 5 µl Nextera XT Index Kit indices and sequencing adapters (set D) (Illumina Inc., USA). The remaining volume was made up with nuclease-free water. A negative control (nuclease-free water) was also prepared for every set of PCR reactions. PCR amplification was performed as follows: 95°C for 3 minute initial denaturation; 12 cycles of denaturing at 95 °C for 30 seconds, annealing at 58 °C for 30 seconds and elongating at 72 °C for 30 seconds; and a final elongation of 72 °C for 5 minutes. Product size was then checked by gel electrophoresis in a 1 % agarose gel. The indexed PCR amplicons were purified using AMPure XP beads and then quantified using PicoGreen fluorescence, as previously described (see Section 2.2.4.1.1).

2.2.4.2.5 Sequencing on mixed communities

Indexed PCR amplicons were pooled to produce a single library with a final concentration of 15 nM, which was confirmed using PicoGreen quantification. Samples were pooled by concentration (nM) to obtain the correct number of reads per sample in the final pooled library. Molar concentrations were used to account for different amplicon lengths. The

[41] The ratio of sample to beads is of critical importance in ensuring primer removal and amplicon retention.

amplicon size for primers 799F and 1193R is 415 bp and the mean amplicon size for primers ITS3 and ITS4 is 374.5 bp (adapters are 33 and 34 bp respectively and must also be added to the amplicon length, along with the primer sequence). The concentration of the samples was calculated to yield a sequencing depth of 100,000 reads for each prokaryotic sample and 10,000 reads for each eukaryotic sample and was based on their individual starting concentrations, which was confirmed by PicoGreen quantification. The combined sample was sequenced at The Genome Analysis Centre in Norwich (TGAC) using an Illumina MiSeq sequencer, using a MiSeq Reagent Kit v2 (500 cycles) (Illumina Inc., USA).

2.2.4.2.6 Bioinformatics analysis

Demultiplexed sequence data was received from TGAC in five files; unpaired reads from the forward and reverse primers, paired reads from the forward and reverse primers and unpaired reads containing a mixture of both forward and reverse primers that did not match the other four data sets. The quality score of the data was checked using FastQC (Babraham Bioinformatics) and samples selected that had a quality score of >Q20[42] score above a read length of approximately 200 bp. Pair read data was selected and processed using a QIIME pipeline (Caporaso *et al*. 2010a).

Each data file was filtered with USEARCH8.1 (Edgar 2010) and the paired .FASTQ files merged and converted to .FASTA file format, with a minimum read length of 350 bp for prokaryotes and 300 bp for eukaryotes. A mapping file was used to add QIIME labels to the .FASTA data files and the data combined into one file. Primers were removed from both ends of the sequences (18 bp for the prokaryotic primers and 22 bp for the eukaryotic primers). Index sequences had already been removed by TGAC during demultiplexing.

Chimaeras were then removed using a combination of *de novo* (abundance based) checks and by comparison with a reference database a) RDP gold database (Wang *et al*. 2007) for prokaryotes or b) its_12_11_otus, provided by the UNITE database (Abarenkov *et al*. 2010) for eukaryotes. A parameter file was created and OTUs were assigned to the sequences at two levels of sequence identity (97% and 99%), against both the Greengenes (DeSantis *et al*. 2006; Caporaso *et al*. 2010b; McDonald *et al*. 2012; Werner *et al*. 2012) and Silva databases (Quast *et al*. 2013), for prokaryotes and at 97% sequence identity against the UNITE database for eukaryotes. Data was then rarefied, so that both rarefied and unrarefied data sets could

[42] Q30 is 1 in 1000 base pair errors, Q20 is 1 in 100 base pair errors and Q10 is 1 in 10 base pair errors.

be used in downstream analysis (Lozupone & Knight 2005; Vázquez-Baeza *et al*. 2013). Processing scripts are in Appendix C.

2.2.4.2.7 Data quality checks

The DNA samples were analysed by sequencing 16S rRNA genes (prokaryotes) and ITS and 5.8S rRNA genes (eukaryotes). DNA sequence data was provided by TGAC in 5 files; sequences that matches both forward and reverse primers (both paired and unpaired) and any remaining sequence data that did not match either of the primer sets, which was a mixture of forward and reverse reads. Both forward and reverse reads (paired and unpaired) were analysed with FastQC (Babraham Bioinformatics) to check the data quality. The forward paired data had Q values of Q20 or greater at read lengths of 200 bp and above, with the eukaryotic reads overall having lower Q values than the prokaryotes. Read length quality decreased in the reverse paired reads - however sufficient overlap was present between the forward and reverse sequences in the prokaryotic data set to use paired-end reads, extending the length of the 16S rRNA sequence used for comparison. For the eukaryotic data set, the forward paired and unpaired reads were combined into one dataset and the reads truncated to 200 bp (see Figure 2.8 and Figure 2.9). (Although some samples could be paired, this introduced biases into the dataset, favouring shorter sequences. Therefore, only forward reads were analysed).

Each data file was filtered with USEARCH8.1 (Edgar 2010). For prokaryotic sequences the read depth ranged between 978 and 943,065 reads per sample with an average of 109,213 reads per sample. Sequences from the forward primer (799F) passed quality filtering at a rate ranging from 47.4 to 88.3 % per sample with an average of 82.1 % (maxEE[43] value of 1.00) for the 250 bp read lengths. Sequences from the reverse primer (1193R) were of lower quality. The pass rate ranged from 17.5 to 77.5 % with an average of 61.6 % (maxEE value of 1.00; 250 bp reads). However, the proportion of sequences passing the criteria increased to an average of 74.0 % when the accepted read length was reduced to 200 bp (maxEE value of 1.00; range 24.9 to 91.7 %). Two samples failed to sequence correctly and were omitted.

Of the 41 samples that contained eukaryotic DNA, the sequence read depth ranged from 9,387 to 80,578 reads per sample with an average of 38,801. Sequences from the forward primer (ITS 3) had a pass rate between 1.9 and 87.5 % with an average of 42.0 % (maxEE value of 1.00) for the 250 bp reads. This indicates that the quality of the 250 bp read lengths was variable. A similar trend in sequence quality was observed with the reverse primer (ITS

[43] A maxEE of 1.00 represents a 1 base pair error per 1000 base pairs.

4) which had a pass rate between 17.8 to 71.8 % per sample with an average 47.2 % (maxEE value of 1.00) for the 250 bp reads. However, the number of reads meeting the criteria increased considerably when the acceptable read length was dropped to 200 bp, averaging 69.1 % for the forward primer (maxEE value of 1.00; range 26.4 to 93.7 %) and 76.1 % for the reverse primer (maxEE value of 1.00; range 62.2 to 84.0 %). Six samples failed to sequence correctly and were not analysed further.

Chimeric sequences were removed using a combination of *de novo* and reference based methods, using the RDP Gold database (Wang *et al*. 2007) for prokaryotes and the UNITE database for eukaryotes (Abarenkov *et al*. 2010). Chimeric sequences were removed from the prokaryotic (169,658) and eukaryotic (6,718) datasets, leaving 6,045,258 and 952,452 sequences respectively. The remaining sequences were then rarefied (prokaryotes to 20,000 reads per sample and eukaryotes to 5,000 reads per sample), the taxonomic ranks assigned, using the Greengenes and Silva databases for prokaryotes and UNITE databases for eukaryotes, and the coverage checked by comparing the number of observed OTUs against the Chao1 index (see Appendix D).

2.2.4.2.8 Statistical analysis

Further analysis was performed in R using the phyloseq package (McMurdie & Holmes 2013). Biom tables (OTU counts and associated taxonomy tables), mapping files (linking sample files to conditions) and representative .FASTA sequence files produced in QIIME were read into phyloseq. For prokaryotic (16S rRNA) sequences, a phylogenetic tree was also included. Samples were filtered for read depth (minimum of 20,000 reads per sample for prokaryotes, 5,000 for eukaryotes) and normalized to 100 (%) relative abundance for ordination analyses. Dominant OTUs were classified as those with a relative abundance greater than 1 % (unless otherwise stated) in any sample. Ordinations were performed using the phylogenetically aware Unifrac distance measure for prokaryotic sequences, weighted for relative abundance (Lozupone *et al*. 2011). For eukaryotes, a Bray-Curtis measure was used, again weighted for relative abundance. A statistical analysis of differences between samples was performed using the R package mvabund (Wang *et al*. 2012). Generalised Linear Models for Multivariate Abundance were fitted to the normalised data (with 999 bootstrap iterations) assuming a negative binomial distribution of OTU abundance. A Likelihood-Ratio-Test was calculated for each comparison and used to derive a *p* value, adjusted for false discovery. OTUs whose relative abundance differed between samples were identified using DESEQ2 (Love *et al*. 2014), again assuming a negative binomial distribution of OTU abundance, with correction

for false discovery using the Benjamini-Hochberg method. DESEQ2 uses unnormalised sequence counts rather than normalised counts, so these data were supplied to the program.

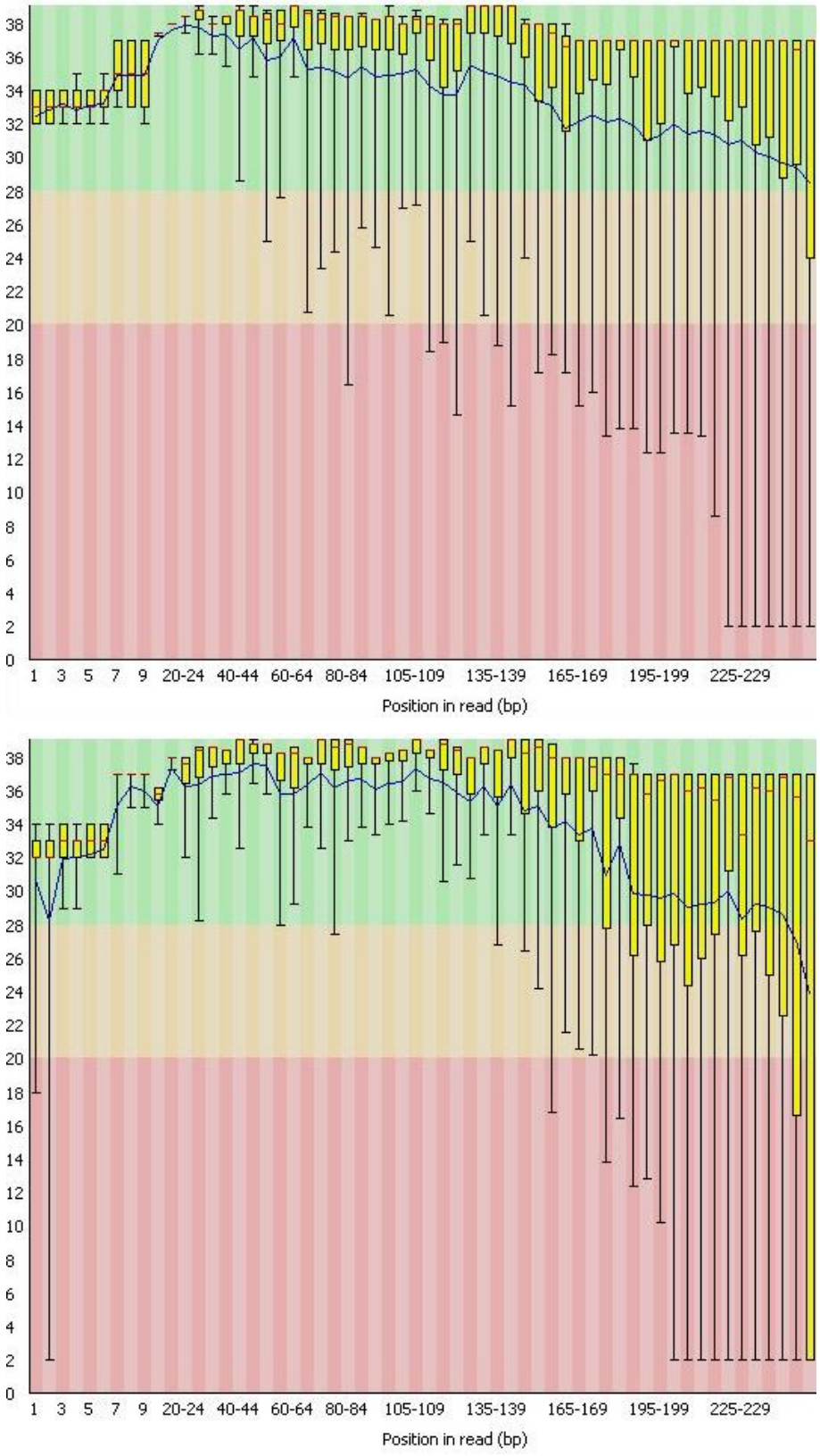

Figure 2.8 – An example quality report from a single prokaryotic sample showing the quality scores (Q value) across all 250 bases of the forward (top) and reverse (bottom) paired primer (FastQC, Babraham Bioinformatics).

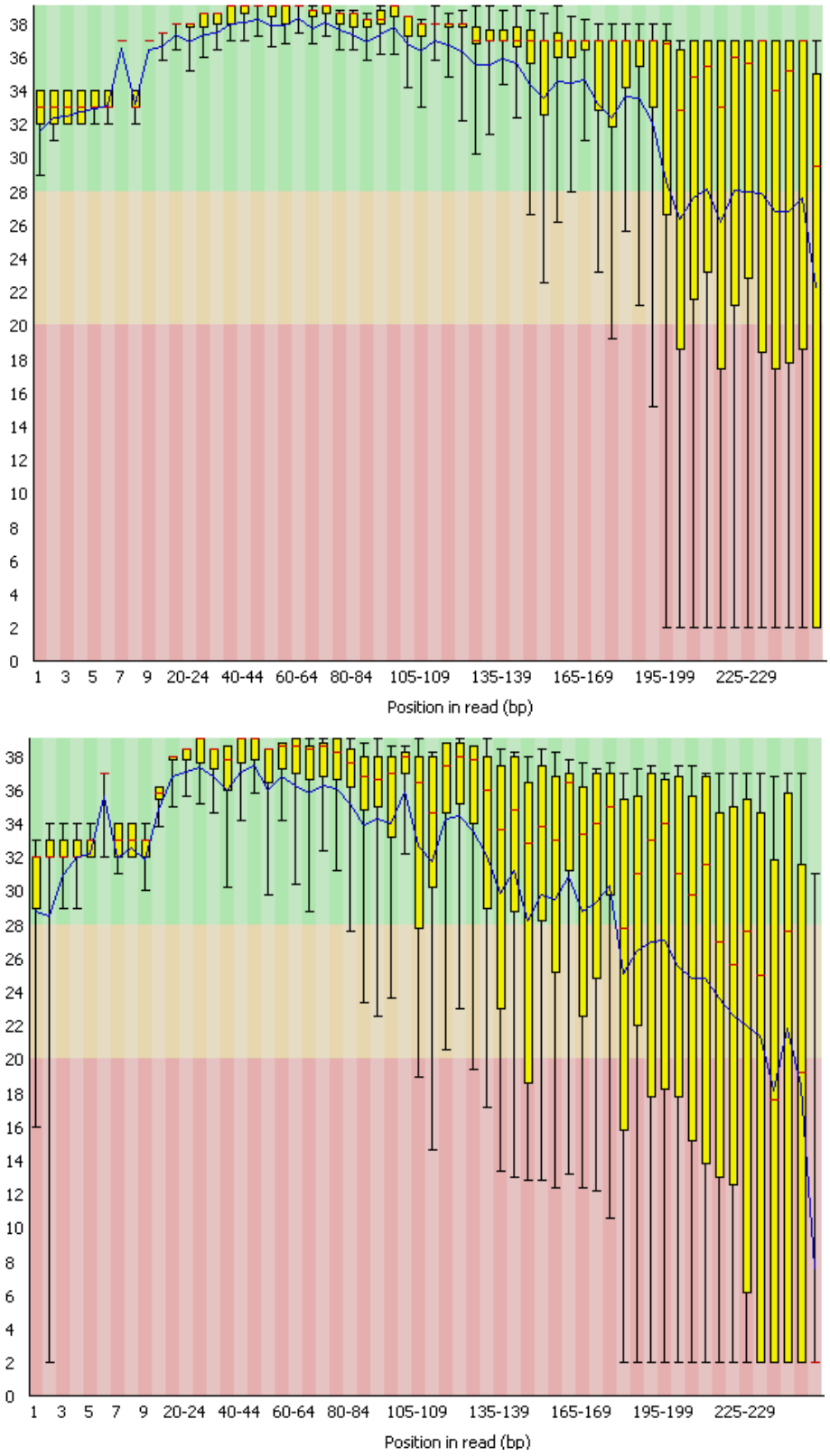

Figure 2.9 – An example quality report from a single eukaryotic sample showing the quality scores (Q value) across all 250 bases of the forward (top) and reverse (bottom) paired primer (FastQC, Babraham Bioinformatics).

2.3 Results

To characterise microbial communities in jet fuel systems, contaminated fuel and water samples were taken from fuel systems and aircraft across Europe and the Middle East. Two types of sample were received: contaminated fuel (A) or a mixture of contaminated fuel and water (B). The contaminated fuel (100 ml) from these samples was used as an inoculum in microcosms containing either sterile water (C) or a sterile defined mineral medium (Bushnell-Haas) (D), which were overlaid with the contaminated fuel. Contaminated water (1 ml) was used as an inoculum in microcosms containing sterile Merox-treated Jet A-1 and Bushnell-Haas (E). Planktonic growth was assessed after 90 days in all of the microcosms by direct sequencing (culture-independent) and by isolating microorganisms and sequencing (culture-dependent). For heavily-contaminated water samples, DNA was extracted directly without incubation and sequenced - microorganisms were also isolated (see Figure 2.10). In total, these analyses were undertaken on 78 samples. Fourteen samples were taken directly from water drains from aircraft and fuel tanks in the field. Ten samples of contaminated water were used as inocula in the microcosms and contaminated fuel was used as inocula in 29 microcosms containing Bushnell-Haas and 25 containing distilled water (see Appendix B).

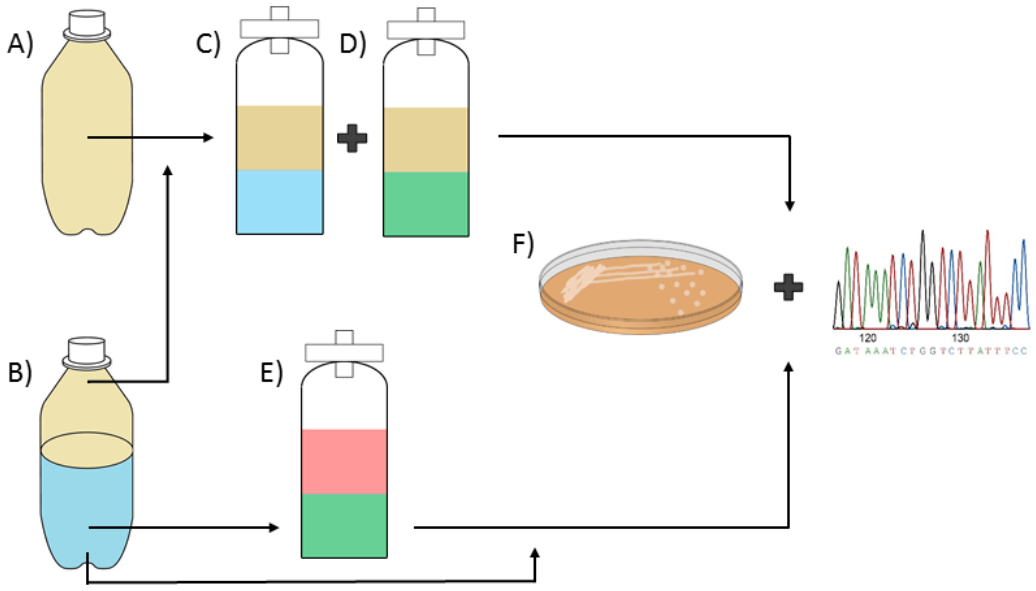

Figure 2.10 – The analysis protocol for identifying microorganisms and microbial communities from contaminated jet fuel/water samples.

2.3.1 General results figure key

Throughout this chapter, samples that have been used for direct sequencing (culture-independent) have been divided into four main groups: 1) Microcosms inoculated with contaminated fuel, overlaid on Bushnell-Haas, 2) microcosms inoculated with contaminated fuel overlaid on distilled water, 3) microcosms containing sterile Merox-treated Jet A-1 overlaid on Bushnell-Haas and inoculated with 1 ml of contaminated water and 4) contaminated water from environmental (field) samples. For comparative purposes, these different treatments have been displayed on the same figures. Therefore, a consistent colour code and labelling has been used across all figures in this chapter (unless otherwise stated) (see Table 2.3).

Table 2.3 – General figure key for all samples within this chapter.

Group	Fuel phase	Aqueous phase	Inoculum	Label	Colour
1	*Contaminated fuel*	*Bushnell-Haas*	*Fuel*	*Bushnell-Haas*	*Red*
2	*Contaminated fuel*	*Distilled water*	*Fuel*	*Water*	*Blue*
3	*Merox-treated Jet A-1*	*Bushnell-Haas*	*Contaminated water (1 ml)*	*Contaminated water*	*Green*
4	*N/A*	*N/A*	*N/A*	*Field samples*	*Orange*

2.3.2 Identification of isolated microorganisms

Isolated microorganisms were obtained from contaminated fuel and water. 16S rRNA genes (prokaryote) or ITS and 5.8S rRNA genes (eukaryote) sequences from 305 organisms were amplified, cloned and sequenced. This resulted in 35 different microorganisms being identified; 24 prokaryotes and 11 eukaryotes (see Table 2.4). To the best of the authors' knowledge, 16 of these species have not been identified in jet fuel systems before, namely: *Cellulosimicrobium sp.*, *Entrophospora sp.*, *Erwinia billingiae*, *Epicoccum nigrum*, *Exiguobacterium arabatum*, *Meyerozyma caribbica*, *Novosphingobium resinovorum*, *Paenibacillus sp.*, *Paracoccus yeei*, *Peniophora sp.*, *Pseudallescheria boydii*, *Rosemonas sp.*, *Sclerostagonospora sp.*, *Stenotrophomonas maltophilia*, *Trametes sp.* and *Yarrowia lipolytica*. Additionally, although their genus has been described, 7 of the species have not been identified to the species level before, namely: *Bacillus simplex*, *Candida krusei*, *Escherichia coli*, *Pantoea eucalypti*, *Pseudomonas fluorescens*, *Pseudomonas graminis and Pseudomonas tolaasii* (see Tables 1.1 and 1.2)[44].

[44] Identifying microorganisms beyond a Genus level is particularly challenging when sequencing 5.8S, 16S and 18S rRNA. For example, two *Pseudomonas sp.* may look identical at >99% similarity, and

Table 2.4 – List of microorganisms obtained from contaminated fuel and water samples.

Prokaryotes	
Bacillus simplex	*Bacillus spp.*
Cellulosimicrobium sp.	*Erwinia billingiae*
Escherichia coli	*Exiguobacterium arabatum*
Flavobacterium sp.	*Kocuria rhizophila*
Novosphingobium resinovorum	*Paenibacillus sp.*
Pantoea eucalypti	*Pantoea spp.*
Paracoccus yeei	*Pseudomonas fluorescens*
Pseudomonas graminis	*Pseudomonas spp.*
Pseudomonas tolaasii	*Rosemonas sp.*
Serratia sp.	*Shigella sp.*
Staphylococcus epidermidis	*Staphylococcus sp.*
Stenotrophomonas maltophilia	*Variovorax paradoxus*
Eukaryotes	
Amorphotheca resinae	*Candida krusei*
Candida sp.	*Entrophospora sp.*
Epicoccum nigrum	*Meyerozyma caribbica*
Peniophora sp.	*Pseudallescheria boydii*
Sclerostagonospora sp.	*Trametes sp.*
Yarrowia lipolytica	

The results show that prokaryotic communities were dominated by Proteobacteria (Alpha-, Beta- and Gamma-), which made up 62.5 % of the prokaryotes isolated, with Gammaproteobacteria being the most frequently isolated (11 species isolated). Firmicutes were also frequently isolated - ~25% of the prokaryotes isolated. Additionally 2 Actinobacteria and 1 Bacteroidetes were identified. The eukaryotes were dominated by Ascomycota, which made up 82% of the eukaryotic isolates (9 species). Within this division, 4 yeasts of the classes of Saccharomycetes were dominant. The remaining organisms in this division were made up of 4 additional classes (Dothidiomycetes, Glomeromycetes, Sordariomycetes and Incertae sedis[45]). Two eukaryotes were also present from the Basidomycota division (*Epicoccum nigrum* and *Sclerostagonospora sp*.).

2.3.3 Quantification of DNA by qPCR

DNA extracted from complex samples may contain both prokaryotic and eukaryotic DNA. To quantify the amount of each, qPCR with prokaryotic and eukaryotic specific primers was

becomes even more challenging when horizontal gene transfer is taken into account. Therefore more accurate methodology, such as qPCR or microarrays should be used to definitively identify microorganisms to a species level.

[45] Incertae sedis is used where a microorganism has been identified, however its broader relationships are unknown/undefined. This is true of a few key microorganisms in jet fuel systems such as *A. resinae*.

performed, using a standard curve of *P. putida* (prokaryotes), *E. coli* (prokaryotes) or *C. tropicalis* (eukaryotes). This was done to a) test whether both prokaryotic and eukaryotic DNA was present in the samples to maximise sequencing efficiency and b) ensure that there was no cross-kingdom amplification by the primer sets.

Cross-kingdom amplification was checked by producing a range of standard curves from 0 to 50 ng/µl using *P. putida* and *C. tropicalis* DNA, as well as a mixture of both types of DNA. DNA was then amplified with primer sets 799F and 1193R (prokaryotes) and ITS 3 and ITS 4 (eukaryotes) and the results presented in genome equivalents for their respective organism. No cross amplification was present with either primer set and the reactions became saturated between 25 and 50 ng in both reactions (see Figure 2.11). The quantity of extracted DNA was then measured.

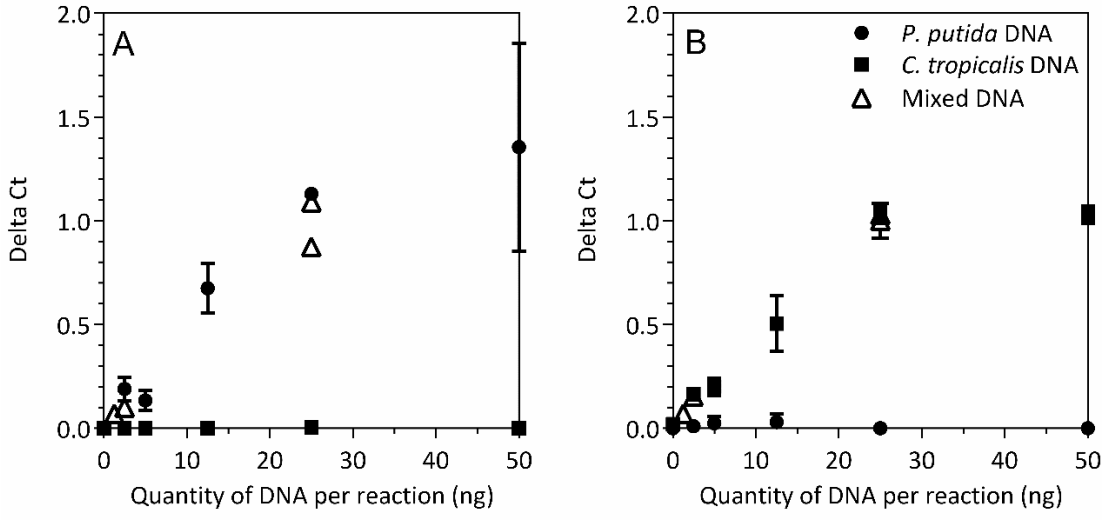

Figure 2.11 – Amplification of *P. putida*, *C. tropicalis* and a mixture of both DNAs by qPCR using primers sets 799F and 1193R (A) and ITS 3 and ITS 4 (B). DeltaCt = $E^{\wedge(minCt - Ct)}$ where E is the amplification efficiency of the primer, Ct is the cycle threshold i.e. the number of cycles for the fluorescent signal to cross the threshold and minCt is the Ct value of the highest standard (in this case the 50 ng).

Figure 2.12 A and B show the genome equivalents per litre of the prokaryotic (*E. coli* genomes) and eukaryotic (*C. tropicalis* genomes) organisms extracted from microcosms and field samples. C and D show an *E. coli* and *C. tropicalis* standard curve respectively and were included in each qPCR data set. Prokaryotic DNA was found in all samples, although the concentration varied markedly (over two orders of magnitude). Eukaryotic DNA was found in only 41 of the 78 samples with an even greater range in observed concentration (over

three orders of magnitude). In some samples where eukaryotic DNA could not be detected directly (e.g. field water samples 29, 33, 34, 35, 36 and 51), eukaryotes did grow when placed in microcosms indicating the eukaryotic contamination was present but at a low level.

There was no obvious pattern in prokaryotic and eukaryotic DNA concentrations related to geographical origin of the sample, nor the way in which they had been treated. In addition, there was no obvious relationship between prokaryotic and eukaryotic DNA concentration, i.e. no indication of competitive effect or coexistence of the contaminants.

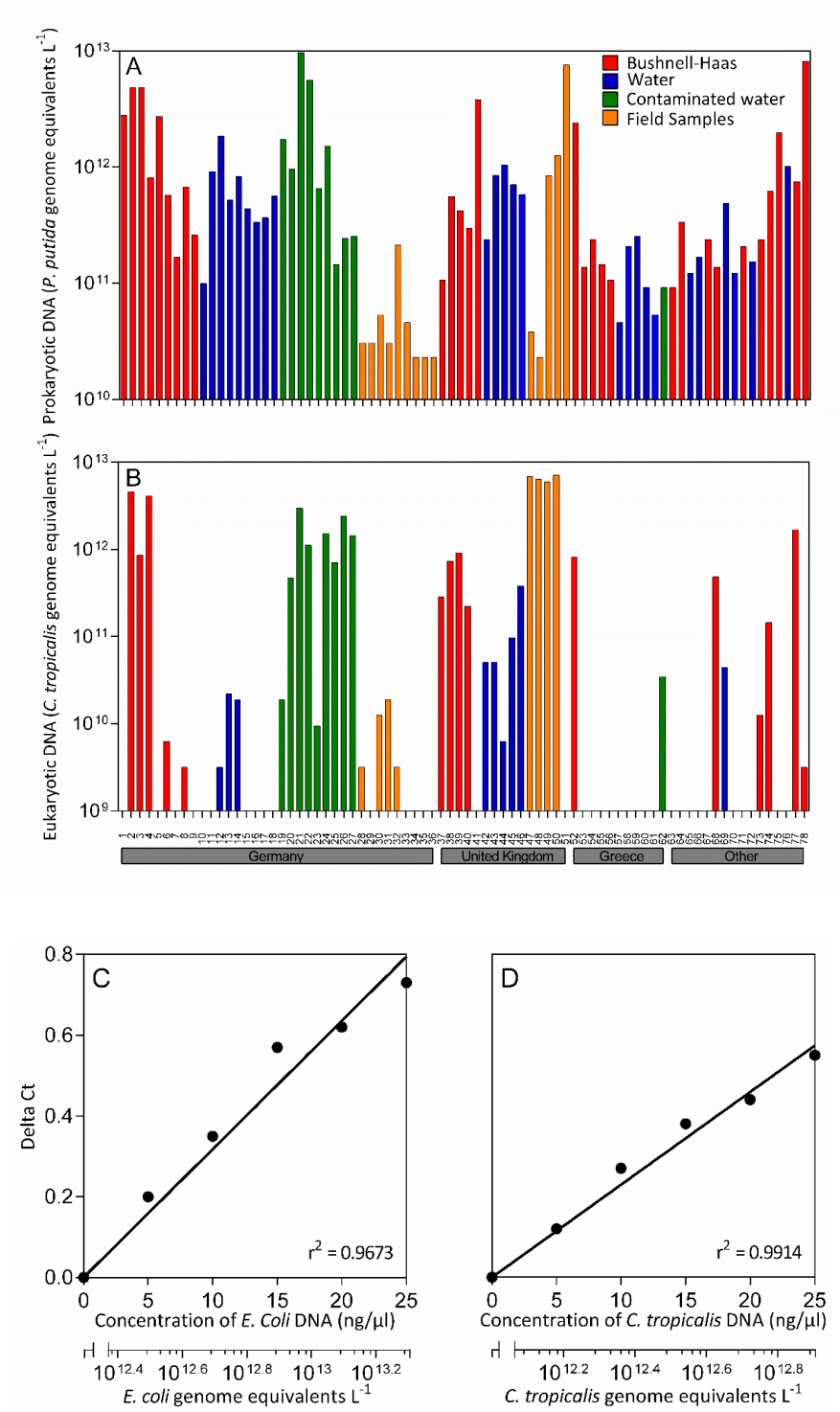

Figure 2.12 – The quantity of *E. coli* (A) and *C. tropicalis* (B) genome equivalents of DNA per litre in each of the microbial communities analysed by qPCR. As well as the standard curve of *E. coli* genome equivalents (C) used to calculate the prokaryotic genomes present and the standard curve of *C. tropicalis* DNA genome equivalents (D) used to calculate the eukaryotic genomes present in the microbial communities.

2.3.4 Culture-independent analysis of microbial communities from aircraft fuel systems

2.3.4.1 Diversity of microbial communities

To examine the diversity of microbial populations found within jet fuel systems, culture-independent analysis was undertaken on field samples obtained from 11 locations across Europe and the Middle East. These samples were used to set up a series of microcosms using contaminated jet fuel or water as an inoculum resulting in a total of 78 samples. The microbial communities were then analysed using next-generation sequencing.

Across the 76 prokaryotic libraries that passed quality control, 145 distinct OTUs were identified by comparison with the Greengenes database at 97 % sequence identity (158 were identified when the sequence identity was increased to 99 %). Similar results were obtained using the Silva database. Further work used the Greengenes database at 97 % similarity.

Across all of the samples, the phylum Proteobacteria dominated, accounting for 50.0 % of the reads in prokaryotic libraries. These belonged to the classes: Alphaproteobacteria (19.0 %), Betaproteobacteria (14.5 %), Gammaproteobacteria (15.5 %) and Deltaproteobacteria (0.7 %). Actinobacteria was the next most abundant phylum, accounting for 26.0% of the reads in prokaryotic libraries. They were predominantly from the class of Actinobacteria (25.0 %), one OTU from class of Acidimicrobia (0.7 %) and one from the class of Thermoleophilia (0.7 %) was also identified in the Silva database. Firmicutes (14.0 %) and Bacteroidetes (6.50 %) made up the remaining two dominant phyla. The Firmicutes were composed of Bacilli (10.0 %) and Clostridia (3.0 %), and the Bacteroidetes composed of Flaviobacteria (4.0 %), Bacteroidia (2.0 %) and Sphingobacteria (0.7 %). The remaining OTUs were made up of one OTU from the class Acidobacteria (0.7 %), one OTU from the class of Chloroflexi (0.7 %), one OTU from the class of Elusimicobia (0.7 %) and two unknown OTUs (1.0 %) (see Figure 2.13).

Across the 35 eukaryotic libraries, 51 species were identified by comparison with the UNITE database at 97 % sequence identity. The dominant phylum was Ascomycota, accounting for 76 % of the ITS sequences generated. These were from the classes: Dothideomycetes (20.0 %), Eurotiomycetes (16.0 %), Sordariomycetes (16.0 %), Leotiomycetes (10.0 %), Saccharomycetales (8.0 %), Lecanoromycetes (6.0 %) and one unidentified Ascomycota (2.0 %). Basidiomycota were the other dominant phylum, accounting for 20.0 % of the reads in eukaryotic libraries. These were the classes: Agaricomycetes (6.0 %), Microbotryomycetes (4.0 %), Tremellomycetes (4.0 %), Exobasidiomycetes (4.0 %), Incertae sedis[45] (2.0 %) and

one unidentified Basidiomycota (2.0 %). The remaining microorganisms were Glomeromycota and one unidentified OTU (2.0 %) (see Figure 2.14).

Although a total of 196 OTUs were identified in this study, only 36 had a relative abundance greater than 1 % in any sample. Of the prokaryotes, two OTUs were present in all 76 of the sequence libraries; *Cellulosimicrobium sp*. and an unidentified Xanthomonadaceae. *Cellulosimicrobium sp*. was particularly prevalent, with an average relative abundance at 70.1 % and observed up to 99.8 % in some samples. *Amorphotheca sp*. were the most common eukaryotic OTU, being present in 33 of the 35 sequence libraries, with an average relative abundance 44.7 % and forming a near monoculture (99.97 % of ITS reads) in some samples. A yeast (*Meyerozyma sp*.) was present in 30 samples with an average relative abundance 25.4 % and observed up to 99.94 % in some libraries. Generally yeasts were observed in most sequence libraries. Table 2.5 outlines the most abundant OTUs seen in all 78 samples. Most of these microorganisms were observed in many of the libraries at a low abundance. However, in some libraries, they were very abundant. For example reads from *Methylobacterium sp*. had a maximum relative abundance of 86.3 %, compared to its average relative abundance of 2.5 %.

Table 2.5 – The most dominant microorganisms observed across the sample set. Microorganisms were selected if they were observed in >40 % of the samples sequenced.

	Maximum relative abundance (%)	Average relative abundance (%)	Number of samples where present
Prokaryotes			
Actinomycetales	13.1	0.2	45
Burkholderia sp.	34.5	1.0	74
Cellulosimicrobium sp.	99.8	70.1	76
Enterobacteriaceae	9.4	0.2	53
Enterobacteriaceae	4.1	0.8	34
Erwinia sp.	77.3	3.3	47
Gluconacetobacter sp.	59.4	2.3	65
Methylobacterium sp.	86.3	2.5	47
Oxalobacteraceae	65.2	1.7	34
Pseudomonas sp.	99.6	6.9	72
Sphingomonas sp.	2.8	0.2	32
Stenotrophomonas sp.	5.5	0.8	71
Xanthomonadaceae	31.8	4.7	76
Eukaryotes			
Amorphotheca sp.	99.9	44.7	33
Candida sp.	95.9	4.2	17
Helotiales	50.7	4.3	23
Meyerozyma sp.	99.9	25.4	30
Penicillium sp.	81.0	7.3	21
Pichia sp.	79.2	4.8	27
Protoventuria sp.	76.2	4.3	17
Unidentified Ascomycota	22.2	0.9	19
Unidentified fungi	99.8	3.0	23

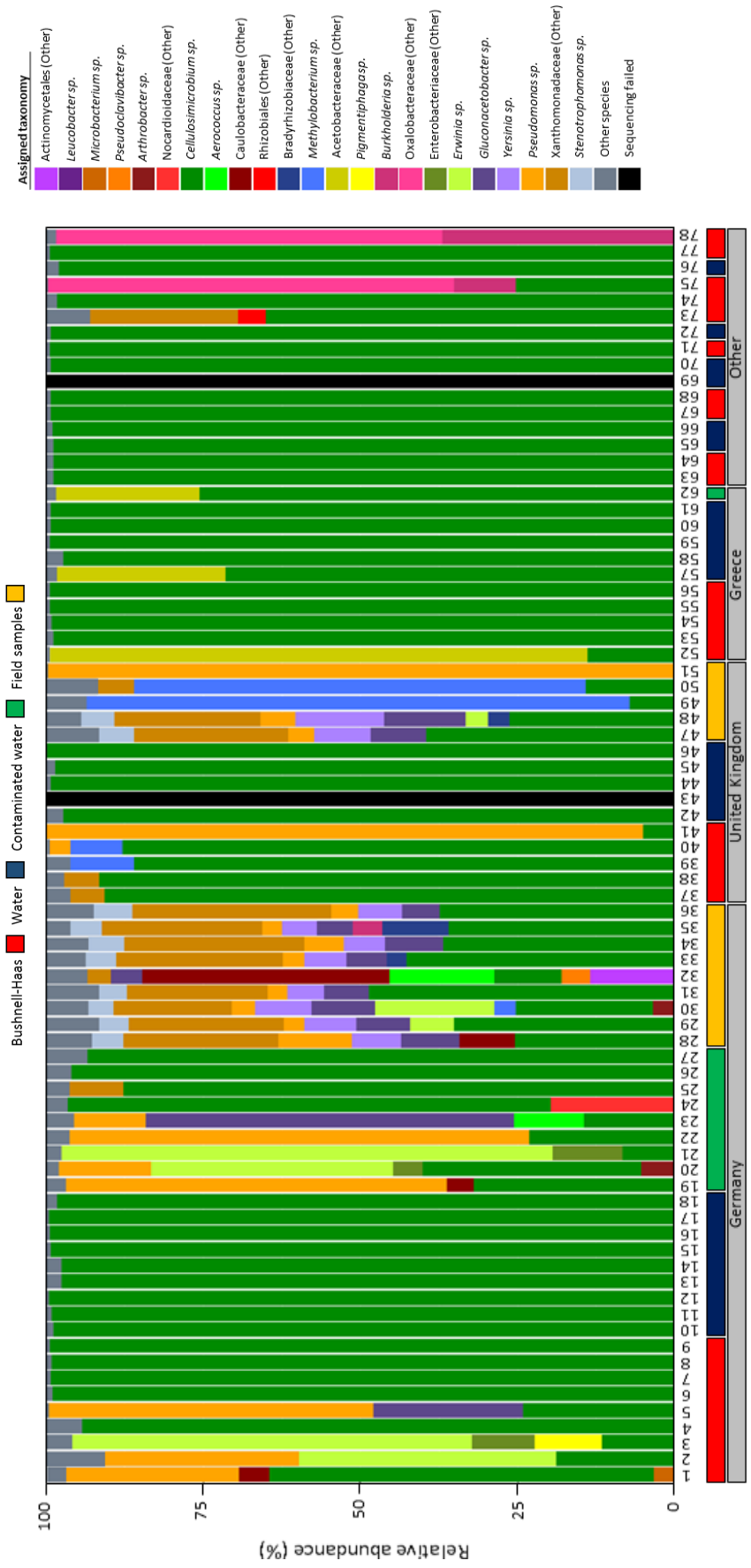

Figure 2.13 – Relative abundance of prokaryotic reads found in aircraft fuel systems. Samples with a completely black bar failed quality control and the data has not been included. Only microorganisms that have a relative abundance >3 % have been displayed, all others have been combined into the "Other species" category.

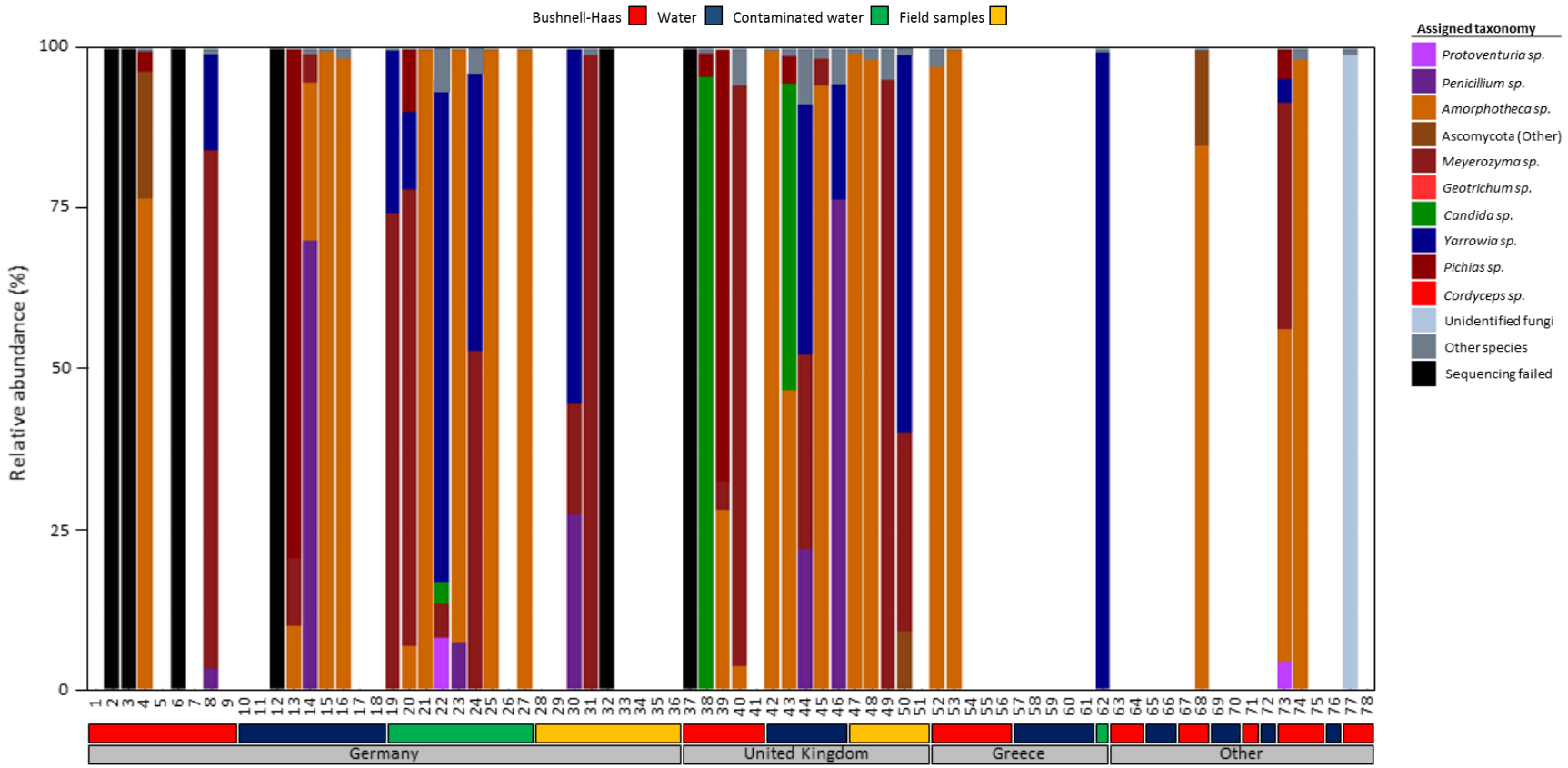

Figure 2.14 – Relative abundance of ITS sequences from eukaryotes found in aircraft fuel systems. Samples with a completely black bar failed quality control and the data has not been included and white bars contained no DNA. Only microorganisms that have a relative abundance >3% have been displayed, all others have been combined into the "Other species" category.

2.3.4.2 Effect of microcosms and mineral media on the relative abundance of microorganisms

To analyse the effect of microbial contamination of fuels, many studies employ a microcosms-based system, using mineral rich mediums, such as Bushnell-Haas, to ensure all nutrient requirements are available (with the exception of a carbon source). These systems have many advantages, however, they are artificially eutrophic environments that are substantially different from those observed in the field. To analyse the effect of introducing a mixed microbial community from a jet fuel system into a microcosm-based environment, 64 microcosms were set up. The microcosms were divided into 3 treatments: 1) contaminated fuel overlaid onto Bushnell-Haas nutrient medium, 2) contaminated fuel overlaid onto sterile distilled water and 3) sterile Merox-treated Jet A-1 overlaid on Bushnell-Hass nutrient medium and inoculated with contaminated water. In each case comparisons were made with the field samples.

2.3.4.3 What is the effect of microcosms on diversity?

The prokaryotic species diversity was much greater than that of eukaryotes. However, in the prokaryotic communities there was a notable difference in diversity between the four treatments. Species richness was highest in the contaminated water taken from the field - when these communities were introduced into a microcosm, species richness decreased considerably (ANOVA, p <0.05 in all cases (see Table 2.6)) (see Figure 2.15 and Figure 2.17). The Chao1 index showed a drop in predicted total species number from ~195 OTUs to ~100 OTUs (see Figure 2.16). Both the inverse Simpson and the Shannon diversity indices showed a significant drop in diversity (ANOVA, p <0.01 (see Table 2.6)) between the field samples and each microcosm treatment, with the exception of the field samples compared with the contaminated water samples using the Shannon diversity index, where no significant difference was observed (AVOVA, p = 0.252 (see Table 2.6) (see Figure 2.17). DESEQ2 analysis show that 26 OTUs were significantly different between the field samples and the contaminated water samples, which account for the observed variation. The significant OTUs with the greatest relative abundance were a *Gluconacetobacter sp., Stenotrophomonas sp., Yersinia sp.* and a *Xanthomonadaceae sp.* (see Table 2.7).

In contrast, the eukaryotic samples showed no significant change in species richness between sample treatments (ANOVA, p >0.05 (see Table 2.6)), averaging 9 OTUs per sample. The Chao1 index predicted an average of 15-20 OTUs across all four treatments (see Figure 2.18). No significant difference in diversity was observed with either the inverse Simpson index or Shannon diversity index (ANOVA, p >0.05 (see Table 2.6)) (see Figure 2.19). Overall these data show that while introducing a mixed community into a microcosm has a

substantial impact on the prokaryotic diversity it appeared to have no significant impact on the eukaryotes.

2.3.4.4 What is the effect of mineral media on diversity?

To explore the impact of nutrient media on microbial diversity, microcosms inoculated with contaminated fuel overlaid on either Bushnell-Haas or distilled water were compared. Species richness was lower in prokaryotic communities in microcosms containing water compared to Bushnell-Haas (see Figure 2.15 and Figure 2.17) (ANOVA, p = 0.007 (see Table 2.6)), with the Choa1 index predicting a drop in OTUs from 55 OTUs (Bushnell-Haas) to 45 OTUs (water) (see Figure 2.16). The Shannon diversity index showed a significant drop in diversity (ANOVA, p = 0.010 (see Table 2.6) though the inverse Simpson index showed no significant differences between the communities (ANOVA, p = 0.091) (see Figure 2.19). The inverse Simpson diversity index is more heavily weighted towards common/dominant species (these communities are dominated by a few microorganisms) in comparison to the Shannon diversity index, which most likely accounts for the difference in results between the two indices. DESEQ2 analysis showed that 7 OTUs accounted for the observed variation in the sample set. OTUs of *Burkholderia sp., Oxalobacteraceae sp.* and *Pseudomonas sp.* all showed a significant increase in the fuel samples incubated in Bushnell-Haas compared to water, whereas OTUs from the genus *Enterobacteriaceae sp., Pseudomonas sp., Erwinia sp.* and *Enterobacteriaceae sp.* all showed a significant decrease (see Table 2.8). The eukaryotic communities showed no statistical difference between microcosms inoculated with contaminated fuel overlaid on either Bushnell-Haas or distilled water (ANOVA, p >0.05 (see Table 2.6)), between species richness and either the inverse Simpson or Shannon diversity index (see Figure 2.19).

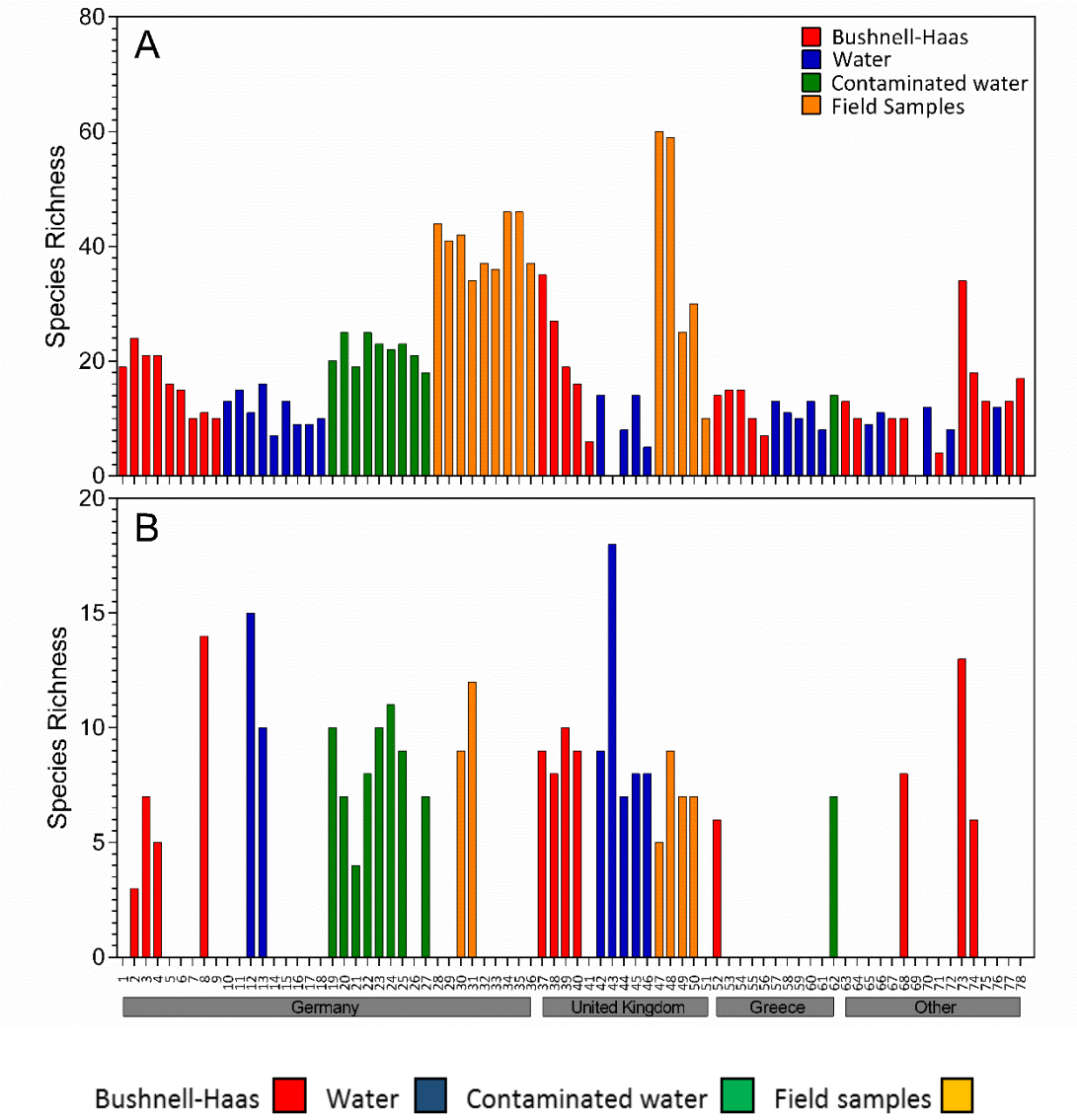

Figure 2.15 – Species richness across all samples. Red samples are contaminated fuel overlaid on Bushnell-Haas nutrient medium. Blue samples are contaminated fuel overlaid on distilled water. Green samples are contaminated water used as in inoculum in microcosms containing Merox-treated Jet A-1 and Bushnell-Haas nutrient medium. Orange samples are contaminated water taken from aircraft fuel systems (no microcosm). A) Prokaryotic species identified by the Greengenes database at 97% similarity. B) Eukaryotic species identified by the UNITE database at 97% similarity.

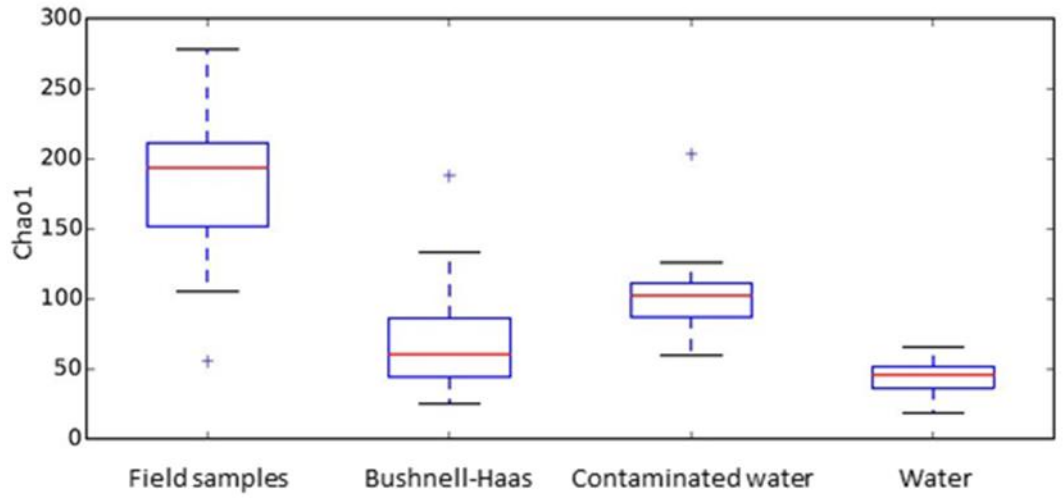

Figure 2.16 – Chao1 index[46] of the prokaryotic samples in relation treatment type. Box and whisker plot, boxes span the interquartile range, horizontal line with the boxes represents the mean. Whisker length extends to 1.5 times the interquartile range, with outliers indicated by a + symbol.

[46] The Chao1 diversity index was included to give an estimation of the observed OTUs in the samples, and therefore an indication of the true species richness. The bias corrected Choa1 formula was used, because all of the singletons are removed during data processing (Chao 1984).

$$S_{Chao1} = S_{obs} + \frac{f_1(f_1 - 1)}{2(f_2 + 1)}$$

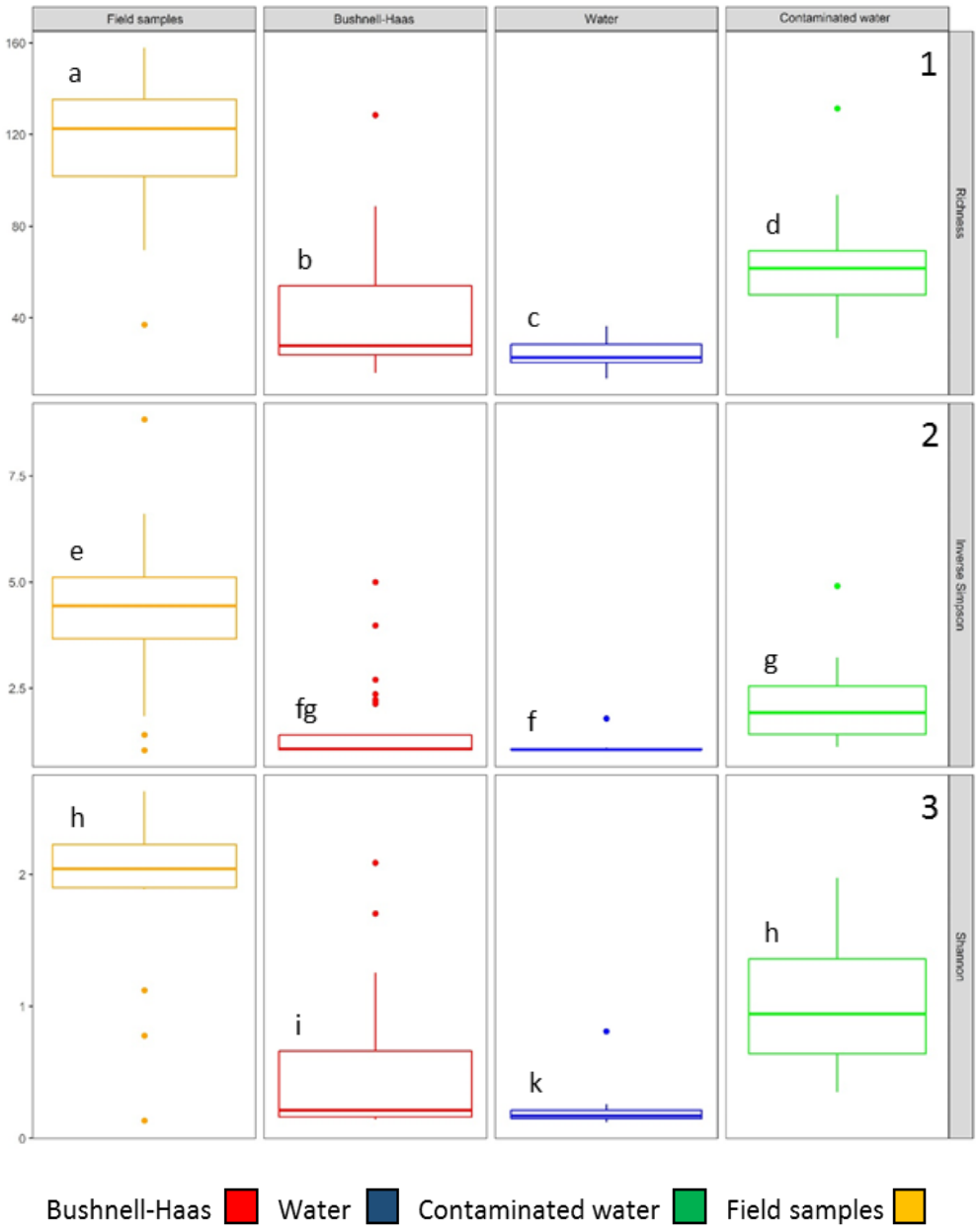

Figure 2.17 – Box and whisker plot showing species richness (1), inverse Simpson[47] (2) and Shannon diversity[48] (3) indices for the prokaryotic samples in relation to treatment type. Boxes span the interquartile boxes span the interquartile range, horizontal line with the

[47] In general, microbial communities in this study contain few very dominant species. Therefore the inverse Simpson diversity index was selected because it accounts for relative abundance, as well as the number of species present (Simpson 1949).

$$D = \frac{1}{\sum_{i=1}^{s} p_i^2}$$

[48] Shannon diversity index is a commonly used diversity index and accounts for both the abundance and evenness of the species present (Shannon 1948; Shannon and Weaver 1949).

$$H = -\sum_{i=1}^{R} \rho i \ln pi$$

boxes represents the mean. Whisker length extends to 1.5 times the interquartile range, with outliers indicated by a ● symbol. Samples which share a letter are not statistically different (*p* values are displayed in Table 2.6).

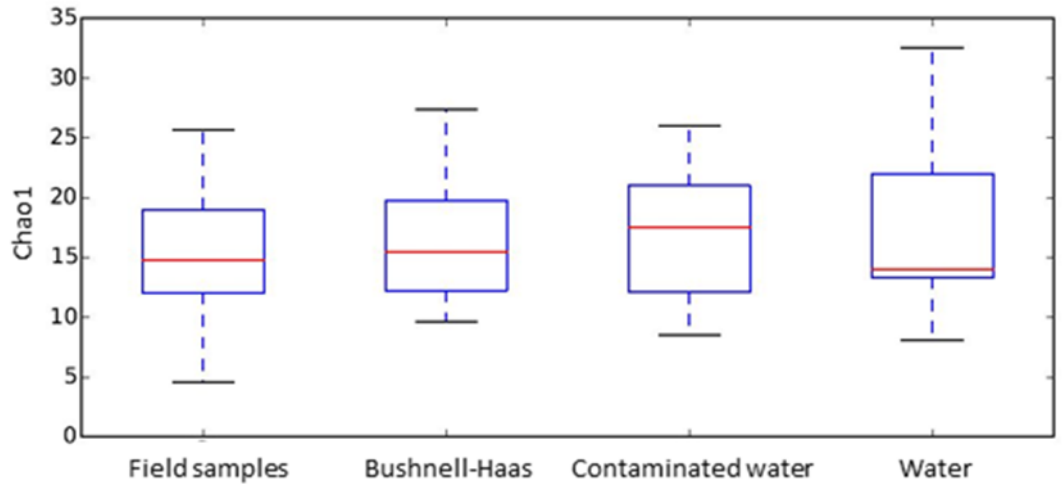

Figure 2.18 – Chao1 index of the eukaryotic samples in relation treatment type. Box and whisker plot, boxes span the interquartile range, horizontal line with the boxes represents the mean. Whisker length extends to 1.5 times the interquartile range, with outliers indicated by a + symbol.

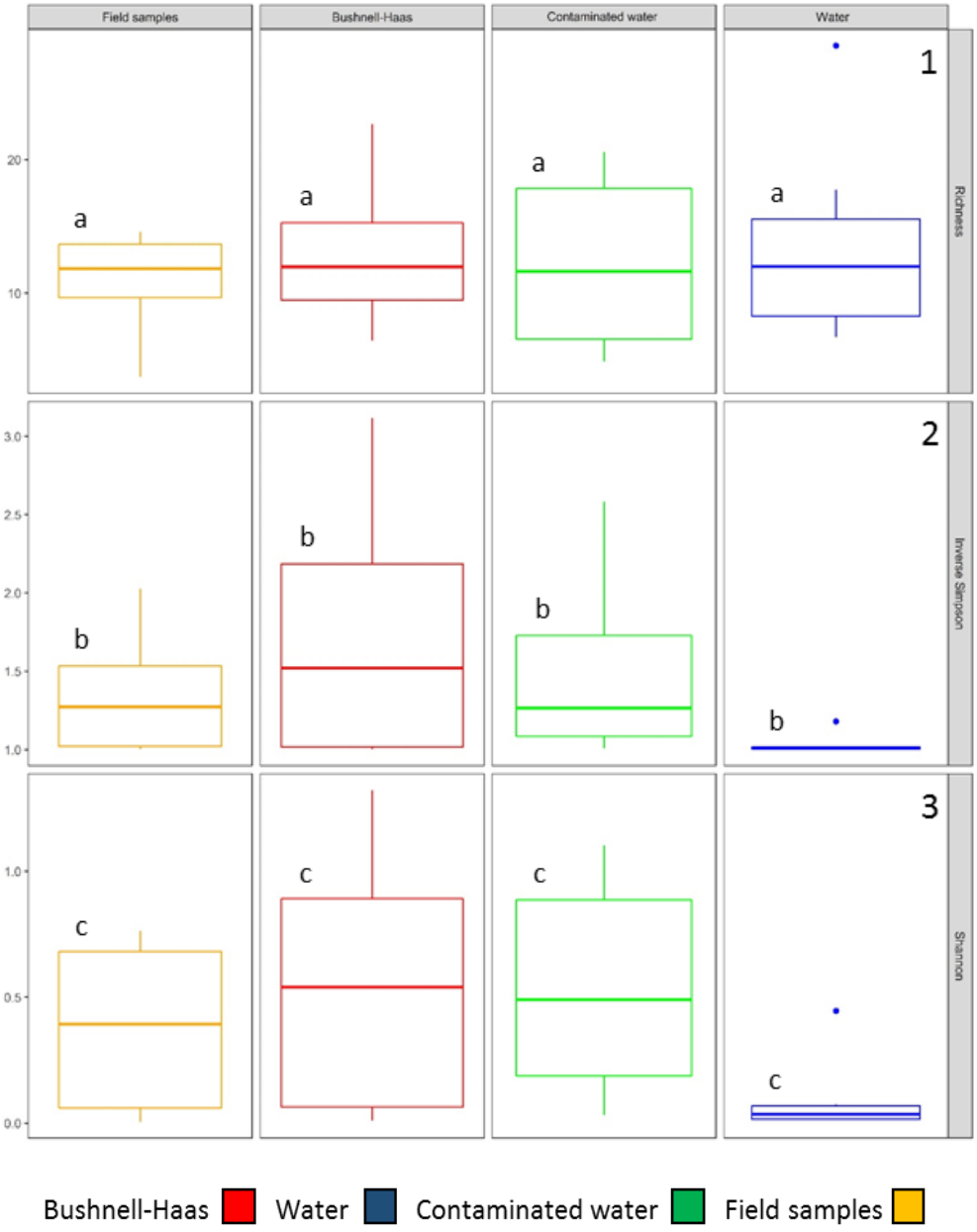

Figure 2.19 – Box and whisker plot showing species richness (1), inverse Simpson (2) and Shannon diversity (3) indices for the eukaryotic samples in relation to treatment type. Boxes span the interquartile boxes span the interquartile range, horizontal line with the boxes represents the mean. Whisker length extends to 1.5 times the interquartile range, with outliers indicated by a ● symbol. Samples which share a letter are not statistically different (*p* values are displayed in Table 2.6).

Table 2.6 – *p* values from ANOVAs performed on log10 transformed prokaryotic and eukaryotic data with a Tukey post hoc test to compare sample treatments against one another for species richness, inverse Simpson diversity and Shannon diversity. *p* values rounded to three decimal places. Analysis performed using the Phyloseq (McMurdie & Holmes 2013) estimate_richness function, using 100 random trials to calculate these values.

		Prokaryotes	
Species Richness	Field samples	Bushnell-Haas	Water
Bushnell-Haas	**<0.001**		
Water	**<0.001**	**0.007**	
Contaminated water	**0.012**	**0.005**	**<0.001**
Inverse Simpson			
Bushnell-Haas	**<0.001**		
Water	**0.000**	0.141	
Contaminated water	**0.002**	0.091	**0.001**
Shannon			
Bushnell-Haas	**<0.001**		
Water	**<0.001**	**0.010**	
Contaminated water	0.252	**0.004**	**<0.001**
		Eukaryotes	
Species Richness			
Bushnell-Haas	0.872		
Water	0.980	0.979	
Contaminated water	0.880	1.000	0.976
Inverse Simpson			
Bushnell-Haas	0.714		
Water	0.978	0.884	
Contaminated water	0.610	0.070	0.302
Shannon			
Bushnell-Haas	0.900		
Water	0.716	0.964	
Contaminated water	0.469	0.090	0.050

Table 2.7 – DESEQ2 analysis identifying which prokaryotic OTUs differed significantly between the field samples and contaminated water samples from the microcosms. OTUs are shown at the genus level where $p \leq 0.05$ and had a mean relative abundance above 0.1 %. The base mean represents the average relative abundance across the sample set. Log 2 fold change represents the change in relative abundance based on the sample treatment. *p* values were derived using DESEQ2 (Love *et al*. 2014), assuming a negative binomial distribution of OTU abundance, with correction for false discovery using the Benjamini-Hochberg method.

OTU	Base Mean	Log 2 Fold change	*p* value	Adjusted *p* value
Gluconacetobacter sp.	1059.08	7.83	7.54E-23	1.37E-20
Stenotrophomonas sp.	702.28	4.41	7.05E-11	6.38E-09
Yersinia sp.	1015.48	10.89	2.04E-10	1.23E-08
Xanthomonadaceae sp.	3652.28	4.85	4.28E-10	1.94E-08
Stenotrophomonas sp.	24.40	4.69	2.66E-09	9.62E-08
Bradyrhizobiaceae sp.	375.60	10.38	9.62E-09	2.90E-07
Yersinia sp.	70.22	9.02	1.92E-07	4.95E-06
Xanthomonadaceae sp.	11.24	4.66	8.18E-07	1.85E-05
Xanthomonadaceae sp.	16.18	4.74	1.14E-06	2.29E-05
Pseudomonas veronii	347.63	4.85	1.75E-06	3.16E-05
Enterobacteriaceae sp.	23.87	4.89	2.62E-06	4.31E-05
Yersinia sp.	35.96	7.95	2.61E-05	3.30E-04
Pseudomonas sp.	10.50	5.53	2.32E-05	3.30E-04
Stenotrophomonas sp.	11.61	4.71	2.80E-05	3.30E-04
Xanthomonadaceae sp.	7.01	4.41	2.86E-05	3.30E-04
Burkholderia sp.	61.39	3.33	2.91E-05	3.30E-04
Burkholderia sp.	308.02	3.23	1.12E-04	1.19E-03
Pseudomonas sp.	424.26	4.42	1.41E-04	1.42E-03
Stenotrophomonas sp.	10.48	3.72	1.60E-04	1.52E-03
Pseudomonas sp.	185.93	-6.11	2.05E-04	1.85E-03
Xanthomonadaceae sp.	3.74	3.42	2.53E-04	2.18E-03
Propionibacterium acnes	4.70	4.63	5.67E-04	4.67E-03
Enterobacteriaceae sp.	2.87	4.50	1.13E-03	8.92E-03
Brevibacterium sp.	7.22	6.02	1.44E-03	1.09E-02
Enterobacteriaceae sp.	19.31	5.06	3.15E-03	2.28E-02
Stenotrophomonas sp.	4.46	3.79	5.07E-03	3.53E-02

Table 2.8 – DESEQ2 analysis to identify which prokaryotic OTUs differed significantly between the microcosms containing Bushnell-Haas nutrient medium and water and inoculated with contaminated jet fuel. OTUs are shown at the genus level where $p \leq 0.05$ and had a mean relative abundance above 0.1 %. The base mean represents the average relative abundance across the sample set. Log 2 fold change represents the change in relative abundance based on the sample treatment. *p* values were derived using DESEQ2 (Love *et al*. 2014), assuming a negative binomial distribution of OTU abundance, with correction for false discovery using the Benjamini-Hochberg method.

OTU	Base Mean	Log 2 Fold change	*p* value	Adjusted *p* value
Enterobacteriaceae sp.	78.15	-6.68	2.73E-09	2.61E-06
Pseudomonas sp.	185.93	-7.18	1.39E-06	6.64E-04
Erwinia sp.	336.70	-5.28	4.48E-06	1.43E-03
Burkholderia sp.	188.09	5.34	7.71E-05	1.84E-02
Oxalobacteraceae sp.	1091.92	6.18	1.55E-04	2.87E-02
Enterobacteriaceae sp.	10.95	-5.47	1.80E-04	2.87E-02
Pseudomonas sp.	424.26	3.81	2.49E-04	3.40E-02

2.3.4.5 Is the sample location or microcosm treatment an important factor driving differences between microbial communities?

Weighted and unweighted principle coordinate analysis (PCoA), using UniFrac distances was undertaken on the prokaryotic microbial communities, to assess the impact of sample location and microcosm treatment (see Figure 2.20). The analysis was undertaken on microcosms containing either a) contaminated water in Bushnell-Haas, b) contaminated fuel in Bushnell-Haas, c) contaminated fuel in water, or d) the field samples. The first two components explained 72.8 % of the variation in the weighted analysis and 43.8 % of the variation in the unweighted analysis. Due to a low percentage variation explained in the unweighted sample, a third axis was also analysed, however this did not provide any additional information and has therefore been omitted. Samples were also separated by microcosm treatment to assist in interpretation (see Figure 2.23).

The analysis showed that there was little variation in microbial communities taken from the field, as both the field samples from Germany and the UK clustered together. However, once the contaminated water containing these communities was introduced into a microcosm

containing Bushnell-Haas and Merox-treated Jet A-1, the variation between the microbial communities increased.

Introducing contaminated fuel to microcosms containing Bushnell-Haas resulted in more variation between the microbial communities than compared to microcosms containing water. Presumably, the increase in nutrients produced a more favourable environment for a diverse population, causing this difference. The location of the samples had little impact on the deviation, with the largest deviation being seen in the UK dataset. However, this included the largest number of sample sites and is therefore to be expected. PCoA analysis also shows this trend, though less variation is observed in the water samples (see Figure 2.21). The variation appears to be entirely stochastic in nature and it is possible that during the earlier stages of a community forming that there is more fluctuation in the community composition compared to a more established community. No analysis was undertaken on the eukaryotic communities because no statistical differences between microcosm treatments were observed (see Table 2.6).

Overall these data show that prokaryotic microbial populations from the field are relatively similar in composition. This is to be expected, as environmental conditions at the two main sample sites in Germany and the UK are similar and it is likely that the microclimates and local fauna have an influence on the microbial populations in jet fuel systems within these locations. Additionally, these data indicate a large population shift occurred in these samples after been introduced into microcosms; diversity drops significantly compared to the field samples and single microorganisms, such as *Cellulosimicrobium sp*. become dominant (forming near monocultures in some cases). Therefore it is likely that the use of microcosms and Bushnell-Haas has been the driving factor in the diversity observed within this sample set.

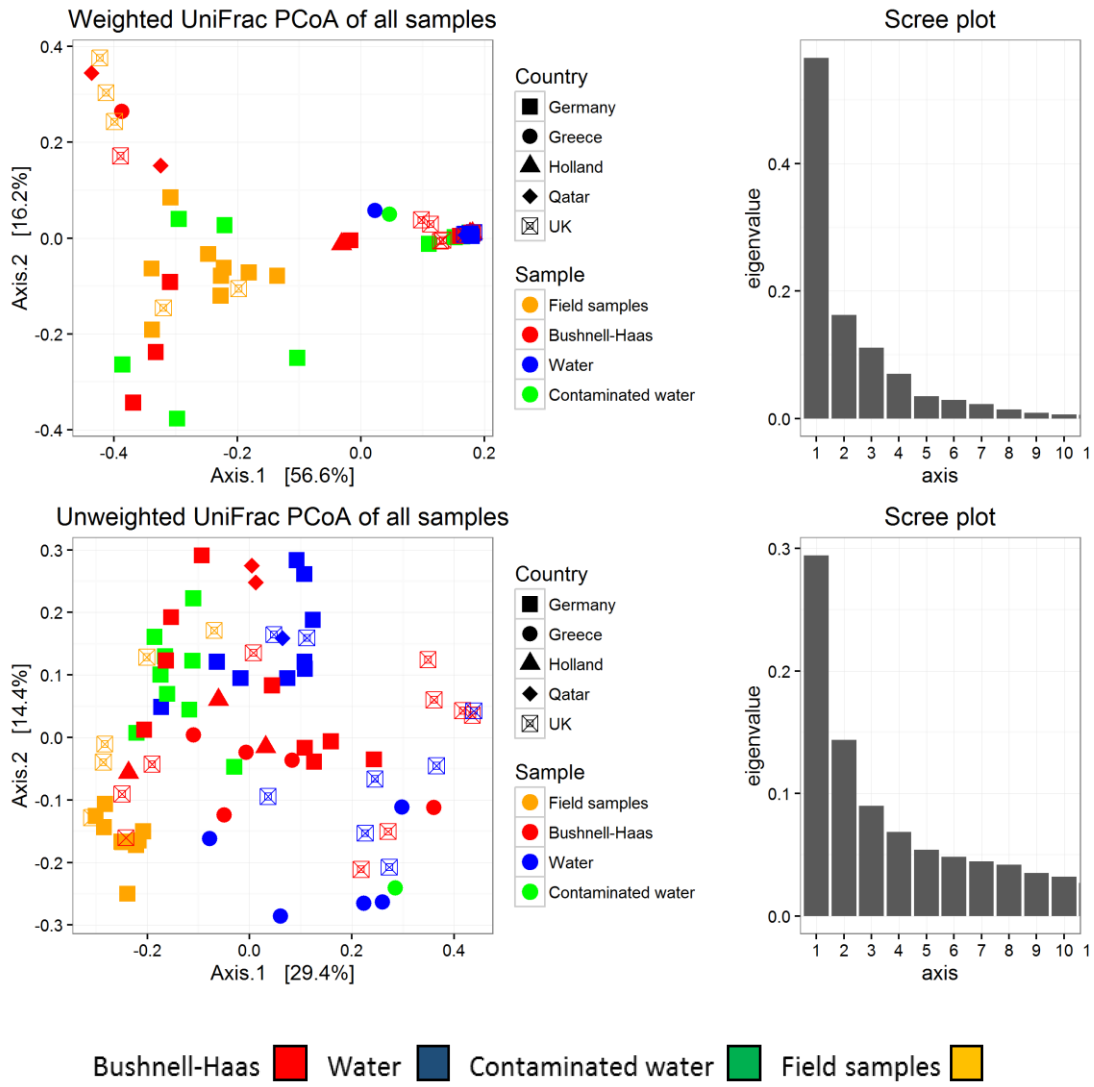

Figure 2.20 – Weighted and unweighted PCoA, using a UniFrac distance measurement on all prokaryotic samples showing the effect of treatment type on samples taken from different geographical locations.

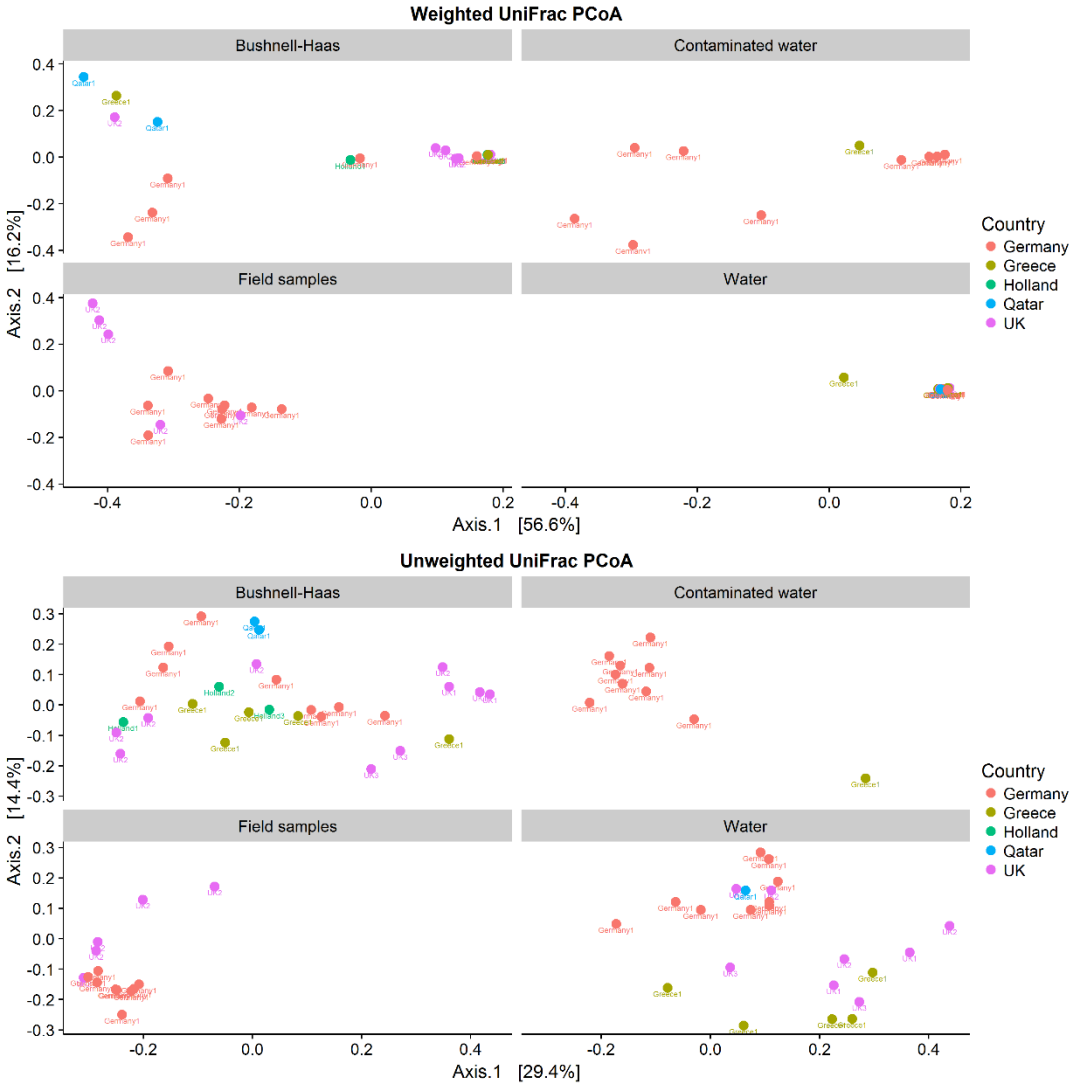

Figure 2.21 – Weighted and unweighted PCoA, using a UniFrac distance measurement on all prokaryotic samples. Plots separated out by treatment type and show the effect of each treatment type on samples taken from different geographical locations.

2.3.4.6 Community differences in aircraft fuel tanks compared to terrestrial fuel tanks

Shannon and inverse Simpson diversity indices were calculated for the prokaryotic microbial communities taken directly from aircraft and terrestrial fuel tanks (i.e. only the field water samples). ANOVA of log10 normalised values show that terrestrial tank diversity (Shannon and inverse Simpson) was lower than aircraft samples (ANOVA, p <0.05 in both cases) (see Figure 2.22).

PCoA was also used to compare samples taken from ground storage tanks and samples from aircraft (see Figure 2.23). The prokaryotic communities of field samples from aircraft compared to those from ground storage tanks. DESEQ2 showed that 8 OTUs accounted for

the variation. OTUs from the genus *Oxalobacteraceae sp.* The relative abundances of *Methylobacterium sp.* (two OTUs)*, Burkholderia sp., Sphingomonas sp.* and *Pseudomonas sp.* were significantly less in aircraft fuel tanks, whereas the relative abundance of OTUs from the genus *Caulobacteraceae sp.* and *Erwinia sp*. were significantly greater (see Table 2.9).

Presumably the harsher environment experienced during flight (extreme temperature cycling) exerts a selection pressure on the microbial communities within aircraft tanks. However, more work needs to be undertaken in this area before firmer conclusions can be drawn.

Table 2.9 – DESEQ2 analysis to identify which prokaryotic OTUs differ significantly between the aircraft fuel tanks and terrestrial fuel tanks. OTUs are shown at the genus level where *p* ≤0.05 and had a mean relative abundance above 0.1 %. The base mean represents the average relative abundance across the sample set. Log 2 fold change represents the change in relative abundance based on the sample treatment. *p* values were derived using DESEQ2 (Love *et al*. 2014), assuming a negative binomial distribution of OTU abundance, with correction for false discovery using the Benjamini-Hochberg method.

OTU	Base Mean	Log 2 Fold	*p* value	Adjusted
Oxalobacteraceae sp.	127.95	-7.95	1.93E-09	3.66E-07
Methylobacterium sp.	16436.86	-7.18	5.46E-06	5.19E-04
Burkholderia sp.	100.28	-5.23	6.53E-05	3.10E-03
Methylobacterium sp.	78.20	-6.69	6.12E-05	3.10E-03
Sphingomonas sp.	27.32	-4.89	9.82E-05	3.73E-03
Pseudomonas sp.	26.17	-5.98	1.91E-04	6.04E-03
Caulobacteraceae sp.	157.74	6.72	2.58E-04	7.01E-03
Erwinia sp.	53.06	6.06	9.09E-04	2.16E-02

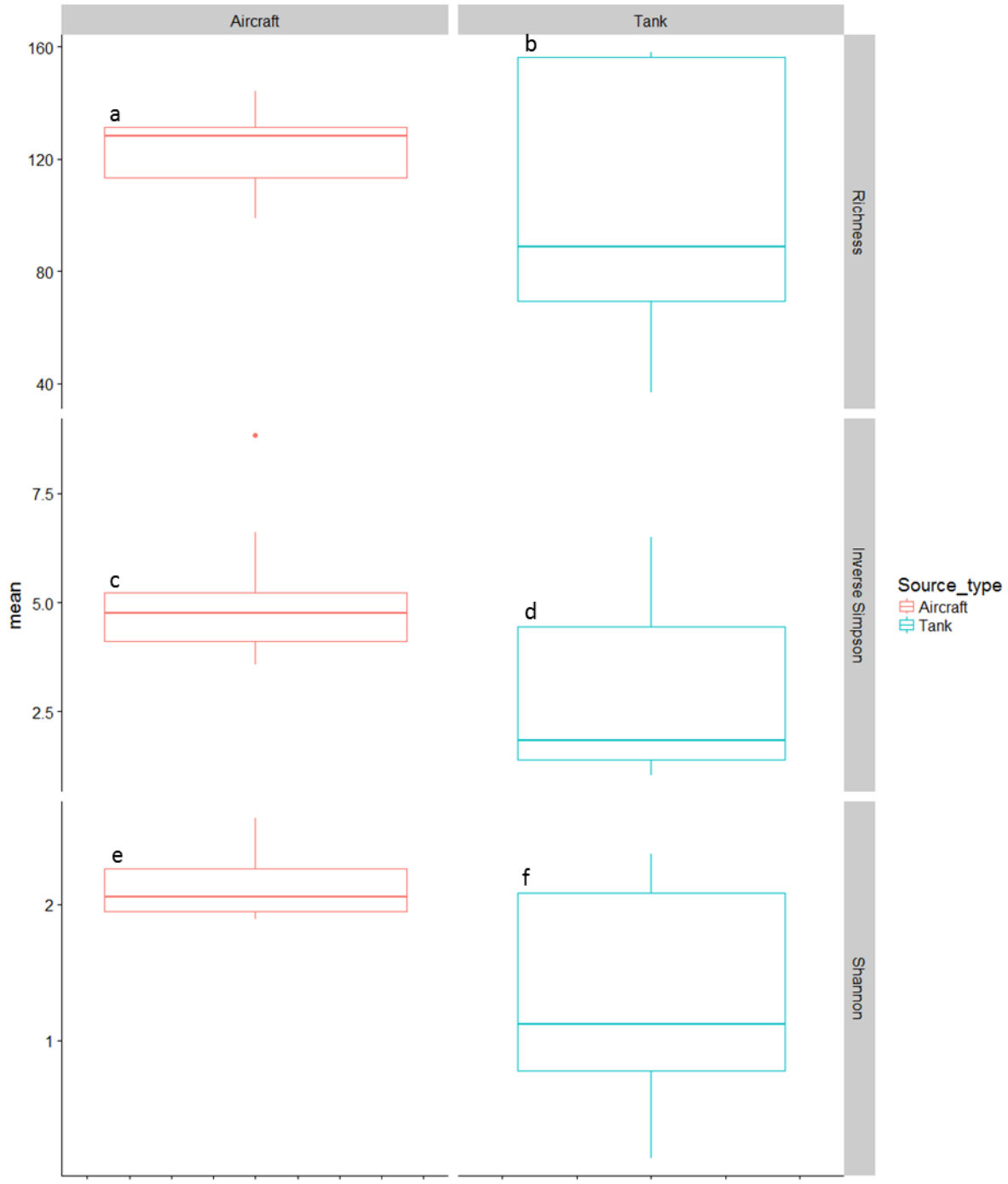

Figure 2.22 – Box and whisker plot showing species richness, as well as inverse Simpson and Shannon diversity indices for the prokaryotic samples based on source location (either aircraft or terrestrial fuel tank). Boxes span the interquartile boxes span the interquartile range, horizontal line with the boxes represents the mean. Whisker length extends to 1.5 times the interquartile range, with outliers indicated by a ● symbol. Samples that share a letter are not statistically different.

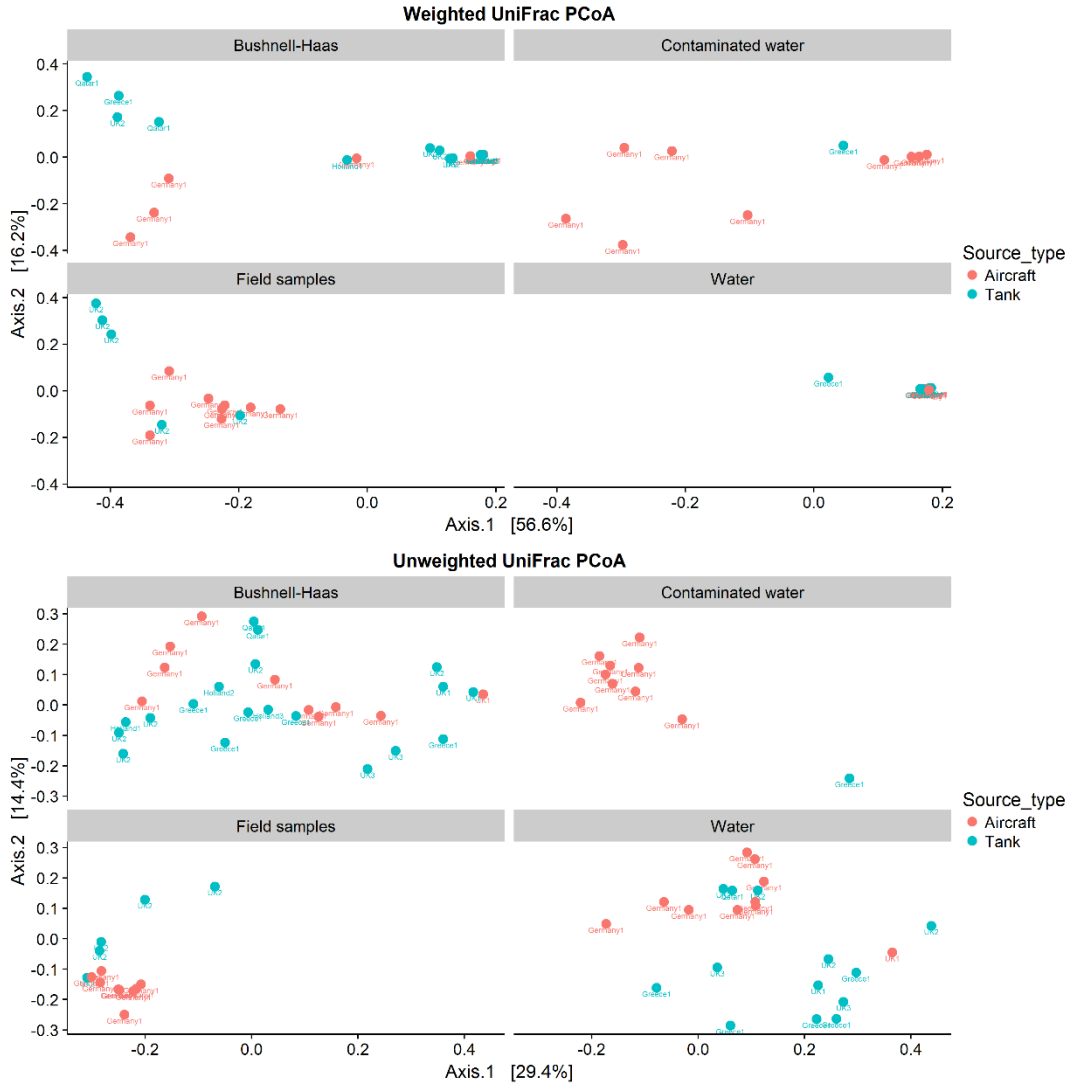

Figure 2.23 – Weighted and unweighted PCoA, using a UniFrac distance measurement on all prokaryotic samples. Plots show the distances between communities taken from aircraft in comparison to ground storage tanks for each treatment type and location.

2.4 Discussion

It has long been known that environments rich in hydrocarbons, such as n-alkanes can support microbial growth (Miyoshi 1895), but problems arising from microbial contamination of aircraft have only been documented since the 1950s and 60s (Balster *et al*. 2009). Historically culture-dependent methods have been used to identify microbial contamination in aircraft (Gaylarde *et al*. 1999; Rauch *et al*. 2006; White *et al*. 2011). Ruiz *et al.* used culture-independent methods to analyse the impact of jet fuel exposure to marine bacterial communities (Ruiz *et al*. 2015), though no culture-independent analysis has been done on microbial communities in aircraft. Using culture-dependent methods introduces a well-documented bias during analysis, specifically underestimating microbial numbers within a community as microorganisms most able to grow on the selected media are preferentially selected. Therefore, it is highly likely that previous studies have underestimated the number and diversity of microorganisms within the jet fuel supply chain.

Another common method for analysing microbial contamination in jet fuel supply is the use of laboratory microcosms - controlled environments used to replicate environmental conditions found in the field. When analysing fuel systems, typically a nutrient-rich mineral medium, Bushnell-Haas, is used in place of water (Bento *et al*. 2005; Ruiz *et al*. 2015; Soriano *et al*. 2015). Bushnell-Haas is preferred, as it provides all of the nutrients required for growth, with the exception of carbon, which is provided by the fuel; thus ensuring that there are no growth limitations within the microcosm. However, in the field, microbial communities are not exposed to such eutrophic conditions. Therefore, it is likely that these enriched environments select for the microorganisms best suited to utilising them, introducing another bias.

In this study typical microbial communities found in jet fuel systems have been examined. To get an idea of the true composition of these communities, both culture-dependent and culture-independent techniques have been used, with a view to understanding their likely response to changes in environmental conditions, such as geographical location. Comparative studies between microbial communities found in ground storage tanks, against those from aircraft wing tank, have also been undertaken. Potential biases introduced by using culture-dependent techniques and nutrient rich mineral media have also been explored.

2.4.1 How do cultured-dependent and cultured-independent microorganisms compare?

The results show that Proteobacteria, Actinobacteria, Firmicutes and Bacteroidetes are all present in jet fuel systems. The most frequently isolated microorganisms when employing culture-dependant techniques were Proteobacteria, with Gammaproteobacteria dominant. Ascomycota were the most frequently isolated eukaryotes, though Basidiomycota and a Glomeromycota were also identified.

When isolating microorganisms, a richer prokaryotic community was obtained with approximately twice as many prokaryotic taxa identified compared to eukaryotic taxa (24 prokaryotes, 11 eukaryotes). This may be due to there being a higher diversity of prokaryotes present in the field samples, or the media used may provide more favourable growth conditions for a wider range of prokaryotes. Culture-dependent techniques cited in the literature show that Proteobacteria and Ascomycota are the most frequently isolated phyla for prokaryotes and eukaryotes respectively. However, in the literature, Actinobacteria make up approximately 25-30 % of the microorganisms isolated (Rauch *et al*. 2006). This suggests that Actinobacteria are largely underrepresented in the microorganisms isolated in this study. Most eukaryotic microorganisms currently known to exist in jet fuel systems are Ascomycota, with the remaining organisms from the division Basidiomycota (Rauch *et al*. 2006). However, the predominant class of known microorganisms are Eurotiomycetes, which were not isolated in this study, suggesting they are underrepresented in this sample set (see Tables 1.1 and 1.2). It is unclear as to why these classes are underrepresented, potentially changes in media or other growth condition, such as temperature may account for this. With the above exceptions, the microorganisms identified in this study correlate well with the literature.

Comparatively, the culture-independent analyses also show that Proteobacteria, Actinobacteria, Firmicutes and Bacteroidetes were the dominant prokaryotic phyla, with Ascomycota and Basidiomycota the dominant eukaryotic phyla. This correlates well with the cultured microorganisms. However, approximately 220 unique OTUs (158 prokaryotes, 64 eukaryotes) were identified using culture-independent analysis compared to 35 unique OTUs (24 prokaryotes, 11 eukaryotes) using culture-dependent analysis. This would suggest that using culture-dependent analysis identifies approximately 16 % of the microorganisms in jet fuel systems and over represents eukaryotic microorganisms in these communities. These results highlight the implicit bias between culture-dependent and culture-independent analyses.

This is of particular significance for the field analysis of microbial contamination in jet fuel systems, by operators. Four of the seven currently approved test kits recommended by IATA are culture-dependent methods (including the reference test method) (Anon. 2015). Though it is likely that cultivable microorganisms will be present in samples taken from the field, it is not definite and the quantity of viable microorganisms would be unknown. Additionally, it is thought that "*the majority of biomass fouling fuel tanks and filters will be due to a relatively few fungal species*" (Anon. 2016a). This study has found, using qPCR, that eukaryotes are not always present at detectable levels in field samples (eukaryotic DNA was present in ~53 % of the field and microcosm samples); though they have grown when field samples with no detectable eukaryotic DNA present were used as an inoculum in a microcosm and must therefore be present in low levels. Therefore, kits that are specifically designed to detect eukaryotes may not be fit for purpose when detecting microbial contamination of jet fuels. This could potentially lead to underestimating the levels of contamination in an aircraft or in the worst case return a false negative result, increasing maintenance costs and potentially impacting on aircraft safety.

2.4.2 What are the dominant microorganisms?

Although approximately 150 prokaryotic OTUs were observed across the sample set, only 23 were present at a relative abundance above 3 %. Notably *Cellulosimicrobium sp*. was particularly dominant, present in all of the samples and accounting for more than 99 % of the OTUs in some samples (minimum ~0.3 %). To the author's knowledge, this has not been identified as a contaminant in jet fuel systems before. Other prokaryotes were present in a large abundance, predominantly from the phyla of Proteobacteria and Actinobacteria.

The *Cellulosimicrobium* genus was originally reclassified in 2001 by Schumann *et al*. from *Cellumonas sp*. (Metcalfe & Brown 1957). Gram-positive Actinobacteria from the family Promicromonosporaceae, they have been identified in environments such as soils (*C. cellulans* and *C. terreum*) (Schumann *et al*. 2001; Yoon *et al*. 2007) and fresh water reservoirs (*C. aquatile*) (Sultanpuram *et al*. 2015). In rare cases *C. funkei* has also been recorded as an opportunistic human pathogen (Brown *et al*. 2006)[49].

Both aerobes and facultative anaerobes, *Cellulosimicrobium sp*. are chemoorganotrophs; organisms with the ability to oxidise chemical bonds in organic compounds to obtain carbon.

[49] Additionally, *C. variabile* was isolated from the hindgut of Australian termites (*Mastotermis darwiniensis* (Froggatt)) (Bakalidou *et al*. 2002), though this has since been reclassified to *Isoptericola variabilis* (Stackebrandt *et al*. 2004).

They favour temperatures ranging between 4-55 °C (25-30 °C optimal) and pH of 6.0-9.0 (6.5-7.5 optimal) in a weak saline environment (0-9 % (w/v) NaCl solution (1-5 % (w/v) optimal)) (Sultanpuram *et al*. 2015; Yoon *et al*. 2007). Laboratory studies have demonstrated the *Cellulosimicrobium sp*. utilise a wide range of sugars as a carbon source (Sultanpuram *et al*. 2015; Yoon *et al*. 2007). However, field studies have demonstrated that *Cellulosimicrobium sp*. have the ability to degrade n-alkanes and polyaromatic hydrocarbons (PAHs) from biodiesel and crude oil contaminated waters and soils (Davolos & Pietrangeli 2007; Nken *et al*. 2016; Yenn, 2015).

Jet fuel systems, are carbon rich and regularly provide optimal growth conditions for *Cellulosimicrobium sp*. These systems typically become contaminated by water ingress and soil particulates (Rauch 2006), environments where *Cellulosimicrobium sp*. are well documented. It is likely that *Cellulosimicrobium sp*. enter jet fuel systems through airborne particulates and, in conjunction with their chemoorganotrophic ability, utilise the abundance of n-alkanes to thrive in a relatively niche environment that provides favourable growth conditions.

Of the eukaryotes, approximately 50 distinct OTUs were observed, with only 11 being present at a relative abundance above 3 %. These were dominated by the yeasts of the order of Saccharomycetales, where 6 different OTUs were observed. Since the 1950s, the fungus *Hormoconis resinae* (formerly *Cladosporium resinae* and now *Amorphotheca resinae*) has been the predominant microorganism attributed to microbial contamination of jet fuel systems (Hendey 1964; Finefrock & London 1966; Mcdougall 1966). *Amorphotheca sp.* was found in 33 of the 35 samples sequenced where eukaryotic DNA was detectable. However, 2 of the samples returned no *Amorphotheca sp.* OTUs and 37 samples contained no eukaryotic DNA. The lack of *Amorphotheca sp*. in all samples has a similar significance to the culture-dependent techniques. One of the International Air Transport Association (IATA) approved field test kits is an enzyme-linked immunosorbent assay (ELISA) detecting *Amorphotheca resinae* (Anon. 2015). Without the presence of *A. resinae* this test kit will not work, potentially returning false negative results. However, it should be noted that a new generation of ELISAs has been produced for use with contaminated free water associated with jet fuel, identifying general bacteria and fungi, as well as *A. resinae,* which potentially mitigates the reliance on one species. The molecules being detected by this kit are proprietary information, however, similar to the single species test kit, if the molecules being

detected are not present, this test kit will not work, potentially returning false negative results.

Historical culture-dependent analyses of jet fuel system contamination has suggested that microbial communities are dominated by eukaryotic microorganisms (Elphick 1970; Salvarezza *et al*. 1981; Stowe 1995). More recent data has suggested that prokaryotes are more dominant (Smith 1991; Raikos *et al.* 2011). The culture-independent analysis undertaken in this study has shown that across this sample set the richness of prokaryotic taxa was higher than eukaryotic taxa and qPCR data has definitively shown that prokaryotic taxa were present in all of the field samples compared to the eukaryotic taxa, which were not always present at detectable levels (thought they were present, as eukaryotes grew in microcosms inoculated with field samples where no eukaryotic DNA was detected).

One OTU of the Glomeromycota phylum was detected in the eukaryotic data set during sequencing. Glomeromycota are arbuscular mycorrhizal fungi, which form symbiotic relationships with plant roots. Though there is some circumstantial evidence that mycorrhizal fungi can exist outside of their symbiotic relationships and in the presence of *Paenibacillus sp*. (Hildebrandt *et al*. 2006; Hempel *et al*. 2007), it is unlikely that they are commonly found or playing a key role in microbial contamination of jet fuel systems and this is either a) a misidentification in the sequencing database, b) a potential bias in the primers (particularly common in eukaryotes) or c) a contaminant that has been brought into the fuel with airborne dirt particles. Strong correlations have been previously observed between the taxonomic profiles of jet fuel systems and nearby soil samples (Rauch *et al*. 2006). This issues could also be applied to other microorganisms detected in this study, such as *E. coli* (common in the gut microbiome) or *Erwinia sp.* (a plant pathogen). The likelihood of misidentifying microorganisms at a 97 % similarity is high, as species share similar or even identical 16S rRNA sequences at this similarity (Janda & Abbott 2007). Further samples would need to be analysed to determine whether Glomeromycota and other such taxa are a common contaminant of jet fuel systems.

2.4.3 How diverse are the microbial populations in different samples?

The jet fuel supply chain is a global network, spanning many countries and crucially many different environments. Environmental influences such as geographical location and climate, as well as the type of tank[50] that samples are drawn from are bound to have an influence on

[50] Tank design will have a large impact on microbial contamination, due is impacts the ability to remove free water. Typically jet fuel tanks are cone down, so that water can be drained from the tanks lowest

the microbial communities found in those systems. However, due to the restrictive nature of the samples taken in this study it is not possible to make statements about these factors. Further study, with an increased number of replicates from the sample location and an increase knowledge of the climate and tank conditions would be needed to draw any firm conclusions.

2.4.4 How does introducing the microbial communities to a microcosm affect diversity?

Nutrient rich microcosms have typically been used to analyse microbial communities found in jet fuel systems for decades (Passman *et al*. 2001). Coupled with culture-dependent techniques, this method has been used to build up a picture of microbial community structure. However, these techniques come with well-documented biases (Staley 1985; Brock 1987; Amann *et al*. 1995), as outlined above. Having examined the diversity of microbial communities found in jet fuel systems, using culture-independent techniques, analysis was undertaken in an effort to understand the effects of nutrient rich mineral media (Bushnell-Haas) on community structures.

The results showed that introducing a prokaryotic community into a microcosm containing Bushnell-Haas nutrient medium reduced the species diversity. However, this decrease in species diversity is observed in all the microcosm treatments. Conversely no statistical difference in the diversity of the eukaryotic communities was observed after introduction into a microcosm. Eukaryotes accounted for approximately 7 % of the overall population (predicted by the Chao1 index) before being introduced into the microcosms, rising to around 15 % after incubation a microcosm. These favourable conditions provided to eukaryotic communities, may be one reason why historically it was thought that eukaryotes dominated aircraft fuel systems microorganisms (Elphick 1970; Salvarezza *et al*. 1981; Stowe 1995; Racicot *et al*. 2007). However, although it appears as though utilising a microcosm-based system does affect the microbial communities within them, the results are not conclusive. Further investigations need to take place incubating field samples under differing conditions in conjunction with controls (untreated field samples) over time to more rigorously show the effects of different treatments. This would require repeat samples from an aircraft or storage tank over time, which were unavailable for this study.

point. However, designs such a floating roofs, fixed roofs or underground storage tanks affect this. There is also a great deal of diversity in aircraft fuel tank design.

2.4.5 How does utilising Bushnell-Haas instead of water affect microbial communities in microcosms?

As well as examining the impact of microcosms on microbial communities, the impact of replacing water with a nutrient-rich mineral medium (Bushnell-Haas) was also examined. These experiments used contaminated jet fuel, instead of contaminated water, so it was expected that diversity in these samples would decrease as a result. Results show an approximate 50 % drop in species diversity when compared against communities taken from microcosms inoculated with contaminated water (75 % compared to the field samples).

Using nutrient-rich mineral media had an impact on prokaryotic communities. Species richness was significantly different between the Bushnell-Haas and water microcosms. Whilst no significant difference was observed in the inverse Simpson index, differences were observed using the Shannon index. This indicates that these treatments had no effect on diversity when taking into account the relative abundance of the microorganisms present. However, when relative abundance is not taken into account, diversity decreases less in the Bushnell-Haas treated microcosms compared to the water treated microcosms. Additionally, no growth measurements were undertaken during this experiment, so the impact of the Bushnell-Haas and water treatment cannot be examined. Further work needs to be undertaken to monitor the growth of microorganisms in these systems over time.

From the literature, Bushnell-Haas is typically used in microcosms to grow microbial communities found in jet fuel systems (Edmonds & Cooney 1967; Stowe 1995; Jung *et al*. 2002; Buddie *et al*. 2011). Our results show that this does not have a significant impact on the species diversity in these experiments, when taking into account the relative abundance of the microorganisms compared to water treatment. However, significant differences are observed when comparing the field samples with the microcosm samples indicating that incubations affect the microbiology of the fuel systems. Another approach could be to use a water-based system, with regular replenishment of jet fuel plus associated micronutrients, which may potentially yield a more representative result, because it more closely replicates conditions observed in the field. This would be best employed on sessile communities (biofilms), as planktonic communities would be removed whilst replenishing the system, though further experimental work needs to be undertaken to test this concept.

Initial work was done on attached communities formed from planktonic field samples; obtaining biofilms samples from the field is difficult as it requires tanks to be taken out of

service, drained and vented to gain access. It would however, be beneficial to characterise biofilm samples from the field if they could be obtained.

2.4.6 How do microbial communities in aircraft wing tanks compare to ground storage tanks?

The PCoA and DESEQ2 analysis showed the microbial communities from aircraft wing tanks differed from those found in ground storage tanks. These differences are likely to arise from the harsher aircraft wing tank environment compared to ground storage tanks (Zabarnicm & Ervin 2010); this exerts a powerful selection pressure on the aircraft wing tank communities.

Aircraft wing tanks differ from ground storage tanks in two significant ways. Firstly, the air space in wing tanks is rendered inert during flight[51] (nitrogen is pumped into the tanks to prevent the fuel from igniting). This nitrogen rich atmosphere, restricts the level of available oxygen to around 12 %. Though we do not expect that this will have a significant impact on the microbial communities, as oxygen levels are still relatively high, it is a possible selection pressure. Further experimental work needs to be done to analyse the effect of fluctuating oxygen levels on microbial communities in aircraft wing tanks. The second significant difference is temperature cycling of aircraft fuel systems. The maximum freeze point of the commonly available jet fuels (Jet A and Jet A-1), are -40 °C and -47 °C respectively. During flight, bulk fuel temperatures are required to be 3 °C higher than the maximum freeze point (Zabarnicm & Ervin 2010). However, the extremities of the tank (where the microbial communities are typically found as attached biofilms) are subjected to the harshest conditions. In these areas it is conceivable temperatures could range between +40 °C and -50 °C, between take-off and landing. This extreme temperature fluctuation causes any free water to go through freeze-thaw cycles. Any microbial communities must be able to withstand this. Therefore, it is likely that fewer microorganisms are adapted to these conditions possibly leading to less variation in aircraft wing tank communities compared to those in ground storage tanks.

Also, the majority of the samples taken from aircraft wing tanks were taken from one airport in Germany. Little diversity in the sampling location would also account for lower variation

[51] Inerting systems have been utilised in the aviation industry since 1996. Explosions on board 3 aircraft have been attributed to an explosive atmosphere being generated on warm day within the centre tank of aircraft with minimal fuel volumes on board. Therefore, oxygen levels are restricted to 12 % in the fuel tanks, to prevent explosions.

in the communities. Therefore further analysis needs to be done on a more diverse sample set to see how variable microbial communities are within aircraft wing tanks.

2.5 Conclusion

In conclusion, this study has found that:

- Microbial communities in jet fuel systems are composed of the phyla of Proteobacteria, Actinobacteria, Firmicutes, Bacteroidetes, Ascomycota and Basidiomycota. Within these phyla Gammaproteobacteria and Saccharomycetes are dominant for prokaryotes and eukaryotes respectively. More prokaryotic OTUs are present in these communities than eukaryotic OTUs.
- Although culture-dependent and culture-independent analyses identified OTUs from similar Classes, culture-dependent analysis detected significantly fewer OTUs and therefore underestimated the diversity of the microorganisms present in these systems Prokaryotic DNA was present in all samples, whereas eukaryotic DNA was present in approximately 50 % of the samples. There was no discernible pattern in relation to geographic location or treatment type. Therefore, eukaryotes are a poor choice as an indicator species for test kits assessing microbial contamination in the field.
- *Cellulosimicrobium sp*. a previously undocumented genus in aviation systems, is the dominant microorganism within these systems and is present in all of the samples.
- *Hormoconis resinae* is not present in all of the samples as previously stated, which potentially impacts field operating procedures as current field test kits may return false negatives. This has the potential to a) increased maintenance and repair costs and b) impact on aircraft safety.
- Culture-independent analysis showed that although microbial communities in jet fuel systems are diverse they are dominated by relative few OTUs.
- Geographic location appears to have little impact on microbial community composition. However, this is a limited dataset and more research needs to be undertaken to fully understand the impact of geographical location on microbial community dynamics with aircraft fuel systems.
- Introducing a prokaryotic microbial community taken from the field, into a microcosm in this study caused a significant decrease in species diversity regardless of treatment type. Conversely, no significant differences were observed in the eukaryotic microbial communities.
- Although species richness in the prokaryotic communities decreased across all treatment types, utilising Bushnell-Haas nutrient medium to incubate fuel samples

caused less of a decrease in species richness when compared with water. No significant change in the eukaryotic communities was observed.

- The richness of microbial communities taken from aircraft wing tanks is higher than those taken from ground storage tanks.

Chapter Three

How will novel fuels impact microbial contamination in jet fuel systems?

This chapter was published at IASH 2015. See Appendix A.

McFarlane, A. E., Thornton, S. F. and Rolfe, S. A. (2015). How will novel fuels and materials impact microbial contamination in aircraft fuel systems? *International Association for Stability, Handling and Liquid Fuels (IASH)*. Charleston, South Carolina.

3.1 Introduction

For over 50 years, the uncontrolled bio-deterioration of fuel has been problematical in the aviation industry (Balster *et al*. 2006; Raikos *et al*. 2011). The abundance of hydrocarbons found within jet fuel systems provides a significant carbon source for those microorganisms that are able to survive exposure to fuel and have the capacity to metabolise components within it. Additional components within the fuel also have a large impact on the growth of microbial communities. Jet fuel systems inevitably contain water, which is also essential for active microbial growth (Mara & Horan 2003). Whilst water ingress can be minimised by tightly-controlled facility designs, handling procedures and housekeeping measures (Anon. 2015), even small amounts of water can lead to accumulation of microbial biomass. Microbial growth can also lead to fuel/additive degradation, corrosion and production of metabolic by-products that can disarm filter coalescers (White *et al*. 2011). Water enters fuel systems via fuel handling and storage activities, as vapour from natural gas exchange or rain water ingress, and in aircraft, significant amounts of water enter the fuel tanks during descent. Once associated with the fuel, water can exist in three states: dissolved, free water in suspension or free settled water. This fuel/water mixture forms a complex multiphasic system in contact with the fuel container surface and creates a diverse range of environments for microbial growth. Microbial growth in planktonic and sessile phases is a widely documented problem, and several previous studies have characterised microorganisms in jet fuel systems (Denaro *et al*. 2005; Rauch *et al*. 2006; Brown *et al*. 2010; Raikos *et al*. 2011).

Our understanding of the factors that govern microbial growth in current fuel systems is far from complete. In addition, the introduction of alternative fuels and novel composite materials into the supply chain is likely to significantly alter microbial community structure and function. For example, modern fuels differ in composition from conventional jet fuel in terms of hydrocarbon content and reduced aromatic/sulphur levels (Stratton *et al*. 2011). There is also a shift in construction materials moving from traditional metallic compounds to carbon composites. As well as altering physical properties (and thus influencing microbial attachment and biofilm formation), surface chemistry will also change (for example the ability to act as a redox acceptor or donor). It is to be expected therefore that these changes in environmental conditions will influence microbial growth and dynamics, potentially altering risks in the jet fuel supply chain.

The main goal of this chapter is to determine how microbial development and fuel degradation respond to the introduction of alternative fuels. A laboratory microcosm-based

approached was used to examine how isolates of industry-relevant microorganisms respond to alterations in fuel composition. Spectrophotometry and fluorescent microscopy were used to assess their growth rate. Gas chromatography-mass spectrometry (GC-MS) and ion chromatography were used to identify hydrocarbon and nutrients required for growth. These studies were then extended to explore the response of complex microbial communities to variations in fuel type, using a culture-independent approach. Overall this study increases our understanding of how the introduction of alternative fuels is likely to impact current microbial populations in jet fuel systems, which is central to maintaining aircraft safety.

3.1.1 Chapter aims and objectives

This study aims to determine the main factors governing microbial development and fuel degradation in jet fuel systems, and how industry-relevant isolates and complex communities respond to the introduction of alternative fuels.

The main objectives of this chapter are:

a) To understand the factors that govern the growth of industry-relevant microorganisms in jet fuel systems, and;
b) Using these data, explore how these microorganisms respond to the introduction of novel fuels;
c) To expand the study using culture-independent methods to understand how complex communities respond to variations in fuel composition, and;
d) Using these data, understand how the introduction of alternative fuels is likely to affect these communities and predict any potential problems that may arise.

3.2 Materials and methods

3.2.1 Microorganisms

For the monoculture experiments, 4 microorganisms with a known capacity for hydrocarbon degradation were selected. Three of these were obtained from stock centres and represent industry-relevant microbial contaminants: a bacterium *Pseudomonas putida* (Strain designation: F1[PpF1]; ATCC reference number: 700007), a yeast *Candida tropicalis* (Strain designation: AL-6981-X; ATCC reference number: 48138), and a filamentous fungus *Hormoconis resinae* (Strain designations: CBS 174.61, NRRL 6437, QM 7998; ATCC reference number: 20495). Another bacterium (*Pseudomonas graminis*) isolated previously from contaminated fuel in this study was also included. The identity of each organism was confirmed by sequencing of the 16S rRNA genes (prokaryotes), and the ITS and 5.8S genes (eukaryotes).

For experiments on environmental isolates, 64 microorganisms isolated previously in this study from contaminated fuel/water were selected. The identity of these organisms was confirmed by sequencing both 16S rRNA (prokaryotes) genes and the ITS and 5.8S rRNA (eukaryotes). Some of these microorganisms remain unidentified because the ligation reactions outlined in Section 2.2.3 were unsuccessful and therefore the cloning process failed for these samples.

For experiments on fuel degradation, 12 microorganisms (a subset of the 64 isolates described above) were selected with suspected capacity for hydrocarbon degradation, based on the experiments outlined in Section 3.3.2. These were the 4 microorganisms noted above, and 6 additional identified microorganisms: *Novosphingobium resinovorum*, *Paracoccus sp.*, *Stenotrophomonas maltophilia* (prokaryotes), *Amorphotheca resinae*, *Sclerostagonospora sp.*, and *Yarrowia lipolytia* (eukaryotes), and two unidentified microorganisms.

For experiments with complex communities, a mixed community was obtained by combining 5 different microbial communities from contaminated Jet A-1 fuel storage systems.

3.2.2 Materials

Three fuels were supplied by Shell Research Ltd.: Merox-treated Jet A-1, Hydro-treated Jet A-1, and Gas to liquid kerosene (GTL). From these two fuel blends were created: 50:50 Merox-treated Jet A-1 : GTL kerosene and a 50:50 Hydro-treated Jet A-1 : GTL kerosene. Blends were created at a 50:50 ratio because this is how GTL kerosene is likely to be implemented in the field and therefore a direct comparison can be made between the pure

jet fuels, GTL kerosene and the fuel blends. Fuels and blends were sterilised by passing them through 0.22 µm nitrocellulose filter paper. To form a fuel/water interface the fuels were overlaid on sterile Bushnell-Haas nutrient medium (Sigma-Aldrich, UK).

For those microcosms that included a surface, a 304 stainless steel coupon (63 x 10 x 1 mm) was introduced. Coupons were degreased with acetone and then sterilized by soaking in absolute ethanol for 1 hour prior to use.

3.2.3 Microcosms

3.2.3.1 Monocultures

For experiments with monocultures, sterile 20 ml microcosms were set up using 7 ml of fuel or fuel blend and 7 ml of Bushnell-Haas medium (Sigma Aldrich, UK). This was placed in a gas chromatograph (GC) headspace vial sealed with a 20 mm polytetrafluoroethylene (PTFE)/Butyl rubber crimp lid. Gas exchange was allowed by introducing a 1-inch sterile needle capped with a PTFE 0.2 µm filter. A stainless steel coupon was added to each microcosm, so that the fuel-water interface was approximately a third of the way up the coupon. The coupon was angled at approximately 20^{o} to the vertical. Microcosms were inoculated with monocultures of the isolates at an optical density at 600 nm (OD^{600}) of 0.05. Sterile controls were also prepared. Microcosms were incubated at 25 ^{o}C and sampled destructively every week for 4 weeks. Three independent replicates were performed in each case, giving a total of 300 microcosms (see Figure 3.24).

3.2.3.2 Microcosm set up for GC-MS analysis

Separate microcosms were also set up for GC-MS analysis[52]. These contained 900 µl of sterile Bushnell-Haas medium and 100 µl of either Merox-treated Jet A-1, Hydro-treated Jet A-1 or GTL kerosene. Microcosms were otherwise treated as described above (see Section 3.2.3.1) but were not vented. Four independent replicates were performed for each organism, as well as a sterile control, giving a total of 60 microcosms (see Figure 3.24).

[52] Separate microcosms were set up separately for the GC-MS analysis because the carbon source (i.e. the jet fuel) in Section 3.2.3.1 was present in such excess that any hydrocarbon degradation could not be observed. This was discovered during preliminary experiments where 7 ml of jet fuel was used in the microcosms and subsampled for GC-MS analysis (the same set up from Section 3.2.3.1 was used and analysed as described in Section 3.2.5.2). It was found that a volume of 100 µl of jet fuel in conjunction with 900 µl Bushnell-Haas nutrient medium was a sufficiently small volume that hydrocarbon degradation could be observed, but was also sufficiently large not to volatilise entirely into the air space above the sample. Microcosms were not vented to prevent the jet fuel from volatilising into the atmosphere.

3.2.3.3 Environmental isolates

For growth studies on environmental isolates, sterile 15 ml microcosms were set up using 5 ml of Merox Jet A-1 or GTL kerosene and 5 ml of quarter strength Bushnell-Haas medium (Sigma Aldrich, UK). This was placed in a 15 ml glass tissue culture tube (Thermo Fisher Scientific, USA) and sealed with a vented aluminium LABOCAPS (VWR International, USA). Microcosms were inoculated with monocultures of the isolates at an OD^{600} of 0.05. Sterile controls were also prepared. Microcosms were incubated at 25 °C and sampled destructively after 2 weeks (see Figure 3.24).

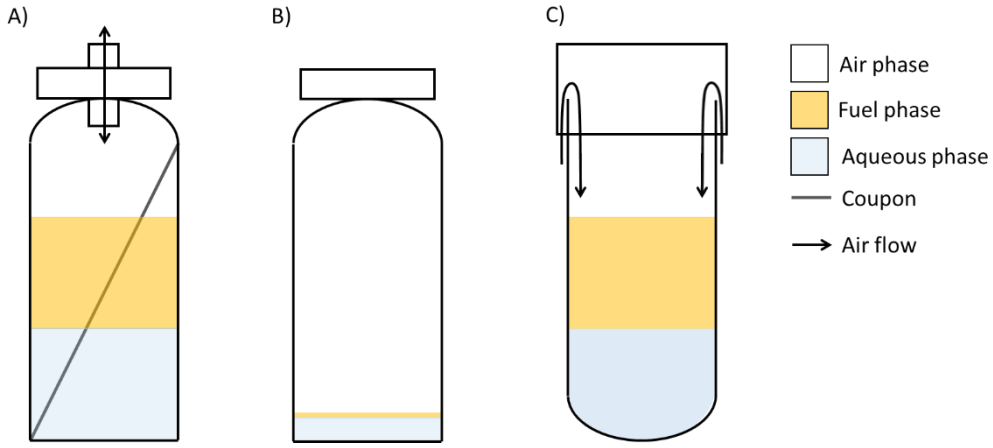

Figure 3.24 – Microcosms used in this experimental work. A) Microcosms used for monoculture experiments. B) Microcosms used for GC-MS analysis. C) Microcosms used for environmental isolates.

3.2.3.4 Mixed communities

Microcosms were set up using 100 ml of each fuel and 95 ml of sterile Bushnell-Haas nutrient medium. This was placed in a 250 ml Duran bottle with a polypropylene cap; gas exchange was allowed as above. Microcosms were inoculated with 5 ml of contaminated water and incubated at 25 °C for 14 days. After 14 days, 5 ml of the aqueous phase was withdrawn and used to inoculate a second set of microcosms with either the same, or a different fuel type. These were incubated at 25 °C for 14 days and then destructively harvested. Three independent replicates were performed in each case giving a total of 39 microcosms (see Figure 3.25).

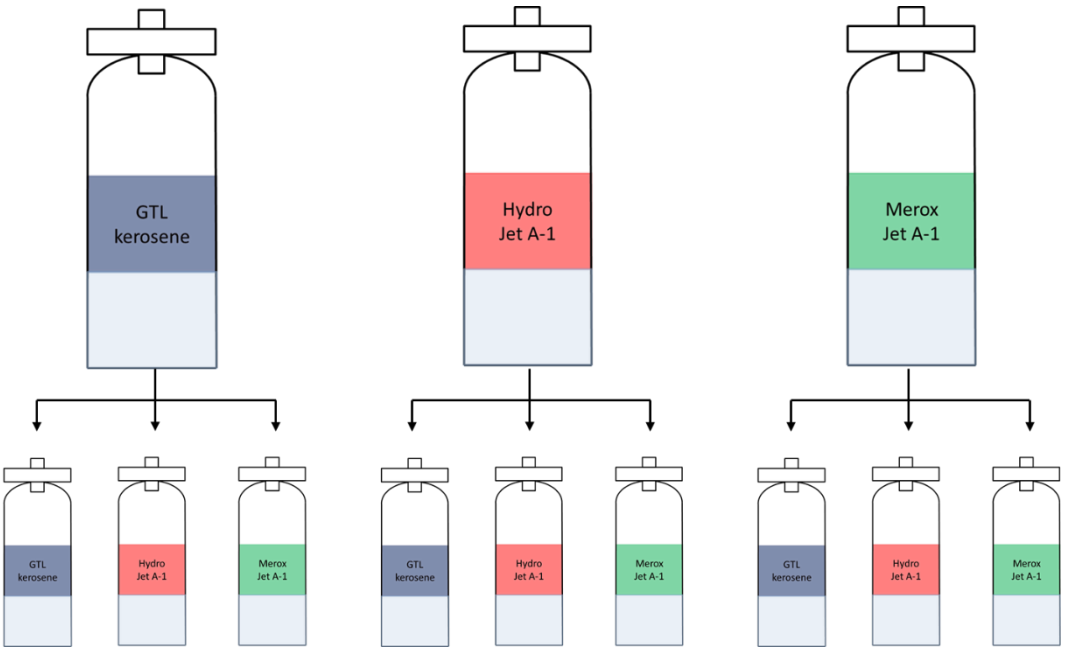

Figure 3.25 – Example of how the inoculum was transferred between the first and second series of microcosms.

3.2.4 Enumeration of microorganisms

For the enumeration of microbes in the aqueous phase, 2 ml aliquots of the Bushnell-Haas nutrient medium were withdrawn and the OD^{600} determined by spectrophotometry. For analysis of microorganisms attached to the coupons, the coupons were removed from the microcosms and fixed in a 4% (v/v) formaldehyde solution, then stained with SYTO 9 DNA stain to visualise microbial cells and SYPRO Ruby Biofilm Matrix Stain to visualise biofilm matrix components (proteins) (Life Technologies, USA). One millilitre of the SYPRO Ruby was applied to the surface of each coupon and incubated in the dark at room temperature for 25 minutes, then 800 µl of filtered 1x SYTO 9 solution was applied and incubated for a further 5 minutes. The coupons were washed gently with filtered deionised water, a coverslip applied and imaged immediately by either a) epifluorescence microscopy (Olympus BX-51) or b) confocal laser scanning microscopy (CLSM) (Zeiss LSM510 Meta). Epifluorescence images were taken using 10x and 40x objectives and CLSM images were collected using an EC Plan-Neofluar 40x objective with excitation at 488 nm from an argon laser. SYTO 9 fluorescence was selected using a 500-550 nm band pass filter whilst SYPRO Ruby was selected using a 650-710 nm band pass filter. CLSM images were 1252 x 1252 pixels in size (0.17 µm/pixel) and acquired at 0.89 µm intervals. Typically, 15-20 image stacks were taken per sample, which were processed using Axiovision software (Zeiss, Germany).

3.2.5 Chemical analyses of microcosms

3.2.5.1 Major ions

Samples were passed through a 0.2 µm polycarbonate syringe filter (Thermo Fisher Scientific, USA) to remove particulates. A two-fold dilution was prepared in filtered distilled water and samples analysed on an ICS 3000 ion chromatography system with auto-sampler and eluent regeneration (Thermo Fisher Scientific, USA). Ten microliters of each sample were analysed for anions in a 31 mM sodium hydroxide solution at a flow rate of 0.25 ml/min on 2 x 250 mm AS18 columns with AG18 guards (Thermo Fisher Scientific, USA). Twenty microliters of each sample were analysed for cations in a 48 mM methane sulphonic acid solution at a flow rate of 0.42 ml/min on 4 x 250 mm CS16 columns with a CG16 guards. Chromatograms were analysed using the Chromeleon v6.80, and the data analysed using Metaboanalyst v3.0 (Xia & Wishart 2011).

3.2.5.2 Gas chromatography-Mass spectrometry (GC-MS)

Microcosms were centrifuged at 2,500 x *g* for 2 minutes to prior to sampling to collect condensates from the microcosm walls. Both fuel and aqueous layers were then pipetted into a 2 ml microcentrifuge tube and 1 ml of ≥99% Dichloromethane (DCM) (Sigma-Aldrich, UK) was added. Samples were vortexed vigorously for 30 seconds and then incubated in a sonic bath for 10 minutes. Samples were then centrifuged at 10,000 x *g* for 1 minute and the bottom layer (DCM) was transferred to a 2 ml Cromacol crimp top GC vial (Supelco, USA) for GC-MS analysis.

Samples were analysed using an Agilent 7890B GC system coupled to a 7200 Accurate-Mass Quadrupole Time-of-Fight (Q-TOF) GC-MS (Agilent Technology, USA). The column was a 30 m x 0.25 mm i.d., 0.25 µm film thickness Zebron ZB-5MS column coated with 5% phenyl and 95% dimethyl polysiloxane (Phenomenex, UK). The oven temperature was programmed linearly from 60 to 300 °C at 10 °C per minute (with a 5 minute hold at 60 °C after injection). Mass spectra were scanned at 0.15 s intervals.

The raw Retention time/mass spectrum (Rt:m/z) data was converted from the Agilent .D format into .mzdata format using Agilent MassHunter Qualitative Analysis Workstation B.06.00 (Agilent Technology, USA) and processed using the xcms package (Smith *et al*. 2006) in R[53] (R Development Core Team 2008) (see Appendix E for script). This package identifies and aligns peaks, correcting for small changes in retention time. The range of scans for peak

[53] Additional packages used were: CAMERA 1.28.0, multtest 2.28.0, RANN 2.5, xcms 1.48.0, Biobase 2.32.0, ProtGenerics 1.4.0, BiocGenerics 0.18.0 mzR 2.6.3 and Rcpp 0.12.6.

detection was set from 900 to 9500 scans for the Merox- and Hydro-treated Jet A-1 samples. For GTL the scan range was smaller (950-6500 scans), reflecting the simpler hydrocarbon composition of this fuel (1 scan = 0.15 seconds). These scan ranges were selected so that only peaks attributed to the samples were analysed; the initial solvent peak and any background peaks from cleaning the column between samples were ignored. The peak width for peak detection was set at 6 fwhm, (50% of the peak width in seconds) and the maximum number of masses per peak was set at 200. The data were grouped to the nearest peak and retention times were adjusted by a maximum 2 seconds. The corrected Rt:m/z data were exported as a .csv file for further analysis in Metaboanalyst v 3.0 (Xia & Wishart 2011). Prior to statistical testing, data were filtered by interquartile range to identify and remove variables unlikely to be of use during modelling, and then normalised by median, log transformed and scaled by mean-centring the data, and dividing by the standard deviation. Statistical differences between m/z values in live microcosms and the sterile control were detected at each Rt and corrected for false discovery using the Benjamini-Hochberg option. Inspection of the data showed that a requirement for 10 or more masses to differ significantly between samples ($p \leq 0.05$) provided a useful balance between sensitivity and rejecting noise. Once the peaks of interest were identified, the background spectra were subtracted and the mass spectrum of each peak compared against the National Institute of Standards and Technology (NIST) mass spectral library for identification (see Appendix E for the analysis script). This produced a list of candidate peaks with tentatively assigned identification. Finally, the corrected m/z data for the complete mass spectrum of candidate molecules (normalised to the total ion count of the run) were obtained. The ratio of ion counts for each m/z peak in the mass spectrum was calculated and a t-test used to determine if this differed significantly from 1 (Minitab v17). The dataflow for the GC-MS analysis has been outline in Figure 3.26.

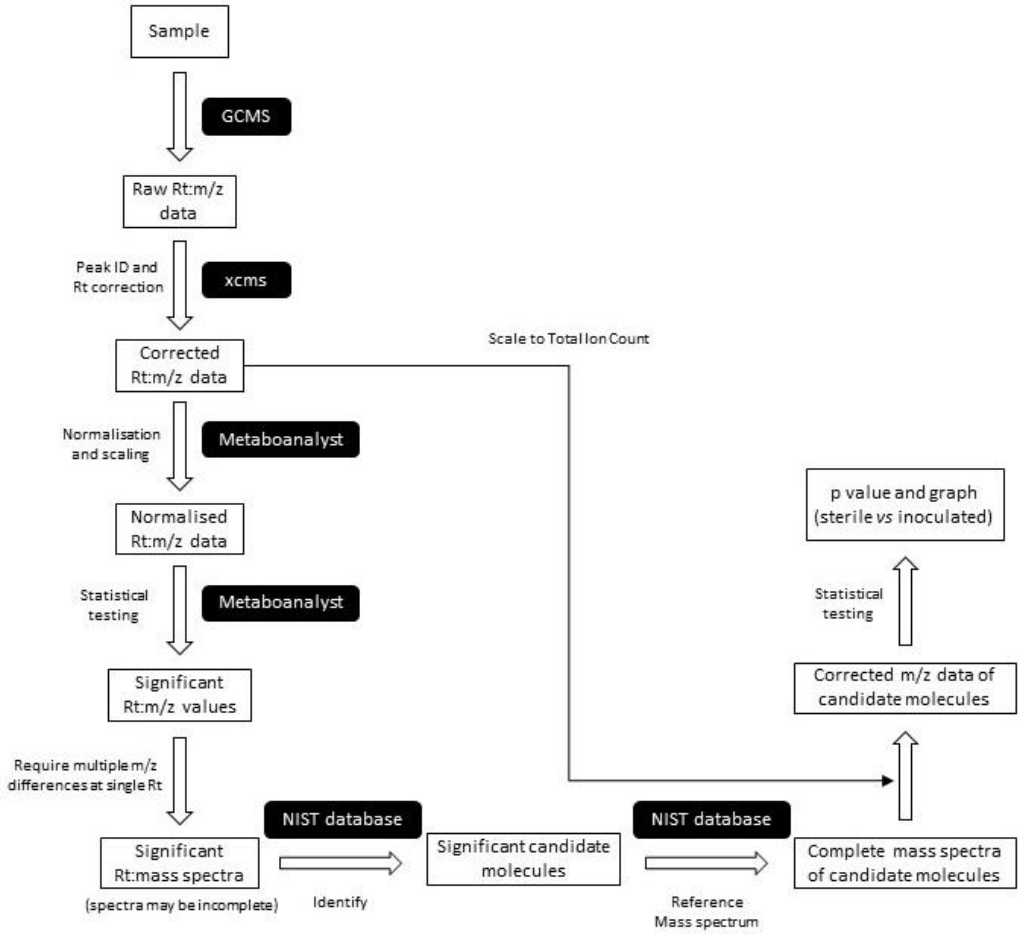

Figure 3.26 – Summary of the data flow for GC-MS analysis

3.2.6 Microbial community structure analyses

3.2.6.1 DNA extraction

Samples were collected from the microcosms, using a 2-inch sterile needle and 5 ml sterile syringe and filtering through a 0.2 µm polycarbonate filter paper, which was then placed into a 2 ml Eppendorf tube. One hundred and fifty microliters of sorbitol buffer[54], was added to the tube along with 3 x 3 mm sterile tungsten beads. Filters were then ground in a SPEX Centriprep 8000M Mixer/Mill (Glen Creston, UK) for 5 minutes. Fifty units of lyticase (Sigma-Aldrich, UK) were then added and the samples incubated at 30 °C for 30 minutes in a water bath. DNA extractions were performed using an UltraClean® Microbial DNA Isolation kit (MO BIO Laboratories, USA), directly following the manufacturer's instructions.

3.2.6.2 Amplification of 16S rRNA genes for T-RFLP

Two microliters of extracted DNA was amplified by PCR using 799F-FAM (5'-AACMGGATTAGATACCCKG-3', end labelled with 6-carboxyfluorescein (FAM)) (Chelius & Triplett 2001) and 1193R (5'-ACGTCATCCCCACCTTCC-3') (Bodenhausen *et al*. 2013). PCR was

[54] 1 M sorbitol, 500 mM EDTA (pH 8) and 10 mM 2-mercaptoethanol.

performed with an initial incubation period of 94 °C for 5 minutes, then 30 cycles of 94 °C for 30 seconds, 53 °C for 30 seconds and 72 °C for 1 minute with a final incubation step of 10 minutes at 72 °C. PCR products were confirmed by gel electrophoresis on 1% agarose gels and stained with ethidium bromide. Amplicons were purified using a QIAquick PCR purification kit (Qiagen, Germany), following the manufacturer's instructions. DNA was then quantified using PicoGreen fluorescence.

3.2.6.3 T-RFLP

Bacterial samples were analysed using terminal-restriction fragment length polymorphism (T-RFLP). Twenty five nanograms of purified 16S rRNA amplicons were digested with 10 U *Alu1*[55] (Promega, USA) in a 20 µl reaction at 37 °C for 3 hours. Five microliter aliquots were desalted by precipitation for 2 hours with 16.65 µl ice-cold 95% ethanol and 10 % (v/v) 3 M sodium acetate (pH 5.2) with 0.25 µl of 20 mg/ml glycogen as a carrier. Samples were then centrifuged at 14000 x *g* at 4 °C for 20 minutes and the pellets washed twice in 70 % (v/v) ethanol. The pellets were resuspended in 10 µl hi-di formamide containing 0.5% GeneScan 500 ROX internal size standard (Applied Biosystems, USA). Samples were then denatured at 95 °C for 5 minutes, cooled on ice and the DNA fragments separated using capillary electrophoresis using an ABI 3730 PRISM capillary DNA analyser (Applied Biosystems, USA). The T-RFLP electropherograms were analysed using Peak Scanner v1.0 (Thermo Fisher Scientific, USA). Noise was removed by only analysing T-RFs with peak heights >50 fluorescent units. Fingerprinted fragments were expressed in terms of peak area and aligned using T-REX (Culman *et al*. 2009) with a confidence interval of 0.8 nt.

3.2.6.4 Illumina sequencing

Samples were sequenced using the same pipeline described in Chapter 2 (see Section 2.2.4.2). However, demultiplexing was undertaken at the University of Sheffield, which provided data in four formats; unpaired reads from the forward and reverse primers, as well as paired reads from the forward and reverse primers. Reads which did not match any of these categories (taking into account a 1 bp mismatch in the primer) were discarded. Data quality checks showed that the forward paired data had Q values of Q20 and above at read lengths of 150 bp and above, with the eukaryotic reads overall having lower Q values than the prokaryotes. However, the quality of the reverse reads (paired and unpaired) was poor

[55] *Alu1* was selected because good separation of the *P. putida* 16S rRNA gene (the model organism in this study) was observed in Restriction Mapper (7 restriction sites) (Blaiklack, 2017). Additional analysis was also performed using the restriction enzyme *Cfo1* (Promega, USA) (5 restriction sites, *P. putida*) and the primer 1193R-HEX (Hexachloro-fluorescein), both as a separate end label and as a pair with 799F-FAM. None of these analyses yielded a T-RFLP electropherogram, therefore data not shown.

and were therefore discarded. The forward paired and unpaired reads, for both prokaryotes and eukaryotes, were merged to produce one dataset for each type of microorganism.

Prokaryotic sequences had a read depth that ranged between 68 and 309,978 reads per sample with an average of 74,405 reads per sample, and a pass rate ranging from 79.5 % to 92.0 % per sample, with an average of 87.9 % (maxEE value of 1.00) for the 150 bp read lengths. Eukaryotic sequences had a read depth ranged from 32 to 6,332 reads per sample with an average of 1,790, and a pass rate between 85.2 % and 93.4 % with an average of 91.5 % (maxEE value of 1.00) for the 150 bp reads. Chimeras were removed as previously described from the prokaryotic (2,967,711) and eukaryotic (70,701) datasets, leaving 2,901,804 and 69,825 sequences respectively. Taxonomy was then assigned using the Greengenes (prokaryotes) and UNITE (eukaryotes) databases (see Appendix D).

3.3 Results

To assess the response of common industry microorganisms to variation in fuel type, microcosms were set up consisting of a fuel or fuel blend overlaid on a defined mineral medium. The mineral medium provided all of the necessary nutrients for microbial growth with the exception of a carbon supply (provided by the fuel). The microcosms were inoculated with either microorganisms in monoculture or a mixed community sourced from a contaminated Jet A-1 storage tank. Growth in the monocultures was assessed at weekly intervals in the planktonic phase and as biofilms developed on a stainless steel coupon placed within each microcosm. Growth of the environmental isolates and fuel-degrading microorganisms was measured after two weeks. The impact of microbial growth on the composition of the aqueous and fuel phases was measured. Growth in the mixed community was determined by T-RFLP analysis of amplified 16S rRNA genes and by culture-independent analysis of both the 16S rRNA genes (prokaryotes) and ITS and 5.8S rRNA genes (eukaryotes), to determine how fuel type influenced community composition over time.

3.3.1 Growth of monocultures in different fuel types

Planktonic growth of the monocultures was compared across the five fuel types by measuring the OD^{600} of the aqueous phase (see Figure 3.27). Four microorganisms were tested: two prokaryotes (*Pseudomonas putida* and *Pseudomonas graminis*) and two eukaryotes (the fungus *Hormoconis resinae* and a yeast *Candida tropicalis*). Five hydrocarbon sources were used: Hydro-treated Jet A-1, Merox-treated Jet A-1, GTL kerosene and 50:50 blends of each Jet A-1 fuel with GTL kerosene. In microcosms containing a jet fuel, whether as a single component (Hydro- or Merox-treated Jet A-1) or as 50:50 blends of either with GTL kerosene, rapid growth from a starting OD^{600} of 0.05 to ~1 was seen in the first week in all cases. The microorganisms then entered the stationary phase with little change in OD over weeks 2-4 with the exception of *C. tropicalis* where there was a slight decline, due to the yeast precipitating out of solution over time. This difference was significant in the Merox-treated Jet A-1 and the Hydro-treated Jet A-1 (ANOVA, $p = 0.02$), but not in the two blends (ANOVA, $p > 0.05$). In contrast, much less growth occurred in the pure GTL kerosene samples with all 4 microorganisms tested. For *P. putida, P. graminis* and *C. tropicalis* growth in GTL kerosene was ~10% of that seen in the other fuels. For *H. resinae* it was somewhat higher at ~30% but this declined in weeks 2-4.

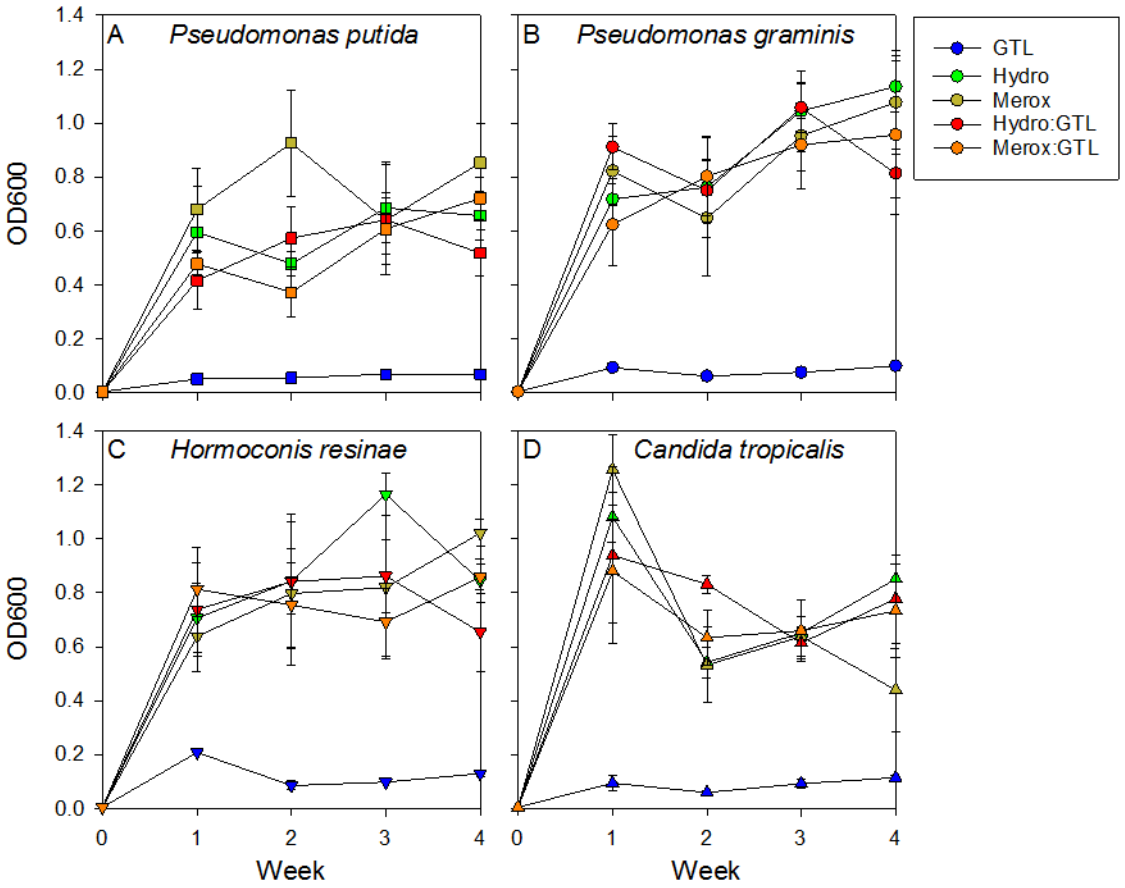

Figure 3.27 – Growth of isolated organisms in fuels or fuel blends. Results are means (n = 3) +/- S.E.

Biofilm formation on the stainless steel coupons mirrored the growth patterns seen in the planktonic phase. Figure 3.28 to Figure 3.31 show examples of typically observed biofilms formed by each isolate on a stainless steel coupon after 4 weeks incubation in microcosms containing Merox-treated Jet A-1 (A-C) and GTL kerosene (D-F), using epifluorescence microscopy. In the main images (A-F) and insert 1 cells fluoresce green (SYTO 9), whist in insert 2 matrix components fluoresce red (SYPRO Ruby)[56]. In all of the Merox-treated Jet A-1 samples, a heterogeneous biofilm of each isolate had formed. In each aqueous phase individual cells had attached with only a few colonies of cell clusters present. The individual cells and colonies had little EPS associated with them. Cell density was greatest in the proximity to the fuel-aqueous interface in all coupons. As well as many individual cells, larger colonies of cells were evident. Some limited production of EPS was evident in these colonies

[56] The images shown in this thesis are typical examples of the biofilms observed during this experimental programme. At present these images are purely qualitative in nature and no quantitative analysis has been undertaken.

as seen in inserts Figure 3.28 B-2. Many cells had also attached in the fuel phase with numerous but somewhat smaller colonies developing. This pattern was observed in all samples which contained a conventional jet fuel. In contrast, less growth was seen in the microcosms with prokaryotes containing GTL kerosene. For the eukaryotes similar growth to Jet A-1 was observed (although quantification of the attached growth would be required to confirm these observations).

Wide-field epifluorescence microscopy provided an overview of the colonisation of the coupons. Confocal Laser Scanning Microscopy (CLSM) was used to obtain more detailed images. As the growth patterns in the microcosms were similar only the *P. putida* samples were imaged in this manner. Figure 3.32 shows the *P. putida* biofilm in both the Merox-treated Jet A-1 (A-C) and the GTL kerosene (D-F). The main images and inserts shown are the same as the previous figures, with the exception of insert 3, which shows the combined emission signal from both stains. The faint green scaling seen in the CLSM images is not of biological origin. It developed in coupons placed in sterile microcosms during extended incubations. CLSM images showed that the cell clusters in the aqueous phase were 12-15 µm in height, with little matrix associated with them. At the fuel-aqueous interface the larger colonies were up to 50 µm across and 20 µm high. Some limited production of matrix was evident in these colonies as seen in Figure 3.32, B-2. The more numerous but smaller colonies attached in the fuel phase were typically 5-10 µm across and >10 µm high. Significant amounts of matrix were associated with the cells as shown by the strong SYPRO Ruby signal in Figure 3.32, A-2. This was not observed as clearly in the epifluorescence microscopy. Again, little growth was seen in the microcosms containing GTL kerosene.

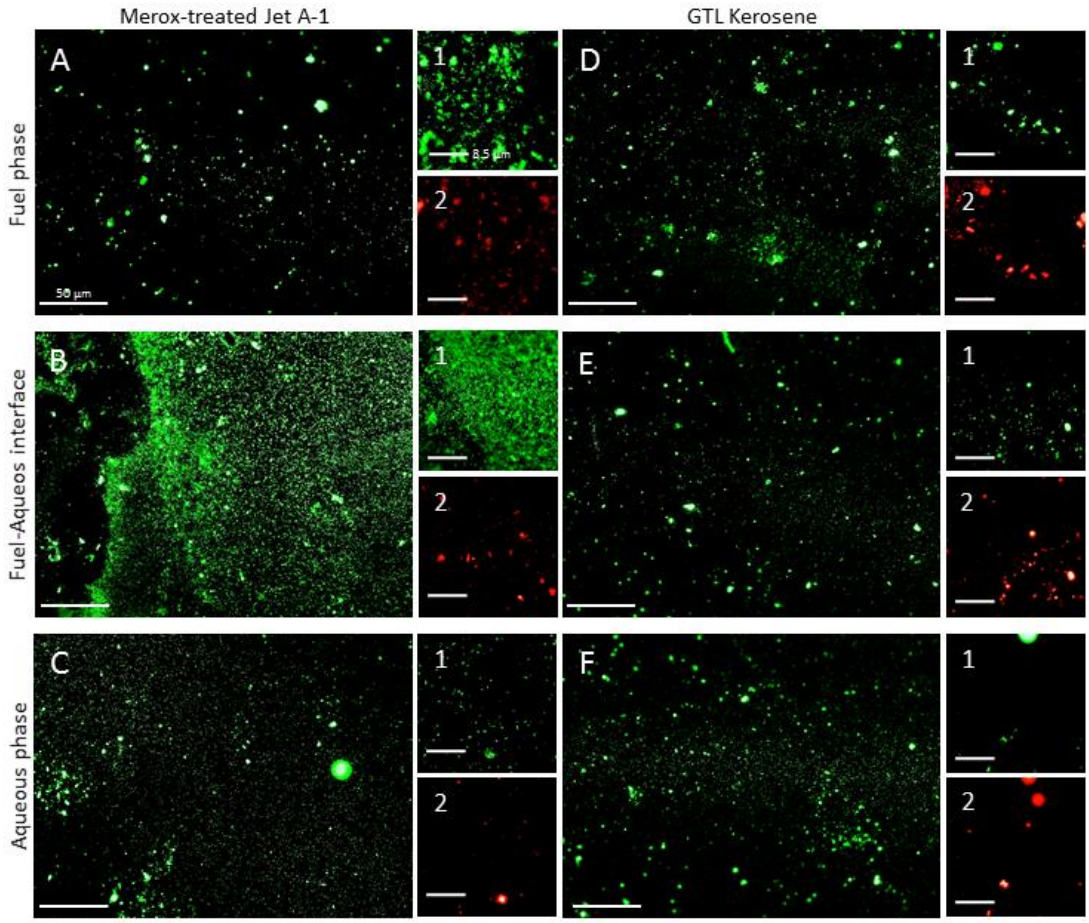

Figure 3.28 – Epifluorescence images of *P. putida* biofilms on stainless steel coupons incubated for 4 weeks in microcosms containing Merox-treated Jet A-1 (A-C) and GTL kerosene (D-F). Images were taken at different points along the coupon in the aqueous phase, at fuel-aqueous interface and in the fuel phase. The main image is a maximum intensity projection image in X and Y dimensions of the DNA stain SYTO 9. Close up images are shown as inserts of the SYTO 9 (1) and SYPRO Ruby (2) signals. Scale bars are 50 µm (main images) and 8.5 µm (insets).

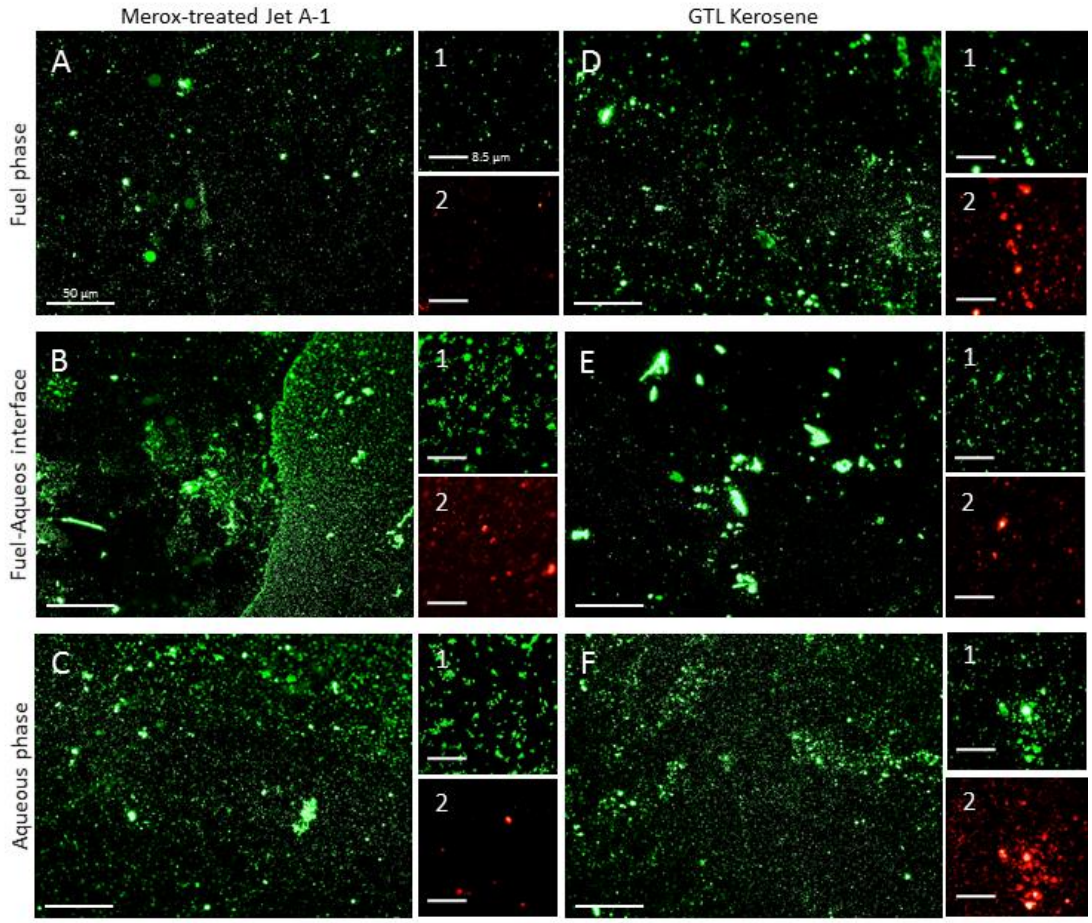

Figure 3.29 – Epifluorescence images of *P. graminis* biofilms on stainless steel coupons incubated for 4 weeks in microcosms containing Merox-treated Jet A-1 (A-C) and GTL kerosene (D-F). Images were taken at different points along the coupon in the aqueous phase, at fuel-aqueous interface and in the fuel phase. The main image is a maximum intensity projection image in X and Y dimensions of the DNA stain SYTO 9. Close up images are shown as inserts of the SYTO 9 (1) and SYPRO Ruby (2) signals. Scale bars are 50 µm (main images) and 8.5 µm (insets).

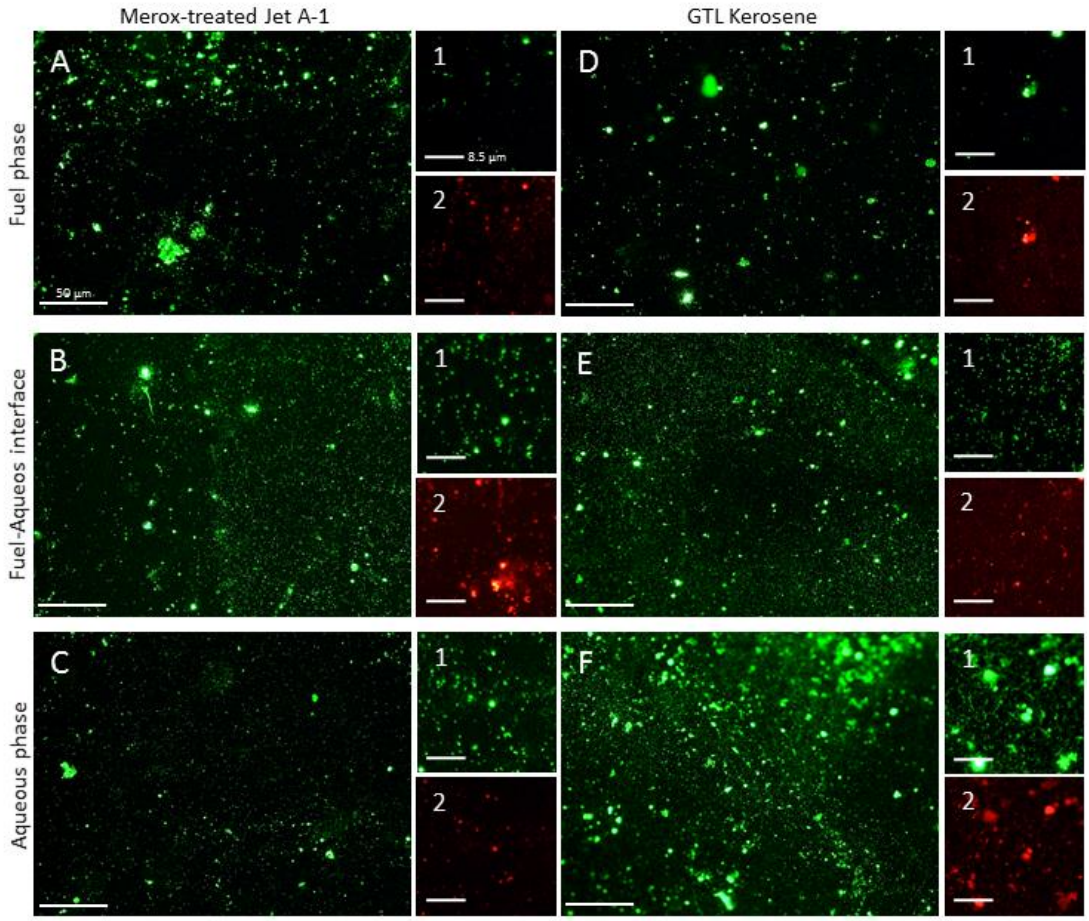

Figure 3.30 – Epifluorescence images of *H. resinae* biofilms on stainless steel coupons incubated for 4 weeks in microcosms containing Merox-treated Jet A-1 (A-C) and GTL kerosene (D-F). Images were taken at different points along the coupon in the aqueous phase, at fuel-aqueous interface and in the fuel phase. The main image is a maximum intensity projection image in X and Y dimensions of the DNA stain SYTO 9. Close up images are shown as inserts of the SYTO 9 (1) and SYPRO Ruby (2) signals. Scale bars are 50 µm (main images) and 8.5 µm (insets).

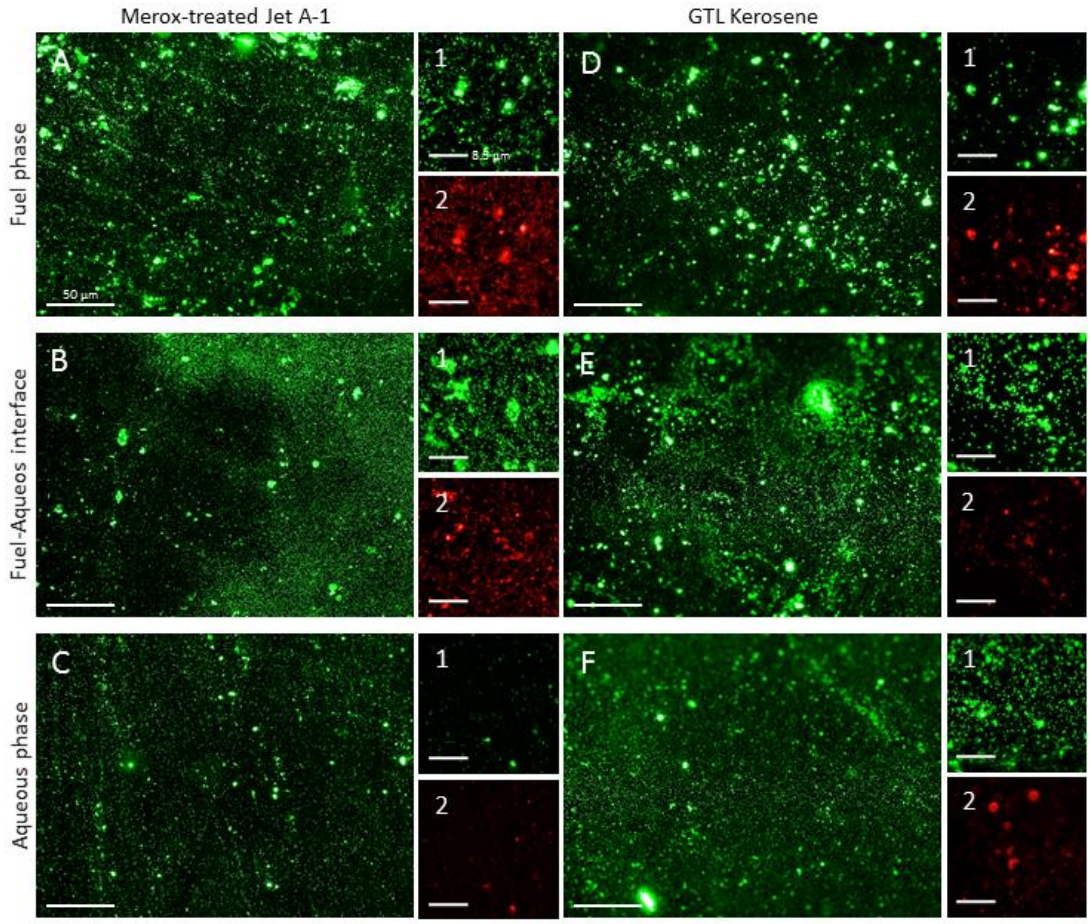

Figure 3.31 – Epifluorescence images of *C. tropicalis* biofilms on stainless steel coupons incubated for 4 weeks in microcosms containing Merox-treated Jet A-1 (A-C) and GTL kerosene (D-F). Images were taken at different points along the coupon in the aqueous phase, at fuel-aqueous interface and in the fuel phase. The main image is a maximum intensity projection image in X and Y dimensions of the DNA stain SYTO 9. Close up images are shown as inserts of the SYTO 9 (1) and SYPRO Ruby (2) signals. Scale bars are 50 µm (main images) and 8.5 µm (insets).

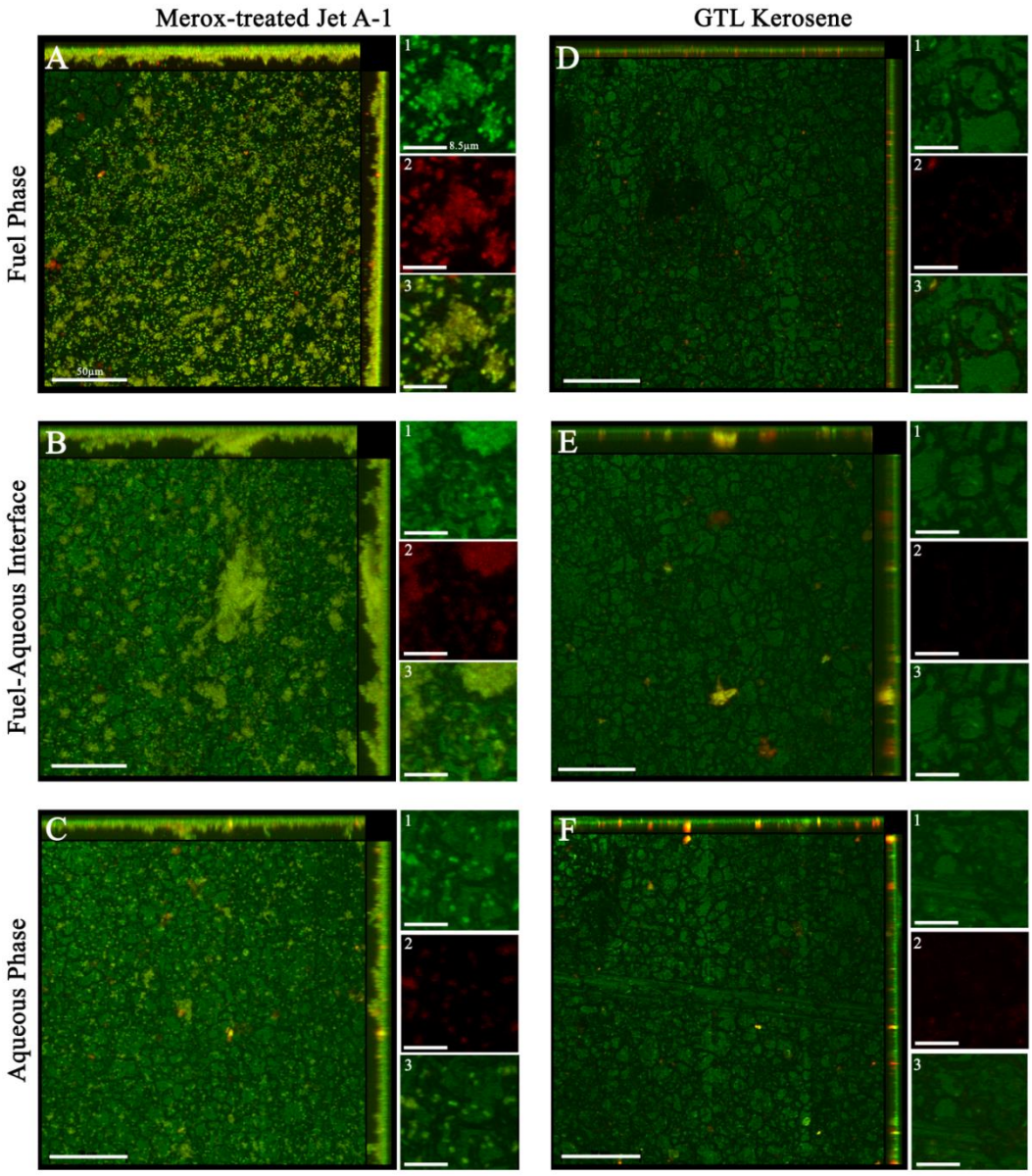

Figure 3.32 – CLSM images of *P. putida* biofilms on stainless steel coupons incubated for 4 weeks in microcosms containing Merox-treated Jet A-1 (A-C) and GTL kerosene (D-F). Images were taken at different points along the coupon in the aqueous phase, at fuel/aqueous interface and in the fuel phase. The main image is a maximum intensity projection image in X, Y and Z dimensions of the DNA stain SYTO 9 (light green) and the EPS stain SYPRO Ruby (red). Non-specific staining shows as dark green and is of non-biological origin. Close up images are shown as inserts of the SYTO 9 (1), SYPRO Ruby (2) and combined signals (3). Scale bars are 50 µm (main images) and 8.5 µm (insets).

3.3.2 Growth of monocultures in different fuel types

Planktonic growth of environmental isolates was compared across two fuel types by measuring the OD^{600} of the aqueous phase (see Figure 3.33). Sixty-four microorganisms were tested (both prokaryotes and eukaryotes). Two hydrocarbon sources were used: Merox-treated Jet A-1 and GTL kerosene. Microcosms with absorbance >0.06 (starting inoculum and instrument error) were considered to have exhibited microbial growth. In total 42 microorganisms grew in the two fuels, representing ~66 % of the microorganisms tested. Therefore, these microorganisms have the potential to utilise hydrocarbons as a carbon source. Of these, 14 grew into observable biofilms in at least one of the two fuel types.

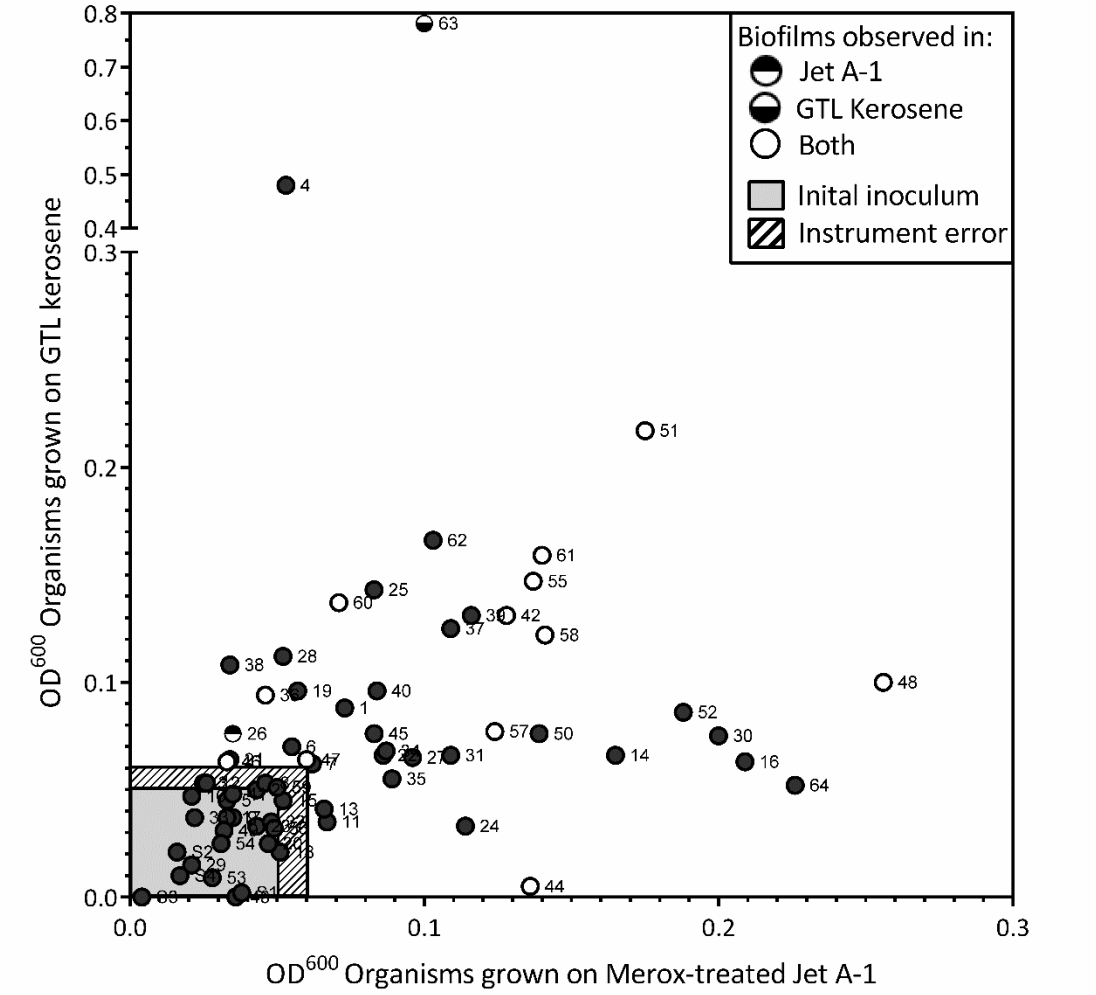

Figure 3.33 – A comparison between the isolated environmental microorganisms grown in either Merox-treated Jet A-1 or GTL kerosene, at an OD^{600}. Black circles represent the growth of microorganisms in both fuel types. White circles represent microcosm where a clear biofilm was formed, and therefore some of the OD^{600} may under represent the true growth rate. Black semicircles represent biofilm formation in one of the two fuel types. Data points

outside of the instrument error shown were considered to have grown. A detailed list of these microorganisms can be seen in the table below (see Table 3.10).

Table 3.10 – List of the isolated microorganisms used in the growth studies.

1) *Kocuria sp.*	23) *Pantoea sp.*	45) Unknown organism
2) *Erwinia sp.*	24) *Pseudomonas sp.*	46) Unknown organism
3) *Pseudomonas sp.*	25) *Paracoccus sp.*	47) Unknown organism
4) *Stenotrophomonas sp.*	26) Unknown organism	48) Unknown organism
5) Unknown organism	27) *Roseomonas sp.*	49) *Pantoea sp.*
6) *Pseudomonas sp.*	28) Unknown organism	50) *Amorphotheca sp.*
7) *Meyerozyma sp.*	29) *Flaviobacterium sp*.	51) Unknown organism
8) *Serratia sp.*	30) Unknown organism	52) Unknown organism
9) *Exiuobacterium sp.*	31) *Meyerozyma sp.*	53) *Shigella sp.*
10) Unknown organism	32) Unknown organism	54) *Staphylococcus sp.*
11) *Candida tropicalis*	33) Saccaromycetales	55) *Amorphotheca sp.*
12) Unknown organism	34) Unknown organism	56) *Staphylococcus sp.*
13) Unknown organism	35) *Variovorax sp.*	57) *Amorphotheca sp.*
14) *Pseudomonas putida*	36) Unknown organism	58) *Entrophospora sp.*
15) Unknown organism	37) Unknown organism	59) *Pseudomonas sp.*
16) *Yarrowia sp.*	38) *Hormoconis resinae*	60) *Amorphotheca sp.*
17) *Panteao sp.*	39) *Bacillus sp.*	61) *Amorphotheca sp.*
18) *Pseudomonas graminis*	40) *Bacillus sp.*	62) Unknown organism
19) *Cellulosimicrobium sp.*	41) *Bacillus sp.*	63) *Sclerostagonospora sp.*
20) *Pseudomonas sp.*	42) Unknown organism	64) *Novosphingobium sp.*
21) *Stenotrophomonas sp.*	43) *Escherichia sp.*	
22) *Pseudomonas sp.*	44) *Bacillus sp.*	

3.3.3 Chemical analysis of microcosms

3.3.3.1 Ion chromatography

To better understand the chemical differences in microcosms containing different fuel types and blends, chemical analysis was performed on the major ions in the aqueous phase (using ion chromatography) and the hydrocarbon content of the fuel phase (using GC-MS). Significant changes in the ion content of the aqueous phase were detected. These were analysed by Partial Least Squares-Discriminant Analysis (PLS-DA) to identify differences in ions associated with the growth differences seen between microcosms (see Figure 3.34, A). The microcosms containing GTL kerosene alone clearly separated from the other fuel types and blends. The loading plot (Figure 3.34, B) showed that this separation was driven by nitrate and ammonium, which was confirmed by analysis of the variable importance in projections (VIP). Nitrate was the most important factor in both component 1 and 2 with additional contributions from ammonium and sulphate. Figure 3.34, C shows plots of selected ions.

There was little change in the phosphate concentration of the microcosms, but both nitrate and ammonium were utilised in those microcosms containing conventional jet fuels. In contrast, little nitrate or ammonium was consumed in the GTL kerosene systems with the exception of *C. tropicalis* where ammonium was consumed. This correlated with the slightly better growth of *C. tropicalis*, in the GTL kerosene systems, compared to other organisms. Figure 3.34, D shows a plot of growth versus nitrate concentration, indicating a close correlation between nitrate consumption and growth.

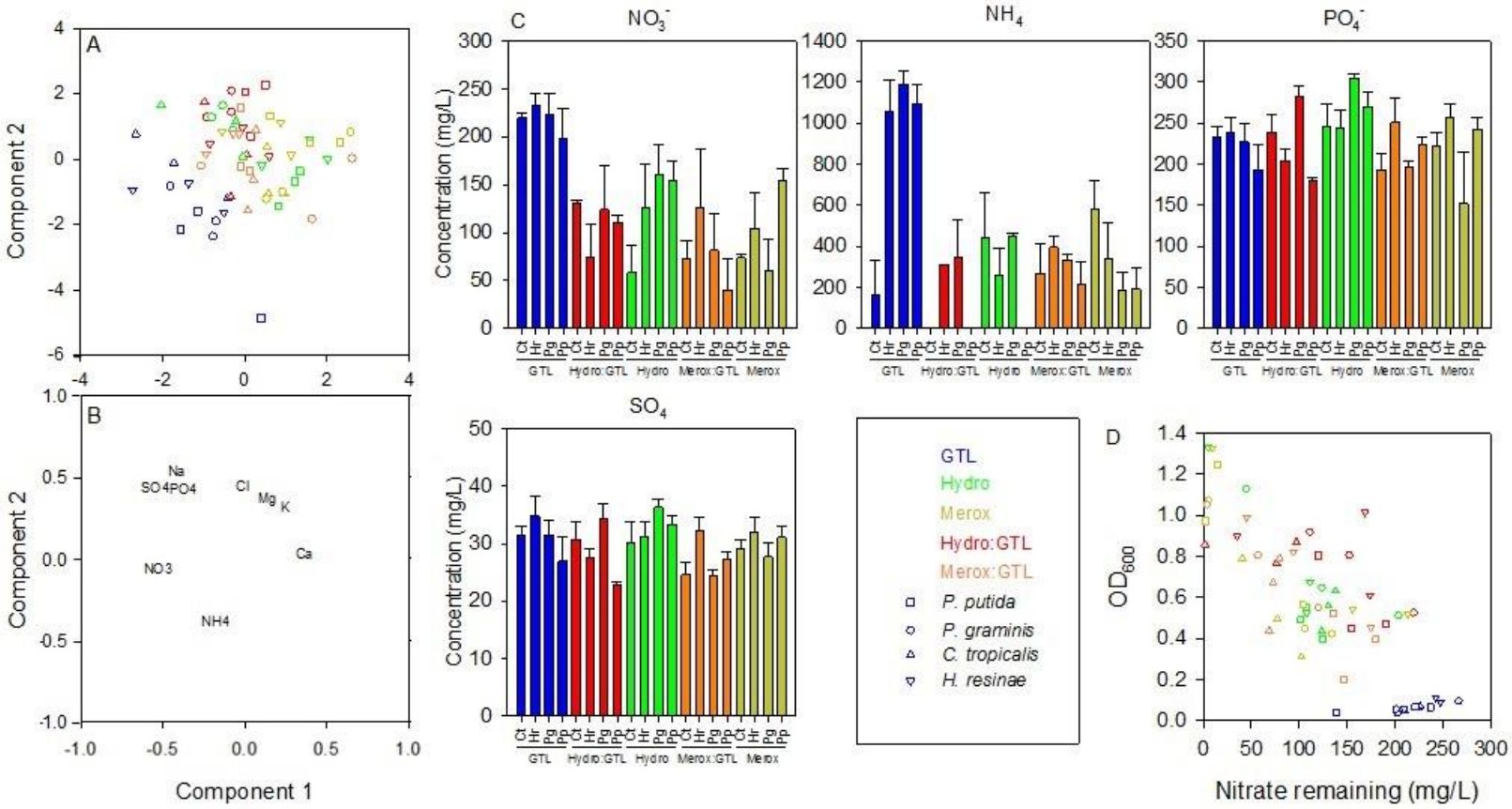

Figure 3.34 – Analysis of the concentration of selected anions in the aqueous phase of the microcosms. A, PLS-DA plot of samples based on all major ions in solution (Cl, SO_4, NO_3, PO_4 Na, NH_4, K, Mg, Ca). B, Loading plots. C, Concentration of selected ions (means +/- SE, n = 3). D, Nitrate remaining in the microcosm vs. growth.

3.3.3.2 Gas Chromatography-Mass Spectrometry

The hydrocarbon composition of jet fuels (Merox- and Hydro-treated Jet A-1) and GTL kerosene was analysed using GC-MS before and after 2 weeks growth of the isolated microorganisms in a microcosm. All three fuels are a complex mixture of hydrocarbons. The two conventional jet fuels are composed of varied aliphatic, aromatic and heterocyclic compounds, with carbon chain lengths of approximately C_{10}-C_{16} (see Figure 3.35) and a boiling range between 150 and 260 °C, as well as hetero-atomic species (e.g. sulphur, nitrogen and oxygen compounds). The Hydro-treated Jet A-1 contains more aromatic species (~22 % compared to ~19 %), and the Merox-treated Jet A-1 contains more sulphur species (325 mg/kg compared to <100 mg/kg) (see Appendix F). In comparison, the GTL kerosene is a simpler fuel, with carbon chain lengths of approximately C_{10}-C_{14} (see Figure 3.35). It contains no aromatics or hetero-atomic species (see Appendix F), consisting of only straight chained and branched aliphatic compounds in an approximate ratio of 4:1. For further compositional information (such as C:H ratios) see Snijders *et al*. (2011), where the same fuels have been used. As the Merox-treated and Hydro-treated jet fuels have a relatively similar composition, only the Merox-treated Jet A-1 and GTL kerosene have been used for this analysis.

During initial method development, microcosms containing an excess (7 ml) of jet fuel overlaying 7 ml nutrient medium were used. In these microcosms fuel was in vast excess so that the microorganisms had an abundant carbon source for the duration of the experiment (precluding it from being a growth-limiting factor). As the microorganisms degraded only a small proportion of the fuel, differences in composition could not be detected by GC-MS (data not shown). Ruiz *et al.* (2015) recognized this problem and developed microcosms where only small volumes of fuel were added, so that specific molecules limited growth and became depleted from the fuel phase allowing their detection. Therefore, additional microcosms were set up (see Section 3.2.3.2) containing a minimal amount (100 µl) of jet fuel to allow specific hydrocarbon degradation to be observed.

Twelve microorganisms (both prokaryotes and eukaryotes) were incubated in monoculture in these microcosms, containing either Merox-treated Jet A-1 or GTL kerosene and comparisons made against sterile controls. All microcosms were sealed to prevent losses of volatile components. Sufficient headspace was present to ensure that the systems remained aerobic. At the end of the incubation time, fuel composition was analysed by GC-MS and candidate molecules that showed a significant reduction in the live microcosms identified (see 3.2.5.2).

After analysis, 8 candidate molecules that differed significantly were identified in the Merox-treated Jet A-1 microcosms and 10 candidate molecules in the GTL kerosene microcosms, from the selected 12 microorganisms (see Table 3.11 and Table 3.12). In the Merox-treated Jet A-1 *P. putida* showed a significant decrease in naphthalene and 2-methyl-naphthalene, whilst *Paracoccus sp*., *Y. lipolytica* and an unidentified microorganism (#51) showed a significant decrease in 2,4,6-trimethyldecane and decane (see Figure 3.36). In the GTL kerosene *P. putida* showed a significant decrease in tridecane, *P. graminis* in undecane and tridecane, *H. resinae* in 2,3,6-trimethyldodecane, undecane and 2-ethyl-hexanol, *Paracoccus sp.* and *S. maltophilia* in decane and *Y. lipolytica* in nonane and decane (see Figure 3.37). No candidate molecules were identified as being degraded by the remaining 5 microorganisms.

For the 7 of the 12 microorganisms where hydrocarbon degradation was putatively identified, in general simpler straight chained n-alkanes were degraded more favourably than the more complex branched and ring structured molecules (particularly in the GTL kerosene, where molecules with ring structures are not present). *Paracoccus sp.*, *Y. lipolytica* and *P. putida* showed the ability to degrade hydrocarbons in both fuels, with *Paracoccus sp.*, *Y. lipolytica* degrading n- and iso-alkanes in both fuel types. *P. putida* preferentially degraded straight chain alkanes when grown with GTL kerosene. However, in Merox treated Jet A-1, *P. putida* no longer degraded these compounds to a significant extent, but preferentially degraded the polycyclic aromatic compounds naphthalene and 2-methyl-napthalene. The remaining four microorganisms showed a preference for either Merox-treated Jet A-1 (unidentified microorganism #51) or GTL kerosene (*P. graminis*, *H. resinae* and *S. maltophilia*). Overall, significant mass changes were observed across all 12 microorganisms and, in conjunction with the growth data (see Figure 3.33), this suggests that these microorganisms could grow in one or both of these two fuel types, so significant degradation of compounds would be expected in at least one fuel type. However, in the remaining five cases, although growth was visible in the microcosm (see Figure 3.33), it was not possible to identify specific compounds that were being degraded. It is likely that GC-MS is not sensitive enough to detect low level changes in the degradation of hydrocarbons associated with these microorganisms. Further work needs to be undertaken to develop this method.

Table 3.11 –A) the total number of peaks in the GC-MS spectra where a significant ($p \leq 0.05$) change in at least one m/z occurred in the Merox-treated Jet A-1 samples, and B) the number of peaks where a significant change in ≥10 m/z occurred. The predicted compounds by comparison to the NIST database are listed. The isolate number shown in Table 3.10 and Figure 3.33 and whether visible growth was observed in the microcosms is provided.

Microorganism	A	B	Compounds	Visible growth
P. putida (14)	9	2	Naphthalene, 2-methyl-naphthalene	Yes
P. graminis (18)	31	0	N/A	Limited
C. tropicalis (11)	15	0	N/A	Yes
H resinae (38)	18	0	N/A	No
A. resinae (55)	40	0	N/A	Yes
N. resivorium (64)	19	0	N/A	Yes
Paracoccus sp. (25)	84	2	2,4,6-trimethyldecane, decane	Yes
Sclerostagonospora sp. (63)	30	0	N/A	Yes
S. maltophilia (4)	74	0	N/A	Yes
Unidentified 51	72	2	2,4,6-trimethyldecane, decane	Yes
Unidentified 62	44	0	2,4,6-trimethyldecane, decane	Yes
Y. lipolytica (16)	132	2	2,4,6-trimethyldecane, decane	Yes

Table 3.12 – A) the total number of peaks in the GC-MS spectra where a significant ($p \leq 0.05$) change in at least one m/z occurred in the GTL-treated Jet A-1 samples, and B) the number of peaks where a significant change in ≥10 m/z occurred. The predicted compounds by comparison to the NIST database are listed. The isolate number shown in Table 3.10 and Figure 3.33 and whether visible growth was observed in the microcosms is provided.

Microorganism	A	B	Compounds	Visible growth
P. putida (14)	36	1	Tridecane	Yes
P. graminis (18)	34	2	Undecane, tridecane	Limited
C. tropicalis (11)	16	0	N/A	No
H resinae (38)	33	3	2,3,6-trimethyldodecane, Undecane, 2-ethyl-hexanol	Yes
A. resinae (55)	22	0	N/A	Yes
N. resivorium (64)	4	0	N/A	No
Paracoccus sp. (25)	21	1	Decane	Yes
Sclerostagonospora sp. (63)	16	0	N/A	Yes
S. maltophilia (4)	23	1	Decane	Yes
Unidentified 51	17	0	N/A	Yes
Unidentified 62	17	0	N/A	Yes
Y. lipolytica (16)	27	2	Nonane, decane	Yes

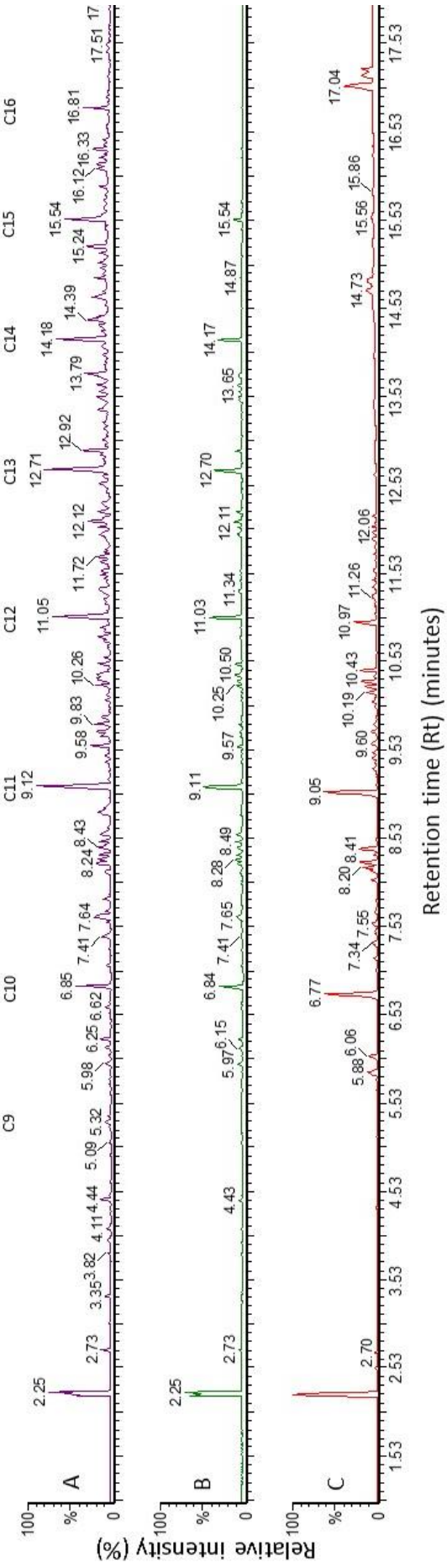

Figure 3.35 – GC-MS chromatograms of the Merox-treated Jet A-1 (A), Hydro-treated Jet A-1 (B) and GTL kerosene (C). Straight chain alkane peaks are indicated by CX, where X is the number of carbon molecules in the chain. These traces are not corrected for small inter-run differences in retention time.

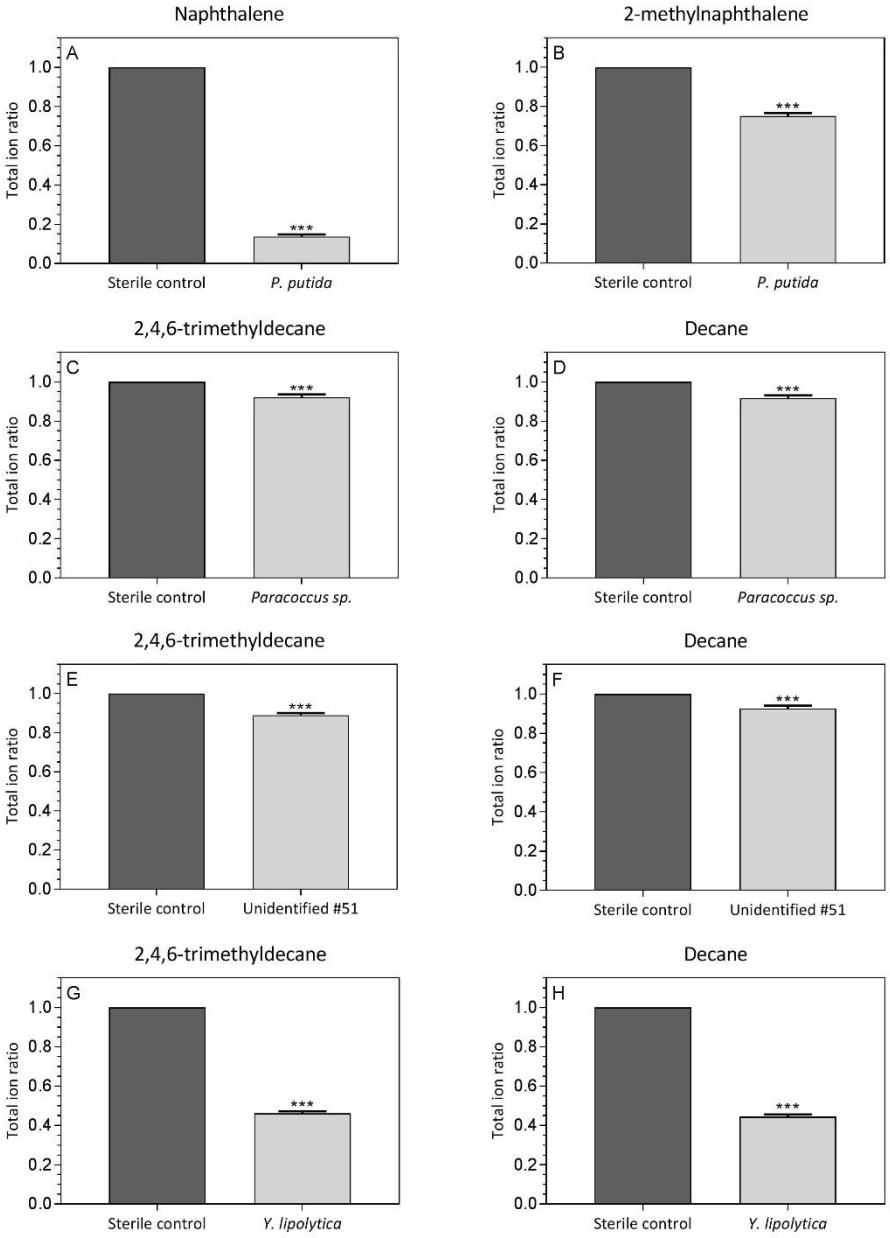

Figure 3.36 – Compounds that were degraded in microcosms containing Merox-treated Jet A-1 and isolated microorganisms. Compounds were selected if ≥ 10 m/z values differed between the live microcosm and the sterile control. The mean (+ SE) total ion counts for the candidate molecules are shown, normalised to that in the sterile control. Significant differences are indicated (t-test, * p <0.05, ** p <0.01, *** p <0.001). Graphs A and B show the degradation of naphthalene (A) and 2-methyl-naphthalene (B) by *P. putida*. Graphs C and D show the degradation of 2,4,6-trimethyldecane (C) and decane (D) by a *Paracoccus sp.* Graphs E and F show the degradation of 2,4,6-trimethyldecane (E) and decane (F) by an unidentified microorganism (#51). Graphs G and H show the degradation of 2,4,6-trimethyldecane (G) and decane (H) by *Y. lipolytica*.

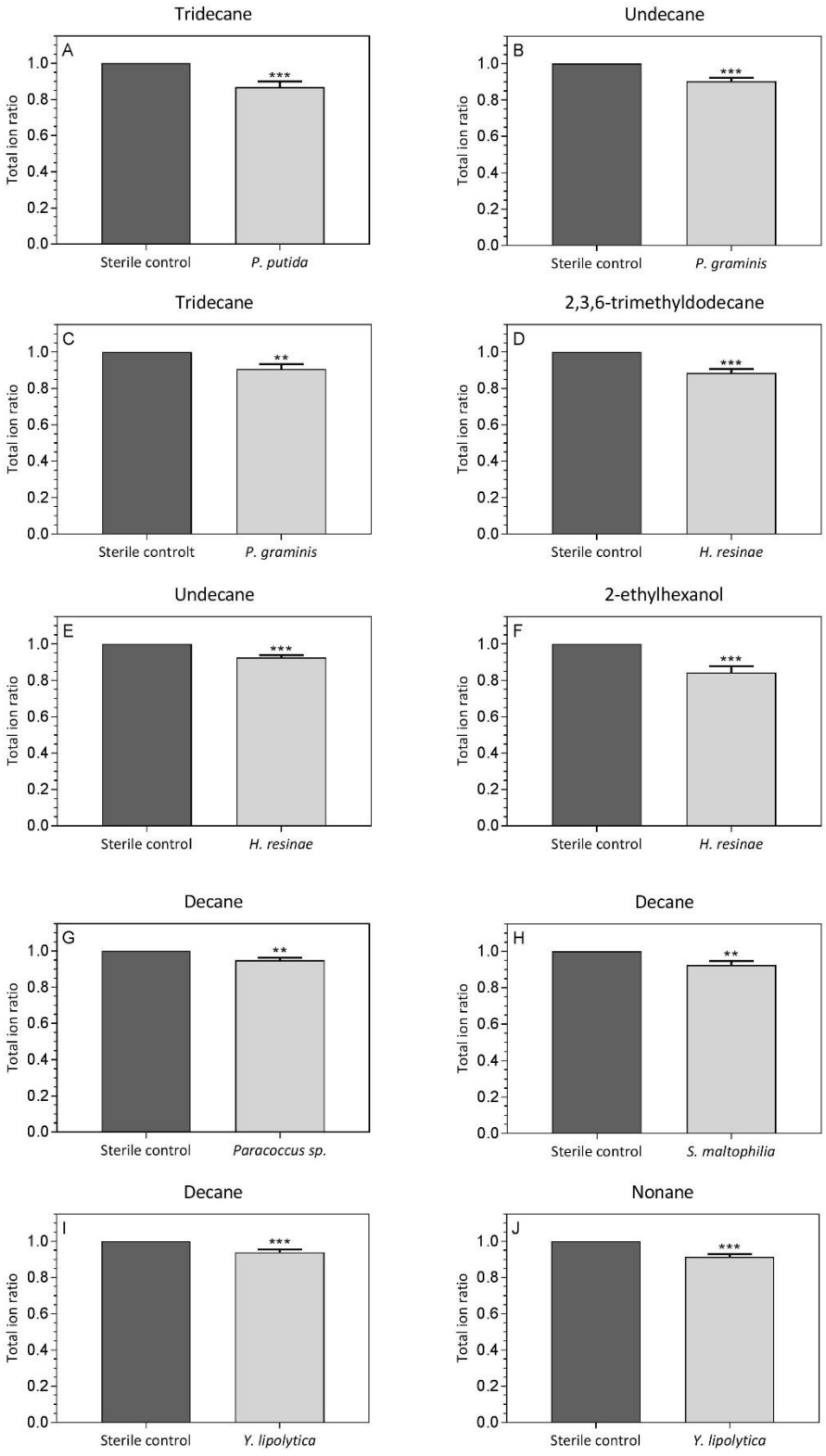

Figure 3.37 – Compounds that were degraded in microcosms containing GTL-treated Jet A-1 and isolated microorganisms. Compounds were selected if ≥ 10 m/z values differed between the live microcosm and the sterile control. The mean (+ SE) total ion counts for the candidate molecules are shown, normalised to that in the sterile control. Significant differences are indicated (t-test, * p <0.05, ** p <0.01, *** p <0.001). (A) degradation of tridecane by *P.*

putida, (B ,C) degradation of undecane (B) and tridecane (C) by *P. graminis,* (D) degradation of decane by a *Paracoccus sp., (*E,F G) degradation of undecane (E), 2-ethyl-hexanol (F) and 2,4,6-trimethyldodecane (G) by *H. resinae*, (H) degradation of decane by *S. maltophilia,* (I, J) degradation of nonane (I) and decane (J) by a *Y. lipolytica.*

3.3.3.3 Sample key

From this point in Chapter 3, figures will be labelled with the unique codes assigned to them during analysis. This was done because there are multiple variables within the sample set, which could not be otherwise fitted into the figures. These represent the fuels used at each stage of the analyses and the biological replicate. These codes consisting of numbers and letter; one letters denote the initial inoculum, two letter codes denote the microcosm samples after two weeks (exposure to one fuel) and three letter codes denote the microcosm samples after four week (see Table 3.13). For example:

G1 would denote: G – GTL kerosene (first fuel), no second letter – this was incubated for two weeks, and 1 - Biological replicate number 1.

HM3 would denote: Hydro-treated Jet A-1 (first fuel), Merox-treated Jet A-1 (second fuel), and 3 - Biological replicate number 3.

Table 3.13 – Chapter 3 sample key

Sample code	Definition
First letter:	This is the fuel used weeks zero to two
G	GTL kerosene
H	Hydro-treated Jet A-1
M	Merox-treated Jet A-1
Second letter:	This is the fuel used for weeks two until four
G	GTL kerosene
H	Hydro-treated Jet A-1
M	Merox-treated Jet A-1
No letter	This microcosm was only incubated for two weeks
Third number:	This is the biological replicate
1	Biological replicate 1
2	Biological replicate 2
3	Biological replicate 3
Other:	If the sample is only one letter e.g. G, H or M, and no number
Single letter	This is the inoculum

3.3.3.4 The impact of fuel type on microbial community structure

Although the four isolates grew poorly on GTL kerosene compared to the other fuel types, it is unlikely that this was a general phenomenon when compared to the 63 environmental isolates, but rather a requirement in those specific isolates for compounds present in the more complex conventional fuels compared to the simpler GTL kerosene. Therefore, it was hypothesised that taking a mixed community from a Jet A-1 contaminated fuel tank and growing it on different fuels would select communities of microorganisms better able to degrade specific fuel types. Therefore, larger (200 ml) microcosms were set up with the different fuel types, inoculated with a mixed community and allowed to grow for 2 weeks. An aliquot of the aqueous phase was then removed, used to inoculate new microcosms containing the same or different fuel types, and then incubated for a further 2 weeks. Experiments were performed in triplicate. Microbial cells were harvested from the aqueous phase/interface, DNA extracted and bacterial diversity assessed by T-RLFP of amplified 16S rRNA gene fragments. These results were then used as a basis to assess diversity using next generation sequencing to profile both the prokaryotic and eukaryotic populations, by analysing both the 16S rRNA and the ITS and 5.8s rRNA genes respectively.

3.3.3.5 Terminal-restriction fragment length polymorphism (T-RFLP)

Between 10 and 51 terminal restriction fragments (T-RF) were produced per sample following digestion with *AluI*. There was considerable variation between samples with a slight increase in species richness in the older microcosms compared to the starting inoculum. The average number of T-RFs and variation between microcosms is shown in Figure 3.38, A. Of the 90 different T-RFs detected, 8 were common to all samples and included the most dominant bands. T-RFs of 78 and 258 bp were the most abundant and the shared T-RFs represented, on average, 92% of the total signal intensity in each lane.

Principle Component Analysis (PCA) was then used to identify factors that controlled variance in the samples (see Figure 3.38, B). The first two components explained 81 % of the variation in the samples. The analysis was weighted for signal intensity identifying major T-RFs at 55, 75, 78 and 285 bp, as the major drivers of diversity within the microcosms (see Figure 3.38, C). Figure 3.38, D-F show PCA analysis for microcosms containing GTL kerosene, Hydro-treated Jet A-1 and Merox-treated Jet A-1 separately. In each case only the first two components are shown, as these explained the majority of the variation between the samples.

The PCAs show that the microbial communities from microcosms containing GTL kerosene and Hydro-treated Jet A-1 were relatively constant and did not deviate much from that seen in the initial inocula. However, as the incubation proceeded, variation tended to increase, presumably as conditions became more favourable for a more diverse population of microorganisms. Variation in the Merox-treated Jet A-1 tended to be much greater after 2 weeks than with the other fuel types, a pattern which persisted after 4 weeks of incubation, most likely due to the high sulphur content of this fuel. The biggest variation was seen when the fuel type was changed from GTL kerosene to a conventional jet fuel or vice versa. The data indicated a large population shift occurred in these samples.

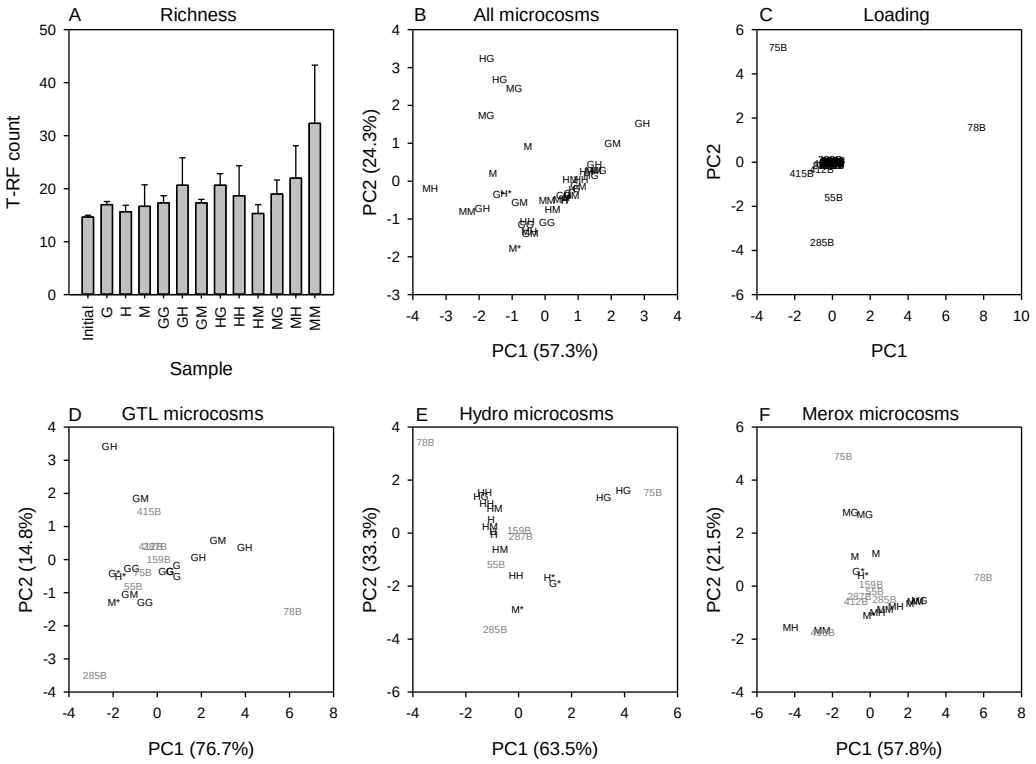

Figure 3.38 – A, T-RF count in each microcosm. B and C, PCA of all samples and loading plots. D, E and F, PCA of microcosms containing each fuel type. T-RFs which account for 1% or more of the variation (weighted for signal intensity) are shown in grey. * indicates initial inoculum. G, H, M represent samples from microcosms after 2 weeks incubation with GTL kerosene, Hydro- and Merox-treated Jet A-1 respectively. Where two letters are shown (e.g. HG) the first two weeks incubation was in Hydro-treated Jet A-1 that was then used to inoculate a microcosm containing GTL kerosene. Numbers are the T-RFs driving the variation in each direction.

3.3.3.6 Structure of the microbial communities

To examine the impact of alternative fuels on the community dynamics of microbial populations found within jet fuel systems, culture-independent sequencing analysis was undertaken on a microbial community after 14 and 28 days. After 14 days the fuel type in some on the microcosms was switched (see Figure 3.25), to assess the impact of introducing alternative fuels into a fuel system containing conventional fuels.

Across the 38 prokaryotic libraries that passed quality control, 57 distinct OTUs were identified by comparison with the Greengenes database at 97 % sequence identity. Across all of the samples, the phylum Proteobacteria dominated, accounting for 47.5 % of the prokaryote sequences. These belonged to the classes: Alphaproteobacteria (21.0 %), Betaproteobacteria (12.0 %), and Gammaproteobacteria (14.0 %). Actinobacteria were the next most abundant phylum, and accounted for 40.0 % of the prokaryotes sequenced; all from the family of Actinomycetales. Firmicutes (5.0 %), Bacteroidetes (1.5 %) and Verrucomicrobia (1.5 %) made up the remaining phyla, as well as two unassigned OTUs (see Figure 3.39).

Across the 39 eukaryotic libraries, 38 distinct OTUs were identified by comparison with the UNITE database at 97 % similarity. The microorganisms were evenly split between the phyla Ascomycota and Basidiomycota (47.0 % each). The Ascomycota were made up of the classes: Dothideomycetes (13.0 %), Saccharomycetales (13.0 %), Sordariomycetes (11.0 %), Eurotiomycetes (5.0 %), Lecanoromycetes (2.5 %) and one unidentified Ascomycota (2.5 %). Basidiomycota were made up of the classes: Agaricomycetes (26.0 %), Microbotryomycetes (5.0 %), Incertae sedis (5.0 %), Agaricostilbomycetes (2.5 %), Atractiellomycetes (2.5 %), Tremellomycetes (2.5 %), and one unidentified Basidiomycota (2.5 %) (see Figure 3.40). Two other unidentified microorganisms were also present.

Although a total of 95 distinct OTUs were identified in this study, only 26 microorganisms had a relative abundance greater than 1% in any sample. Of the prokaryotes, the communities were dominated by two OTUs; *Cellulosimicrobium sp*. and *Stenotrophomonas sp.*; *Stenotrophomonas sp.* was particularly prevalent, with an average abundance at ~63% and observed up to ~79% in some samples. Nine OTUs were present in more than 80% of the samples sequenced, but at much lower levels than the dominant two. Likewise, the eukaryotic communities were dominated by two OTUs: *Pseudallescheria sp.* and *Amorphotheca sp*., with average abundances of ~57% and 29% respectively, and were observed in all of the samples sequenced. *Candida sp.* were also dominant in a few samples

(particularly the starting inoculum), though the relative abundance dropped significantly after being introduced into the microcosms (see Table 3.14).

Table 3.14 – The most dominant microorganisms observed across the sample set. Microorganisms were selected if they were observed in >40 % of the samples sequenced.

	Maximum relative abundance (%)	**Average relative abundance (%)**	**Number of samples where present**
Prokaryotes			
Stenotrophomonas sp.	78.65	62.65	38
Cellulosimicrobium sp.	45.62	28.74	38
Dermacoccus sp.	7.52	1.29	38
Burkholderia sp.	1.09	0.26	38
Xanthomonadaceae	0.47	0.18	38
Actinomycetales	0.47	0.06	37
Microbacterium sp.	3.2	0.70	36
Xanthomonadaceae	0.26	0.08	36
Methylobacterium sp.	10.89	1.98	33
Kocuria sp.	4.14	0.71	31
Nocardioidaceae	5.33	0.49	29
Dietzia sp.	0.17	0.03	24
Sanguibacteraceae	0.23	0.03	23
Sanguibacter sp.	0.23	0.03	20
Actinotalea sp.	0.09	0.02	20
Intrasporangiaceae	0.06	0.01	16
Eukaryotes			
Amorphotheca sp.	72.87	28.60	39
Pseudallescheria sp.	96.58	57.42	39
Candida sp.	87.33	10.07	33
Unidentified fungi	13.42	1.10	24
Cryptococcus sp.	6.99	0.54	16

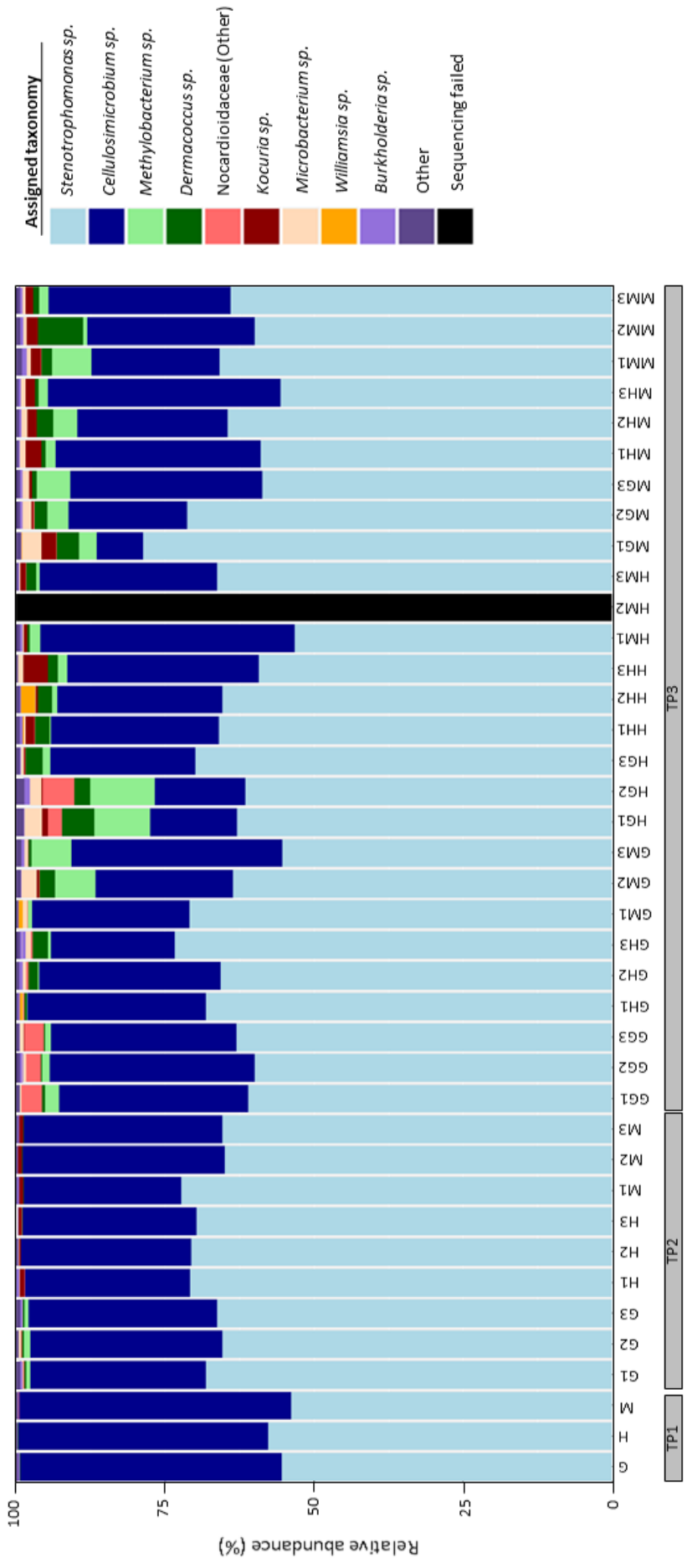

Figure 3.39 – Relative abundance of prokaryotic microorganisms found in aircraft fuel systems. Samples with a completely black bar failed quality control and the data has not been included. Only microorganisms that have a relative abundance >1 % have been included, all others have been combined into the "Other species" category. Time point one (TP1) is the inoculum, time point two (TP2) are the communities after two weeks and time point three (TP3) are the communities after four weeks, where the fuel type has either been maintain or varied in the microcosm.

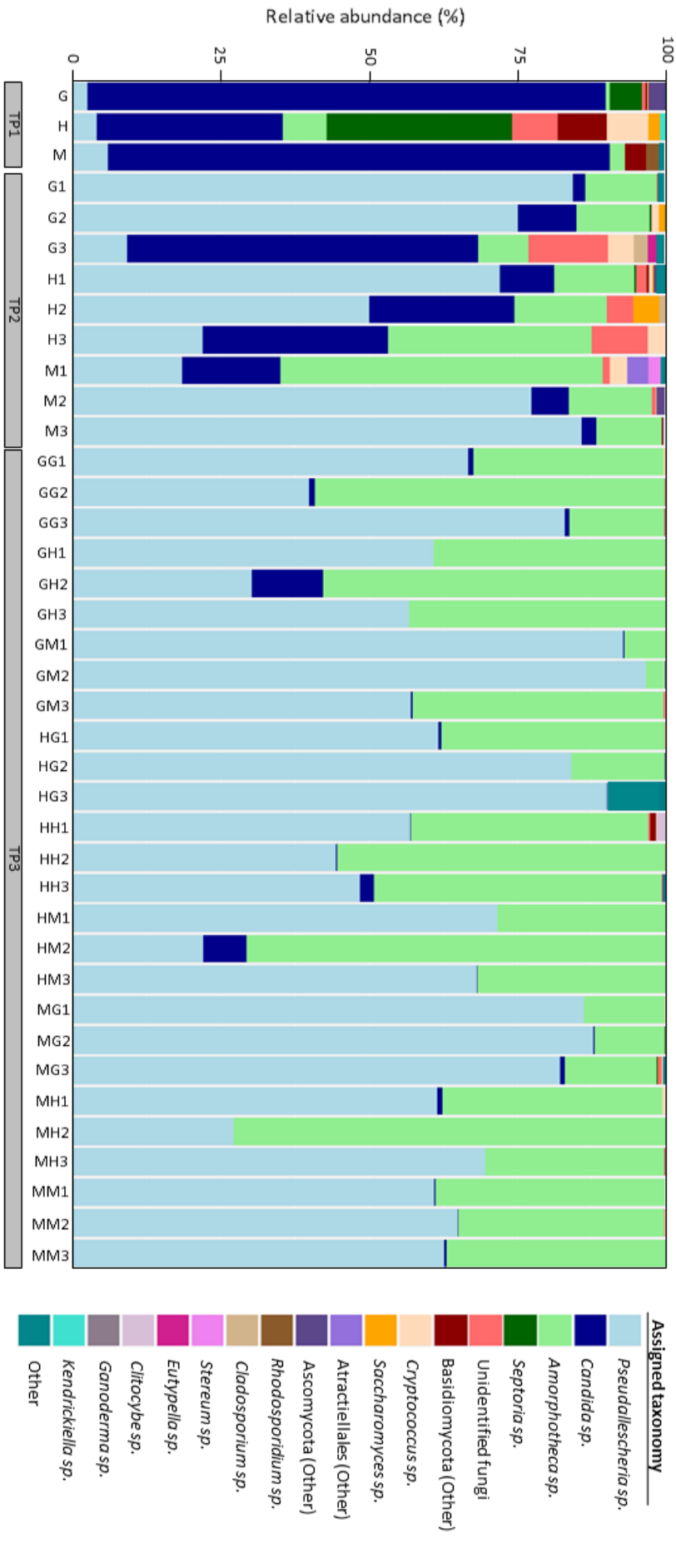

Figure 3.40 – Relative abundance of eukaryotic microorganisms found in aircraft fuel systems. Only microorganisms that have a relative abundance >1% have been included, all others have been combined into the "Other species" category. Time point one (TP1) is the inoculum, time point two (TP2) are the communities after two weeks and time point three (TP3) are the communities after four weeks, where the fuel type has either been maintain or varied in the microcosm.

To assess the impact of different treatments on the prokaryotic and eukaryotic microbial communities, 3 measures of microbial richness and diversity were calculated; species richness, inverse Simpson and Shannon indices. ANOVA was used to determine whether these indices differed significantly. Figure 3.41 and Figure 3.42 show boxplots of these indices with statistical comparisons between each treatment shown in Table 3.16 and Table 3.18. ANOVAs were also performed with time as a factor to identify trends across samples (see Table 3.15).

Table 3.15 – ANOVAs on the prokaryotic communities to assess the impact of fuel treatments over time on species richness and diversity (Simpson and Shannon indices).

Comparison	Time 1 *vs* 2	Time 1 *vs* 3	Time 2 *vs* 3
Richness	0.462	**0.001**	**0.001**
Inverse Simpson	0.629	0.412	**0.003**
Shannon	0.888	**0.001**	**<0.001**

For the prokaryotic samples, none of the indices showed a significant difference between the starting inoculum (Time 1) and time 2 (2 weeks growth in a microcosm containing G, H, M fuels). All the indices (with the exception of the inverse Simpson) showed an increase in value between the starting inoculum (Time 1) and time 2 (2 weeks) and time 3 (4 weeks growth in G, H or M fuels and transfer between fuel types). Overall, there was an increase in the diversity of prokaryotic communities over time in the microcosms. However, more detailed analysis comparing each treatment did not resolve further clear patterns (see Table 3.15). Differences were observed between some microcosms but the majority of these could be explained by time.

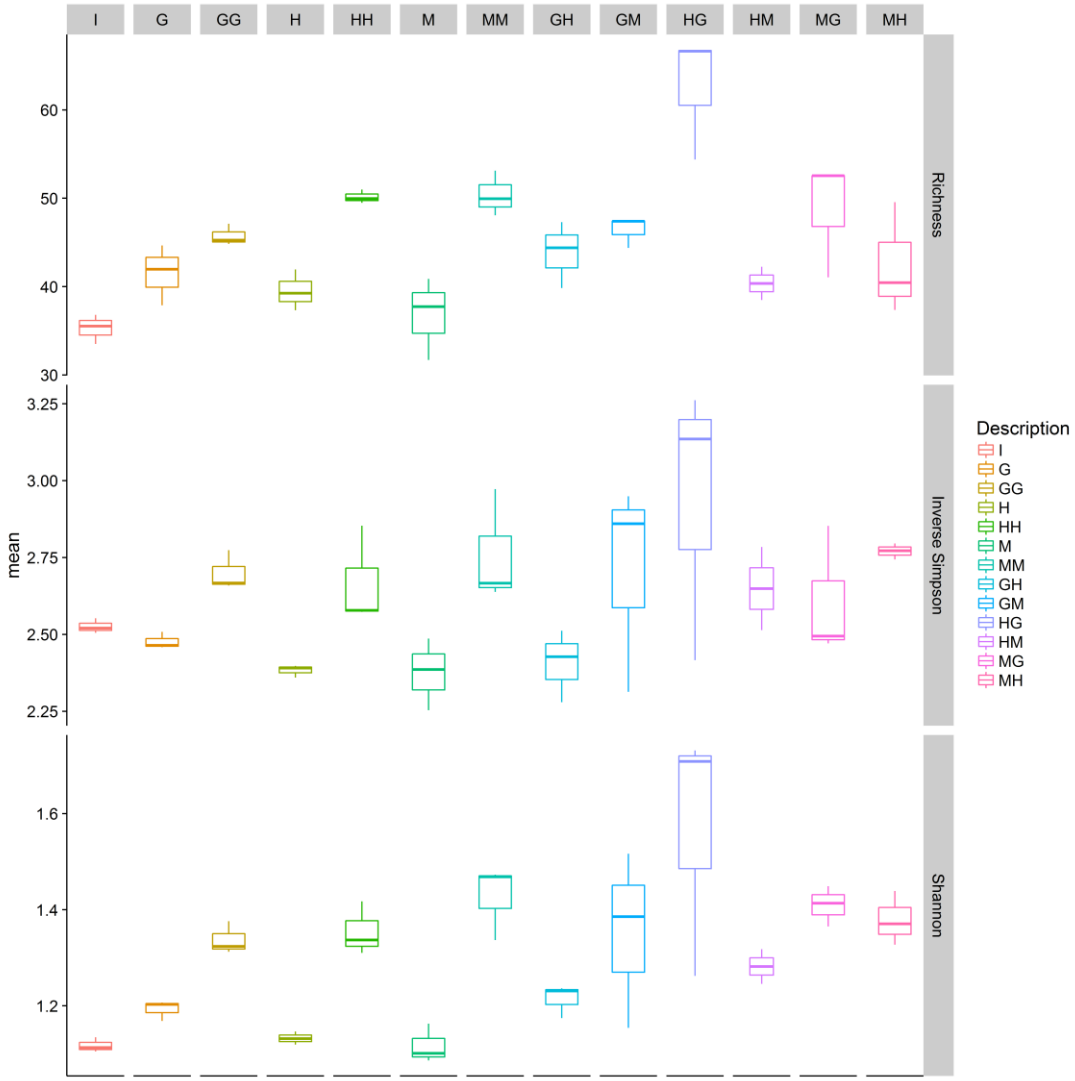

Figure 3.41 – Box and Whisker plot showing the species richness and diversity using the inverse Simpson and Shannon diversity indices for the prokaryotic communities. Boxes represent the upper and lower interquartile ranges, line in the middle of the box represents the mean (n = 3), whiskers show the lowest and highest values.

Table 3.16 – *p* values derived from ANOVAs with a Tukey post hoc test applied, to show the significant differences between treatment types in prokaryotic communities. (A) Species richness (B) inverse Simpson index (C) Shannon index. Numbers highlighted in green show as significant difference ($p \leq 0.05$).

(A) Species Richness

	I	G	H	M	GG	GH	GM	HG	HH	HM	MG	MH
G	0.595											
H	0.059	0.971										
M	0.930	1.000	0.710									
GG	**0.003**	0.345	0.984	0.107								
GH	1.000	0.875	0.163	0.997	**0.010**							
GM	**0.003**	0.318	0.977	0.096	1.000	**0.009**						
HG	0.120	0.999	1.000	0.963	0.793	0.441	0.764					
HH	**0.039**	0.927	1.000	0.589	0.996	0.112	0.994	0.999				
HM	**0.001**	**0.001**	**0.013**	**0.001**	0.190	**0.001**	0.209	**0.003**	**0.020**			
MG	0.898	1.000	0.930	1.000	0.320	0.989	0.296	0.998	0.868	**0.001**		
MH	**0.010**	0.636	0.999	0.261	1.000	**0.032**	1.000	0.966	1.000	0.073	0.571	
MM	0.444	1.000	0.994	0.999	0.485	0.753	0.453	1.000	0.978	**0.001**	1.000	0.781

(B) Inverse Simpson index

	I	G	H	M	GG	GH	GM	HG	HH	HM	MG	MH
G	1.000											
H	0.994	0.956										
M	0.998	1.000	0.666									
GG	0.999	0.987	1.000	0.792								
GH	0.997	0.999	0.626	1.000	0.757							
GM	0.953	0.840	1.000	0.453	1.000	0.416						
HG	0.999	1.000	0.757	1.000	0.866	1.000	0.547					
HH	0.996	0.965	1.000	0.694	1.000	0.655	1.000	0.783				
HM	0.482	0.301	0.983	0.091	0.946	0.079	0.999	0.123	0.977			
MG	0.999	0.998	1.000	0.923	1.000	0.904	1.000	0.958	1.000	0.957		
MH	1.000	0.999	1.000	0.951	1.000	0.934	0.998	0.978	1.000	0.781	1.000	
MM	0.930	0.793	1.000	0.399	1.000	0.363	1.000	0.489	1.000	0.999	0.999	0.996

(C) Shannon Index

	I	G	H	M	GG	GH	GM	HG	HH	HM	MG	MH
G	0.994											
H	0.152	0.736										
M	1.000	0.999	0.232									
GG	0.099	0.602	1.000	0.157								
GH	1.000	0.993	0.147	1.000	0.096							
GM	**0.014**	0.161	0.995	**0.024**	0.999	**0.014**						
HG	0.959	1.000	0.887	0.989	0.785	0.955	0.275					
HH	0.131	0.688	1.000	0.201	1.000	0.126	0.997	0.853				
HM	**0.001**	**0.006**	0.376	**0.001**	0.504	**0.001**	0.949	**0.013**	0.421			
MG	0.653	0.994	1.000	0.776	0.999	0.642	0.900	0.999	0.999	0.199		
MH	**0.022**	0.228	0.999	**0.038**	0.999	**0.021**	1.000	0.372	0.999	0.8896	0.951	
MM	0.053	0.415	1.000	0.086	1.000	0.051	1.000	0.602	1.000	0.695	0.994	1.000

Table 3.17 – ANOVAs on the eukaryotic communities to assess the impact of fuel treatments over time on species richness and diversity (Simpson and Shannon indices).

Comparison	Time 1 *vs* 2	Time 1 *vs* 3	Time 2 *vs* 3
Richness	0.740	**<0.001**	**0.001**
Inverse Simpson	**0.034**	**0.004**	0.893
Shannon	0.287	**0.005**	0.138

For the eukaryotic samples, there was a general trend for a decrease in richness and diversity over time. The richness of the eukaryotic community increased the microcosms containing Hydro-treated fuel, but did not differ in Merox-treated fuel or GTL kerosene after 2 weeks. However, richness was significantly lower in the majority of samples after 4 weeks incubation. These differences are evident in the individual comparisons shown in Table 3.17. A similar decrease in diversity was seen with the inverse Simpson and Shannon indices; the decrease in the inverse Simpson index was evident between the inoculum (Time 1) and later time points (Times 2 and 3) whereas the reduction in the Shannon index was only evident between Times 2 and 3 (see Table 3.17).

Due to the limited sequencing depths obtained from the eukaryotic samples, differences between inverse Simpson and Shannon indices were not apparent when individual comparisons were made (see Table 3.18).

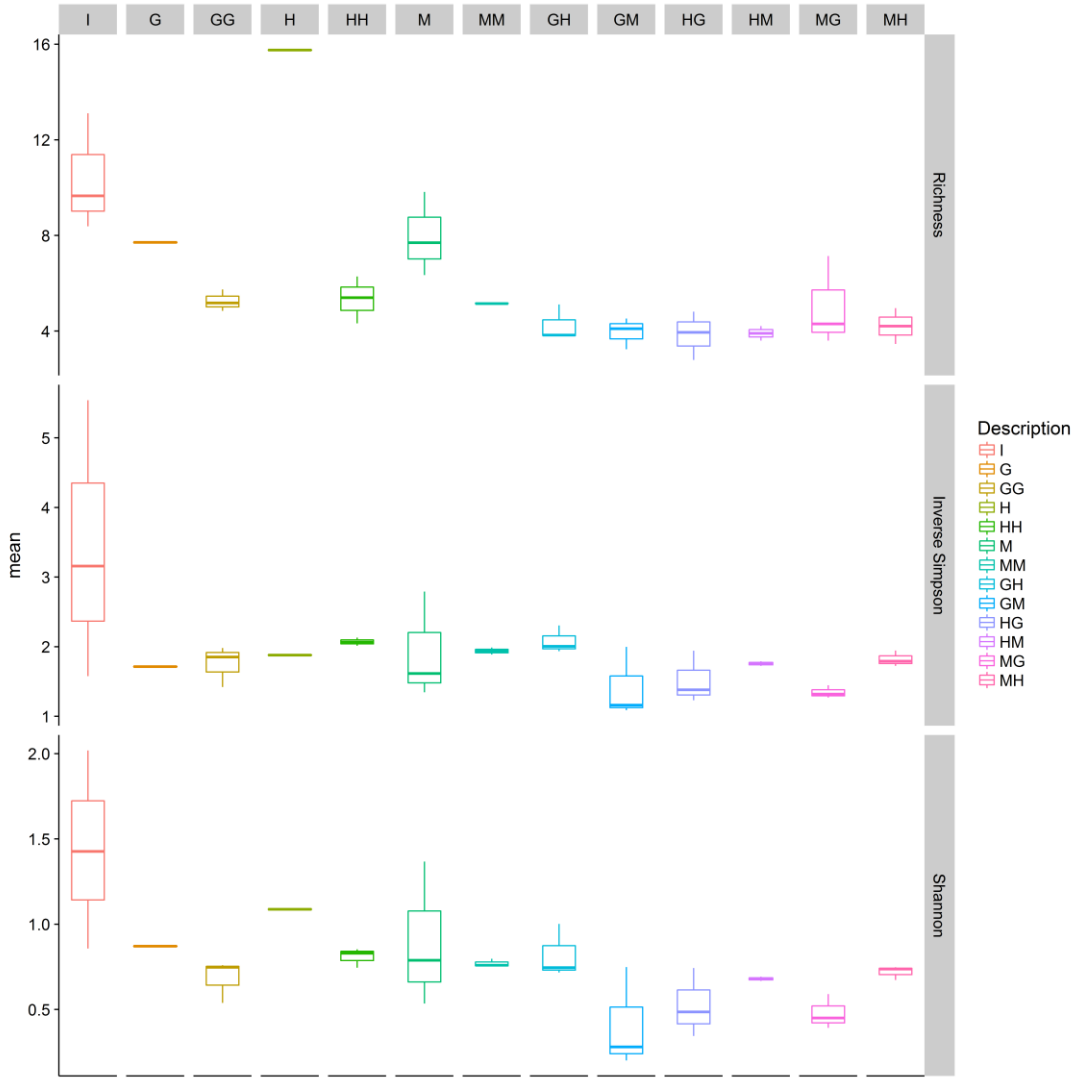

Figure 3.42 – Box and Whisker plot showing the species richness and diversity using the inverse Simpson and Shannon diversity indices for the eukaryotic samples. Boxes represent the upper and lower interquartile ranges, line in the middle of the box represents the mean (n = 3), whiskers show the lowest and highest values.

Table 3.18 – *p* values derived from ANOVAs with a Tukey post hoc test applied, to show the significant differences between treatment types in eukaryotic communities. (A) Species richness (B) inverse Simpson index (C) Shannon index. Numbers highlighted in green show as significant difference ($p \leq 0.05$).

(A) Species Richness

	I	G	H	M	GG	GH	GM	HG	HH	HM	MG	MH
G	0.990											
H	**0.029**	0.901										
M	0.812	0.442	**0.007**									
GG	**0.031**	0.910	1.000	**0.007**								
GH	0.917	1.000	0.483	0.211	0.504							
GM	**0.024**	0.877	1.000	**0.006**	1.000	0.431						
HG	**0.002**	0.387	0.976	**0.001**	0.971	0.050	0.986					
HH	**0.001**	0.247	0.858	**0.001**	0.842	**0.021**	0.893	1.000				
HM	**0.001**	0.184	0.730	**0.001**	0.709	**0.012**	0.780	1.000	1.000			
MG	**0.002**	0.308	0.916	**0.001**	0.905	**0.049**	0.939	1.000	1.000	1.000		
MH	**0.009**	0.722	1.000	**0.003**	1.000	0.224	1.000	0.999	0.987	0.950	0.994	
MM	**0.001**	0.368	0.968	**0.001**	0.962	**0.045**	0.980	1.000	1.000	1.000	1.000	0.999

(B) Inverse Simpson index

	I	G	H	M	GG	GH	GM	HG	HH	HM	MG	MH
G	0.817											
H	0.404	1.000										
M	0.932	1.000	1.000									
GG	0.863	1.000	0.999	1.000								
GH	0.539	1.000	1.000	1.000	1.000							
GM	0.707	1.000	1.000	1.000	1.000	1.000						
HG	0.869	1.000	0.999	1.000	1.000	1.000	1.000					
HH	0.059	0.999	0.994	0.997	0.773	0.974	0.908	0.766				
HM	0.130	1.000	0.999	0.999	0.940	0.999	0.988	0.937	1.000			
MG	0.594	1.000	1.000	1.000	1.000	1.000	1.000	0.999	0.997	0.999		
MH	0.052	0.999	0.991	0.995	0.739	0.964	0.886	0.731	1.000	1.000	0.995	
MM	0.530	1.000	1.000	1.000	1.000	1.000	1.000	1.000	0.976	0.999	1.000	0.966

(C) Shannon Index

	I	G	H	M	GG	GH	GM	HG	HH	HM	MG	MH
G	0.992											
H	0.378	0.999										
M	1.000	1.000	0.983									
GG	0.773	1.000	1.000	0.999								
GH	0.831	1.000	0.999	0.999	1.000							
GM	0.670	1.000	1.000	0.999	1.000	1.000						
HG	0.784	1.000	0.999	0.999	1.000	1.000	1.000					
HH	**0.003**	0.477	0.452	0.200	0.159	0.129	0.217	0.153				
HM	0.052	0.950	0.994	0.699	0.839	0.782	0.911	0.829	0.973			
MG	0.552	1.000	1.000	0.991	1.000	0.999	1.000	1.000	0.592	0.997		
MH	**0.033**	0.907	0.974	0.605	0.723	0.656	0.820	0.711	0.993	1.000	0.987	
MM	0.511	1.000	1.000	0.995	1.000	1.000	1.000	1.000	0.325	0.972	1.000	0.922

Weighted principle coordinate analysis (PCoA), using UniFrac distances, was used to visualise factors that controlled variance in the prokaryotic samples (see Figure 3.43). Unweighted

analysis was performed, but did not show any additional information and is therefore not shown. In addition, unweighted analysis lends equal importance to OTUs that are present at very low abundance which is not the focus of these experiments. A PERMANOVA (using the R package mvabund) was then performed to identify which samples were statistically significantly different, although this analysis is not phylogenetically corrected (see Table 3.19).

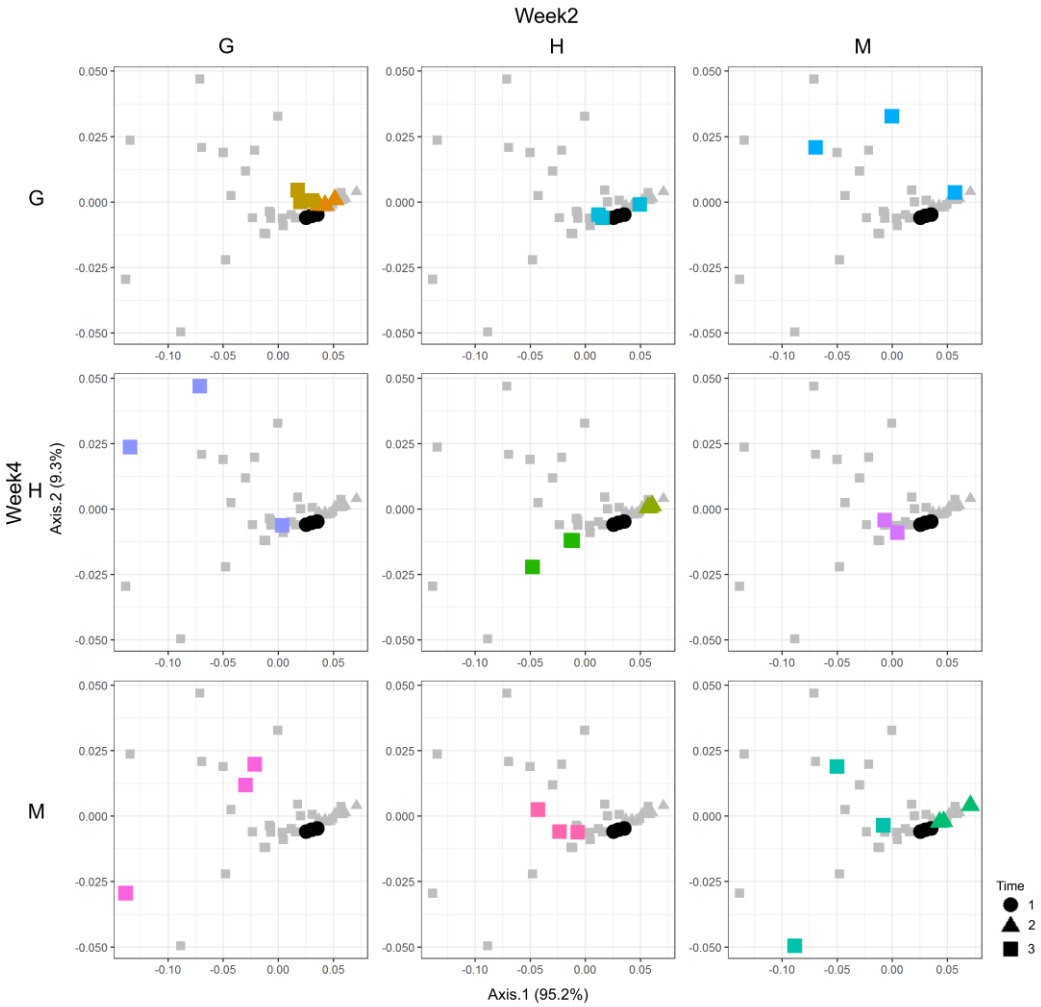

Figure 3.43 – Weighted PCoA of the prokaryotic communities at all three time points, using UniFrac measurements to calculate the distance between the samples. Samples have been separated by sample treatment. G (GTL), H (Hydro) and M (Merox) fuels were used as a carbon source in microcosms grown for 2 weeks (Time 2) and 4 weeks (Time 3). The starting inoculum (Time 1) is shown as black circles. Small grey symbols show all samples in all treatments.

Table 3.19 – Probability that prokaryotic samples differ using PERMANOVAs with a Likelihood Ratio correction. Samples highlighted in green show a statistical difference from one another.

	I	G	H	M	GG	GH	GM	HG	HH	HM	MG	MH
G	**0.001**											
H	**0.001**	**0.008**										
M	**0.001**	**0.007**	0.606									
GG	**0.001**	**0.010**	**0.001**	**0.001**								
GH	**0.001**	**0.012**	**0.001**	**0.002**	**0.001**							
GM	**0.001**	**0.019**	**0.001**	**0.001**	**0.005**	**0.003**						
HG	**0.001**	**0.002**	**0.001**	**0.001**	**0.004**	**0.001**	**0.029**					
HH	**0.001**	**0.020**	**0.003**	**0.002**	**0.003**	**0.006**	**0.012**	**0.003**				
HM	**0.001**	**0.008**	**0.002**	**0.001**	**0.010**	**0.001**	**0.021**	**0.001**	**0.048**			
MG	**0.001**	**0.005**	**0.001**	**0.001**	**0.001**	**0.001**	**0.018**	**0.011**	**0.007**	**0.004**		
MH	**0.001**	**0.004**	**0.001**	**0.002**	**0.003**	**0.001**	**0.017**	**0.001**	**0.036**	0.241	**0.003**	
MM	**0.001**	**0.002**	**0.001**	**0.002**	**0.001**	**0.002**	**0.037**	**0.014**	0.077	**0.018**	**0.009**	**0.032**

The PCoAs and PERMANOVAs of the prokaryotic communities showed that the majority of samples differed from each other. The inoculum (I – Time 1) differed from samples incubated for two weeks (G, H and M – Time 2) and 4 weeks in the microcosms (GG, HH, MM, GH, GM, HG, HM, MH and MG – Time 3). Similarly, samples from Time 2 differed significantly from those at Time 3. There was also an increase in variation within a treatment over time, with Time 3 samples showing greater variation than Time 2 or the inoculum (Time 1).

Fuel type also had a significant impact on the prokaryotic microbial communities. At both time points 2 and 3, the Merox- and Hydro- treated fuels did not differ significantly from each other (i.e. H *vs* M or HH *vs* MM). However, these communities did differ significantly from those grown in GTL kerosene.

These data show that the significant factors that influenced prokaryotic microbial community structure were time of growth in the microcosm and conventional (H and M) *vs* alternative (G) fuels.

To determine which OTUs were significantly influenced by fuel type, DESEQ2 analysis was used to identify OTUs that differed between G and H or M, and GG and HH or MM. These comparisons identify the impact of conventional *vs* alternative fuel correcting for time in the microcosm.

Figure 3.44 and Figure 3.45 show boxplots of normalised OTU abundance for OTUs that grew preferentially in either conventional or alternative fuels.

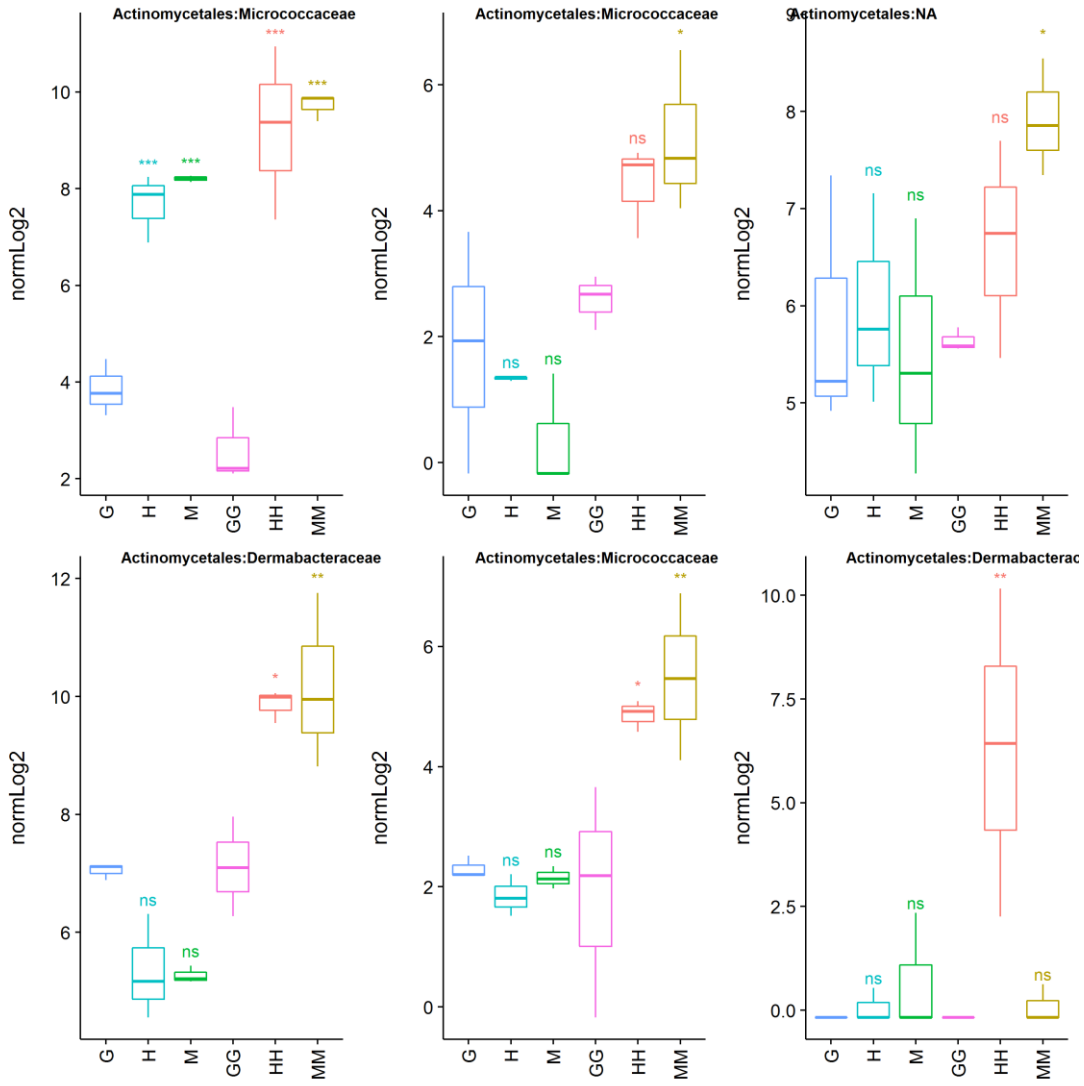

Figure 3.44 – Prokaryotic OTUs that grow preferentially in one or more treatments containing conventional fuel (H, M or HH, MM) compared to growth in alternative fuel (G or GG). Boxplots are of variance stabilised OTU abundance (log2). The mean is shown as a solid line within the interquartile ranges with the whiskers showing maximum and minimum values. Statistical comparisons are shown within a time point i.e. G *vs* H, G *vs* M, GG *vs* HH and GG *vs* MM. (ns – not significant, * p <0.05, ** p <0.01, *** p <0.001). The order and family are shown for each OTU.

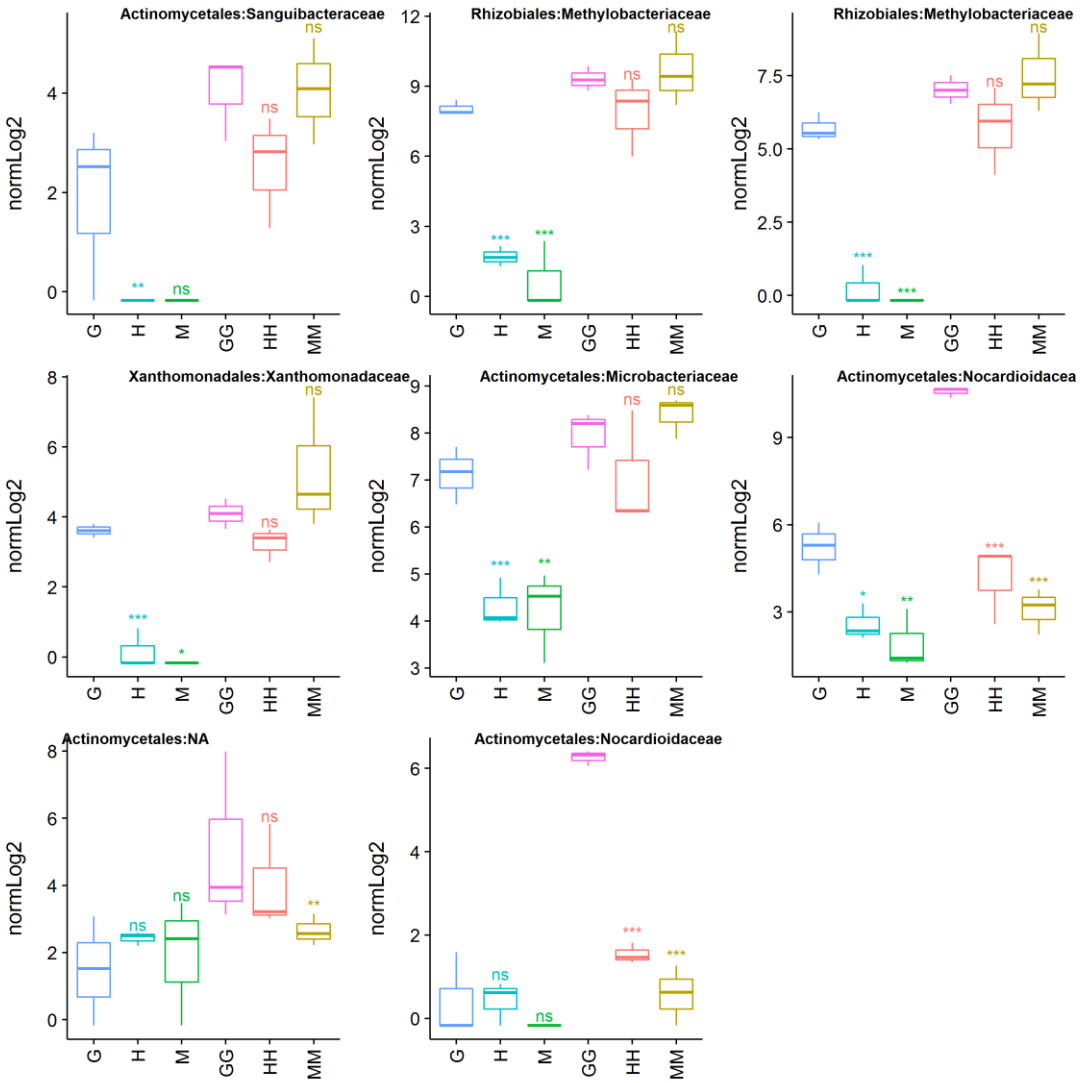

Figure 3.45 – Prokaryotic OTUs that grow preferentially in one or more treatments containing alternative fuel (G or GG) compared to growth in conventional fuel (H, M or HH, MM). Boxplots are of variance stabilised OTU abundance (log2). The mean is shown as a solid line within the interquartile ranges with the whiskers showing maximum and minimum values. Statistical comparisons are shown within a time point i.e. G *vs* H, G *vs* M, GG *vs* HH and GG *vs* MM. (ns – not significant, * p <0.05, ** p <0.01, *** p <0.001). The order and family are shown for each OTU.

Six OTUs showed a preference for growth in conventional fuels under one or more conditions. All were Actinomycetales *sp*. One Micrococcaceae sp. showed a strong preference for conventional fuels (G *vs* H, M and G *vs* HH, MM) at both time points – the other two showed greater abundances after 4 weeks growth. With the Dermatabactereaceae, changes in relative abundance were only statistically significant after 4 weeks. One of these OTUS only showed significant growth in Hydro treated fuels (HH).

OTUs which showed a greater relative abundance in one or more GTL treatments compared to conventional fuels included members of the Actinomycetales, Rhizobiales and Xanthomonadales. In many cases, differences were apparent only after 2 weeks growth in the microcosm – after 4 weeks there were no significant differences. The exceptions were two Norcardioaceae sp. that showed much greater relative abundances in GTL compared to conventional fuels after 4 weeks growth.

Weighted principle coordinate analysis (PCoA), using Bray Curtis distance measurements was then used to identify factors that controlled variance in the eukaryotic samples (see Figure 3.46). A PERMANOVA (using the R package mvabund) was then performed to identify which samples were statistically significantly different, although this analysis is not phylogenetically corrected. These data show that the analysis is heavily driven by the starting inoculum. PERMANOVA was used to identify samples that differed significantly (see Table 3.20).

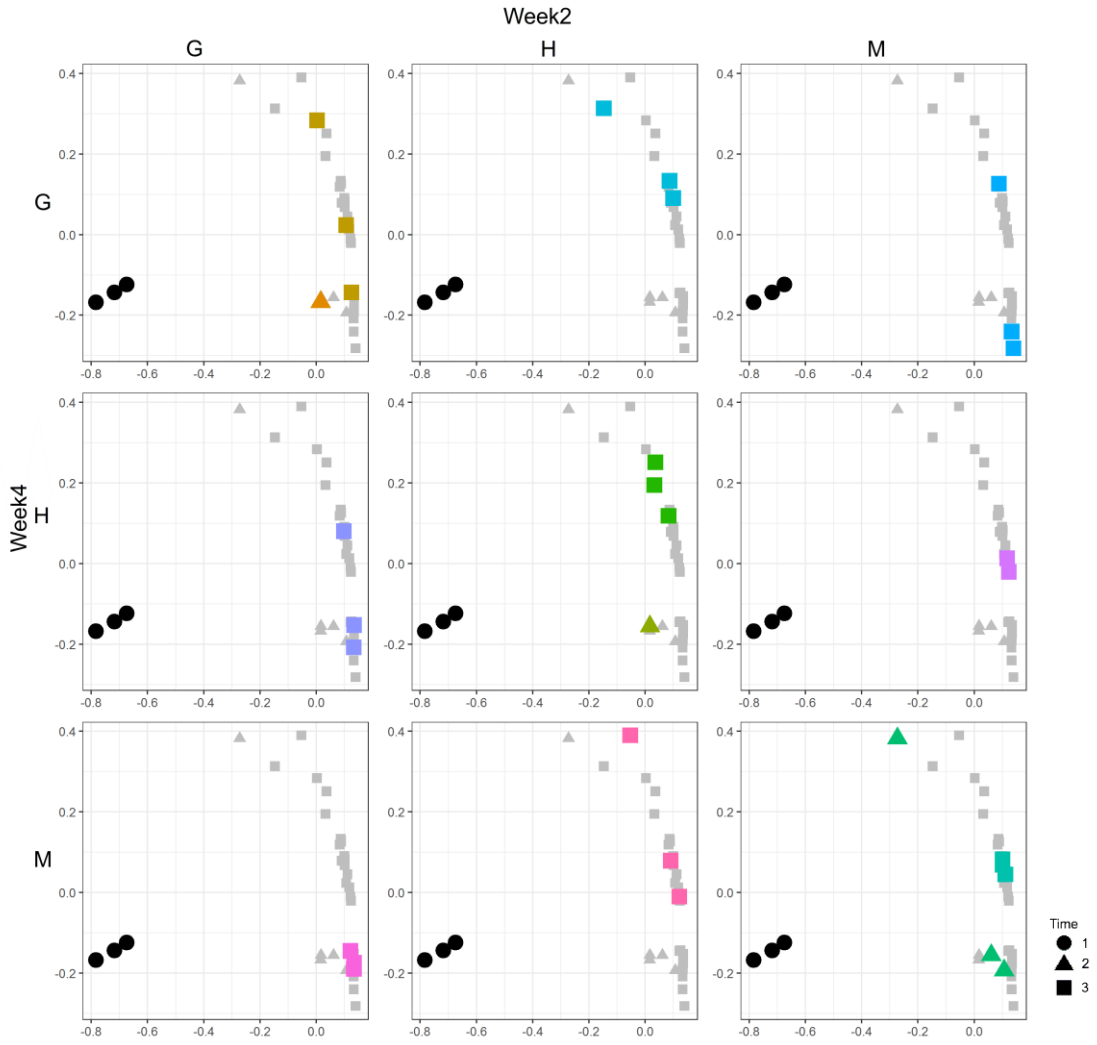

Figure 3.46 – Weighted PCoA of the eukaryotic communities at all three time points, using Bray-Curtis measurements to calculate the distance between the samples. Samples have been separated by sample treatment. G (GTL), H (Hydro) and M (Merox) fuels were used as a carbon source in microcosms grown for 2 weeks (Time 2) and 4 weeks (Time 3). The starting inoculum (Time 1) is shown as black circles. Small grey symbols show all samples in all treatments.

Table 3.20 – Probability that eukaryotic samples differ using ANOVAs with a LR correction. Samples highlighted in green show a statistical difference from one another.

	I	G	GG	GH	GM	H	HG	HH	HM	M	MG	MH
G	**0.001**											
GG	**0.001**	**0.016**										
GH	**0.001**	**0.033**	0.310									
GM	**0.001**	**0.009**	**0.006**	**0.002**								
H	**0.001**	0.298	**0.003**	**0.005**	**0.001**							
HG	**0.001**	**0.007**	0.171	**0.020**	0.056	**0.001**						
HH	**0.001**	**0.013**	0.141	0.104	**0.002**	**0.002**	**0.021**					
HM	**0.001**	**0.007**	0.087	**0.025**	0.055	**0.002**	0.338	**0.010**				
M	**0.001**	**0.048**	**0.013**	**0.045**	**0.002**	**0.006**	**0.004**	**0.004**	**0.008**			
MG	**0.001**	**0.011**	**0.029**	**0.001**	**0.033**	**0.002**	0.191	**0.002**	0.080	**0.006**		
MH	**0.001**	**0.003**	0.062	**0.034**	**0.008**	**0.001**	0.062	**0.014**	0.405	**0.001**	**0.007**	
MM	**0.001**	**0.002**	0.073	**0.028**	**0.005**	**0.001**	0.206	**0.008**	0.497	**0.001**	**0.009**	0.465

As is evident from the ordination plots, all the samples incubated in the microcosm differed from the inoculum. As with the prokaryotic samples, time of incubation also resulted in statistically significant differences between samples. The communities also responded to fuel type but in a complex way. One factor that appeared to influence these differences was the presence/absence of Merox-treated Jet A-1; a high sulphur fuel. The eukaryotic communities in conventional fuels were not statistically significantly different (G *vs* H, GG *vs* HH) but G *vs* H and H *vs* M were significantly different. These differences were less evident at time 3 (after 4 weeks' growth in the microcosm) but HH *vs* MM was significantly different.

Further exploration of the impact of Merox-treated fuels on eukaryotic communities using DESEQ2 analysis did not identify specific OTUs that responded to Merox treatment (i.e. OTUs that differed in relative abundance in the comparisons G *vs* M, H *vs* M, GG *vs* MM and HH *vs* MM). Inspection of the data (and the richness/diversity indices) showed that many of the OTUs present in the inoculum did not become established in the microcosms which limits the effectiveness of the analysis. The microcosms were dominated by 3 eukaryotic OTUs (*Amorphotheca sp.*, *Candida sp.* and *Pseudallescheria sp*.), which did not differ significantly between treatments. Also, when the data set was filtered to remove noise, only single samples remained for several treatments so no statistical analysis was possible. Identification of specific eukaryotic OTUs that respond to Merox-treated Jet A-1 will require greater sequencing depth, but this would be of limited use as the microcosms are dominated by one or two eukaryotic organisms. A more appropriate analysis would be of field samples obtained from different fuel types, but these were not available.

3.4 Discussion

Jet fuels are a complex mixture of hydrocarbons, typically containing thousands of compounds. These can be broadly categorised into aliphatic (~66 %) and aromatic (≤ 25 %) hydrocarbons, along with a variety of heteroatomic compounds, asphaltenes and resins (Mbadinga *et al*. 2011; Passman 2013; Gaylarde *et al*. 1999). These groups vary in their susceptibility to degradation by microorganisms, but in general aliphatic hydrocarbons show the highest degradation rates (Atlas 1981) with high molecular weight aromatics and polar compounds the lowest (Fuchs 2008; Leahy & Colwell 1990). Many previous studies have looked at the microbial degradation of hydrocarbons (Fuchs *et al*. 2011; Xia *et al*. 2014), however, most field studies focus on remediation of environmental contamination (Chandankere *et al*. 2014; Lisiecki *et al*. 2014; Yanto & Tachibana 2014) and not degradation within fuel systems. This study has examined how microorganisms respond to changes in hydrocarbon composition, to predict responses following the introduction of alternative fuels. Specifically, we have looked at how industry-relevant single isolates and mixed communities responded to GTL kerosene.

3.4.1 The effect of fuel type on monocultures

When microcosms were inoculated with *P. putida*, *P. graminis*, *H. resinae* and *C. tropicalis* in monoculture, both planktonic growth and biofilm formation was significantly lower in pure GTL kerosene when compared to fuels containing conventional jet fuels. This is not due to a toxicity effect of GTL kerosene as this reduction was not seen in 50:50 blends of GTL kerosene with conventional fuels. Therefore these isolates, in monoculture, grew slowly in fuels containing only normal- and iso-alkanes, presumably due to limited ability to metabolise these compounds (Mueller *et al*. 2011). The one exception to this was *P. putida*, which utilised both normal- and iso-alkanes in the GTL kerosene. GTL kerosene differs from conventional jet fuels as it contains only alkanes and iso-alkanes and no aromatic or cyclic compounds (DeWitt *et al*., 2008). Presumably *P. putida* utilised these alkanes less efficiently, accounting for the lower growth rate in GTL kerosene.

When this study was expanded to a larger range of microorganisms, it became apparent that many microorganisms were capable of degrading GTL kerosene, utilising both normal- and iso-alkanes; however, no degradation of cyclo-alkanes was observed. At present, it is still unclear as to whether there are any specific hydrocarbons components required for microbial growth in jet fuel systems. Acquisition of specific hydrocarbon degradation capacities by microorganisms is highly likely over time if such genes exist within a community. Hydrocarbon degradation genes are commonplace (approximately two thirds of the isolates

tested grew on Jet A-1 and/or GTL kerosene) within mixed communities. Horizontal gene transfer is likely to occur, particularly in prokaryotes, and other microorganisms would gain the ability to utilise these hydrocarbons (Keeling & Palmer 2008; Thomas & Nielsen 2005).

The complexity of the hydrocarbon mixtures meant that it was often difficult to identify by GC-MS specific components that were being degraded by GC-MS. To help identify hydrocarbons of interest, a number of alternative approaches could be taken. Initial method development showed that the ratio of jet fuel to water was critical to observing degradation (Ruiz *et al*. 2015). In a system with excess fuel, no degradation was observed due to abundance of hydrocarbons (the proportion degraded was so small that the decrease could not be detected). In systems with too little fuel, the jet fuel volatised and no hydrocarbons were recovered. A ratio of 900 µl of water to 100 µl fuel was found to work well. However, this could be optimised further to identify more compounds. Also, the experiments were run for two weeks. This choice of time was based on the initial growth data, which showed that these systems became nitrogen limited after this time, slowing growth. The incubation time could be extended, and therefore more of the hydrocarbons would be degraded, which would aid in their identification. Finally, two dimensional gas chromatography (GCxGC) could be utilised in place of the GC-MS, better separate the hydrocarbons making it easier to identify the compounds as there is a reduced chance of peaks co-eluting.

The identification of hydrocarbons by comparison to the NIST database is not definitive, but the closest matching spectra to the compound of interest were selected with an appropriate retention time. Therefore, compound identification was not always definitive. To address this, experiments utilising pure compounds could be undertaken and the growth responses of isolates analysed to test whether these microorganisms are able to utilise the identified hydrocarbons.

Microorganisms have also been isolated from microcosms containing both GTL kerosene and conventional fuel so a comparative genomic analysis could be used to identify key degradative genes. Once identified, it may also be possible to use stable isotope analysis to assess which microorganisms within a community are primary degraders and how these carbon sources are utilised within biofilms. Overall, it is clear from these results, that the standard industry isolates used for analysing microbial contamination in fuels are not appropriate when analysing potential for biodegradation of alternative fuels (Anon. 2001).

All of the microcosms in this study were designed as eutrophic systems, with the aqueous phase providing all of the mineral nutrients required for microbial growth. Analysis of the aqueous phase showed that in most cases growth continued until nitrogen became limiting. This is to be expected as the typical C:N ratio of bacterial cells is in the range of 5-10 whilst C:P ratios are ~10-fold higher (Goldman *et al*. 1987). A large amount of planktonic and biofilm biomass had developed at this point. We recognise that jet fuel systems will be oligotrophic (and other environmental factors such as low temperature and associated freeze/thaw cycles) are likely to strongly influence microbial communities. For example, low nutrients and the removal of the water phase by routine tank drainage will favour biofilm formation (Garrett *et al*. 2008; Koch *et al*. 2001). Future studies will explore biofilm communities in oligotrophic environments, building upon the baseline knowledge about hydrocarbon utilisation described in this chapter. Biofilms are of particular importance as they can lead to operational problems such as filter plugging and corrosion. In these systems the surfaces to which microorganisms attach will be of key importance, as both the physical and chemical properties of these surfaces will have an impact on biofilm formation (Percival *et al*. 1999).

The microscopy undertaken in this chapter was preliminary and purely qualitative in nature. Further work needs to be undertaken to develop a quantitative measure of biofilm formation on surfaces within jet fuel systems, as this will allow changes in cell density to be assessed. Future work will study the effect of varying surface type on cell attachment and biofilm formation in representative oligotrophic systems.

3.4.2 The effect of fuel type on complex communities

These results demonstrate that the selected industry-relevant isolates used GTL kerosene much less efficiently than conventional fuels. However, the impact of altering fuel types on mixed communities was much less marked. T-RFLP analysis showed that the dominant bacteria in the microcosms were present irrespective of fuel type. Next generation sequencing showed these to be *Stenotrophomonas sp.* and *Cellulosimicrobium sp.*, as well as identifying *Amorphotheca sp., Pseudallescheria sp.* and *Candida sp.* in the eukaryotic communities. In Chapter 2, all of these species were successfully isolated from the field samples (where the inoculum for this experiment was sourced).

Over the course of four weeks, species richness and diversity increased in the prokaryotic communities but decreased in the eukaryotic microbial communities suggesting these conditions were more favourable for a wider variety of prokaryotic species. Similar results to the prokaryotic microcosms have been seen in other xenobiotic degrading microcosms;

initially the systems are dominated by a few, highly competitive organisms but as the systems mature, a wider diversity of microbes becomes apparent (Elliott *et al*. 2010). This highlights the need to regularly remove conditions favourable for microbial growth i.e. free water, when operating in the field.

DESEQ2 analysis identified prokaryotic organisms that favoured the alternative fuel GTL over conventional and *vice versa*. This suggests that introducing alternative jet fuels into systems containing conventional jet fuel will cause a shift in the microbial population and that prokaryotic communities are more likely to be susceptible to such changes in fuel composition than the eukaryotic communities. Therefore, we can hypothesise that the observed shift in microbial community dynamics will be more marked in the prokaryotic communities. However, data from the industry-standard isolates suggests that in fuel systems where conventional and alternative fuels are mixed together, it is likely that less impact will be observed. More work needs to be undertaken to confirm whether mixing fuel types will influence a complex mixed community.

It should be noted that both conventional and alternative fuel microcosms were numerically dominated by *Stenotrophomonas sp.* and *Cellulosimicrobium sp*. whose relative abundance did not change. However, members of the *Actinomycetales* were particularly responsive. All of the OTUs whose relative abundance increased in conventional fuels compared to GTL were members of this Order (*Micrococcaceae* and *Dermatobacteraceae*), whilst *Norcardioidaceae, Microbactericeae* and *Sanguibacteraceae* showed increased relative abundance in GTL (as did the *Rhizobiales, Methylobaceriaceae*). Members of the *Actinomycetales* have been identified in many diverse hydrocarbon-degrading environments and may therefore be particularly responsive to changing fuel composition.

Overall, these results have demonstrated that the introduction of GTL kerosene into the jet fuel supply system is likely to impact the microbial communities present, with implications for current operating procedures and test methods. This impact is likely to be less marked in systems where GTL kerosene is used in mixtures with conventional fuels. Many questions are still to be addressed, including the identity of genes able to degrade GTL kerosene; how these may be transferred between microorganisms in the fuel system environment; the role of biofilms and the impact of new surfaces on biofilm formation and the complex physical and metabolic interactions between members of microbial consortia. By using microcosms to disassemble these systems and drawing comparisons with research on the environmental

impacts of fuel release this work will provide a greater understanding of the problem of microbial contamination in jet fuel systems of the future.

3.5 Conclusions

In conclusion, this study has found that:

- Industry standard isolates grow poorly in GTL kerosene. This is not due to toxicity effects, but limitations in hydrocarbon degradation in these systems. These microorganisms are either unable to utilise GTL kerosene (i.e. alkanes) as a carbon sources, or break down GTL kerosene less efficiently than aromatic species (i.e. benzenes/naphthalenes).
- Other isolates are able to utilise GTL kerosene, so it probable that these microorganisms will become dominant in systems primarily associated with GTL kerosene, or horizontal gene transfer will occur.
- Therefore, the isolates currently used as an industry standard to assess microbial contamination of fuels are not appropriate for analysing alternative fuels.
- When utilising eutrophic systems containing a mineral medium, the availability of nitrogen is the growth limiting factor. It is therefore likely that nitrogen is the limiting factor in an oligotrophic system (like seen in the field), but further analysis needs to be undertaken.
- Fuel systems are dominated by prokaryotes and any change in fuel type will have a more marked effect on the prokaryotic communities vs. the eukaryotic communities.
- GTL kerosene will undoubtedly have an impact on the microbial communities exposed to it yielding potential for new microorganisms to become dominant and for unforeseen safety concerns to arise. However, this is less likely when GTL kerosene is mixed with a conventional jet fuel.

Chapter Four

How will novel surfaces impact microbial contamination in jet fuel systems?

4.1 Introduction

Microorganisms are ubiquitous in the environment, commonly found in the air, soil and water (Passman 2003; Raikos *et al*. 2012). They are typically thought of as planktonic; free-floating and growing independently from one another. However, when introduced to a surface they begin to accumulate, amalgamating into complex communities known as biofilms, which is a community of microorganisms where cells are embedded in a self-produced matrix of water and biopolymers adhering to each other and surfaces.

Both single and multi-species biofilms have been documented across a range of different natural environments and surfaces, dating further back than the 1930s (Angst 1923). Cells within a biofilm are physiologically distinct from their planktonic counterparts, specifically altering their genetic pathways to trigger biofilm development. Biofilms are formed by producing a nutrient-rich matrix, known as EPS, largely composed of extracellular DNA, proteins and polysaccharides, which comprises over 90 % of the total biomass within a biofilm.

These three components play a key role in the aggregation, cohesion and adhesion of biofilms. However, these EPS components also confer a number of other benefits to the cells encapsulated within. Polysaccharides and proteins form a barrier, offering the cells resistance to antimicrobial agents and biocides and specific and nonspecific host defences during infection. They also shield cells from predation by protozoa.

Hydrophilic polysaccharides retain water within the biofilm, creating a hydrated microenvironment, offering protection against environmental stresses such as desiccation in arid environments. Charged polysaccharides and proteins facilitate the sorption of organic and inorganic compounds into the biofilms. Nutrients are accumulated from the environment, for example carbon, nitrogen and phosphorus containing compounds, which can be utilised by the biofilm community. Extra-cellular DNA provides a foundation for extra-cellular communication and the exchange of genetic information (horizontal gene transfer) (Flemming & Wingender 2010). These EPS matrices are so successful that it is estimated that over 99% of all life may exist within a biofilm (Vu *et al*. 2009; Andrews *et al*. 2010).

The protective nature of biofilms is particularly relevant to microorganisms found within jet fuel systems. Jet fuel is a rich carbon source for those microorganisms that able to utilise it. However, short-chain length hydrocarbons ($<C_8$), can be toxic and any microorganisms must be able to withstand such exposure. Aircraft systems are subject to extreme ranges of

temperature during flight; it is conceivable that temperatures could range between +40 °C and -50 °C, between take-off and landing. These temperature fluctuations cause any free water to go through freeze-thaw cycles, restricting its bioavailability (Zabarnicm & Ervin 2010) and disrupting cell membranes (Morley *et al*. 1983).

Biofilms undoubtedly play a key role in the microbial contamination of jet fuel systems, allowing the microorganisms encapsulated within them to survive these harsh conditions. Therefore, the surfaces within jet fuel systems are particularly important, as their properties will influence biofilm attachment. Historically, aircraft fuel tanks have been constructed of lightweight aluminium alloys, such as T2024 and latterly T7075-T6. These surfaces were typically coated in a chromate-leaching epoxy paint, offering increased protection against chemical corrosion. However, advances in technology have led to aluminium alloys being replaced with proprietary carbon composites; lightweight woven mats of carbon embedded in plastic. These materials offer increased strength at a lower weight than their aluminium alloy counterparts. Additionally, due to environmental concerns, chromate-leaching paints have been banned in jet fuel systems and have been replaced with less toxic epoxy coatings.

These factors will undoubtedly have an impact on biofilm formation in jet fuel systems and it is important to understand how this change of substrate impacts the microbial communities. This chapter uses next-generation sequencing and microscopy to characterise two representative microbial communities (one from conventional jet fuels and one from alternative fuels). Using these data, the impact of varying surface chemistry (including chromate-leaching epoxy paint) on biofilm formation, in both jet fuel and its associated free water, is explored.

4.1.1 Chapter aims and objectives

This chapter aims to examine biofilm formation within typical jet fuel systems. Culture-independent techniques are employed to characterise and compare the planktonic and sessile microbial communities and these data used to explore the impact of varying tank coatings on biofilm structure.

The main objectives of this chapter are:

a) To use culture-independent methods to characterise representative microbial communities found in both the fuel and aqueous phases and, using these data, examine the variation in both the planktonic and sessile communities within these systems;
b) To explore the impact of using representative surface coatings on the microbial community dynamics of the attached biofilms;
c) To examine how the removal of chromate-leaching paint will likely affect the microbial communities found in these systems. Specifically, i) the ability of the organisms to form biofilms and ii) the diversity of microorganisms within these biofilms.

4.2 Materials and methods

4.2.1 Materials

4.2.1.1 Surfaces

Three hundred and twenty 60 x 11 x 1 mm aluminium alloy 7075-T6 coupons were machined and then naturally anodised by Oxton Engineering (UK). Coupons were degreased with acetone and dried. The coupons were divided into 3 groups: 160 coupons had a layer of Epoxy Coating EA 42217 (3M Scotchkote, USA) applied to them, 80 had a layer of Aerowave 2001 Primer (AkzoNobel, Netherlands) (a chromate-leaching paint) applied and 80 coupons were left unpainted. The epoxy paint was composed of 4 parts paint and 1 part epoxy coating activator EA 42217 (3M Scotchkote, USA) and diluted to 65 % (v/v) with Cleaner 3000 (3M Scotchkote, USA). The chromate-leaching paint was composed of 3 parts paint and 1 part Curing Solution 6005 (AkzoNobel, Netherlands) and diluted to 70 % (v/v) with distilled water. Both paints were then applied in 4 thin layers, approximately 1 per hour, on the upper side of the coupon and then left to dry overnight, before repeating the process on the underside of the coupon. Paint was applied using a 4 inch foam roller (Hamilton, UK). Coupons were then left for 48 hours to dry before being sterilised in a bench top autoclave (Prestige Medical, UK).

4.2.1.2 Fuels

Two fuels were supplied by Shell Research Ltd.: Merox-treated Jet A-1 and GTL kerosene. Fuels were sterilised by passing them through a 0.22 µm nitrocellulose filter paper (Merck Millipore, USA). To form a fuel/aqueous interface the fuels were overlaid on sterile Bushnell-Haas nutrient medium (Sigma-Aldrich, UK).

4.2.1.3 Microorganisms

Two mixed communities were obtained by combining contaminated water from 5 Jet A-1 samples for microcosms containing Merox-treated Jet A-1 and contaminated water from 5 GTL kerosene samples for microcosms containing GTL kerosene.

4.2.1.4 Microcosms

Sterile 20 ml microcosms were set up using 5 ml of Merox-treated Jet A-1 and 5 ml of Bushnell-Haas medium (Sigma Aldrich, UK) placed in a GC headspace vial sealed with a 20 mm PTFE/Butyl rubber crimp lid. Gas exchange was allowed by introducing a 1 inch sterile needle capped with a PTFE 0.2 µm filter. An aluminium coupon, coated in either epoxy paint, chromate-leaching paint or uncoated was added to each microcosm, so that the fuel/aqueous interface was approximately a third of the way up the coupon. A subset of

these microcosms was also set up containing no coupon, so that planktonic communities could be analysed. The coupon was angled at approximately 20° to the vertical. Microcosms were inoculated with a mixed culture of microorganisms drawn from 5 different contaminated water samples taken from fuel tanks containing conventional fuel, at an OD^{600} of 0.05. Sterile controls were also prepared. Microcosms were incubated at 25 °C and sampled destructively after 2 weeks. Four independent replicates were performed in each case and an individual set of replicates set up for each experimental technique, giving a total of 176 microcosms (see Table 4.21).

A set of sterile microcosms were also set up in the same way, except 5 ml of GTL kerosene was used as a fuel source and only epoxy coated coupons added to the microcosms. A subset of these microcosms was also set up containing no coupon, so that planktonic communities could be analysed. Microcosms were inoculated with a mixed culture of microorganisms drawn from 4 different contaminated water samples taken from contaminated fuel samples containing GTL kerosene, at an OD^{600} of 0.05. Sterile controls were also prepared. Microcosms were incubated at 25 °C and destructively sampled after 2 weeks. Four independent replicates were performed, accounting for 36 of the total number of microcosms in this study. Microcosms were also set up for GC-MS analysis. These contained 900 µl of Bushnell-Haas medium and 100 µl of either Merox-treated Jet A-1 or GTL kerosene, but were otherwise treated as described above (but were not vented). Four independent replicates were performed in each case, accounting for 16 of the total number of microcosms in this study (see Section 3.2.3.2).

Table 4.21 – Sample matrix indicating the number of microcosms set up for each type of analysis. The same number of microcosms was also set up containing no microbial community for use as sterile controls.

Fuel	Coupon	Community	DNA extraction	SEM	Confocal	GC-MS
Jet fuel	AA 7075	1	8	4	4	-
	Epoxy		8	4	4	-
	Chromate		8	4	4	-
	None		8	-	-	4
GTL kerosene	Epoxy	2	8	4	4	-
	None		8	-	-	4
Total			48	16	16	8

4.2.2 Methods

4.2.2.1 Confocal microscopy

Coupons with attached microbes were analysed by removing the coupons from the microcosms and fixing them in a 4 % (v/v) formaldehyde solution. The coupons were stained with 50 µM SYTO 9 solution (to visualise microbial cells) and 100 % SYPRO Ruby Biofilm Matrix Stain (v/v) (Life Technologies, USA), (to visualise matrix components). One millilitre of the SYPRO Ruby was applied to the surface of each coupon and incubated in the dark at room temperature for 25 minutes, then 800 µl of filtered SYTO 9 solution was applied and incubated for a further 5 minutes. The coupons were gently washed with filtered deionised water, a coverslip applied and imaged immediately by confocal laser scanning microscopy (CLSM) (Zeiss LSM510 Meta). Images were collected using an Olympus FV1000 microscope using a 10x objective with excitation at 488 nm from an argon laser. SYTO 9 fluorescence was selected using a 500-550 nm band pass filter whilst SYPRO Ruby was selected using a 650-710 nm band pass filter. Images were 1252 x 1252 pixels in size (0.17 µm/pixel) and acquired at 0.89 µm intervals. Images were false coloured using ImageJ (a green channel was selected for SYTO 9 and a red channel for SYPRO Ruby) (Rasband 1997).

4.2.2.2 Scanning electron microscopy (SEM)

Thirty two coupons were removed from the microcosms; 16 each incubated with the mixed cultures of microorganisms and their respective sterile controls. The coupons consisted of 8 uncoated aluminium coupons, 8 aluminium coupons coated in epoxy paint, 8 aluminium coupons coated with chromate leaching paint, all incubated in Merox-treated Jet A-1 and 8 aluminium coupons coated in epoxy paint incubated in GTL kerosene. The coupons were drained gently by touching the lower edge to tissue paper and the fuel removed by incubating for 15 minutes in a humid atmosphere, with a gentle airflow. The bottom 20 mm of the coupons was removed so that the fuel, fuel-aqueous interface and aqueous phases were sampled and then fixed in 0.1 M cacodylate buffer, with 3 % glutaraldehyde and stored overnight at 4 °C. Coupons were then fixed in 2 % osmium tetroxide (aqueous) for one hour at room temperature and then gradually dehydrated in increasing concentrations of ethanol solution (75 %, 95 %, 100 %, 100 % (v/v)) for 15 minutes each (one hour total). Ethanol was then removed by drying the coupons over anhydrous copper sulphate for 15 minutes and the residual ethanol removed with hexamethyldisilazane. Coupons were then placed in a 50:50 (v/v) mixture of ethanol and hexamethyldisilazane for 30 minutes, followed by a further 30 minutes 100% (v) hexamethyldisilazane and allowed to air dry overnight. Coupons were then mounted on a 12.5 mm diameter stub, using carbon sticky tabs and then sputter

coated (Edwards S150B) with approximately 25 nm of gold. Images were collected using a Philips XL-20 scanning electron microscope at an accelerating voltage of 20 kV.

4.2.2.3 GC-MS

GC-MS analysis was undertaken as described previously (see Section 3.2.5.2).

4.2.2.4 DNA extractions

Planktonic microorganisms were extracted from the microcosms by drawing 4 ml of both the aqueous phase and fuel phase from the microcosms using a 5 ml sterile syringe and 2 inch sterile needle and passing it through separate 0.22 µm nitrocellulose filter (this was done for both the microcosms containing coupons as well as microcosms that did not include coupons). Biofilms were sampled by separately swabbing both the aqueous and fuel phases of the coupons with sterile foam-tipped swabs (Puritan, USA).

Each filter/swab was then transferred into a 2 ml microcentrifuge tube and 720 µl of SET buffer[57] and 81 µl of 10 mg/ml lysozyme (Sigma Aldrich, UK) added and vortexed for 10 seconds to mix thoroughly. The filters/swabs were then incubated at 37 °C for 30 minutes. After incubation, 90 µl of 10 % (v/v) sodium dodecyl sulphate (SDS) (Sigma-Aldrich, UK) and 25 µl of 20 mg/ml proteinase K (Applied Biosystems, USA) were added to the tubes and incubated at 55 °C for 2 hours. The lysate was then transferred into a fresh 2 ml microcentrifuge tube and 137 µl of 5 M sodium chloride, 115 µl of hexadecyltmethyl ammonium bromide (CTAB) and sodium chloride solution[58] and 8 µl of 20 mg/ml glycogen added. Samples were then vortexed for 10 seconds to mix and incubated for a further hour at 65 °C. After incubation, 838 µl of chloroform (Sigma-Aldrich, UK) was added to the tubes, vortexed for 10 seconds and centrifuged at 17,900 x *g* for 5 minutes. The upper, aqueous layer was then removed into a fresh 2 ml microcentrifuge tube and cleaning with chloroform repeated. Eight hundred and fifteen microliters of isopropyl alcohol were then added to the lysate, which was vortexed for 10 seconds and incubated overnight at -20 °C. Samples were centrifuged at 17,900 x *g* for 30 minutes at 4 °C and the supernatant removed. One millilitre of 70 % (v/v) ethanol solution was added to the tube and mixed by finger tapping. Samples were centrifuged at 17,900 x *g* for a further 10 minutes at 4 °C, the ethanol solution removed and this step repeated. After a second centrifugation, the ethanol solution was again removed and the sample centrifuged for 1 minute at 17,900 x *g*. The final ethanol was removed and samples left to air dry. The pellet was resuspended in 50 µl of 10 mM TE buffer[59]

[57] 40 mM Ethylenediaminetetraacetic acid (EDTA), 50 mM Tris-HCl (pH 9.0), 0.75 M sucrose.
[58] 4.1 g Sodium Chloride, 10 g CTAB and 100 ml distilled water.
[59] 5 ml of 1 M Tris-base, 1 ml 0.5 M EDTA in 494 ml distilled water, pH 8

and incubated on ice for 1 hour, periodically mixed by finger tapping (approximately every 15 minutes) (Fish *et al*. 2015).

4.2.3 Illumina sequencing and bioinformatics analysis

The sequencing process was undertaken as outlined in Chapter 3. Prokaryotic sequences had a read depth ranging between 185 and 260,742 reads per sample with an average of 33,977 reads per sample, with a pass rate ranging from 2.0 to 82.2 % per sample with an average of 53.5 % (maxEE value of 1.00) for the 250 bp read lengths. Eukaryotic sequences had a read depth ranging from 7 to 21,446 reads per sample with an average of 3,730, with a pass rate between 3.6 and 83.8 % with an average of 52.9 % (maxEE value of 1.00) for the 250 bp reads. This indicates that the quality of the 250 bp read sequences was quite variable. Chimeric sequences were removed from the prokaryotic (3,295,478) and eukaryotic (358,062) datasets, leaving 3,057,953 and 335,659 sequences and rarefied to 4,000 and 1,000 reads per sample respectively. Taxonomy was assigned as previously described (see Section 2.2.4.2) and bioinformatics analysis performed as described in section 2.2.4.2.6.

4.3 Results

To examine the differences between planktonic and sessile microbial communities, microcosm systems were step up. These consisted of two fuel types and three surfaces, each containing a defined mineral medium. The mineral medium provided all of the necessary nutrients for microbial growth, with the exception of a carbon supply that was provided by the fuel. The microcosms were inoculated with two different communities, one taken from water phase of contaminated GTL kerosene and the second from conventional jet fuels. These were then used to inoculate microcosms containing the same fuel type. After two weeks, culture-independent methods were used to measure the impact of varying surface type on both the planktonic and the sessile communities within the microcosms. Surfaces were also assessed using epifluorescent microscopy and SEM to determine how variations in surface type and surface finish altered attached communities. Fuel degradation was assessed using GC-MS.

4.3.1 Microscopy

Biofilm formation on the aluminium alloy 7075-T6 coupons was assessed using epifluorescent and scanning electron microscopy. Figure 4.47to Figure 4.50 show examples of mixed community biofilms formed on three different types of aluminium alloy 7075-T6 coupons after 2 weeks incubation in microcosms containing Merox-treated Jet A-1 (see Figure 4.48 to Figure 4.50) and GTL kerosene (see Figure 4.47). In each figure, images A-C are from epifluorescent microscopy, where cells fluoresce green and matrix components fluoresce red. Images D-F are SEM.

In chapter 3, SYPRO Ruby was used successfully to image matrix components of biofilms associated with steel coupons, but a strong background fluorescence was observed in the coupons used in these microcosms. It is difficult to distinguish between matrix components of a biological and non-biological origin in these images (unless associated with filamentous structures clearly of a biological origin). In the future, alternative stains will need to be considered.

Figure 4.47 shows epoxy coated aluminium alloy 7075-T6 coupons in GTL kerosene. Epifluorescent microscopy shows a heterogeneous biofilm formed after two weeks. SEM images show that individual cells had attached in the aqueous phase with only a few colonies of clustered cells present. Numerous cell morphologies were observed (most notably fungal hyphae). As well as many individual cells, some large colonies of cells were evident, up to 10 µm across. Some limited production of EPS was evident in the aqueous phase as seen in

Figure 4.47, F. A limited number of cells had also attached in the fuel phase with epifluorescent microscopy showing numerous, but somewhat smaller colonies, developing. There was little evidence of fungal growth in this phase.

Figure 4.49 shows epoxy coated aluminium alloy 7075-T6 coupons in the Merox-treated Jet A-1. Morphologically, results in this sample set were similar to those observed in the GTL kerosene, though different communities were used for inoculation. Epifluorescent microscopy showed a heterogeneous biofilm formed after two weeks. SEM images showed that individual cells had attached in the aqueous phase. However, no clusters of cells were observed. The highest variety in cell morphology was observed in this sample (see Figure 4.48). Cell density increased with proximity to the aqueous/fuel interface and was greatest in this region of the coupon. Here multiple eukaryotic cells were observed, consisting of a dense layer of fungal hyphae and fungal spores in Figure 4.48, E. Many cells were also observed in the fuel phase. Typically, numerous large colonies were evident, up to 10 µm across. There was little evidence of fungal growth in this phase.

The most evident difference was noted in Figure 4.49, which shows aluminium alloy 7075-T6 coupons coated in chromate-leaching paint in Merox-treated Jet A-1. Similarly to the epoxy coated coupons, epifluorescent microscopy showed a heterogeneous biofilm had formed after two weeks. Cells in the aqueous phase increased in density with proximity to the aqueous/fuel interface. In the fuel phase cells tended to cluster together and stacked on top of one another (clustering was noted in all phases, but was much more apparent in the fuel phase). The diversity of cell morphology was also lower, compared to the epoxy coated coupons. Observed cells were larger in size. Presumably the toxic nature of the chromate leaching paint was exerting a selection pressure on this community. A hypothesis is that cells towards the bottom of the cluster were most likely dead, with the viable cells stacking on top to form the biofilm.

Figure 4.50 shows uncoated aluminium alloy 7075-T6 coupons, in Merox-treated Jet A-1. Unfortunately, image quality was poor due to a poor signal to noise ratio (possibly due to reflection from the coupon surface), so little can be deduced from these images. SEM indicated that there was sparse attachment of single cells in both phases. The images shown in this thesis are typical examples of the biofilms observed during this experimental programme. At present these images are purely qualitative in nature and no quantitative analysis has been undertaken.

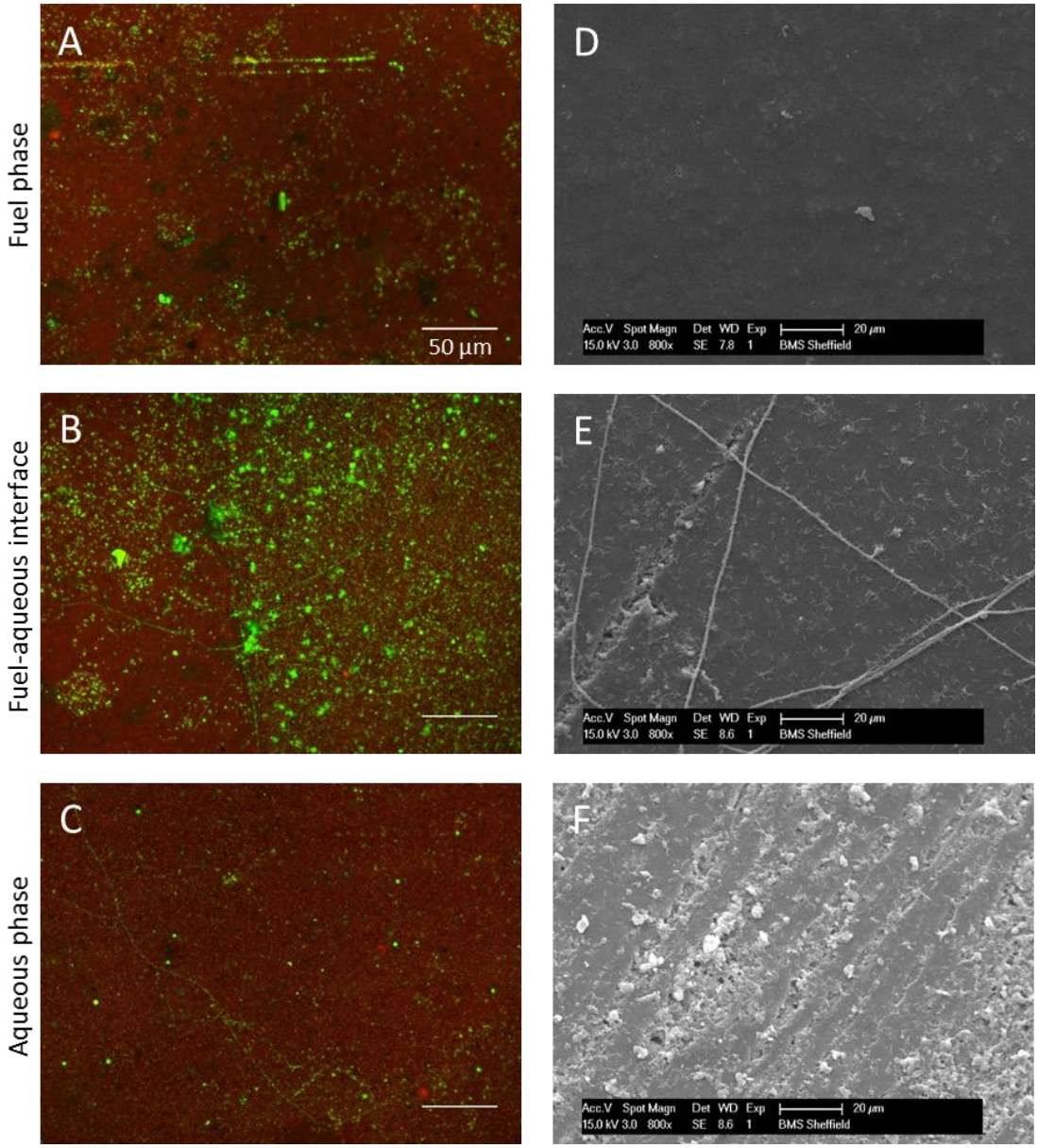

Figure 4.47 – CLSM (A-C) and SEM (D-F) images of a biofilm formed from a mixed microbial community on epoxy coated aluminium alloy 7075-T6 coupons incubated for 2 weeks in microcosms containing GTL kerosene. Images were taken at different points along the coupon in the aqueous phase, at fuel-aqueous interface and in the fuel phase. The CLSM images are a maximum intensity projection image of the DNA stain SYTO 9 (light green) and the matrix stain SYPRO Ruby (red). SEM images are a secondary electron image of coupons sputter-coated in gold. Scale bars are 50 µm (CLSM images) and 20 µm (SEM images).

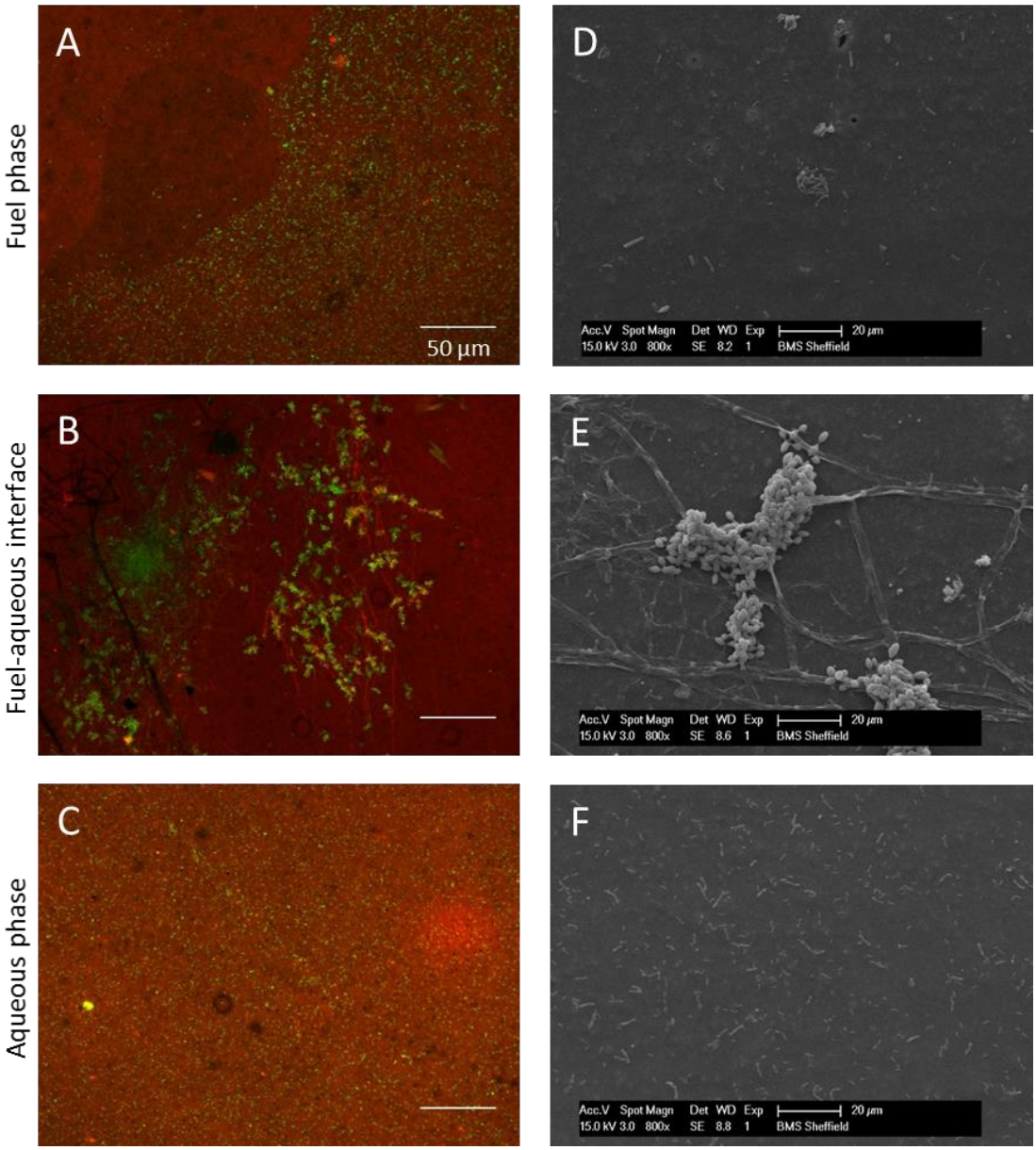

Figure 4.48 – CLSM (A-C) and SEM (D-F) images of a biofilm formed from a mixed microbial community on epoxy coated aluminium alloy 7075-T6 coupons incubated for 2 weeks in microcosms containing Merox-treated Jet A-1. Images were taken at different points along the coupon in the aqueous phase, at fuel-aqueous interface and in the fuel phase. The CLSM images are a maximum intensity projection image of the DNA stain SYTO 9 (light green) and the matrix stain SYPRO Ruby (red). SEM images are a secondary electron image of coupons sputter-coated in gold. Scale bars are 50 µm (CLSM images) and 20 µm (SEM images).

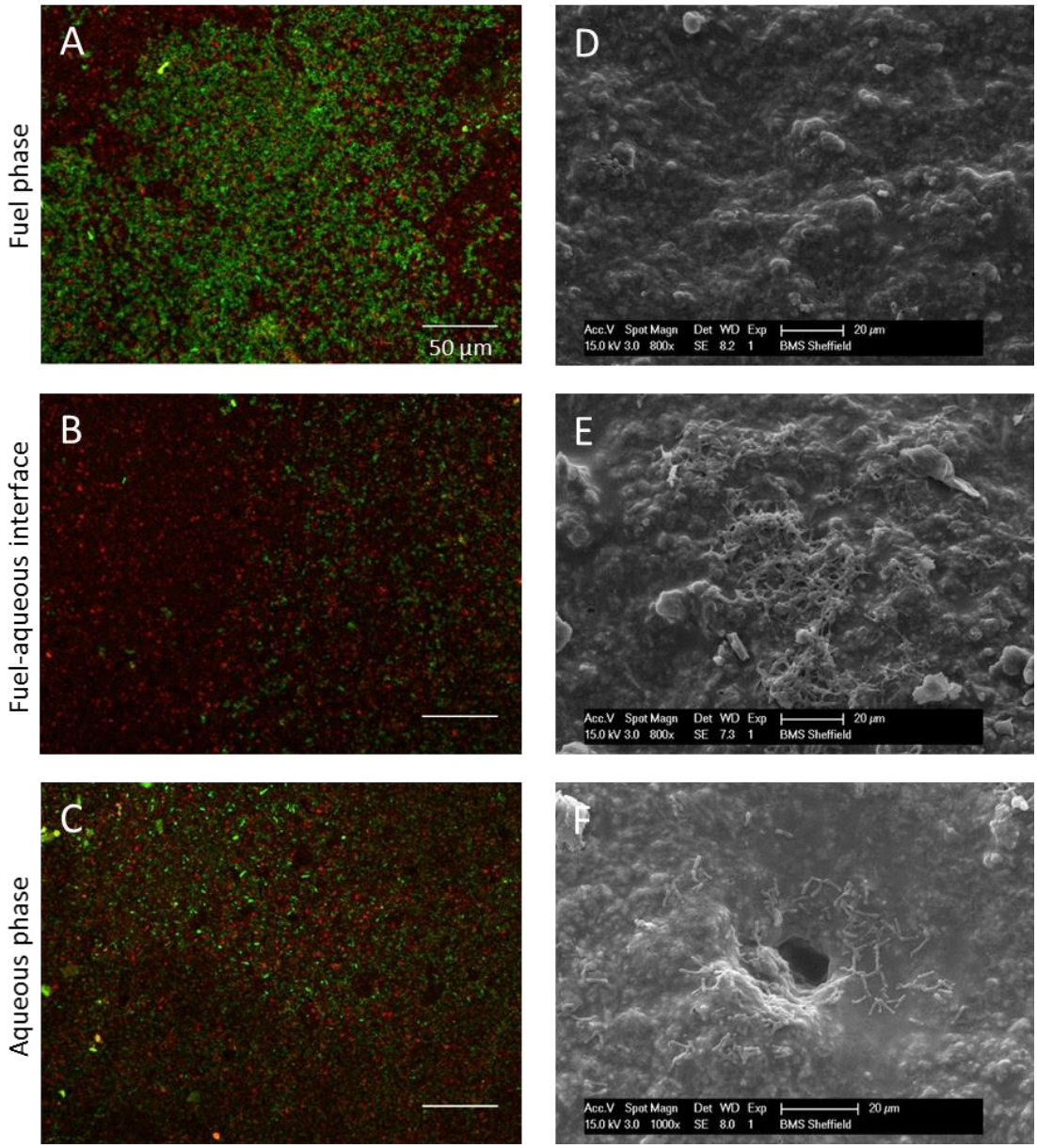

Figure 4.49 – CLSM (A-C) and SEM (D-F) images of a biofilm formed from a mixed microbial community on aluminium alloy 7075-T6 coupons, coated in chromate leaching paint and incubated for 2 weeks in microcosms containing Merox-treated Jet A-1. Images were taken at different points along the coupon in the aqueous phase, at fuel-aqueous interface and in the fuel phase. The CLSM images are a maximum intensity projection image of the DNA stain SYTO 9 (light green) and the matrix stain SYPRO Ruby (red). SEM images are a secondary electron image of coupons sputter-coated in gold. Scale bars are 50 µm (CLSM images) and 20 µm (SEM images).

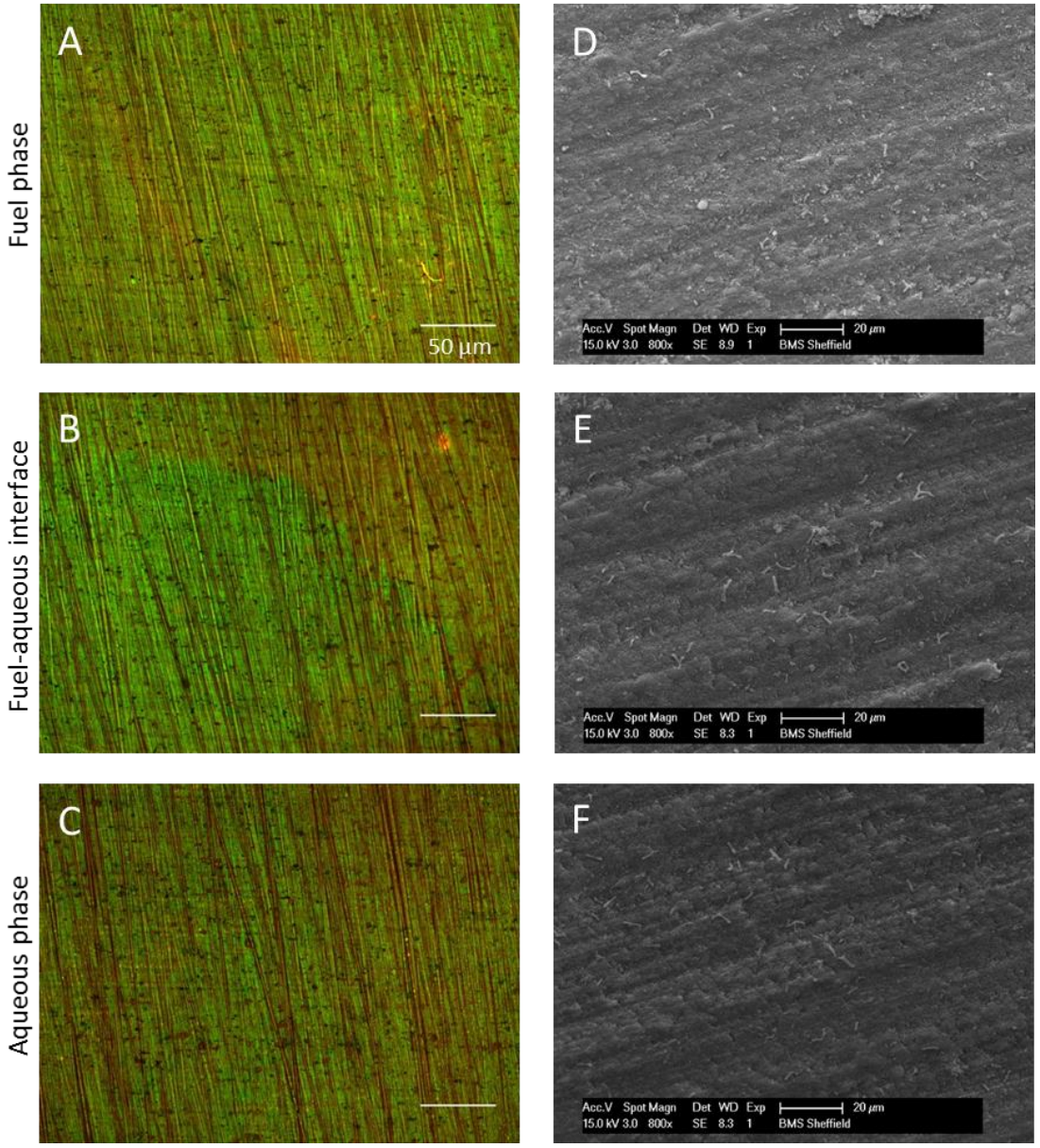

Figure 4.50 – CLSM (A-C) and SEM (D-F) images of a biofilm formed from a mixed microbial community on uncoated aluminium alloy 7075-T6 coupons incubated for 2 weeks in microcosms containing Merox-treated Jet A-1. Images were taken at different points along the coupon in the aqueous phase, at fuel-aqueous interface and in the fuel phase. The CLSM images are a maximum intensity projection image of the DNA stain SYTO 9 (light green) and the matrix stain SYPRO Ruby (red). SEM images are a secondary electron image of coupons sputter-coated in gold. Scale bars are 50 µm (CLSM images) and 20 µm (SEM images).

4.3.2 Gas Chromatography-Mass Spectrometry

The hydrocarbon composition of the Merox-treated Jet A-1 and GTL kerosene was analysed using GC-MS after the growth of two mixed communities; one sourced from conventional fuels (grown on Merox-treated Jet A-1) and the other from alternative fuels (grown on GTL kerosene) for two weeks and comparisons made against the sterile controls. Data was analysed as previously described (see Section 3.2.5.2), using a combination of R (R Team 2008) and Metaboanalyst (Xia & Wishart 2011). All microcosms were sealed to prevent loss of volatile components. Sufficient headspace was present to ensure that the systems remained aerobic. At the end of the incubation time, fuel composition was analysed by GC-MS and candidate molecules that showed a significant reduction in the live microcosms identified by comparison against the NIST database (see 3.2.5.2).

After analysis, 8 candidate molecules that differed significantly were identified in the Merox-treated Jet A-1 and no candidate molecules were identified in the GTL kerosene (see Table 4.22). In the Merox-treated Jet A-1 the mixed community sourced from conventional jet fuels showed a significant decrease in molecules identified as p-xylene, o-xylene, nonane, 1-ethyl-3-methyl-benzene, decane, undecane, 2,3-dimethyl-octane and 2-methyl-naphthalene (see Figure 4.51).

Overall the data showed that the mixed community sourced from conventional jet fuels had the ability to degraded a range on compounds, including n- and iso-alkanes, as well as aromatic and polycyclic aromatics. The community had preferentially degraded the shorter chain n-alkanes, specifically nonane, decane and undecane (C_9 to C_{11}) compared to the larger straight chain alkanes (C_{12} to C_{16}) in this fuel, as well as aromatic rings with two methyl (or one methyl and one ethyl) groups associated with them. Presumably the smaller chain length alkanes required less energy to breakdown and were therefore preferentially degraded compared to longer chain molecules. However, the results of this study are limited. No degradation of hydrocarbons was detected in the GTL kerosene although growth was observed in the microcosm, indicating that hydrocarbon degradation must have occurred. Therefore, it is likely that the GC-MS was not sensitive enough to detect small changes in the hydrocarbons degraded by these microorganisms. Further work needs to be undertaken to develop this method.

Table 4.22 – Shows the number of m/z within a peak in the GC-MS spectra where a significant ($p \leq 0.05$) change occurred in the Merox-treated Jet A-1 samples and the compounds predicted by comparison to the NIST database.

Compound	Number of significant masses degraded
p-xylene	10
o-xylene	12
Undecane	14
Nonane	12
1-ethyl-3-methyl-benzene	11
Decane	11
2,3-dimethyl-octane	10
2-methyl-naphthalene	13

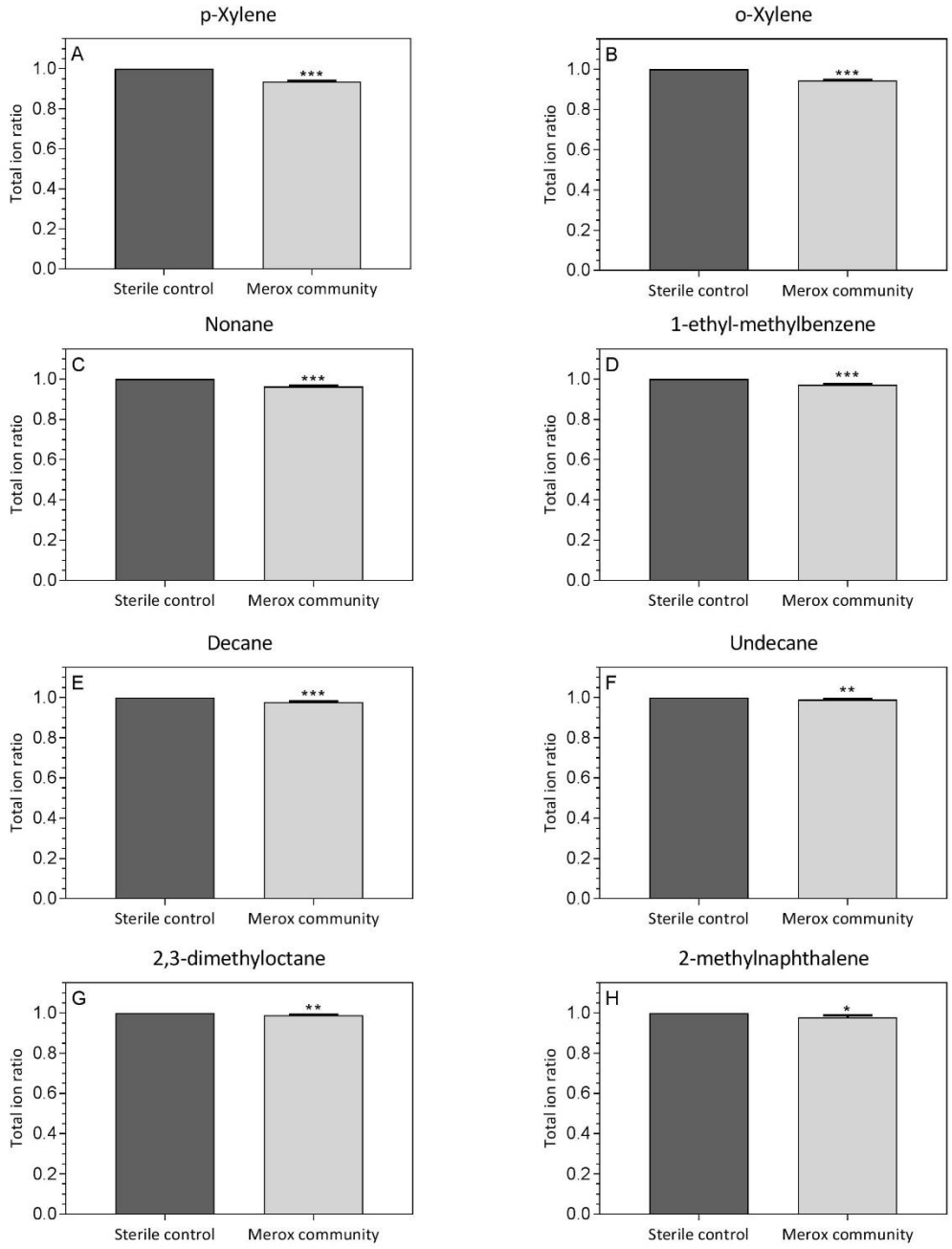

Figure 4.51 – Compounds degraded in microcosms containing Merox-treated Jet A-1 and a mixed microbial community (sourced from conventional fuels). Compounds were selected if ≥ 10 m/z values differed between the live microcosm and the sterile control. The mean (+ SE) total ion counts for the candidate molecules are shown, normalised to that in the sterile control. Significant differences are indicated (t-test, * p <0.05, ** p <0.01, *** p <0.001).

4.3.3 Culture-independent analysis of microbial communities on aluminium surfaces

4.3.3.1 Sample key

From this point onwards in Chapter 4, figures are labelled with the unique codes assigned to them during analysis. This was done because there are multiple variables within the sample set which would not otherwise fit onto the figures. These codes took the form of four to five characters, consisting of numbers and letters; four letters denote the initial inoculum and five letters the microcosm samples (see Table 4.23). For example:

MC1WS would denote: M - Merox-treated Jet A-1, as the fuel, C - Chromate-leaching coupon in the microcosms, 1 - Biological replicate number 1, W - Sample taken from the aqueous (water) and S - Sample is sessile (swabbed).

GN4FF would denote: G - GTL kerosene, as the fuel, N - No coupon associated with the microcosm, 4 - Biological replicate number 4, F - Sample taken from the fuel phase and F - Sample is planktonic (filtered).

Table 4.23 – Chapter 4 sample key

Sample code	Definition
First letter:	This is the fuel that was associated with the microcosm/inoculum
G	GTL kerosene
M	Merox-treated Jet A-1
J	Jet fuel
Second letter:	This is the surface that was associated with the microcosm
A	Aluminium alloy T7075-T6, with no coating
C	Aluminium alloy T7075-T6, with a chromate-leaching epoxy paint
E	Aluminium alloy T7075-T6, with a chromate-leaching epoxy paint
N	No coupon associated with the microcosm
Letter omitted	This is the inoculum
Third number:	This is the biological replicate
1	Biological replicate 1
2	Biological replicate 2
3	Biological replicate 3
4	Biological replicate 4
5	Biological replicate 5
Fourth letter:	Whether the community was taken from the fuel or aqueous phase
F	Fuel phase
W	Aqueous phase
Fifth letter:	Whether the fuel was filter (planktonic) or swabbed (sessile)
F	This sample was filtered and was a planktonic community
S	This sample was swabbed and was a sessile community

4.3.3.2 Diversity of microbial communities

To examine the impact of surface type on the microbial populations within jet fuel systems, culture-independent analysis was undertaken on two microbial communities; one sourced from contaminated jet fuel and one sourced from contaminated GTL kerosene. These communities were introduced into a series of laboratory microcosms, which contained different surfaces and either Merox-treated Jet A-1 or GTL kerosene. The inoculating communities were introduced into microcosms containing the same fuel type from which they were sourced. The surfaces used were: bare aluminium alloy 7075-T6 coupons, epoxy coated aluminium alloy 7075-T6, epoxy coated aluminium alloy 7075-T6 containing chromate. All surfaces were incubated in microcosms with Merox-treated Jet A-1 and only epoxy coated aluminium alloy 7075-T6 in the microcosms containing GTL kerosene. Control microcosms containing no coupons were also included. This resulted in a total of 90 samples. The microbial communities were then analysed using next generation sequencing. DNA was taken from the planktonic phase (fuel or water) and the sessile phase (fuel or water, surface type)

In the prokaryotic sequences, 457 distinct OTUs were identified by comparison with the Greengenes database at 97 % sequence identity. Across all of the samples, prokaryotes from 23 phyla were identified. The phylum Proteobacteria was the most dominant accounting for 42.7 % of the prokaryotes sequenced. These belonged to the classes: Alphaproteobacteria (35 %), Betaproteobacteria (26 %), Gammaproteobacteria (25 %), Deltaproteobacteria (13 %) and TA18 (1 %). Actinobacteria were the next most abundant phylum and accounted for 18.8 % of the prokaryotes sequenced. They were predominantly from the class of Actinobacteria (84 %), though microorganisms from classes of Thermoleophilia (7 %), Acidimicrobia (6 %), Rubrobacteria (2 %) and MB-A2-108 (1 %) were also identified. Firmicutes (13.0 %) and Bacteroidetes (7 %) made up the remaining two dominant phyla. The Firmicutes were composed of Bacilli (58.0 %) and Clostridia (42.0 %) and the Bacteroidetes composed of Flavobacteria (35 %), Bacteroidia (16.5 %), Cytophagia (16.5 %), Sphingobacteria (13 %), Saprospirae (13 %), Rhodothermi (3 %) and VC2-1-Bac22 (3 %) (see Figure 4.52).

Across the eukaryotic libraries, 206 OTUs were identified by comparison with the UNITE database at 97 % similarity. The dominant phylum was Basidiomycota, accounting for 54.1 % of the sequences. These were the classes: Agaricomycetes (75 %), Tremellomycetes (9 %), Exobasidiomycetes (5 %), Microbotryomycetes (4 %) and other classes (6 classes; 7 %). Ascomycota made up the other dominant phylum, accounting for 40.4 % of the eukaryotes

sequenced. These were from the classes: Dothideomycetes (27 %), Sordariomycetes (25 %), Saccharomycetales (18 %), Eurotiomycetes (11 %), Lecanoromycetes (7 %), Leotiomycetes (6 %) and other classes (4 classes; 6 %). The remaining microorganisms were from the phyla Zygomycota (2 %), Chytridiomycota (1.5 %), Glomeromycota (1 %) and two unidentified microorganism (1 %) (see Figure 4.53).

A total of 746 microorganisms were identified in this study with only 70 microorganisms having a relative abundance greater than 5 % in any sample. Of the prokaryotes, 11 OTUs were present in more than 50 % of the sequenced samples. *Pseudomonas sp.*, *Burkholderia sp.*, *Cupriavidus sp., Sphingomonas sp.* and *Cellulosimicrobium sp.* appeared to be particularly dominant (>70 % abundance in a single sample), forming near monocultures in some samples (97.1 % maximum relative abundance). Of the eukaryotes 12 OTUs were present in more than 50 % of the sequenced samples. *Candida sp.*, *Rhinocladiella sp.*, *Yarrowia sp.* and an unidentified fungus were particularly dominant (>70 % abundance in a single sample), similarly forming a near monoculture in some samples (99.8 % maximum relative abundance). Table 4.24 and Table 4.25 below list the most dominant microorganisms seen in all 90 samples.

Table 4.24 – The most dominant prokaryotic microorganisms observed across the sample set. Microorganisms were selected if they were observed at relative abundance of >5 % in any of the samples sequenced.

	Maximum relative abundance (%)	Average relative abundance (%)	Number of samples where present
Prokaryotes			
Sphingomonas sp.	72.0	13.4	81
Bradyrhizobium sp.	36.0	5.3	80
Pseudomonas sp.	97.1	33.3	76
Cupriavidus sp.	74.0	13.7	74
Methylobacterium sp.	54.3	6.4	70
Unidentified bacteria	7.1	0.4	60
Burkholderia sp.	92.2	10.6	59
Xanthomonadaceae (Other)	36.5	1.8	59
Rhodospirillaceae (Other)	12.1	1.5	54
Comamonadaceae (Other)	5.6	0.4	42
Rhizobiales (Other)	5.3	0.5	41
Dermacoccus sp.	6.8	0.3	35
Bacillus sp.	57.5	1.3	35
Gluconacetobacter sp.	25.2	0.5	32
Enterobacteriaceae (Other)	5.8	0.4	31
Staphylococcus sp.	7.8	0.3	30
Sphingobium sp.	5.2	0.3	29
Sphingomonadaceae (Other)	1.0	6.1	28
Cellulosimicrobium sp.	91.5	1.4	26
Flavobacterium sp.	10.6	0.3	22
Sinobacteraceaae (Other)	6.7	0.2	18
Acetobacteraceae (Other)	5.9	0.1	13
Syntrophobacteraceae (Other)	5.3	0.1	10

Table 4.25 – The most dominant eukaryotic microorganisms observed across the sample set. Microorganisms were selected if they were observed at relative abundance of >5 % in any of the samples sequenced.

	Maximum relative abundance (%)	Average relative abundance (%)	Number of samples where present
Eukaryotes			
Candida sp.	99.8	41.3	89
Unidentified fungi	88.9	6.5	80
Geotrichum sp.	64.9	6.9	75
Rhinocladiella sp.	99.6	17.5	71
Saccharomycetaceae (Other)	95.2	1.1	6
Strophariaceae (Other)	94.9	1.4	26
Meyerozyma sp.	50.4	2.8	63
Basidiomycota (Other)	42.7	2.3	63
Yarrowia sp.	71.0	2.8	60
Amorphotheca sp.	40.8	1.6	59
Ascomycota (Other)	61.9	3.6	59
Unidentified organism	32.2	1.9	50
Pichia sp.	20.9	1.4	49
Dothideomycetes (Other)	20.8	1.3	46
Polyporales (Other)	10.6	0.4	37
Cortinarius sp.	18.7	0.2	5
Piptoporus sp.	16.6	0.2	8
Ampelomycetes sp.	11.1	0.2	6
Phaeosphaeriaceae (Other)	11.1	0.2	4
Peniophora sp.	46.7	0.8	26
Hyphodontia sp.	17.6	0.6	24
Saccharomyces sp.	44.4	0.6	22
Malasseziales (Other)	17.3	0.3	21
Aspergillus sp.	7.7	0.3	20
Tilletiopsis sp.	22.0	0.4	20
Cladonia sp.	11.2	0.2	19
Antrodia sp.	7.1	0.1	2
Xylariales (Other)	7.1	0.1	5
Cystofilobasidiales (Other)	16.3	0.2	17
Trametes sp.	5.2	0.1	16
Septoria sp.	5.4	0.1	13
Penicillium sp.	12.5	0.2	13

Sample key: 1st letter: Fuel; GTL (G), Merox (M) and Jet fuel (J). 2nd letter: Surface; Aluminium (A), Chromate (C), Epoxy (E), None (N). 3rd number: bio. rep. 4th letter: Phase; Fuel (F), Aqueous (A). 5th letter: State; Planktonic (F), Sessile (S).

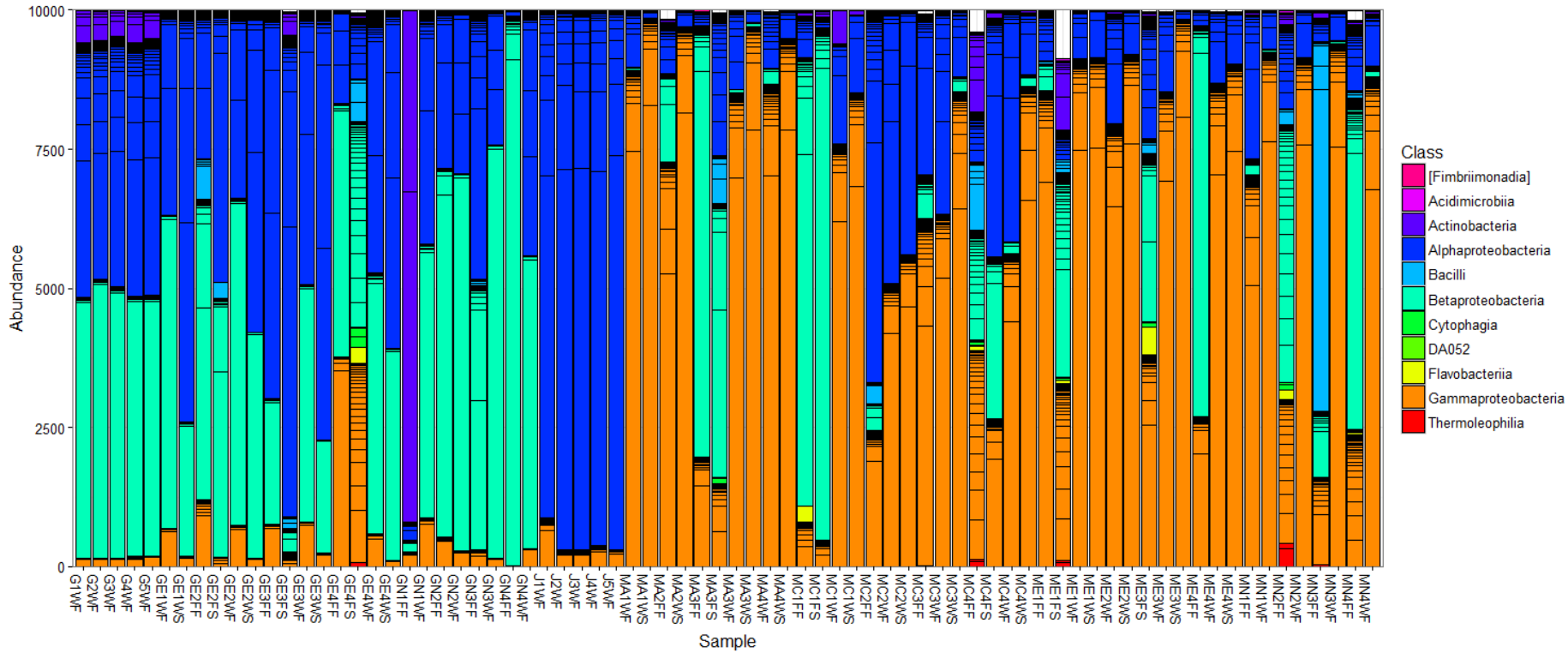

Figure 4.52 – Relative abundance of the classes of prokaryotic microorganisms found in both the Merox Jet A-1 communities and GTL kerosene communities. Both planktonic and sessile communities have been included, as well as communities from both the fuel and aqueous phases. Samples were rarefied to 10,000 counts (shown on Y axis). White bars indicate unknown microorganisms. Boxes within the bars represent a different OTU within the class.

Sample key: 1st letter: Fuel; GTL (G), Merox (M) and Jet fuel (J). 2nd letter: Surface; Aluminium (A), Chromate (C), Epoxy (E), None (N). 3rd number: bio. rep. 4th letter: Phase; Fuel (F), Aqueous (A). 5th letter: State; Planktonic (F), Sessile (S).

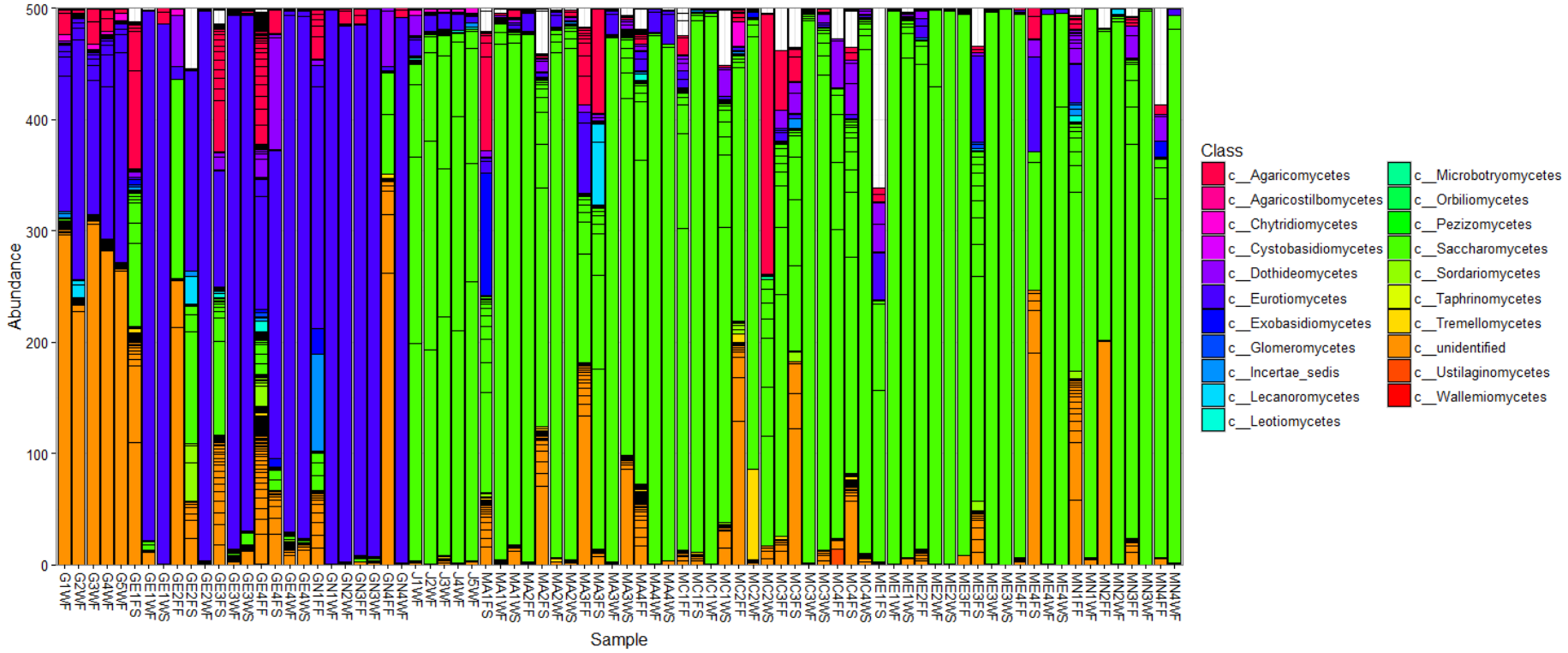

Figure 4.53 – Relative abundance of the classes of eukaryotic microorganisms found in both the Merox Jet A-1 communities and GTL kerosene communities. Both planktonic and sessile communities have been included, as well as communities from both the fuel and aqueous phases. Samples were normalised to 500 counts (shown on Y axis). White bars indicate unknown microorganisms. Boxes within the bars represent a different OTU within the class.

4.3.3.3 Richness and diversity measurements

Species richness and inverse Simpson and Shannon diversity indices were calculated for prokaryotic and eukaryotic communities (see Appendix G for Box and Whisker plots). To assess the difference in species richness and diversity, ANOVAs were performed to test the impact of State (Sessile vs Planktonic), Phase (Fuel vs Water) and Surface (Aluminium, Chromate-leaching epoxy and Epoxy for Merox-treated Jet A-1 and Epoxy for GTL kerosene) as well as the interactions between these three factors. Tukey multiple comparisons were used to determine which interactions were significant (see Table 4.26 and Table 4.27).

For both the prokaryotes and the eukaryotes in microcosms containing Merox-treated Jet A-1, both the species richness and diversity indices were strongly influenced by Phase, with indices higher in fuel compared to water. For prokaryotes, differences in these indices were not strongly influenced by State or Surface, but complex interactions between all 3 parameters were observed. For the eukaryotes, indices were generally higher in the sessile state compared to the planktonic state, particularly in the water phase of Merox-treated Jet A-1 microcosms. The surfaces also affected the diversity indices, with Aluminium and Chromate having similar values, but Epoxy being lower. In GTL, eukaryotic indices were strongly influenced by phase only. The prokaryotic indices were similar to each other except that values were higher for samples from the sessile, fuel phase. Other comparisons were not informative (hence data not shown).

Table 4.26 – *p* values derived from ANOVAs with a Tukey post hoc test applied, to show the significant differences between phase, state, surface, as well as interactions between phase:state, phase:surface, state:surface and phase:state:surface in the prokaryotic communities. Species richness, the inverse Simpson index and the Shannon index are shown. Numbers highlighted in green show as significant difference ($p \leq 0.05$).

	Richness	Inverse Simpson	Shannon
Phase	**<0.001**	**<0.001**	**<0.001**
State	0.115	0.913	0.074
Surface	0.247	0.473	**0.045**
Phase:State	0.174	0.339	**0.021**
Phase:Surface	0.145	0.258	**0.008**
State:Surface	0.292	0.107	0.056
Phase:State:Surface	**0.009**	**0.0384**	**<0.001**

Table 4.27 – *p* values derived from ANOVAs with a Tukey post hoc test applied, to show the significant differences between phase, state, surface, as well as interactions between phase:state, phase:surface, state:surface, phase:state:surface and differences in surface type in the eukaryotic communities. Species richness, the inverse Simpson index and the Shannon index are shown. Numbers highlighted in green show as significant difference ($p \leq 0.05$).

	Richness		Inverse Simpson		Shannon	
	Merox	**GTL**	**Merox**	**GTL**	**Merox**	**GTL**
Phase	**<0.001**	**<0.001**	**<0.001**	**<0.001**	**<0.001**	**<0.001**
State	**0.004**	0.309	**<0.001**	0.289	**0.007**	0.096
Surface (overall)	**<0.001**		**0.041**		**<0.001**	
Al vs Cr	**<0.001**		0.985		0.996	
Al vs Ep	**<0.001**		0.096		**0.002**	
Cr vs Ep	**<0.001**		**0.039**		**<0.001**	
Phase:State	0.254	0.726	0.211	0.453	0.465	0.737
Phase:Surface	0.306		0.265		0.118	
State:Surface	0.978		0.514		0.798	
Phase:State:Surface	0.218		**0.038**		0.070	

4.3.3.4 How do the samples differ?

Weighted principle coordinate analysis (PCoA) was used to visualise factors that controlled variance in the prokaryotic and eukaryotic samples using Unifrac and Bray-Curtis distances respectively (see Figure 4.54 and Figure 4.55). Unweighted analysis was performed, but did not show any additional information and is therefore not shown. A PERMANOVA (using the R package mvabund) was then performed to identify which treatments were statistically significantly different (see Table 4.28 and Table 4.29), although this analysis is not phylogenetically corrected.

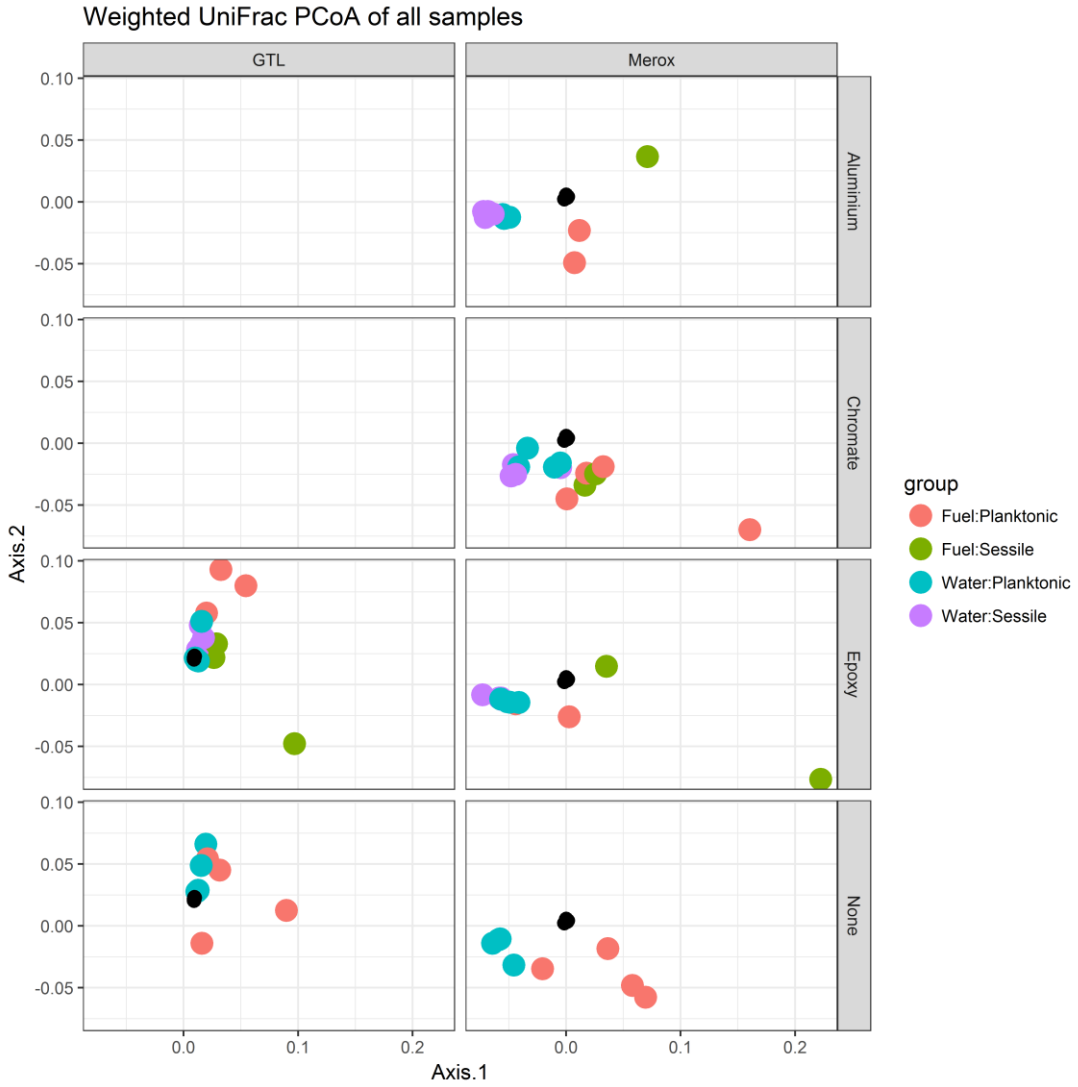

Figure 4.54 – Weighted PCoA of the prokaryotic communities, using UniFrac measurements to calculate the distance between the samples. Samples have been separated by sample treatment i.e. fuel type, phase (fuel vs. aqueous), state (planktonic vs. sessile) and surface (aluminium, chromate-leaching epoxy, epoxy and none). Small black symbols show the respective starting inoculum in all treatments.

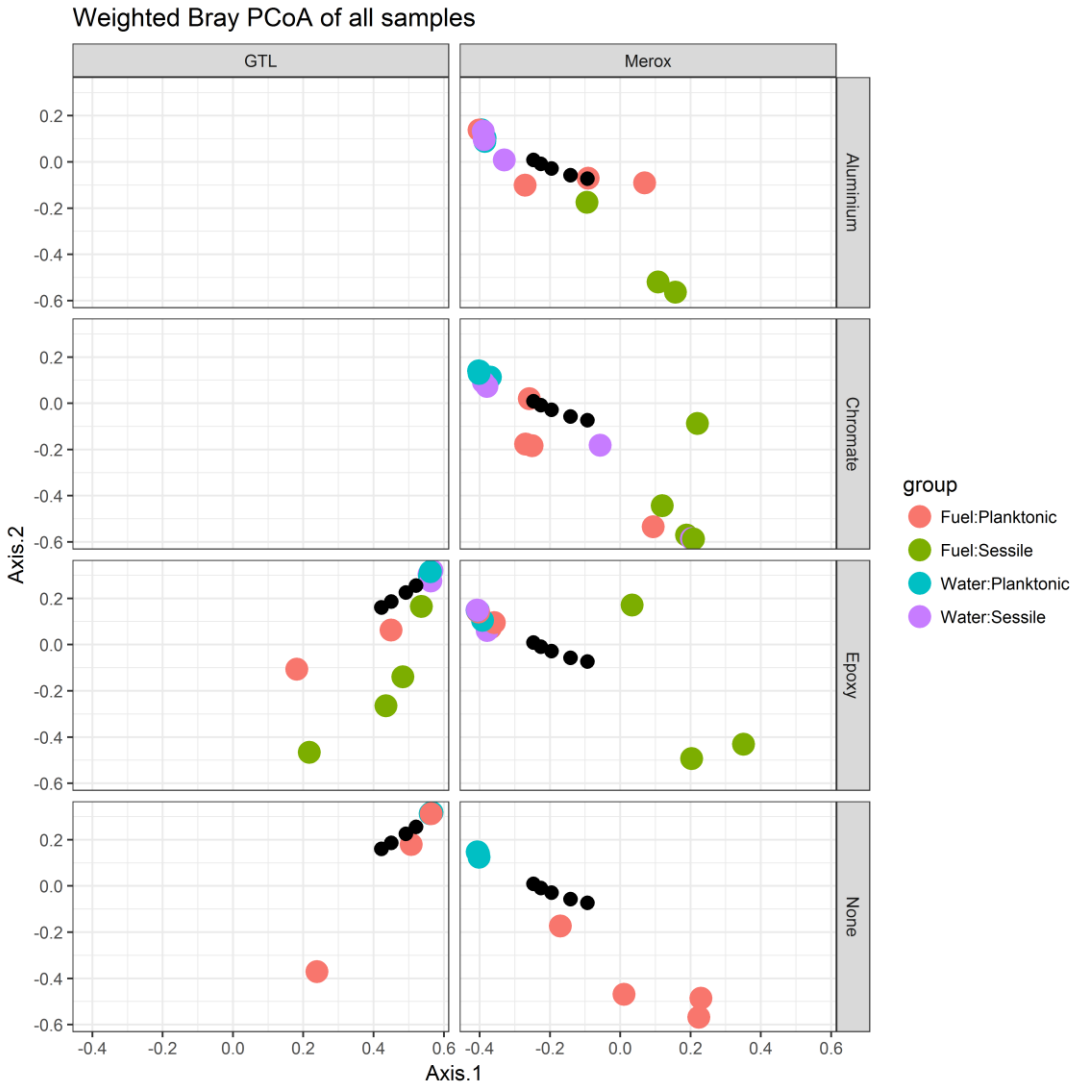

Figure 4.55 – Weighted PCoA of the eukaryotic communities, using Bray Curtis measurements to calculate the distance between the samples. Samples have been separated by sample treatment i.e. fuel type, phase (fuel vs. aqueous), state (planktonic vs. sessile) and surface (aluminium, chromate-leaching epoxy, epoxy and none). Small black symbols show the respective starting inoculum in all treatments.

Table 4.28 – PERMANOVA testing of differences between prokaryotic communities. Likelihood ratios were tested using mvabund with 999 resampling iterations.

Test	Significance (*p*)	
Fuel type: GTL *vs* Merox	0.001	
Phase: Fuel *vs* Water	0.002	
State: Planktonic *vs* Sessile	0.001	
Surfaces:		
	Aluminium	Epoxy
Epoxy	0.015	
Chromate-leaching epoxy	0.002	0.008

Table 4.29 – PERMANOVA testing of differences between eukaryotic communities. Likelihood ratios were tested using mvabund with 999 resampling iterations.

Test	Significance (*p*)	
Fuel type: GTL *vs* Merox	0.001	
Phase: Fuel *vs* Water	0.001	
State: Planktonic *vs* Sessile	0.001	
Surfaces:		
	Aluminium	Epoxy
Epoxy	0.004	
Chromate-leaching epoxy	0.087	0.001

4.3.3.5 How do the communities taken from the fuel phase and the aqueous phase differ?

The most evident variation between the samples shown by the PCoAs was between the phases (Fuel *vs* Water). PERMANOVAs showed that the variation observed between the fuel and water phases were statistically different in both the prokaryotic and eukaryotic communities (see Table 4.28 and Table 4.29). For all treatments, both the planktonic and sessile communities in the fuel and water phases differed from one another, with the exception of the eukaryotic planktonic community with an epoxy coupon, where little variation was observed. Additionally, in the prokaryotic communities, separation was more evident in the Merox-treated Jet A-1 communities in comparison to the GTL kerosene communities. To determine which OTUs were significantly influenced by phase was used to

identify OTUs that differed between the fuel *vs* water phases (see Figure 4.56) in those microcosms that contained a surface.

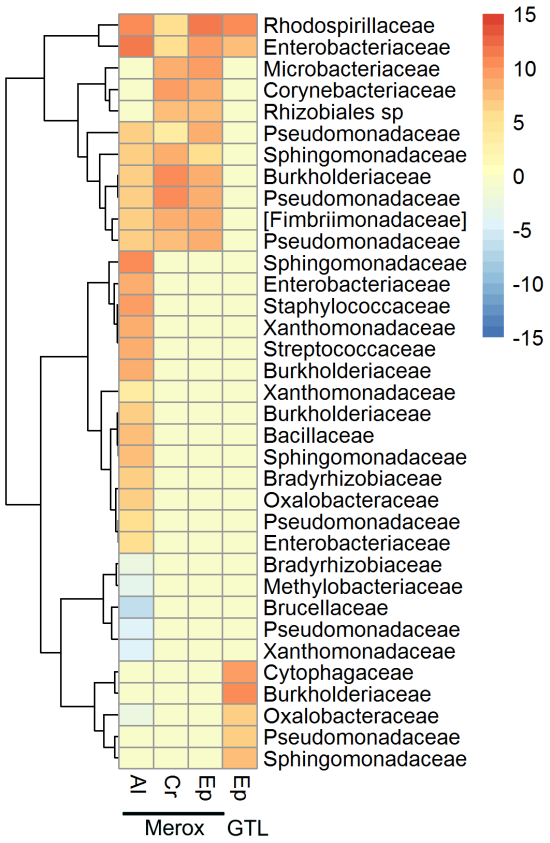

Figure 4.56 – A heat map of prokaryotic OTUs that were more abundant in either the fuel or water phases of microcosms with varying treatments in relation to one another. Both the Merox-treated Jet A-1 community and the GTL kerosene community are shown. Changes are log 2 fold scale – positive values (red) favour growth in the fuel phase. Sample key: Al = aluminium coupons, Cr = Chromate-leaching coupons, Ep = Epoxy coupons.

Of the OTUs that were influenced by phase, relatively few were the same in the GTL and Merox treated microcosms (only 2 shared) confirming the importance of fuel type as a factor controlling prokaryotic microbial community structure. In both types of microcosms, the majority of changes in relative abundance observed were of OTUs that favoured growth in the fuel phase (red colours in Figure 4.56).

In microcosms containing Merox Jet-A1 fuel, 21 OTUs changed on the Aluminium surface with approximately half that number showing changes on epoxy and Chromate-leaching Epoxy surfaces. These responsive OTUs were generally members of the alpha, beta and gamma Proteobacteria (Orders: Rhizobiales, Sphingomonadales, Burkholderiales,

Enterobacteriales and Pseudomonadales). The OTUs that responded to phase on Chromate-leaching epoxy and epoxy surfaces were similar and also responded on Aluminium.

Fewer eukaryotic OTUs responded to phase. In the GTL microcosm, a single *Candida* sp. showed an increased relative abundance in the fuel phase (red colours in Figure 4.57) compared to the water phase. Four OTUs differed in the microcosms containing Merox-treated Jet A-1 and an Aluminium surface and two OTUs differed in the Epoxy and Chromate-leaching epoxy surfaces. These OTUs were all Ascomycota with the exception of a single unidentified Basidiomycota.

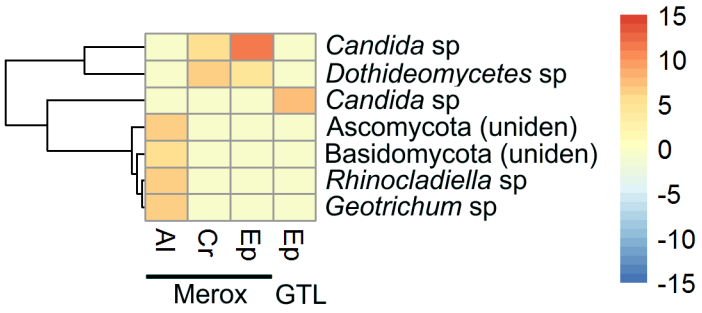

Figure 4.57 – A heat map of eukaryotic OTUs that were more abundant in either the fuel or water phases of microcosms with varying treatments in relation to one another. Both the Merox-treated Jet A-1 community and the GTL kerosene community are shown. Changes are on a log 2 fold scale – positive values (red) favour growth in the fuel phase. Sample key: Al = aluminium coupons, Cr = Chromate-leaching coupons, Ep = Epoxy coupons.

4.3.3.6 How do planktonic and sessile communities compare?

The PCoA analysis and PERMANOVAs of the microcosm samples showed that both the prokaryotic and eukaryotic communities differed in the planktonic and sessile states, particularly in Merox treated fuel.

To determine which OTUs were responsible for these changes, DESEQ2 analysis was performed of planktonic and sessile states comparing samples from microcosms with the same fuel type, surface and phase (i.e. fuel *vs* water). OTUs which showed significant differences in relative abundance were identified and results have been presented in a heat map as the log 2 fold-change between the two states. For example, the column 'MAF' in Figure 4.58 is the log 2 fold change in OTU relative abundance between the planktonic (sample MAFP) and sessile (sample MAFS) states of prokaryotes grown in a microcosm with

Merox fuel, in the fuel phase and on an Aluminium surface. OTUs that had greater relative abundance in the planktonic state are coloured red, those that had a greater relative abundance in the sessile state are coloured blue.

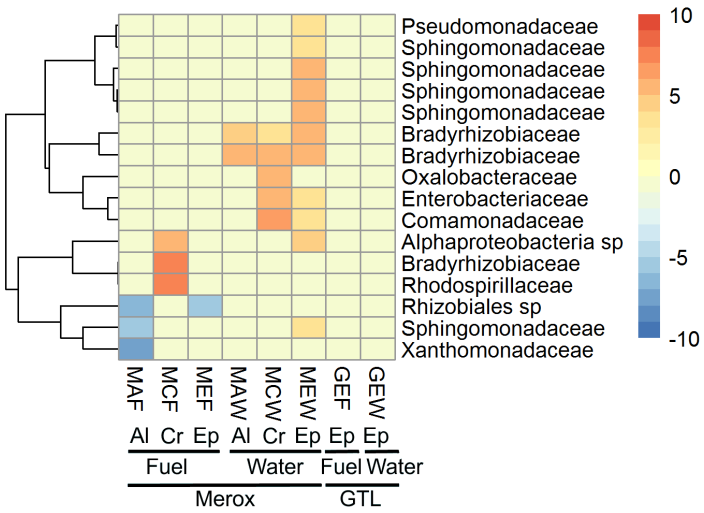

Figure 4.58 – A heat map of prokaryotic OTUs that are more abundant in either the sessile or planktonic state of microcosms with varying treatments. Both the Merox-treated Jet A-1 and the GTL kerosene communities are shown. Changes in relative abundance are log 2 fold changes with positive (red) colours indicating increased relative abundance in the planktonic state. Sample key: 1st letter, M = Merox-treated Jet A-1, G = GTL kerosene. 2nd letter, A = aluminium, C = chromate, E = epoxy. 3rd letter, F = fuel, W = water.

All of the OTUs that showed a difference in relative abundance between the planktonic and sessile states in water favoured growth in the planktonic state. In the fuel phase 3 OTUs favoured the planktonic state and 3 the sessile state. There were no obvious taxonomic patterns in the response to state but all were Proteobacteria (alpha, beta and gamma). None of these was numerically dominant in the samples indicating that the impact of state (sessile *vs* planktonic) on the total prokaryotic community was relatively low.

Figure 4.59 shows the differences in relative abundance between eukaryotes in the sessile and planktonic state. The majority of eukaryotes that showed a difference favoured the sessile state. These differences were most apparent in two microcosms, Merox-treated Jet A-1 with an epoxy coated coupon in the fuel phase and a Chromate-leaching coupon in the water phase (other treatments may not show significant differences if sampling depth was insufficient). These OTUs included those that were numerically dominant in the microcosms,

particularly the yeast identified as a *Geotrichum* sp. indicating that the impact of state (sessile *vs* planktonic) on the overall eukaryotic community was high.

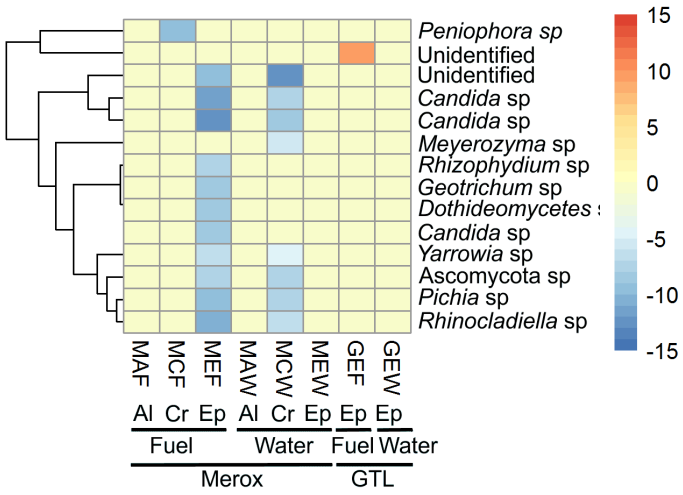

Figure 4.59 – A heat map of eukaryotic OTUs that are more abundant in either the sessile or planktonic state of microcosms with varying treatments. Both the Merox-treated Jet A-1 and the GTL kerosene communities are shown. Changes in relative abundance are log 2 fold changes with positive (red) colours indicating increased relative abundance in the planktonic state. Sample key: 1st letter, M = Merox-treated Jet A-1, G = GTL kerosene. 2nd letter, A = aluminium, C = chromate, E = epoxy. 3rd letter, F = fuel, W = water.

4.3.3.7 How does surface type affect community structure?

The analysis of differences between samples showed that surface influenced both prokaryotic and eukaryotic microbial communities with all treatments showing a difference except Chromate-leaching epoxy *vs* Aluminium in the eukaryotic samples.

DESEQ2 analysis was used to identify the OTUs that were responsible for these differences. Results for OTUs that showed differences between one or more pairs of surfaces are shown in Figure 4.60 and Figure 4.61. Results are shown as variance stabilised log 2 relative abundances to enable comparisons to be drawn between multiple comparisons.

In the prokaryotic samples, those OTUs that differed between surfaces were alpha, beta and gamma Proteobacteria. Most differences were seen between two treatments: (1) Aluminium surfaces and Chromate-leaching epoxy in the fuel phase where growth was favoured on the Aluminium surface and (2) Chromate-leaching epoxy and epoxy surfaces in the water phase

although different OTUs showed different preferences for these surfaces. The relative abundances of many of the OTUs were high and as such contributed significantly to the total prokaryotic community within the sample.

In the eukaryotic samples, differences were found in the water phase between Aluminium *vs* Chromate-leaching epoxy and Epoxy *vs* Chromate-leaching epoxy. Surprisingly, where these differences occurred, the increase in relative abundance was greatest on the Chromate-leaching epoxy surface indicating that chromate did not deleteriously affect those OTUs that were influenced by the surface.

Overall, the results show that phase, state and surface all influence the variation within these communities. However, the biggest driver in variation is whether the community exists within the fuel phase or the aqueous phase of the jet fuel system. Chromate-leaching paint did impact the microbial community within these systems, but only detrimentally in the fuel phase.

Sample key: 1st letter: Fuel; Merox (M). 2nd letter: Surface; Aluminium (A), Chromate (C), Epoxy (E). 3rd letter: Phase; Fuel (F), Aqueous (A). 4th letter: State; Sessile (S).

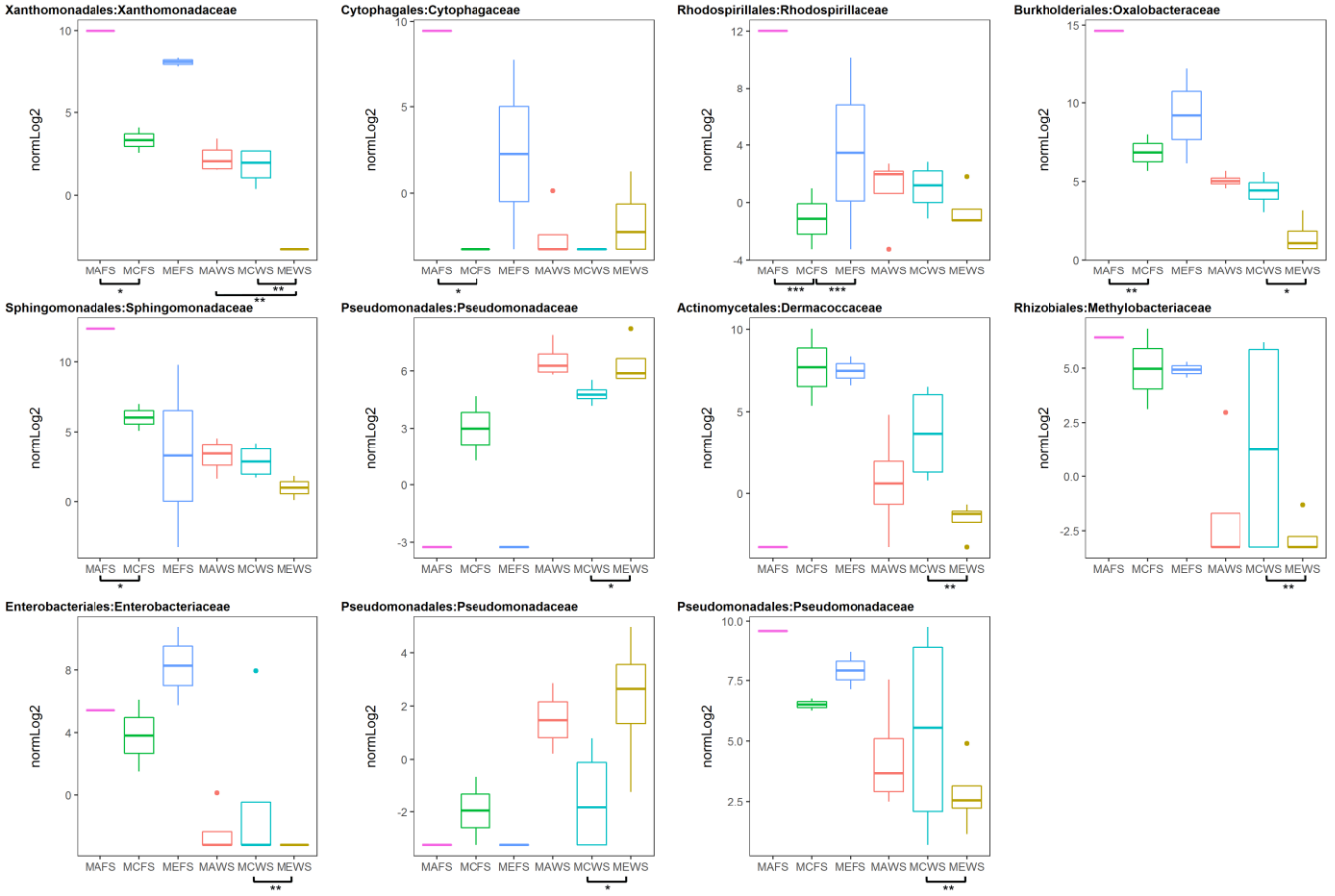

Figure 4.60 – Box and Whisker plots of prokaryotic OTUs that are more abundant on surfaces in the Merox-treated Jet A-1 Changes in relative abundance are log 2 fold changes. Boxes represent the upper and lower interquartile ranges, line in the middle of the box represents the mean (n = 4), whiskers show the lowest and highest values and dots the outliers. Significant differences are indicated (PERMANOVA, * p <0.05, ** p <0.01, *** p <0.001).

Sample key: 1st letter: Fuel; Merox (M). 2nd letter: Surface; Aluminium (A), Chromate (C), Epoxy (E). 3rd letter: Phase; Fuel (F), Aqueous (A). 4th letter: State; Sessile (S).

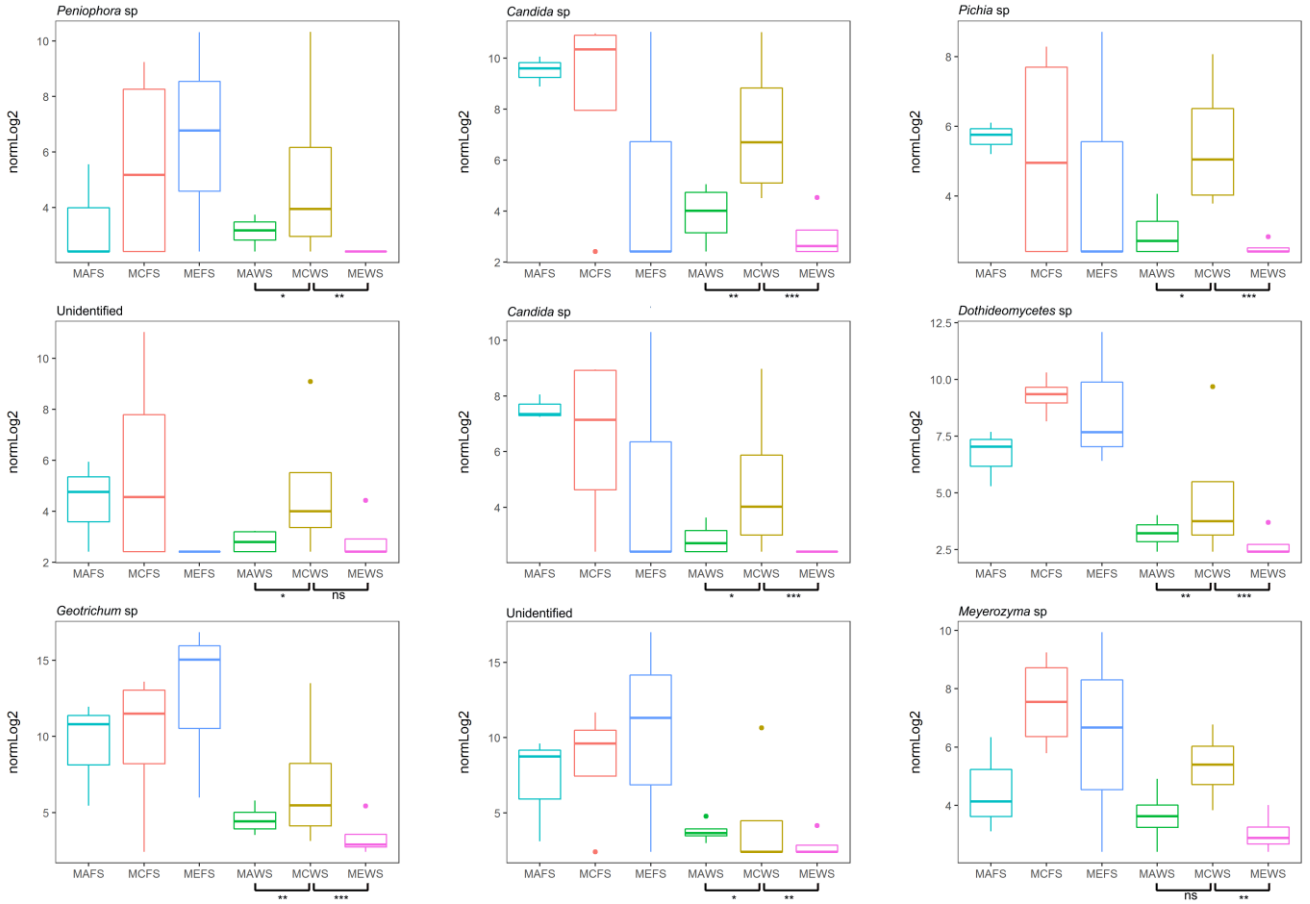

Figure 4.61 – Box and Whisker plots of eukaryotic OTUs that are more abundant on surfaces in the Merox-treated Jet A-1 Changes in relative abundance are log 2 fold changes. Boxes represent the upper and lower interquartile ranges, line in the middle of the box represents the mean (n = 4), whiskers show the lowest and highest values and dots the outliers. Significant differences are indicated (PERMANOVA, * p <0.05, ** p <0.01, *** p <0.001).

4.4 Discussion

To ensure aircraft safety and reduce operational costs associated with decontamination, it is increasingly important to understand the composition of microbial biofilms within aircraft and how they interact with the surfaces found in these systems and their associated coatings. This knowledge can be used to predict how the introduction of novel fuel and materials is likely to impact these communities, averting unforeseen issues with microbial contamination that may arise.

In this study, two typical microbial communities found in jet fuel systems have been examined; one sourced from conventional fuels and the other from alternative fuels. GC-MS, microscopic and culture-independent techniques have been used characterise these communities, as well as the hydrocarbons they degrade. The aim was to understand the differences in planktonic and sessile communities, as well as the differences in communities found fuel and water phases. These data were then used to look at the impact chromate-leaching epoxy paint on microbial community dynamics, to provide an understanding on how the removal of chromate-leaching paints may affect microbial community dynamics in jet fuel systems.

The results showed that Proteobacteria, Actinobacteria, Firmicutes and Bacteriodetes were the most common prokaryotic phyla and Ascomycota and Basidiomycota were the most common eukaryotic phyla. These are the same phyla that dominated the field samples (see Chapter 2). From these data it would appear that microbial communities from jet fuel systems are primarily composed of microorganisms from these phyla. Across the sample set the abundance of Proteobacteria was relatively evenly split between Alpha-, Beta- and Gammaproteobacteria (35 %, 26 % and 25 % respectively). Actinobacteria were dominated by the class Actinobacteria (84 %), Firmicutes by Bacilli (58.0 %) and Clostridia (42.0 %) and to a lesser extent, Bacteroidetes by Flavobacteria (35 %). In the eukaryotic samples, more unique Basidiomycota OTUs were observed (54 %), however, many Ascomycota, particularly yeast species from the order of Saccharomycetales dominated many of the eukaryotic communities. This dominance suggests that yeasts either a) play a significant role in biofilms, or b) the growth conditions in this experiment were particularly suited to yeast species. More work needs to be undertaken to fully understand the role that yeasts play in microbial biofilms found within jet fuel systems. Once again, over twice the number of unique prokaryotic OTUs were observed, compared to eukaryotic OTUs (457 prokaryotic, 206 eukaryotic), suggesting (at least during the early stages of biofilm growth) that these biofilms

were dominated by prokaryotes. Also, the two microbial communities, one sourced from conventional fuels and used in Merox-treated Jet A-1 microcosms and one sourced from alternative fuels and used in GTL kerosene microcosms (see Section 4.2.1.2), were significantly different from one another. This is most likely due to the fact that they were sourced from fuel tanks containing different fuel types.

A. resinae is historically considered the main eukaryotic contaminant of jet fuel systems (Raikos *et al*. 2011) and industry experts have suggested that jet fuel contamination is largely down to a few key filamentous fungi (Anon. 2016a). In Chapter 2 it was observed that eukaryotic contamination was not present in all field samples at detectable levels (though when these communities were introduced into a microcosm, eukaryotes were observed and therefore must be present at low levels). In this experiment *A. resinae* was present in both of the communities used to inoculate the microcosms. However, after two weeks *A. resinae* was not detected in 31 of the microcosms. There was no observable pattern in *A. resinae* presence or absence. These experiments were only run for 14 days; it may be that *A. resinae* is not a primary contaminant and becomes established in the secondary succession of a biofilm and therefore is an indicator of heavily contaminated jet fuel. Alternatively *A. resinae* may not be as significant a contaminant of jet fuels as initially thought, instead being ideally suited to the culture-dependent analyses undertaken throughout the past 50 years (Anon. 2001; Passman 2013) and is therefore grossly over-represented as a contaminant. More research utilising culture-independent methods needs to be undertaken on microbial communities from jet fuel systems, to fully understand how what role community members play in biofilm formation.

4.4.1 Fuel degradation within the microcosms

In this study GC-MS was utilised to identify hydrocarbons degraded by both the mixed community sourced from conventional fuels and the mixed community sourced from alternative fuels. It appears that the conventional jet fuel community, when growing on Merox-treated Jet A-1, broke down aromatic rings with associated methyl groups and iso-alkanes, as well as preferentially degrading shorter chain n-alkanes (C_9 to C_{11}) compared to longer chain molecules (C_{12} to C_{16}). Presumably shorter chain alkanes require less energy to degrade and are therefore preferentially degraded over the loner chain length molecules. No evidence by either community of cycloalkanes degradation was observed, again most like because they require more energy to degrade compared to straight chain molecules (Das & Chandran 2011). No significant degradation was recorded by the community sourced from alternative fuels, growing in GTL kerosene. This result should be treated with caution.

Although analysis has shown that there was a statistical difference in some of the GC-MS peaks, it is difficult to identify with certainty the compounds within a complex mixture such a jet fuel. The limitations of this test method have been discussed previously, see Section 3.4 for more details.

4.4.2 How do the fuel and aqueous phases affect the communities?

When introduced into microcosms, microbial communities from the fuel phase and aqueous phases differed. PCoA analysis showed a clear separation in both the prokaryotic and eukaryotic communities found in the fuel and aqueous phases, although few of these were shared between the two fuel types. This highlights the importance of fuel type as a factor for controlling prokaryotic community structure. In microcosms containing Merox-treated Jet A-1 *Burkholderia sp*. were typically the dominant prokaryotes in the fuel phase, compared to *Pseudomonas sp*. in the aqueous phase. *Geotrichum sp*. were the dominant eukaryotes in the fuel phase, compared to *Candidia sp*. in the aqueous phase. The GTL communities showed a similar pattern with *Burkholderia sp*. being the dominant prokaryotes in the fuel phase, as well *Cellulosimicrobium sp*., with *Cupriavidus sp.* dominant in the aqueous phase. For the eukaryotes *Rhinocladiella sp.* were dominant in the fuel phase compared to an unidentified fungi in the aqueous phase. The majority of these organisms showed a significant difference between phases when analysed using DESEQ2. Additionally, communities taken from the fuel phase were much more variable than those taken from the aqueous phase and species richness and diversity were greater. This is an unexpected result, as the environment within the fuel phase is harsher than the aqueous phase. One hypothesis is that growth in the fuel phase requires the production of hydrophobic extracellular polymeric substances to retain water in the vicinity of the biofilm. It was noticeable that water was entrained on the surface near the fuel/water interface. This EPS, in turn, allowed for the increased absorption of nutrients in an otherwise oligotrophic environment creating a more diverse biofilm. Unfortunately, biofilm visualisation using SYBRO Ruby was problematical on these surfaces so alternative approaches will be considered in future. Survival within jet fuels may require a more diverse microbial community to fill all of the niches required to exist within liquid hydrocarbons.

4.4.3 Do the planktonic and sessile communities differ?

In this experiment, both planktonic and sessile microbial communities were sampled and significant differences in both the prokaryotic and eukaryotic communities observed. In general, the prokaryotic communities showed an increase in planktonic abundance in the water phase and a more even change in diversity in sessile abundance (3 OTUs significantly

increased in relative abundance and 3 decreased). This is mostly likely due to the toxic nature of the fuel. Communities in the fuel phase most likely need more protection from the surrounding environment (provided by a biofilm) than in the water phase. Therefore the water phase is likely to see more planktonic growth as a result.

Eukaryotic communities showed an increase in the sessile phase on epoxy (fuel phase) and chromate-leaching (water phase) coupons. Little difference was observed in the planktonic communities. This suggests that eukaryotes may preferentially form a biofilm in aircraft fuel systems. However, this is a limited study incorporating only two communities. Further work needs to be done in this area (preferentially including biofilm samples from the field), to ascertain the differences in planktonic and sessile communities as well as absolute quantification of the community composition.

4.4.4 How does surface type affect the community structure?

The culture-independent sequencing undertaken in this study has shown that surface type affected the community structure of the sessile microorganisms. In the prokaryotic communities, most differences were observed between the aluminium surfaces (higher relative abundance) and chromate-leaching surfaces (lower relative abundance) in the fuel phase and chromate-leaching surfaces (higher relative abundance) and epoxy surfaces (lower relative abundance) in the water phase. In the eukaryotic communities an increase in relative abundance was also seen in the water phase of microcosms containing a chromate-leaching surface, compared to the other two surface types. This may be due to the solubility of chromate; chromate is soluble in jet fuel, but not in water. On Chromate-leaching surfaces in the water phase it may be that the basal layer of microorganisms (those in contact with the surface) are dead, providing an inert surface to which the microbial community then attaches (SEM images of these coupons appeared to show microorganisms stacking on top of one another in the chromate leaching systems) and protecting the communities from the toxic nature of the chromate. However, in the fuel phase, the chromate goes into solution, exposing the communities to an increased amount of toxic chromate *vs* the communities in the water phase and therefore exerts a greater selection pressure on these microorganisms. Visualisation of live and dead microbes can be achieved using LIVE/DEAD staining systems (e.g. propidium iodide which is excluded from viable cells and SYTO9 which stains both live and dead cells). In combination with detailed confocal laser scanning microscopy, the distribution of live and dead cells can be observed.

It is unclear at this point whether the coupons' surface properties affected the ability of microorganisms to attach and whether the microorganisms produced conditioning films on these surfaces. Further work incorporating drop shape analysis (DSA), confocal-Raman and microscopy (in a quantitative manor to allow a measure of biofilm formation on surfaces within jet fuel systems and changes in cell density to be assessed) will need to be undertaken to evaluate the EPS layer on the coupons. DSA will provide an insight into whether the hydrophobicity of the surface is being altered by the biofilm to facilitate attachment and confocal-Raman will be used to understand the composition of the EPS (e.g. Andrews *el al* 2010).

Overall, this study has shown that the biggest driver of variation within a community is whether it exists within the fuel phase or the aqueous phase of the jet fuel system. Chromate leaching paint does impact the microbial communities that develop in different phases of jet fuel system, although it does not prevent a biofilm from forming. Therefore the phasing out of the use of chromate leaching paints may impact microbial community dynamics within the fuel phase of an aircraft.

4.5 Conclusions

In conclusion, this study has found that:

- Culture-independent analysis has been used to characterise representative microbial communities within aircraft fuel systems, showing that fuel type, phase (fuel *vs* water) and state (planktonic *vs* sessile) all significantly influence these communities.
- However, it phase is the main driver for variation in the microbial communities that were sampled.
- These fuels were dominated by a few microorganisms, predominantly from the phyla of Proteobacteria and Actinobacteria for prokaryotes and Ascomycota (particularly yeasts) and Basidiomycota for eukaryotes.
- Varying the surface type between bare aluminium alloy, epoxy paint and chromate-leaching paint has an impact on the microbial communities within these microcosms, causing an increase in relative abundance in the water phase and a decrease in the fuel phase.
- Chromate leaching paint does not prevent microorganisms growing on these surfaces, but does cause variation in the composition of the attached communities.
- Overall, the removal of chromate leaching paint from these microcosms systems, had a greater influence on communities in the fuel phase than the water phase.

Chapter Five

General discussion

5.1 Summary of findings

The aim of this thesis was to examine the microbial communities found in jet fuel systems and investigate how the introduction of alternative fuels and novel components would impact these communities. This was done by first, gaining a better understanding of the diversity of microbial communities found in conventional jet fuel systems using a combination of culture-dependent and culture-independent techniques. The latter has not been applied to conventional aviation fuels before. Complex communities were introduced into microcosms to investigate their responses to environmental variations. In addition, GC-MS and ion chromatography were used to examine alterations in chemical composition and microscopy techniques used to investigate changes in physical structure.

In Chapter Two, field samples were obtained from different geographical locations across Europe and the Middle East, representing a wide range of microbial communities and environments. These communities were characterised using metagenomics approaches and the impact of using industry standard techniques evaluated; for example, comparisons were made between contaminated water collected directly from the field and communities that had developed in microcosms when supplied with nutrient media or pure water. A number of isolates were obtained from these communities (as well as stock centre microorganisms), and in Chapter Three, these microorganisms were analysed (in monoculture). These isolates were exposed to different fuel types. It was found that changes in hydrocarbon composition had a profound effect on growth rate. Chemical analyses were also undertaken, which identified the growth-limiting factors in both alternative and conventional fuels. These studies were further expanded to microbial communities, which showed that altering fuel type has an impact on community structure. Finally, surface composition was varied as described in Chapter Four, and attached communities analysed for their response to the introduction of a toxic, chromate-leaching paint. These studies showed that the toxicity of the surface had little effect on the attached community. Instead the key driver for variation was the phase (fuel or water) in which community was developed. A brief discussion and an overview of the key research findings for each chapter are summarised below.

5.1.1 The diversity of microbial communities within conventional jet fuel systems

The initial study in this thesis characterised the typical microbial communities found in jet fuel systems. Both culture-dependent and culture-independent techniques were used to assess the response of the microbial communities to changes in environmental conditions, such as geographical location. The biases introduced by using culture-dependent techniques, microcosm systems and nutrient-rich mineral media were also explored.

In contrast to some of the existing literature, these results showed that communities were dominated by prokaryotic, not eukaryotic, microorganisms (Elphick 1970; Salvarezza *et al*. 1981; Stowe 1995), supporting the findings of more recent studies (Smith 1991; Raikos *et al.* 2011). Approximately two to three times more unique prokaryotic OTUs were recovered compared to eukaryotic OTUs.

In general, the prokaryotic communities were dominated by the phyla Proteobacteria, Actinobacteria, Firmicutes and Bacteroidetes and the eukaryotic communities by Ascomycota and Basidiomycota. This limited data set indicated that geographic location had little impact on microbial community dynamics (though more research needs to be undertaken to fully understand this). Most significantly, eukaryotic DNA was not present at detectable limits in ~47 % of the samples sequence and the fungi *Hormoconis resinae,* was not detected in all of the communities where eukaryotic DNA was recovered. This is important as some commercial test kits rely on the presence of such 'indicator' organisms as a marker of microbial contamination.

This study has shown that conventional jet fuel systems are significantly more diverse than previously documented and comparisons between culture-dependent and culture-independent analyses indicated that only ~16 % of microorganisms in these systems are detectable by culture-dependent methodology. This has a potential impact on field operating procedures as current field test kits may return false negatives, and has the potential to a) increase maintenance and repair costs, and b) impact on aircraft safety.

Finally, utilising microcosm systems and mineral-rich media does impact the microbial communities within them. This impact is much more significant in the prokaryotic communities, compared to the eukaryotic communities, which may account for some of the bias mentioned above, and will have impacted the results of previous studies.

5.1.2 The impact of alternative fuels on microbial communities

The second study examined the main factors governing microbial development and fuel degradation in jet fuel systems, utilising industry-relevant isolates to study their response to alternative fuels, and then expanding these studies to incorporate complex mixed microbial communities sourced from the field.

This study found that growth in microcosms inoculated with *P. putida*, *P. graminis*, *H. resinae* and *C. tropicalis* in monoculture was significantly lower in pure GTL kerosene (both planktonic growth and biofilm formation) than conventional fuels. This is due to these

isolates lacking the ability to metabolise alkanes; they are therefore carbon limited. However, once these studies were expanded to incorporate more field isolates, it became apparent that the ability to utilise alkanes as a carbon source was common within these communities (though the hydrocarbons required for the growth of these microorganisms have not been identified).

Additionally, in a eutrophic system, it was found nitrogen was the growth limiting micronutrient, and not phosphorus as initially predicted. Further analysis needs to be undertaken to understand if this pattern is replicated in an oligotrophic environment.

These results have demonstrated that the selected industry-relevant isolates use GTL kerosene much less efficiently than conventional fuels, and therefore may not be fit for purpose when testing the biodegradation of alternative fuels. However, the impact of altering fuel types on mixed communities was much less marked. The mixed communities grew readily on GTL kerosene, and analysis showed that, over time, prokaryotic communities exposed to GTL kerosene became more variable in comparison to the starting inoculum (when compared to the two conventional fuels). This indicates that the community dynamics are beginning to change in response to the variation in carbon source. In contrast, the eukaryotic communities tended to remain more stable as time progressed. Therefore the introduction of alternative fuels would have a more significant impact on prokaryotic communities.

5.1.3 The impact of varying surface materials on microbial communities

The final chapter describes the use of culture-independent techniques to examine biofilm formation within jet fuel systems, by examining the planktonic and sessile communities on a variety of representative surfaces. In this study two typical microbial communities were used to understand a) the difference in planktonic and sessile communities, b) the differences in communities found fuel and water phases, and c) the impact chromate leaching epoxy paint has on microbial community dynamics. This was done to provide an understanding on how the current practice of removing chromate leaching paint may affect microbial community dynamics in jet fuel systems, and in turn, predict any additional operational concerns that may arise because of their removal.

The results showed that Proteobacteria, Actinobacteria, Fimicutes and Bacteriodetes were the most common prokaryotic phyla, and Ascomycota and Basidiomycota were the most common eukaryotic phyla; the same phyla that dominated the field samples in Chapter 2. It would appear that microbial communities from jet fuel systems are primarily composed of

microorganisms from these phyla. Additionally, although *A. resinae* was present in both of the communities used to inoculate the microcosms, after two weeks *A. resinae* was not detected in 31 of the microcosms. Whether *A. resinae* in present or absent, is stochastic, however these results show that *A. resinae* may not be a keystone species in fuel systems, as once thought.

Additionally, this study has shown that the biggest driver of variation within a community is whether it exists within fuel or water. Chromate leaching paint has little impact on the microbial community dynamics within a jet fuel system (with the exception of a slightly lower species richness), and no impact on biofilm formation. Therefore the removal of chromate leaching paints should have little impact on the microbial communities within aircraft, though alternative fuels may have a more marked one.

5.2 Future work

The work within this thesis significantly increases the current knowledge of the microbial communities found within jet fuel systems, and provides an insight into the impact that the introduction of alternative fuels and novel materials may have on these microorganisms. However, more work needs to be undertaken before we fully understand the impact these future materials will have. The following section includes recommendations and improvements for future investigation of biofilms development and management in aircraft fuel systems.

5.2.1 Varying environmental conditions

Over the course of this experimental programme, robust and repeatable methodology has been developed and implemented to answer questions of key interest to the aviation industry concerning the impact of tank environment on microbial contamination. However, there are many other environmental conditions that would be of interest that remain to be tested. In particular is the impact of varying temperature and oxygen levels on microbial communities to more closely replicate the conditions found during flight. The impact of the harsh conditions experienced during flight on microbial communities has yet to be explored. However, it is critical in understanding how microbial communities proliferate once on board aircraft, as extreme temperature and the freeze-thaw of free water would undoubtedly exert a selection pressure on these communities.

By applying the microcosm system utilised in this thesis, parameters including temperature regimes (constant temperate vs. temperature cycles seen in aircraft fuel tanks) could be varied. The biofilm development and composition could then be compared to communities grown at ambient temperatures, and assessed using a combination of microscopic techniques, 16S and 5.8S/18S rRNA gene sequencing and confocal Raman spectroscopy.

Furthermore, these studies could be expanded to include other variations in environmental conditions, such as variations in fuel type (FAEs, HRJs, other XTLs) to understand if other alternative fuels impact microbial communities or, variation in surface type to understand how materials, such as scavenge pipes and sensors affect the attachment of biofilms. Overall, by analysing more variables, a more complete picture of microbial contamination in aircraft could be obtained.

5.2.2 Improvement to experiments

During this thesis many techniques have been utilised to characterise the microbial communities used, and their impact on the surrounding environment. Many of these

techniques could be further developed, most notable the detection of hydrocarbon degradation by GC-MS. However, these have been discussed in the experimental chapters and therefore will not be discussed further here (see Sections 3.4).

5.2.3 Further analysis of the biofilms

This study provides an insight into the composition of microbial contamination within jet fuel systems, demonstrating the differences in communities from various geographical locations, as well as how fuel and surface type affect biofilm attachment. However, at present these studies have focused on the microorganisms encapsulated within these biofilms, and not on the composition of the biofilms or the ecological role of these microorganisms. Expanding the knowledge of biofilm adhesion within these systems could be critical to understanding how to effectively remove them. EPS could be characterised using techniques such as confocal Raman spectroscopy and compound-specific dyes. Further work could then be undertaken to explore non-chemical routes to remove biofilms.

Additionally, the work undertaken on chromate leaching surfaces focused on the diversity on the microorganisms within the microcosms. At present no work has been undertaken to assess the conditions on the surface of the coupons. Further work needs to be undertaken to understand the composition of the EPS on these surfaces. Confocal Raman and drop shape analysis would allow the EPS to be characterised, as well as the hydrophobicity of the surfaces to see whether these are affected by the chromate leaching paint. This would allow a complete picture of the biofilms on these surfaces to be obtained.

5.2.4 Field studies

Laboratory microcosm systems provide an invaluable insight into the microbial contamination of jet fuel systems. However, it would be beneficial to apply the approaches undertaken in this study to a field environment. Thus allowing for a more realistic, insightful and representative study to take place. However, there are many operational and logistical problems to achieving such a field study, foremost, obtaining representative biofilm samples from the wall of a sealed fuel tank. There are however, other field studies that may be beneficial to the aviation industry as a whole.

Firstly, by sampling more aircraft and ground storage tanks from a wider variety of geographical locations, and utilising the metagenomic approach described in this thesis, a more complete profile of the microbial contamination within jet fuel systems could be obtained. It would be ideal to gain repeat samples from aircraft flying regular routes vs. variable routes, as well as long haul vs. short haul and aircraft operating out on a single

location. This would provide information on how microbial contamination varies between airports. Also, obtaining a range of samples across a variety geographical locations, with varying climates (particularly in humid subtropical regions, where microbial contamination is worse) would allow a true picture of how microbial contamination of jet fuel systems varies around the world. By doing this a "fingerprint" of a typical microbial communities could be obtained. This information could then be used by the industry to better remediate microbial contamination.

Secondly, by setting up small scale fuel tanks in the field and sampling the surrounding microbiomes (soil, rain water, particulates etc.) the development of microbial communities could be tracked overtime, and the data used to identify the key microbiomes contaminating jet fuel systems. Coupling this with an increased knowledge gained from field sampling aircraft would provide a more detail understanding of where microbial contamination of jet fuel systems originates from, and could be used to input into current systems design to help mitigate contamination. For example, if soil particulates are found to be particularly problematic, a filter could be incorporated into the fuel tank air vents.

5.3 Concluding remarks

The aviation industry is changing. Environmental pressures and advances in technology are driving the introduction of novel fuels and materials into the supply chain. This research has shown that the introduction of these novel components will impact the complex, multispecies biofilms found within jet fuel systems. Additionally, this thesis has made a substantial contribution to the field of hydrocarbon microbiology, for the first time profiling the diversity of the microbial communities found. The knowledge generated will provide a better understanding of how to tackle microbial contamination in the field, and further ensure aircraft safety.

Reference List

Reference list

Abarenkov, K., Henrik N., R., Larsson, K., Alexander, I. J., Eberhardt, U., Erland, S., Høiland, K., Kjøller, R., Larsson, E., Pennanen, T., Sen, R., Taylor, A. F. S., Tedersoo, L., Ursing, B. M., Vrålstad, T., Liimatainen, K., Peintner, U., Kõljalg, U., 2010. The UNITE database for molecular identification of fungi - recent updates and future perspectives. *New Phytologist*, 186(2), pp. 281–285.

Ackerman, V. & Dunk-Richards, G., 1991. *Microbiology: An introduction for the health sciences.* Marrickville: Harcourt Brace Jovanovich Group.

Adal, K. A. & Farr, B. M., 1996. Central venous catheter related infections: a review. *Nutrition*, 12(3), pp. 208–213.

Alnnasouri, M., Lemaitre, C., Gentric, C., Dagot, C. & Pons, M., 2011. Influence of surface topography on biofilm development: experiment and modelling. *Biochemical Engineering Journal*, 57, pp. 38–45.

Amann, R. I., Ludwig, W. & Schleifer, K. H., 1995. Phylogenetic identification and in situ detection of individual microbial cells without cultivation. *Microbiological reviews*, 59(1), pp. 143–169.

Andrews, J. S., Rolfe, S. A., Huang, W. E., Scholes, J. D. & Banwart, S. A., 2010. Biofilm formation in environmental bacteria is influenced by different macromolecules depending on genus and species. *Environmental microbiology*, 12(9), pp. 2496–2507.

Angst, E. C., 1923. *The fouling of ships bottoms by bacteria*. Washington DC: Bur. Construction & Repair, US Navy Department.

Anon., 2016a. *Are Culture Methods still reliable for monitoring microbial contamination in fuel and oil?* Available at: http://echamicrobiology.com/are-culture-methods-still-reliable-for-monitoring-microbial-contamination-in-fuel-and-oil [Accessed August 30, 2016].

Anon., 2001. *ASTM E1259-01: Standard test for evaluation of antimicrobials in liquid fuels boiling below 390 °C*. West Conshohocken: ASTM International.

Anon., 2011a. *Biofuel types. UK government, Department for Transport*. Available at: http://www.dft.gov.uk/topics/sustainable/biofuels/fuel-types [Accessed October 23, 2012].

Anon., 2012a. *Corrosion in systems storing and dispensing ultra low sulfur diesel (ULSD), hypotheses investigatio*. Columbus: Battelle Memorial Institute.

Anon., 2015. *Guidance material on microbiological contamination in aircraft fuel tanks 5th Edition*. Montreal / Geneva: International Air Transport Association (IATA).

Anon., 1988. *Handbook of aviation fuel properties/CRC report number 530*. Washington: Society of Automotive Engineers.

Anon., 2005. *IP 385: Determination of the viable aerobic microbial content of fuels and fuel components boiling below 390 °C - Filtration and culture method*. London: Energy Institute.

Anon., 2011b. *Ministry of Defence, Defence Standard 91-91 Turbine Fuel, Aviation Kerosine Type, Jet A-1 NATO Code : F-35 Joint Service Designation*.

Anon., 2011c. *Renewable transport fuel obligation. UK government, Department for Transport*. Available at: http://www.dft.gov.uk/topics/sustainable/biofuels/rtfo [Accessed October 23, 2012].

Anon., 2008. *Risk of contamination of aviation kerosene (jet fuel) with biodiesel*. Joint Inspection Group - Bulletin 21, (21), pp. 1–2.

Anon., 2016b. *Rotor-Gene SYBR® green PCR kit*. Available at: https://www.qiagen.com/gb/shop/automated-solutions/pcr-instruments/rotor-gene-sybr-green-pcr-kit/#productdetails [Accessed January 25, 2016].

Anon., 2009. *Sulphur free diesel BS EN 590 : 2009*. Brussels: European committee for standardisation.

Anon., 2012b. Virent: jet fuel. Virent. Available at: http://www.virent.com/products/jet-fuel/ [Accessed November 12, 2012].

Anon., 2000. *Waiting for the tide: August*. Yachting & Boating World. Available at: http://www.ybw.com/auto/pbo/edletter/19990616114149pboedletter.html.

Atlas, R. M., 1981. Microbial degradation of petroleum hydrocarbons: an environmental perspective. *Microbiological reviews*, 45(1), pp. 180–209.

Auffret, M., Labbé, D., Thouand, G., Greer, C. W. & Fayolle-Guichard, F., 2009. Degradation of a mixture of hydrocarbons, gasoline, and diesel oil additives by *Rhodococcus aetherivorans*

and *Rhodococcus wratislaviensis*. *Applied and environmental microbiology*, 75(24), pp. 7774–82.

Babich, I. & Moulijn, J. A., 2003. Science and technology of novel processes for deep desulfurization of oil refinery streams: a review. *Fuel*, 82(6), pp. 607–631.

Bacha, J., Freel, J., Gibbs, A., Gibbs, L., Hemignaus, G., Hoekman, K., Horn, J., Ingham, M., Jossens, L., Kohler, D., Lesnini, D., McGeehan, J., Nikanjam, M., Olsen, E., Organ, R., Scott, B., Sztenderowicz, M., Tiedemann, A., Walker, C., Lind, J., Jones, J., Scott, D. & Mills, J., 2007. *Diesel fuels technical review*. California: Chevron Corporation.

Bacha, J., Barnes, F., Franklin, M., Gibbs, L., Heminghaus, G., Hogue, N., Lesnini, D., Lind, J., Maybury, J. & Morris, J., 2000. *Technical review: Aviation fuels*. California: Chevron Corporation.

Bakanauskas, S., 1958. *Bacterial activity in JP-4 Fuel*. Technical report WADC 58-21. Dayton: Wright Air Development Centre.

Bakalidou, A., Kämpfer, P., Berchtold, M., Kuhnigk, T., Wenzel, M. & König, H. 2002 *Cellulosimicrobium variabile sp*. *nov*., a cellulolytic bacterium from the hindgut of the termite *Mastotermes darwiniensis*. *International Journal of Systematic and Evolutionary Microbiology*. 52: 1185-1192.

Baker, N., 2012. *Policies: reducing greenhouse gases and other emissions from transport*. HM Government - Department for Transport. Available at: https://www.gov.uk/government/policies/reducing-greenhouse-gases-and-other-emissions-from-transport#background [Accessed November 16, 2012].

Balster, L.M., Chelgren, S. K., Strobel, E. M., Vangsness, M. D. & Bowen, L. L., 2006. Characterization of the bio-burden in United States aviation fuel: a comparison of FTA paper and other methods for obtaining genetic material from aviation fuel microbes. *Prepr. Pap.-Am. Chem. Soc., Div. Petr. Chem*., 51(2), pp. 558–560.

Balster, L. M., Strobel, E. M., Vangsness, M. D. Bowen, L. L., Mueller, S. S., Brown, L. M., Pike, D. D. & Dalrymple, D. L., 2009. Effect of FSII on microbial contamination in jet fuel: DiEGME and TriEGME. In Prague, Czech Republic. *The 11th International Conference on Stability, Handling and Use of Liquid Fuels (IASH)*.

Bento, F. M., Beech, I. B., Gaylarde, C. C., Englert, G. E. & Muller, I. L., 2005. Degradation and corrosive activities of fungi in a diesel-mild steel-aqueous system. *World Journal of Microbiology and Biotechnology*, 21(2), pp. 135–142.

Bhan, O. K., Tang, S. Y., Brinkman, D. W. & Carley, B., 1988. Causes of poor filterability in jet fuels. *Fuel*, 67(2), pp. 227–237.

Blaiklock, P. 2017. Restriction Mapper Version 3. *Restrictionmapper.org*. Accessed: 17th March 2017.

Blakey, S., Rye, L. & Wilson, C. W., 2011. Aviation gas turbine alternative fuels: a review. *Proceedings of the Combustion Institute*, 33(2), pp. 2863–2885.

Bodenhausen, N., Horton, M. W. & Bergelson, J., 2013. Bacterial communities associated with the leaves and the roots of *Arabidopsis thaliana*. *PLoS ONE*, 8(2), pp. 1-9.

Boethling, R. S. & Alexander, M., 1979. Effect of concentration of organic-chemicals on their biodegradation by natural microbial communities. *Applied and Environmental Microbiology*, 37(6), pp. 1211–1216.

Brock, T. D., 1987. The study of microorganisms in situ: progress and problems. In *Symposia of the Society for General Microbiology*, 41. pp. 1-17.

Brown, J. M., Steigerwalt, A. G., Morey, R. E., Daneshvar, M. I., Romero, L. J., & McNeil, M. M. 2006. Characterization of clinical isolates previously identified as *Oerskovia turbata*: proposal of *Cellulosimicrobium funkei sp. nov*. and emended description of the genus *Cellulosimicrobium*. *International Journal of Systematic and Evolutionary Microbiology*. 56: 801-804.

Brown, L. M., McComb, J. P., Vangsness, M. D., Bowen, L. L., Mueller, S. S., Balster, L. M. & Bleckmann, C. A., 2010. Community dynamics and phylogenetics of bacteria fouling Jet A and JP-8 aviation fuel. *International Biodeterioration & Biodegradation*, 64(3), pp. 253–261.

Bücker, F. Bücker, F., Barbosa, C. S., Quadros, P. D., Bueno, M. K., Fiori, P., Huang, C., Frazzon, A. P. G., Ferrão, M. F., de Oliveira Camargo, F. A. & Bento, F. M., 2014. Fuel biodegradation and molecular characterization of microbial biofilms in stored diesel/biodiesel blend B10 and the effect of biocide. *International Biodeterioration & Biodegradation*, 95, pp. 346–355.

Buddie, A., Bridge, P. D., Kelley, J. & Ryan, M J, 2011. *Candida keroseneae sp. nov.*, a novel contaminant of aviation kerosene. *Letters in applied microbiology*, 52(1), pp. 70–75.

Caporaso, J. G., Bittinger, K., Bushman, F. D. Desantis, T. Z., Andersen, G. L., Knight, R., 2010. PyNAST: A flexible tool for aligning sequences to a template alignment. *Bioinformatics*, 26(2), pp. 266–267.

Caporaso, J. G., Kuczynski, J., Stombaugh, J., Bittinger, K., Bushman, F. D. Costello, E. K., Fierer, N., Peña, A. G., Goodrich, K., Gordon, J. I., Huttley, G. A., Kelley, S. T., Knights, D., Koenig, J., E., Ley, R. E., Lozupone, C., A., Mcdonald, D., Muegge, B., D., Pirrung, M., Reeder, J., Sevinsky, J. R., Turnbaugh, P. J., Walters, W. A., Widmann, J., Yatsunenko, T., Zaneveld, J. & Knight, R., 2010. QIIME allows analysis of high-throughput community sequencing data. *Nature Methods*, 7(5), pp. 335–336.

Cavestri, R. C. & Kalley, T. D., 1999. *Leak detection additives for oil or fuel systems*. US5979226 A.

Chandankere, R., Yao, J., Cai, M., Masakorala, K., Jain, A. K. & Choi, M. M. F., 2014. Properties and characterization of biosurfactant in crude oil biodegradation by bacterium *Bacillus methylotrophicus* USTBa. *Fuel*, 122, pp. 140–148.

Chao, A., 1984. Non-parametric estimation of the number of classes in a population. *Scandinavian Journal of Statistics*, 11, pp. 265–270.

Chelius, M. K. & Triplett, E. W., 2001. The diversity of archaea and bacteria in association with the roots of *Zea mays*. *Microbial ecology*, 41(3), pp. 252–263.

Clark, A. Q., Smith, A. G., Threadgold, S. & Taylor, S. E., 2011. Dispersed water and particulates in jet fuel: Size analysis under operational conditions and application to coalescer disarming. *Industrial & Engineering Chemistry Research*, 50(9), pp. 5749–5765.

Corporan, E., Edwards, T., Shafer, L., DeWitt, M. J., Klingshirn, C., Zabarnick, S., West, Z., Striebich, R., Graham, J. & Klein, J., 2011. Chemical, thermal stability, seal swell, and emissions studies of alternative jet fuels. *Energy & Fuels*, 25(3), pp. 955–966.

Costerton, J. W., Geesey, G. G. & Cheng, K. J., 1978. How bacteria stick. *Scientific American*, 238(1), pp. 86–95.

Culman, S. W., Culman, S. W. Bukowski, R., Gauch, H. G. Cadillo-Quiroz, H. & Buckley, D. H., 2009. T-REX: software for the processing and analysis of T-RFLP data. *BMC bioinformatics*, 10, pp. 171.

Cyplik, P., Schmidt, M., Szulc, A., Marecik, R., Lisiecki, P., Heipieper, H. J., Owsianiak, M., Vainshtein, M. & Chrzanowski, Ł., 2011. Relative quantitative PCR to assess bacterial community dynamics during biodegradation of diesel and biodiesel fuels under various aeration conditions. *Bioresource technology*, 102(6), pp. 4347–52.

Daggett, D., Hadaller, O., Hendricks, R. & Walther, R., 2006. *Alternative fuels and their potential impact on aviation*. Cleveland: National Aeronautics and Space Administration (NASA).

Das, N. & Chandran, P., 2011. Microbial degradation of petroleum hydrocarbon contaminants: an overview. *Biotechnology research international*, pp. 1-13.

Davolos, D. & Pietrangeli B. 2007. *Molecular and phylogenetic analysis on bacterial strains isolated from a PAHs wastewater treatment plant*. In: Mendez-Vilas, A. ed. Current research topics in applied microbiology and microbial biotechnology. Tuck Link, Singapore:World Scientific Publishing, pp. 313-316.

Denaro, T. R., Chelgren, S. K., Lang, J. N., Strobel, E. M., Balaster, L. M. T. and Vangsness, M. D., 2005. *DNA Isolation of microbial contaminants in aviation turbine fuel via traditional polymerase chain reaction (PCR) and direct PCR*. Dayton: University of Dayton and the Airforce Research Laboratory.

Denyer, S. P., Gorman, S. P. & Sussman, M., 1993. *Microbial biofilms: Formation and control.* Oxford: Society of applied bacteriology.

Dewanti, R. & Wong, A. C., 1995. Influence of culture conditions on biofilm formation by Escherichia coli O157:H7. *International journal of food microbiology*, 26(2), pp. 147–164.

DeWitt, M. J., Corporan, E., Graham, J. & Minus, D., 2008. Effects of aromatic type and concentration in Fischer-Tropsch fuel on emissions production and material compatibility. Energy and Fuels, 22(4).

Dolan, R. M., 2002. *Intergovernmental communication: Investigation of fuel/water samples collected from fuel tanks of military aircraft*. Atlanta: Biofilm Laboratory, Centres for Disease Control and Prevention.

Dujon, B., 2010. Yeast evolutionary genomics. *Nature reviews*. Genetics, 11(7), pp. 512–524.

Dykhuizen, D.E., 1998. Santa Rosalia revisited: why are there so many species of bacteria? *Antonie van Leeuwenhoek*, 73(1), pp. 25–33.

Ebbinghaus, A. & Wiesen, P., 2001. Aircraft fuels and their effect upon engine emissions. *Air and Space Europe*, 2(1/2), pp. 101–103.

Edgar, R. C., 2010. Search and clustering orders of magnitude faster than BLAST. *Bioinformatics*, 26(19), pp. 2460–2461.

Edmonds, P. & Cooney, J. J., 1967. Microorganisms systems identification of microorganisms isolated from jet fuel systems. *Appl. Microbiol*, 15(2), pp. 411-416.

Elliott, D. R., Scholes, J. D., Thornton, S. F., Rizoulis, A., Banwart, S. A. & Rolfe, S. A., 2010. Dynamic changes in microbial community structure and function in phenol-degrading microcosms inoculated with cells from a contaminated aquifer. *FEMS Microbiology Ecology*, 71(2), pp. 247–259.

Elphick, J., 1970. *Microbial corrosion in aircraft fuel systems*. In: Microbial aspects of Metallurgy J. Miller, ed., New York: Elsevier.

Franke-Whittle, I. H., Walter, A., Ebner, C. Insam, H. (2014) Investigation into the effect of high concentrations of volatile fatty acids in anaerobic digestion on methanogenic communities. *Waste Management*, 34(11), pp. 2080-2089.

Ferrari, M. D., Neirotti, E. & Albornoz, C., 1998. Occurrence of heterotrophic bacteria and fungi in an aviation fuel handling system and its relationship with fuel fouling. *Revista Argentina de microbiología,* 30(3), pp. 105–14.

Finefrock, V. H. & London, S. A., 1966. *Microbial contamination of USAF JP-4 fuels*. Dayton: Wright-Patterson Air Force Base.

Fish, K. E., Collins, R., Green, N. H., Sharpe, R. L., Douterelo, I., Osborn, A. M. & Boxall, J. B., 2015. Characterisation of the physical composition and microbial community structure of biofilms within a model full-scale drinking water distribution system. *PLoS ONE*, 10(2), p.e0115824.

Flemming, H. & Wingender, J., 2010. The biofilm matrix. *Nature reviews. Microbiology*, 8(9), pp. 623–633.

Flemming, H. C., Neu, T. R. & Wozniak, D. J., 2007. The EPS matrix: The “House of Biofilm Cells”. *Journal of Bacteriology*, 189(22), pp. 7945–7947.

Fuchs, G., 2008. Anaerobic metabolism of aromatic compounds. *Annals of the New York Academy of Sciences*, 1125, pp. 82–99.

Fuchs, G., Boll, M. & Heider, J., 2011. Microbial degradation of aromatic compounds - from one strategy to four. *Nature reviews. Microbiology*, 9(11), pp. 803–816.

Gandee, G. & Reed, T., 1964. *Fuel contamination and fuel system corrosion technical report SEG TDR 64–47*. Systems Engineering Group, Research and Technology Division, Air Force Systems Command.

Garrett, T. R., Bhakoo, M. & Zhang, Z., 2008. Bacterial adhesion and biofilms on surfaces. *Progress in Natural Science*, 18(9), pp. 1049–1056.

Gaylarde, C. C., Bento, F. M. & Kelley, J., 1999. Microbial contamination of stored hydrocarbon fuels and its control. *Revista de Microbiologia*, (30), pp. 1–10.

Geiss, K. T. & Frazier, J. M., 2001. In vitro toxicities of experimental jet fuel system ice-inhibiting agents. *The Science of the total environment*, 274(1–3), pp. 209–218.

Ghigo, J. M., 2001. Natural conjugative plasmids induce bacterial biofilm development. *Nature*, 412(6845), pp. 442–445.

Giannekas, M., 2016. mapchart.net. Whidev. Available at: http://mapchart.net/ [Accessed April 21, 2016].

Gibson, G. R., 1990. Physiology and ecology of the sulphate-reducing bacteria. *The Journal of Applied Bacteriology*, 69(6), pp. 769–797.

Goldman, J. C., Caron, D. A. & Dennett, M. R., 1987. Regulation of gross growth efficiency and ammonium regeneration in bacteria by substrate C: N ratio. *Limnol. Oceanogr*, 32(6), pp. 1239–1252.

Graef, H. W., 2003. *An analysis of microbial contamination in military aviation fuel systems fuels*. Ohio: Air Force Institute of Technology.

Guiamet, P. S. & Gaylarde, C. C., 1996. Activity of an isothiazolone biocide against *Hormoconis resinae* in pure and mixed biofilms. *World Journal of Microbiology & Biotechnology*, 12(4), pp. 395–397.

Haggett, R. D. & Morchat, R. M., 1992. Microbiological contamination: Biocide treatment in naval distillate fuel. *International Biodeterioration & Biodegradation*, 29(1), pp. 87–99.

Van Hamme, J. D., Singh, A. & Ward, O. P., 2006. Physiological aspects. Part 1 in a series of papers devoted to surfactants in microbiology and biotechnology. *Biotechnology advances*, 24(6), pp. 604–620.

Harding, M. W., Marques, L. L. R., Howard, R. J. & Olson, M. E., 2009. Can filamentous fungi form biofilms? *Trends in microbiology*, 17(11), pp. 475–480.

Harmsen, M., Yang, L., Pamp, S. J. & Tolker-Nielsen, T., 2010. An update on *Pseudomonas aeruginosa* biofilm formation, tolerance, and dispersal. *FEMS immunology and medical microbiology*, 59(3), pp. 253–268.

Hazlett, R. N., 1969. Fibrous bed coalescence of water. *I&EC Fundamentals*, 8(11), pp. 625–632.

Hazzard, G., 1961. *Fungal Growths in Aviation Fuel Systems 252*. Australian Defence Scientific Service.

Hempel, S., Renker, C. & Buscot, F., 2007. Differences in the species composition of arbuscular mycorrhizal fungi in spore, root and soil communities in a grassland ecosystem. *Environmental microbiology*, 9(8), pp. 1930–1938.

Hendey, N. I., 1964. Some observations on *Cladosporium resinae* as a fuel contaminant and its possible role in the corrosion of aluminium alloy fuel tanks. *Transactions of the British Mycological Society*, 47(4), p.467–475.

Hendrix, R. W., 2002. Bacteriophages: Evolution of the Majority. *Theoretical Population Biology*, 61(4), pp. 471–480.

Hettige, G. E. G. & Sheridan, J. E., 1989. Effects of biocides on microbiological growth in middle distillate fuel. *International Biodeterioration*, 25(1–3), pp. 175–189.

Heukelekian, H. & Heller, A., 1940. Relationship between food concentration and surface for bacterial growth. *J. Bacteriol*, pp. 547–558.

Hildebrandt, U., Ouziad, F., Marner, F. J. & Bothe, H., 2006. The bacterium *Paenibacillus validus* stimulates growth of the arbuscular mycorrhizal fungus *Glomus intraradices* up to the formation offertile spores. *FEMS microbiology letters*, 254, pp. 258–267.

Hill, E. C., 2003. *Microbes in the marine industry*. London: The Institute of Marine Engineering, Science and Technology.

Hill, E. C. & Hill, G. C., 2008. Microbial contamination and associated corrosion in fuels, during storage, distribution and use. *Advanced Materials Research.* 38, pp. 257–268.

Hill, G. C., 2011. *Investigation of microbiological susceptibility of biodiesel and biodiesel blends*. London: Energy Institute.

Hill, G. C., Hill, E. C., Collins, D. J. & Anderson, S., 2005. Investigation of the anti-microbial characteristics of di-ethylene glycol mono methyl ether (Di-EGNE) in relation to its use intermittently and at sub-lethal concentrations. *In Sitges, Spain: 9th International Conference on Stability, Handling and Use of Liquid Fuels (IASH).*

Housecroft, C. E. & Constable, E. C., 2002. *Chemistry 2nd Edition*. Harlow: Pearson Education Limited.

Hugenholtza, P. & Pace, N. R., 1996. Identifying microbial diversity in the natural environment: A molecular phylogenetic approach. *Trends in Biotechnology*, 14(96), pp. 190–197.

Hutchins, S. R., 1991. Biodegradation of mono-aromatic hydrocarbons by aquifer microorganisms using oxygen, nitrate, or nitrous oxide as the terminal electron acceptor. *Applied and Environmental Microbiology*, 57(8), pp. 2403–2407.

Janda, J. M. & Abbott, S. L., 2007. 16S rRNA gene sequencing for bacterial identification in the diagnostic laboratory: pluses, perils, and pitfalls. *Journal of Clinical Microbiology*, 45(9), pp. 2761–2764.

Jung, C. M., Broberg, C., Giuliani, J., Kirk, L. L., Hanne, L. F., 2002. Characterization of JP-7 jet fuel degradation by the bacterium *Nocardioides luteus* strain BAFB. *Journal of basic microbiology*, 42(2), pp. 127–131.

Karatan, E. & Watnick, P., 2009. Signals, regulatory networks, and materials that build and break bacterial biofilms. *Microbiol Mol Biol Rev*, 73(2), pp. 310–347.

Keeling, P. J. & Palmer, J. D., 2008. Horizontal gene transfer in eukaryotic evolution. *Nat. Rev. Genet.*, 9(8), pp. 605–618.

Kinder, J. D., 2010. *Evaluation of bio-derived synthetic paraffinic kerosenes (Bio-SKPs)*. West Conshohoken: ASTM International.

Kivits, R., Charles, M. B. & Ryan, N., 2010. A post-carbon aviation future: Airports and the transition to a cleaner aviation sector. *Futures*, 42(3), pp. 199–211.

Kobrin, G., 1993. *A practical manual on microbiologically influenced corrosion*. Houston: NASE International.

Koch, B., Worm, J. Jensen, L. E., Hojberg, O. & Nybroe, O., 2001. Carbon limitation induces σS-dependent gene expression in *Pseudomonas fluorescens* in soil. *Applied and Environmental Microbiology*, 67(8), pp. 3363–3370.

Leahy, J. G. & Colwell, R. R., 1990. Microbial degradation of hydrocarbons in the environment. *Microbiological reviews*, 54(3), pp. 305–315.

Lee, J. S., Ray, R. I. & Little, B. J., 2010. An assessment of alternative diesel fuels: microbiological contamination and corrosion under storage conditions. *Biofouling*, 26(6), pp. 623–635.

Lisiecki, P., Chrzanowski, Ł., Szulc, A., Ławniczak, Ł., Białas, W., Dziadas, M., Owsianiak, M., Staniewski, J., Cyplik, P., Marecik, R., Jeleń, H. & Heipieper, H. J., 2014. Biodegradation of diesel/biodiesel blends in saturated sand microcosms. *Fuel*, 116(8), pp. 321–327.

Little, B.J. & Lee, J.S., 2013. *Microbiologically Influenced Corrosion*. New Jersey: John Wiley & Sons, pp. 1-261.

Van Loon, G. W. & Duffy, S .J., 2005. *Environmental chemistry: a global perspective 2nd Edition*. Oxford: Oxford University Press.

Love, M. I., Huber, W. & Anders, S. 2014. Moderated estimation of fold change and dispersion for RNA-seq data with DESeq2. *Genome Biology* 15(12): 550.

Lozupone, C. & Knight, R., 2005. UniFrac : a new phylogenetic method for comparing microbial communities. *Applied and environmental microbiology*, 71(12), pp. 8228–8235.

Lozupone, C., Lladser, M. E., Knights, D., Stombaugh, J. & Knight, R. 2011. UniFrac: an effective distance metric for microbial community comparison. *The ISME journal* 5(2): 169-172.

Madigan, M. T. & Marrs, B. L., 1997. Extremophiles. *Scientific American*, 276(4), pp. 82–87.

Mara, D. & Horan, N., 2003. *The handbook of water and wastewater microbiology*. London: Elsevier Ltd.

Margaroni, D., 1998. Fuel lubricity. *Industrial lubrication and tribology*, 50(3), pp. 108–118.

Mbadinga, S. M., Wang, L. Y., Zhou, L., Liu, J. F., Gu, J. D. & Mu, B. Z., 2011. Microbial communities involved in anaerobic degradation of alkanes. *International Biodeterioration & Biodegradation*, 65(1), pp. 1–13.

McDonald, D., Price, M. N., Goodrich, J., Nawrocki, E. P., DeSantis, T. Z., Probst, A., Andersen, G. L., Knight, R., Hugenholtz, P., 2012. An improved Greengenes taxonomy with explicit ranks for ecological and evolutionary analyses of bacteria and archaea. *The ISME journal*, 6(3), pp. 610–618.

Mcdougall, J., 1966. Microbial corrosion of metals. *Anti-corrosion*, 8, pp. 9-13.

McFarlane, E., 2009. Microbial contamination of middle distillate fuels: past, present and future. *In Asrhus, Denmark. 2nd International conference on applied microbiology and molecular biology in oil systems*.

McNamara, C. J., Perry, T. D., Leard, R., Bearce, K., Dante, J. & Mitchell, R., 2005. Corrosion of aluminium alloy 2024 by microorganisms isolated from aircraft fuel tanks. *Biofouling*, 21(5–6), pp. 257–65.

McMurdie, P. J., & Holmes, S. 2013. phyloseq: An R Package for Reproducible Interactive Analysis and Graphics of Microbiome Census Data. *PLoS ONE* 8(4): e61217.

McNamara, J., 2000. *The enemy within: bacteria's appetite for fuel tanks*. ttnews. Available at: http://www.ttnews.com/members/print_edition/weekly.archive/06.23.97.tw5.html.

Meckenstock, R. U., von Netzer, F., Stumpp, C., Lueders, T., Himmelberg, A. M., Hertkorn, N., Schmitt-Kopplin, P., Harir, M., Hosein, R., Haque, S. & Schulze-Makuch, D., 2014. Water droplets in oil are microhabitats for microbial life. *Science*, 345(6197), pp. 673–676.

Metcafe, G. & Brown, M. E. 1957. Nitrogen fixation by new species of *Nocardia*. *Microbiology*. 17:567-572.

Miyoshi, M., 1895. Die durchbohrung von membranen durch pilzfäden. *Jahrbücher für wissenschaftliche Botanik*, (28), pp. 269–289.

Morley, C. R., Trofymow, J. A., Coleman, D. C. & Cambardella, C., 1983. Effects of freeze-thaw stress on bacterial populations in soil microcosms. *Microbial Ecology*, 9(4), pp. 329–340.

Mueller, S. S., Bowen, L. L., Brown, L. M., Brown, N. A., Ruiz, O. N., Vangsness, M., Balster, L., Zabarnick, S., Shafer, L., Cook, R. & Strobel E. M., 2011. A comparison study of the effects of bacterial contamination on alternative fuels versus petroleum-derived. *In Sarasota, Florida. The 12th International Conference on Stability Handling and Use of Liquid Fuels (IASH).*

Muriel, J. M., Bruque, J. M., Olias, J. M. & Jimenez-Sanchez, A., 1996. Production of biosurfactants by *Cladosporium resinae*. *Biotechnology Letters*, 18(3), pp. 235–240.

Murray, B. J., Broadley, S. L. & Morris, G. J., 2011. Supercooling of water droplets in jet aviation fuel. *Fuel*, 90(1), pp. 433–435.

Neihof, R. A., 1988. *Distillate Fuel: Contamination, Storage and Handling*. H. L. Chesneau & M. Dorris, M, eds., Ann Arbor: ASTM International.

Nessel, C. S., Freeman, J. J., Forgash, R. C. & McKee, R. H, 1999. The role of dermal irritation in the skin tumor promoting activity of petroleum middle distillates. *Toxicological sciences: an official journal of the Society of Toxicology*, 49(1), pp. 48–55.

Nicolau, E., Kerhoas, L., Lettere, M., Jouanneau, Y.& Marchal, R., 2008. Biodegradation of 2-ethylhexyl nitrate by *Mycobacterium austroafricanum* IFP 2173. *Applied and environmental microbiology*, 74(20), pp. 6187–6193.

Nkem, B. M., Halimoo, N., Yusoff, F. M., Johari, W. L. W., Zakaria, M. P., Medipally, S. R. & Kannan, N. 2016. Isolation, identification and diesel-oil biodegradation capacities of indigenous hydrocarbon-degrading strains of *Cellulosimicrobium cellulans* and *Acinetobacter baumannii* from tarball at Terengganu beach, Malaysia. *Marine Pollution Bulletin*. 107:261-268.

O'Toole, G., Kaplan, H. B. & Kolter, R., 2000. Biofilm formation as microbial development. *Annu. Rev. Microbiol*, 54, pp. 49–79.

O'Toole, G. A. & Kolter, R., 1998. Flagellar and twitching motility are necessary for *Pseudomonas aeruginosa* biofilm development. *Molecular microbiology*, 30(2), pp. 295–304.

O'Toole, G. A. & Wong, G. C. L., 2016. Sensational biofilms: surface sensing in bacteria. *Current Opinion in Microbiology*, 30, pp. 139–146.

Pande, S. G., Hardy, D. R., Kamin, R. A., Nowack, C. J., Colbert, J. E., Morris, R. E. & Salvucci, L., 2001. Quest for a reliable method for determining aviation fuel thermal stability: comparison of turbulent and laminar flow test devices. *Energy & Fuels*, 15, pp. 224–235.

Passman, F. ed., 2003. *Fuel and fuel system microbiology: fundamentals, diagnosis, and contamination control*. West Conshohocken: ASTM International.

Passman, F., McFarland, B. & Hillyer, M., 2001. Oxygenated gasoline biodeterioration and its control in laboratory microcosms. *International Biodeterioration & Biodegradation*, 47(2), pp. 95–106.

Passman, F. J., 2013. Microbial contamination and its control in fuels and fuel systems since 1980 – a review. *International Biodeterioration & Biodegradation*, 81(7), pp. 88-104.

Percival, S. L., Knapp, J. S., Wales, D. S., Edyvean, R. G. J., 1999. The effect of turbulent flow and surface roughness on biofilm formation in drinking water. *Journal of Industrial Microbiology and Biotechnology*, 22(3), pp. 152–159.

Piggot, P. J. & Coote, J. G., 1976. Genetic aspects of bacterial endospore formation. *Bacteriological reviews*, 40(4), pp. 908–962.

Pratt, L. A. & Kolter, R., 1998. Genetic analysis of *Escherichia coli* biofilm formation: roles of flagella, motility, chemotaxis and type-I pili. *Molecular microbiology*, 30(2), pp. 285–293.

Pray, L. A., 2008. Transposons: the jumping genes. *Nature Education*, 1(1), pp. 204

Quast, C., Pruesse, E., Yilmaz, P., Gerken, J., Schweer, T., Yarza, P., Peplies, J. & Glöckner, F. O., 2013. The SILVA ribosomal RNA gene database project: improved data processing and web-based tools. *Nucleic Acids Research*, 41, pp. 590–596.

Racicot, R. J., Crouch, C. D. & Rauch, M. E., 2007. Microbial influenced corrosion studies of *Bacillus Licheniformis* on AA2024 aluminium alloys. *Corrosion Reviews*, 25(1–2), pp. 97–106.

Rafiq, M. H., 2012. *Experimental studies and modelling of synthesis gas production and Fischer-Tropsch synthesis*. Trondheim: Norwegian University of Science and Technology (NTNU).

Raikos, V., Vamvakas, S. S., Kapolos, J., Koliadima, A. & Karaiskakis, G., 2011. Identification and characterization of microbial contaminants isolated from stored aviation fuels by DNA sequencing and restriction fragment length analysis of a PCR-amplified region of the 16S rRNA gene. *Fuel*, 90(2), pp. 695–700.

Raikos, V., Vamvakas, S. S., Sevastos, D., Kapolos, J., Karaiskakis, G. & Koliadima, A., 2012. Water content, temperature and biocide effects on the growth kinetics of bacteria isolated from JP-8 aviation fuel storage tanks. *Fuel*, 93, pp. 559–566.

Rand, S. J., 2003. *Significance of tests for petroleum products 7th Edition*. West Conshohocken: ASTM International.

Rasband, W. S., 1997. *ImageJ*. Available at: imagej.nih.gov/ij/.

Rauch, M. E., Graef, H. W., Rozenzhak, S. M., Jones, S. E., Bleckmann, C. A., Kruger, R. L., Naik, R. R. & Stone, M. O., 2006. Characterization of microbial contamination in United States Air Force aviation fuel tanks. *Journal of industrial microbiology & biotechnology*, 33(1), pp. 29–36.

Rauch, M. E., Racicot, R. J. & Crouch, C. D., 2005. Investigation of the hydrocarbon degradation mechanisms of *Bacillus licheniformis* strains isolated from United States Air Force aviation fuel tanks. *In Sitges: Spain. The 9th International Conference on Stability Handling and Use of Liquid Fuels (IASH)*.

Ray, B. & Bhunia, A. (2013) *Fundamental food microbiology*. 5th Edition. Bosa Roca: Taylor and Francis Inc.

Renner, L.D. & Weibel, D.B., 2011. Physicochemical regulation of biofilm formation. *MRS bulletin / Materials Research Society*, 36(5), pp. 347–355.

Rugen, P., Hughes, V. & Hunnybun, M., 2007. *API/EI 1550 Handbook on equipment used for the maintenance and delivery of clean aviation fuels*. London: Energy Institute and Energy API.

Ruiz, O. N., Brown, L. M., Striebich, R. C., Smart, C. E., Bowen, L. L., Lee, J. S., Little, B. J., Mueller, S. S., Gunasekera, T. S., 2016. Effect of conventional and alternative fuels on a marine bacterial community and the significance to bioremediation. *Energy and Fuels*, 30(1), pp. 434-444.

Salvarezza, R. C., De Mele, M. F. L. & Videla, H. A., 1981. Redox potential and the microbiological corrosion of aluminium and its alloys in fuel / water systems. *British Corrosion Journal*, 16(3), pp. 162–168.

Schumann, P., Weiss, N. & Stackebrandt, E., 2001. Reclassification of *Cellulomonas cellulans* (Stackebrandt and Keddie 1986) as *Cellulosimicrobium cellulans gen. nov., comb. nov*.. *International Journal of Systematic and Evolutionary Microbiology*. 51:1007-1010.

Semmler, A. B. T., Whitchurch, C. B. & Mattick, J. S., 1999. A re-examination of twitching motility in *Pseudomonas aeruginosa*. *Microbiology*, 145(10), pp. 2863–2873.

Shannon, C. E. (1948) A mathematical theory of communication. *Bell System Technical Journal*, 27, pp. 379– 423.

Shannon, C. E. & Weaver, W. (1949) The mathematical theory of communication. University of Illinois Press, Urbana.

Shelton, B. G., Kirkland, K. H., Flanders, W. D. & Morris, G. K., 2002. Profiles of airborne fungi in buildings and outdoor environments in the United States. *Applied and Environmental Microbiology*, 68(4), pp. 1743–1753.

Shonnard, D. R., Williams, L. & Kalnes, T. N., 2010. Camelina-derived jet fuel and diesel: sustainable advanced biofuels. *Environmental Progress and Sustainable Energy*, 29(3), pp. 382–392.

Simpson, E. H., 1949. Measurement of diversity. *Nature*, 163, pp. 163-688.

Smith, C.A., Want, E.J., O'Maille, G., Abagyan,R., and Siuzdak G., 2006. XCMS: Processing mass spectrometry data for metabolite profiling using nonlinear peak alignment, matching and identification. *Analytical Chemistry*, **78**, pp. 779–787.

Smith, R., 1991. *Developments in fuel microbiology*. London: Elsevier Applied Science.

Smith, R. N., 1988. *Bacterial extracellular polymers: a major cause of spoilage in middle distillate fuels*. In B. D. R. Houghton, R. N. Smith & H. O. W. Eggins, eds. Biodeterioration. Barking: Elsevier, pp. 256–262.

Snijders, T. A., Melkert, J. A., Bauldreay, J. M., Bogers, P. F., Wahl, C. R. M. & Kapernaum M. G. 2011. Impact of fuel composition on emissions and performance of GTL kerosene blends in a Cessna Citation II. In Sarasota, Florida. *The 12th International Conference on Stability, Handling and Use of Liquid Fuels (IASH)*.

Song, C., 2003. An overview of new approaches to deep desulfurization for ultra-clean gasoline, diesel fuel and jet fuel. *Catalysis Today*, 86(1–4), pp. 211–263.

Soriano, A. U., Martins, L. F., Santos de Assumpção Ventura, E., de Landa, T. G., Henrique, F., de Araújo Valoni, É., Dutra F., Fátima R. F., Fragoso, R., Faller, K., Valério, M. C., Rocha, R., de Assis Leite, C., Lima do Carmo, D., Peixoto, F. & Silva R., 2015. Microbiological aspects of biodiesel and biodiesel/diesel blends biodeterioration. *International Biodeterioration & Biodegradation*, 99, pp. 102–114.

Srivastava, R. B., Awasthi, M., Upreti, M. C., Mathur, G. N., 2006. Studies on *Aureobasidium pullulans* forming biofilm on high strength aluminium alloy, a structural component, in aircraft fuel tanks. *Indian Journal of Engineering & Materials Sciences*, 13(4), pp. 135–139.

Staley, J. T., 1985. Measurements of in situ activities of nonphotosynthstic microorganisms in aquatic and terrestrial habitat. *Ann. Rev. Microbiol*, 39, pp. 321–346.

Stackebrandt E., Schumann, P. & Cui, X. L. 2004. Reclassification of *Cellulosimicrobium variabile* Bakalidou *et al*. 2002 as *Isoptericola variabilis gen. nov., comb. nov*. *International Journal of Systematic and Evolutionary Microbiology*. 54:685–688.

Stamper, D. M., Morris, R. E. & Montgomery, M. T., 2012. *Depletion of lubricity improvers from hydro-treated renewable and ultralow-sulfur petroleum diesels by marine microbiota*. West Bethesda: United States Navy.

Stowe, M. B., 1995. Microbially-induced corrosion and fuel-tank protection. *Aircraft Engineering and Aerospace Technology*, 67(2), pp. 5–9.

Stratton, R. W., Wolfe, P. J. & Hileman, J. I., 2011. Impact of aviation non-CO_2 combustion effects on the environmental feasibility of alternative jet fuels. *Environmental science & technology*, 45(24), pp. 10736–10743.

Sultanpuram, V. R., Mothe, T., Chintalapati, S., & Chintalapati, V. R. 2015. *Cellulosimicrobium aquatile sp. nov.,* isolated from Panagal reservoir, Nalgonda, India. *Antonie van Leeuwenhoek*. 108:1357-1364.

Sutherland, J.B., 2004. *Fungal biotechnology in agriculture, food, and environment*. D. K. Arora, ed., New York: Marcel Dekker.

Suttle, C. A., 2005. Viruses in the sea. *Nature*, 437(7057), pp. 356–361.

Swift, S., 1988. *Identification and control of microbial growth in fuel handling systems*. In M. M. Chesneau & H. L. Dorris, ed. Distillate Fuel Contamination, Storage, and Handling. Philadelphia: ASTM International.

Team R, 2008. *R: a language and environment for statistical computing*. Available at: http://www.r-project.org.

Thomas, C. M. & Nielsen, K. M., 2005. Mechanisms of, and barriers to, horizontal gene transfer between bacteria. *Nat. Rev. Microbiol*., 3, pp. 711–721.

Thomsik, T. M., 2008. *Alternative fuels research laboratory construction completed*. Cleveland: National Aeronautics and Space Administration (NASA) Glenn Research Center.

Tissot, B. P. & Welte, D. H., 1984. *Petroleum formation and occurrence*. Berlin: Springer Verlag.

Toole, G. & Toole, S., 1995. *Understanding biology for advance level 3rd Edition*. Cheltenham: Stanley Thornes (Publishers) Ltd.

Vangsness, M., Chelgren, Capt. S., Strobel, E., Balster, L. & Mueller, S., 2007. Microbial contamination studies JP-8 fuelled aircraft. *In Tucson: Arizona. The 10th International Conference on Stability, Handling and Use of Liquid Fuels (IASH).*

Vázquez-Baeza, Y., Pirrung, M., Gonzalez, A. & Knight, R., 2013. EMPeror: a tool for visualizing high-throughput microbial community data. *GigaScience*, 2(1), pp. 16-20.

Videla, H. A., 1989. Metal dissolution redox in biofilms. *Structure and function of biofilms*, 46, pp. 301–320.

Videla, H. A. & Herrera, L. K., 2005. Microbiologically influenced corrosion: looking to the future. *International microbiology : the official journal of the Spanish Society for Microbiology*, 8(3), pp. 169–180.

Vu, B., Chen, M., Crawford, R. J. & Ivanova, E. P., 2009. Bacterial extracellular polysaccharides involved in biofilm formation. *Molecules*, 14(7), pp. 2535–2554.

Vuong, C., Kocianova, S., Voyich, J. M., Yao, Y., Fischer, E. R., De Leo, F. R. & Otto, M., 2004. A crucial role for exopolysaccharide modification in bacterial biofilm formation, immune evasion, and virulence. *The Journal of biological chemistry*, 279(52), pp. 54881–54886.

Wang, Q, Garrity, G. M., Tiedje, J. M. & Cole, J. R., 2007. Naive bayesian classifier for rapid assignment of rRNA sequences into the new bacterial taxonomy. *Applied and Environmental Microbiology*, 73(16), pp. 5261–5267.

Wang, Y., Naumann, U., Wright, S. T., & Warton, D. I. 2012. mvabund– an R package for model-based analysis of multivariate abundance data. *Methods in Ecology and Evolution* 3(3): 471-474.

Watnick, P. I., Fullner, K. J. & Kolter, R., 1999. A role for the mannose-sensitive hemagglutinin in biofilm formation by *Vibrio cholerae* El Tor. *Journal of bacteriology*, 181(11), pp. 3606–3609.

Waynick, J. A., 2001. The development and use of metal deactivators in the petroleum industry: a review. *Energy & Fuels*, 15(6), pp. 1325–1340.

Weisburg, W. G., Barns, S. M., Pelletier, D. A., Lane, D. J., 1991. 16S ribosomal DNA amplification for phylogenetic study. *Journal of Bacteriology*, 173(2), pp. 697–703.

Werner, J. J., Koren, O., Hugenholtz, P., DeSantis, T. Z., Walters, W. A., Caporaso, J. G., Angenent, L. T., Knight, R & Ley, R. E., 2012. Impact of training sets on classification of high-throughput bacterial 16s rRNA gene surveys. *The ISME journal*, 6(1), pp. 94–103.

Westbrook, S. R., 2000. Compatibility and efficacy of selected diesel fuel biocides. *In Graz, Austria: 7th International Conference on Stability and Handling of Liquid Fuels (IASH).*

White, J., Gilbert, J., Hill, G., Hill, E., Huse, S. M., Weightman, A. J. & Mahenthiralingam, E., 2011. Culture-independent analysis of bacterial fuel contamination provides insight into the level of concordance with the standard industry practice of aerobic cultivation. *Applied and Environmental Microbiology*, 77(13), pp. 4527–4538.

White, T. J., Bruns, T., Lee, S. & Taylor, J., 1990. *Amplification and direct sequencing of fungal ribosomal RNA genes for phylogenetics*. In M. A. Innis *et al*., eds. PCR Protocols: A guide to methods and applications. California: Academic Press Inc., pp. 315–322.

Williams, G. R. & Lugg, M., 1980. The significance of bacteria in aviation turbine fuel containing anti-icing additive. *International Biodeterioration Bulletin*, 16(4), pp. 103–106.

Xia, J. & Wishart, D. S., 2011. Web-based inference of biological patterns, functions and pathways from metabolomic data using MetaboAnalyst. *Nature protocols*, 6(6), pp. 743–760.

Yenn, R. 2015. *A study on problems associated with crude oil contamination in Assam and its control using biological methods*. Maharashta, India:Laxmi Book Publication.

Yoon, J. H., Kang, S. J., Schumann P. & Oh, T. K. 2007. *Cellulosimicrobium terreum sp. nov.*, isolated from soil. *International Journal of Systematic and Evolutionary Microbiology*. 57:2493-2497.

Xia, W., Du, Z., Cui, Q., Dong, H., Wang, F., He, P. & Tang, Y. C., 2014. Biosurfactant produced by novel *Pseudomonas sp*. WJ6 with biodegradation of n-alkanes and polycyclic aromatic hydrocarbons. *Journal of hazardous materials*, 276, pp. 489–498.

Yanto, D. H. Y. & Tachibana, S., 2014. Potential of fungal co-culturing for accelerated biodegradation of petroleum hydrocarbons in soil. *Journal of hazardous materials*, 278, pp. 454–63.

Yemashova, N. A., Murygina, V. P., Zhukov, D. V., Zakharyantz, A. A., Gladchenko, M. A., Appanna, V. & Kalyuzhnyi, S. V., 2007. Biodeterioration of crude oil and oil derived products: a review. *Reviews in Environmental Science and Bio-Technology*, 6(4), pp. 315–337.

Young, J.M., Kuykendall, L. D., Martínez-Romero, E. Kerr, A. & Sawada, H, 2001. A revision of *Rhizobium Frank* 1889, with an emended description of the genus, and the inclusion of all species of *Agrobacterium Conn* 1942 and *Allorhizobium undicola* de Lajudie *et al*. 1998 as new combinations: *Rhizobium radiobacter, R. rhizogenes, R. rubi, R. undocola* and *R. vitus*. *International journal of systematic and evolutionary microbiology*, 51(1), pp. 89–103.

Yousefi Kebria, D., Khodadadi, A., Ganjidoust, H., Badkoubi, A. & Amoozegar, M. A., 2009. Isolation and characterization of a novel native *Bacillus* strain capable of degrading diesel fuel. *International Journal of Environment Science and Technology*, 6(3), pp. 435–442.

Zabarnick, S., Adams, R., West, Z., DeWitt, M. J., Shafer, L., Striebich, R., Delaney, C. L. & Phelps, D. K., 2010. Compatibility of DiEGME and TriEGME fuel system icing inhibitor additives with BMS 10-39 aircraft tank topcoat material. *Energy & Fuels*, 24(4), pp. 2614–2627.

Zabarnick, S., West, Z., Dewitt, M. J., Shafer, L., Striebich, R., Adams, R., Delaney, C. L. & Phelps, D., 2007. Development of alternative fuel system icing inhibitor additives that are compatible with aircraft tank topcoat materials. *In Tucson: Arizona. The 10th International Conference on Stability, Handling and Use of Liquid Fuels (IASH).*

Zabarnick, S., DeWitt, M. J., Adams, R., West, Z. J., Shafer, L. M., Williams, T. F., Cook, R., Striebich, R., Balster, L. M., Delaney, C. L. & Phelps, D. K., 2011. *Evaluation of triethylene*

glycol monomethyl ether (TRIEGME) as an alternative fuel system icing inhibitor. Ohio: Air Force Research Laboratory.

Zabarnick, S., 1998. Pseudo-detailed chemical kinetic modelling of antioxidant chemistry for jet fuel applications. *Energy & Fuels*, 12, pp. 547–553.

Zabarnick, S. & Ervin, J., 2010. *The effects of operating jet fuels below the specification freeze point temperature limit*. Washington: Federal Aviation Administration.

Zherebtsov, V. L. & Peganova, M. M., 2012. Water solubility versus temperature in jet aviation fuel. *Fuel*, 102, pp. 831–834.

ZoBell, C. E., 1943. The effect of solid surfaces upon bacterial activity. *J. Bacteriol*, 46(204), pp. 39–56.

Appendix A

IASH paper

Appendix A – IASH paper

IASH 2015, the 14TH INTERNATIONAL SYMPOSIUM ON STABILITY, HANDLING AND USE OF LIQUID FUELS
Charleston, South Carolina USA
4-8 October 2015

HOW WILL NOVEL FUELS AND MATERIALS IMPACT MICROBIAL CONTAMINATION IN AIRCRAFT FUEL SYSTEMS?

Alexander McFarlane[1], Dr. Steve Thornton[2], and Dr. Stephen Rolfe[1]

[1]*University of Sheffield, Department of Animal and Plant Sciences, Alfred Denny Building, University of Sheffield, Western Bank, Sheffield, S10 2TN, United Kingdom*

[2]*University of Sheffield, GPRG, Kroto Research Institute, North Campus, University of Sheffield, Broad Lane, Sheffield, S3 7HQ, United Kingdom*

A.1 Abstract

It well established that jet fuel systems are susceptible to microbial attack as they provide all of the chemical and physiological requirements for biological growth. The introduction of alternative fuels and materials into the supply chain is likely to impact microbial community structure and function with the potential for new risks.

This project explores the impact of alternative fuels and novel composite materials on microbial community structure, biofilm development and function with the aim of identifying the underlying biological, chemical and physical processes. Our work has focused on a) characterising the microbial communities present in conventional aircraft fuel systems and their role in biofilm development, biocorrosion and fuel degradation, and b) the effect of introducing alternative fuels and new material formulations on these processes.

We have used molecular genetic techniques to characterise the microbial communities found in diverse conventional fuel systems and used these data to design multifactorial laboratory microcosm experiments in which parameters such as microbial community structure, fuel type and surface composition were varied. Our data show that alternative fuels and materials strongly influence microbial growth rate, community structure and cell

attachment. This project will help further the understanding of the principles that govern biofilm formation in aircraft fuel systems and the impact of introducing alternative fuels and materials into the supply chain.

KEYWORDS: Jet fuel, alternative fuels, GTL kerosene, middle distillates, hydrocarbon, biofilms, fuel degradation, community dynamics.

A.2 Introduction

For over 50 years, uncontrolled bio-deterioration of fuel has been problematical in the aviation industry[1,2]. The abundance of hydrocarbons found within jet fuel systems provides a significant carbon source for those microbes that are able to survive exposure to fuel and have the capacity to metabolise components within it. Additional components within the fuel also have a large impact on the growth of microbial communities. Aviation fuel systems inevitably contain water, which is also essential for active microbial growth[3]. Whilst water ingress can be minimised by tightly-controlled facility designs, handling procedures and housekeeping measures[4], even small amounts of water can lead to accumulation of microbial biomass. This can lead to fuel/additive degradation, corrosion and production of metabolic by-products that can disarm filter coalescers[5]. Water enters fuel systems via fuel handling and storage activities, as vapour from natural gas exchange or rain water ingress, and in aircraft significant amounts of water enter the fuel tanks during decent. Once associated with the fuel, water can exist in three states: dissolved, free water in suspension or free settled water. This fuel/water mixture forms a complex multiphasic system in contact with the fuel container surface and creates a diverse range of environments for microbial growth. Microbial growth in planktonic and sessile phases is a widely documented problem, and several previous studies have characterised microbes in aviation fuel systems[2,6,7,8].

Our understanding of the factors that govern microbial growth in current fuel systems is far from complete. In addition, the introduction of alternative fuels and novel composite materials into the supply chain is likely to significantly alter microbial community structure and function. For example, modern fuels differ in composition from conventional jet fuel in terms of hydrocarbon content and reduced aromatic/sulphur levels[9]. There is also a shift in construction materials moving from traditional metallic compounds to carbon composites. As well as altering the surfaces physical properties (and thus influencing microbial attachment and biofilm formation), surface chemistry will also change (for example the ability to act as a redox acceptor or donor). It is to be expected therefore that these changes in environmental conditions will influence microbial growth and dynamics, potentially altering risks in the jet fuel supply chain.

This study aims to determine how microbial development and fuel degradation responds to the introduction of alternative fuels. We have examined how isolates of industry-relevant microbes respond to alterations in fuel composition and extended these studies to explore the responses of complex communities. The following paper outlines the initial experimental data in this research programme.

A.3 Materials and methods

A.3.1 Microorganisms

For experiments with single isolates, four microorganisms with known capacity for hydrocarbon degradation were selected. Three of these were obtained from stock centres and represent industry-relevant microbial contaminants. These were a bacterium *Pseudomonas putida* F1 (ATCC 700007), a yeast *Candida tropicalis* (ATCC 48138), and a filamentous fungus *Hormoconis resinae* (ATCC 20495). Another bacterium (*Pseudomonas graminis*) isolated previously from contaminated fuel was also included. The identity of each organism was confirmed by sequencing of the 16S rRNA genes. A mixed community was also used, obtained from a contaminated Jet A-1 fuel storage system.

A.3.2 Materials

Three fuels were supplied by Shell Research Ltd: Merox-treated Jet A-1, Hydro-treated Jet A-1, and Gas to Liquid kerosene (GTL). Two fuel blends were then created: 50:50 Merox-treated Jet A-1:GTL kerosene and a 50:50 Hydrotreated Jet A-1:GTL kerosene. Fuels and blends were sterilised by passing them through a 0.22µm nitrocellulose filter paper. To form a fuel/water interface the fuels were overlaid on sterile Bushnell-Haas nutrient medium (Sigma Aldrich).

Table A.30 – Approximate compositional ratios of each of the major fuel components

Fuels	Normal Paraffins	Other Paraffins	Aromatics
Merox-treated Jet A-	1	1	1
Hydro-treated Jet A-1	2	1	1
GTL Kerosene	4	1	0

For those microcosms that included a surface, a 304 stainless steel coupon (63 x 10 x 1mm) was introduced. Coupons were degreased with acetone and then sterilized by soaking in absolute ethanol for 1 hour prior to use.

A.3.3 Microcosms

For experiments with monocultures, sterile 20ml microcosms were set up using 7ml of fuel or fuel blend and 7ml of Bushnell-Haas medium (Sigma Aldrich). This was placed in a gas chromatography (GC) headspace vial sealed with a 20mm PTFE/Butyl rubber crimp lid. Gas exchange was allowed by introducing a 1 inch sterile needle capped with a PTFE 0.2µm filter. A stainless steel coupon was added to each microcosm, so that the fuel-water interface was approximately a third of the way up the coupon. The coupon was angled at approximately 20^{o} to the vertical. Microcosms were inoculated with monocultures of the isolates at an optical density at 600nm (OD_{600}) of 0.05. Sterile controls were also prepared. Microcosms

were incubated at 25°C and destructively sampled every week for 4 weeks. Three independent replicates were performed in each case, giving a total of 300 microcosms.

For experiments with complex communities, microcosms were set up using 100ml of each fuel or fuel blend and 95ml of sterile Bushnell-Haas nutrient medium. This was placed in a 250ml Duran bottle with a polypropylene cap; gas exchange was allowed as above. Microcosms were inoculated with 5ml of contaminated water and incubated at 25°C for 14 days. After 14 days, 5ml of the aqueous phase was withdrawn and used to inoculate a second set of microcosms with either the same, or a different fuel type. These were incubated at 25°C for 14 days and then destructively harvested. Three independent replicates were performed in each case, giving a total of 39 microcosms.

A.3.4 Enumeration of microorganisms

For the enumeration of microbes in the aqueous phase, 2ml aliquots of the Bushnell-Haas nutrient medium were withdrawn and the optical density at 600nm determined by spectrophotometry. For analysis of microbes attached to the coupons, coupons were removed from the microcosms and fixed in a 4% (v/v) formaldehyde solution. The coupons were stained with SYTO 9 DNA stain to visualise microbial cells and SYPRO Ruby Biofilm Matrix Stain to visualise extracellular polymeric substances (EPS) (Life Technologies). One ml of the SYPRO Ruby was applied to the surface of the coupon and incubated in the dark at room temperature for 25 minutes, then 800µl of filtered 1x SYTO 9 solution was applied and incubated for a further 5 minutes. The coupons were gently washed with filtered deionised water, a coverslip applied and imaged immediately by confocal laser scanning microscopy (CLSM) (Zeiss LSM510 Meta). Images were collected using an EC Plan-Neofluar 40x objective with excitation at 488nm from an argon laser. SYTO 9 fluorescence was selected using a 500-550nm band pass filter whilst SYPRO Ruby was selected using a 650-710nm band pass filter. Images were 1252 x 1252 pixels in size (0.17µm/pixel) and acquired at 0.89µm intervals. Typically 15-20 image stacks were taken per sample, which were processed using Axiovision software (Zeiss).

A.3.5 Chemical analyses of microcosms

Major ions: Samples were passed through a 0.2µm polycarbonate syringe filter (Thermo Fisher Scientific) to remove particulates. A two-fold dilution was prepared in filtered distilled water and samples analysed on an ICS 3000 ion chromatography system with auto-sampler and eluent regeneration (Thermo Fisher Scientific). Ten µl of each sample were analysed for anions in a 31mM sodium hydroxide solution at a flow rate of 0.25ml/min on 2x250mm AS18

columns with AG18 guards (Thermo Fisher Scientific). Twenty µl of each sample were analysed for cations in a 48mM methane sulphonic acid solution at a flow rate of 0.42ml/min on 4x250mm CS16 columns with a CG16 guards. Chromatograms were analysed using the Chromeleon v6.80, and the data analysed using Metaboanalyst v3.0[10].

GC-MS: Dilutions (100mg/L) of the fuels and fuel blends were prepared in ≥97% n-Hexane. These were analysed using a Varian Saturn 2000 MS coupled to a 3800GC (Varian Medical Systems). Volatile, semi-volatile and C_8 to C_{20} mixed n-alkane standards were also run (Sigma Aldrich). The data were analysed using a Saturn GC/MS Workstation v5.41. The column used was a 30m x 0.25mm i.d., 0.25µm film thickness HP-5 column coated with 5% phenyl and 95% methyl polysiloxane (Agilent Technologies). The column temperature was programmed linearly from 50 to 270°C, at an 8°C per minute temperature ramp (with a 5 minute hold at 50°C after injection).

A.3.5 Microbial community structure analyses

DNA extraction: Samples were collected by passage through a 0.2µm polycarbonate filter paper which was then placed into a 2ml Eppendorf tube. 150µl of sorbitol buffer (1M Sorbitol, 500mM EDTA (pH 8), 10mM 2-mercaptoethanol), was added to the tube along with 3 x 3mm sterile tungsten beads. Filters were then ground in a SPEX Centriprep 8000M Mixer/Mill (Glen Creston) for 5 minutes. Fifty units of lyticase (Sigma Aldrich) were then added and the samples incubated at 30°C for 30 minutes in a water bath. DNA extractions were performed using an UltraClean® Microbial DNA Isolation kit (MO BIO Laboratories), directly following the manufacturers' instructions.

Amplification of 16S rRNA genes: Two µl of extracted DNA was amplified by PCR using 799F-FAM (5'-AACMGGATTAGATACCCKG-3', end labelled with 6-carboxyfluorescein (FAM))[11] and 1193R (5'-ACGTCATCCCCACCTTCC-3')[12]. PCR was performed with an initial incubation period of 94°C for 5 minutes, then 30 cycles of 94°C for 30 seconds, 53°C for 30 seconds and 72°C for 1 minute with a final incubation step of 10 minutes at 72°C. PCR products were confirmed by gel electrophoresis on 1% agarose gels and stained with ethidium bromide. Amplicons were purified using a QIAquick PCR purification kit (Qiagen), following the manufacturer's instructions. DNA was quantified using picoGreen as described previously[13].

T-RFLP: Bacterial samples were analysed using terminal-restriction fragment length polymorphism (T-RFLP). Twenty five ng of purified 16S rRNA amplicons were digested with 10U *Alu1* (Promega) in a 20µl reaction at 37°C for 3 hours. Five µl aliquots were desalted by precipitation for 2 hours with 16.65µl ice-cold 95% ethanol and 10% (v/v) 3M sodium acetate

(pH 5.2) with 0.25µl of 20mg/ml glycogen as a carrier. Samples were then centrifuged at 14000 x *g* at 4 °C for 20 minutes and the pellets washed twice in 70% (v/v) ethanol. The pellets were resuspended in 10µl hi-di formamide containing 0.5% GeneScan 500 ROX internal size standard (Applied Biosystems). Samples were then denatured at 95°C for 5 minutes, cooled on ice and the DNA fragments separated using capillary electrophoresis using an ABI 3730 PRISM capillary DNA analyser (Applied Biosystems). The T-RFLP electropherograms were analysed using Peak Scanner v1.0 (Thermo Fisher Scientific). Noise was removed by only analysing T-RFs with peak heights >50 fluorescent units. Fingerprinted fragments were expressed in terms of peak area and aligned using T-REX[14] with a confidence interval of 0.8nt.

A.4 Results

To assess the response of common industry microorganisms to variation in fuel type, microcosms were set up consisting of a fuel or fuel blend overlaid on a defined mineral medium. The mineral medium provided all of the necessary nutrients for microbial growth with the exception of a carbon supply that was provided by the fuel. The microcosms were inoculated with one of four microorganisms in monoculture or a mixed community sourced from a contaminated Jet A-1 storage tank. Growth in the monocultures was assessed at weekly intervals in the planktonic phase and as biofilms that had developed on a stainless steel coupon placed within each microcosm. The impact of microbial growth on the composition of the aqueous and fuel phases was measured. Growth in the mixed community was determined by T-RFLP analysis of amplified 16S rRNA genes to determine how fuel type drove changes in community dynamics over time.

A.4.1 Growth of monocultures in different fuel types

Planktonic growth of the monocultures was compared across the five fuel types by measuring the optical density of the aqueous phase at 600nm (Figure A.62). Four organisms were tested: two bacteria (*Pseudomonas putida* and *Pseudomonas graminis*) and two eukaryotes – the fungus *Hormoconis resinae* and a yeast *Candida tropicalis*. Five hydrocarbon sources were used: Hydro-treated Jet A-1, Merox-treated Jet A-1, GTL kerosene and 50:50 blends of each Jet A-1 fuel with GTL kerosene. In microcosms containing a jet fuel, whether as a single component (Hydro or Merox-treated Jet A-1) or as 50:50 blends of either with GTL kerosene, rapid growth from a starting OD_{600} of 0.05 to ~1 was seen in the first week in all cases. The organisms then entered the stationary phase with little change in OD over weeks 2-4 with the exception of *C. tropicalis* where there was a slight decline. In contrast, much less growth occurred in the pure GTL kerosene samples with all 4 organisms tested. For *P. putida, P. graminis* and *C. tropicalis* growth in GTL kerosene was ~10% of that seen in the other fuels. For *H. resinae* it was somewhat higher at ~30% but this declined in weeks 2-4.

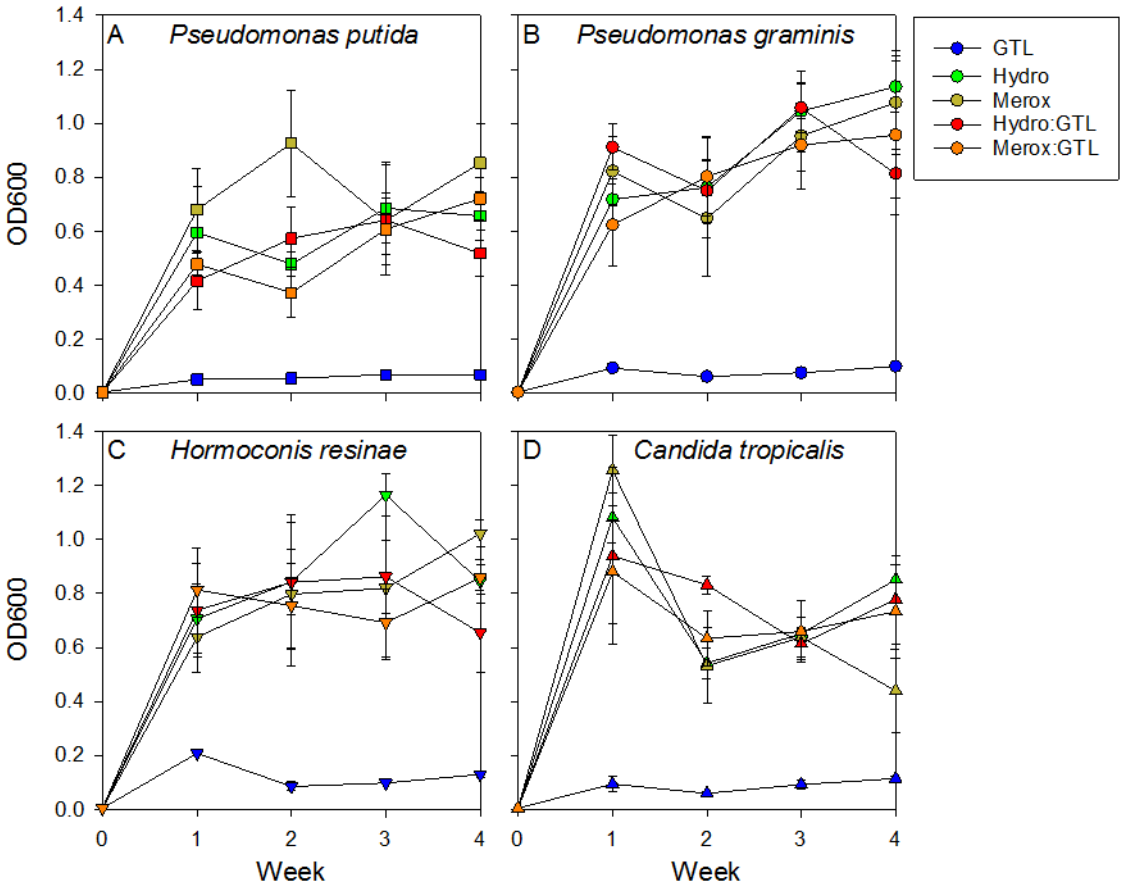

Figure A.62 - Growth of isolated organisms in fuels or fuel blends. Results are means (n = 3) +/- S.E.

Biofilm formation on the stainless steel coupons mirrored the growth patterns seen in the planktonic phase. Figure A.63 shows an example a *P. putida* biofilm formed on a stainless steel coupon after 4 weeks incubation in microcosms containing Merox-treated Jet A-1 (A-C) and GTL kerosene (D-F). The *P. putida* cells fluoresce green whilst EPS fluoresces red (the faint green scaling seen in the images is not of biological origin. It developed in coupons placed in sterile microcosms during extended incubations). In the Merox-treated fuel, a heterogeneous biofilm of *P. putida* had formed. In the aqueous phase individual cells had attached with only a few colonies of cell clusters (12-15µm in height) present. The individual cells and colonies had little EPS associated with them. Cell density increased with proximity to the aqueous:fuel interface and was greatest in this region of the coupon. As well as many individual cells, large colonies of cells were evident, up to 50µm across and 20µm high. Some limited production of EPS was evident in these colonies as seen in Figure A.63, B-2. Many cells had also attached in the fuel phase with numerous but somewhat smaller colonies developing (typically 5-10µm across and >10µm high). Significant amounts of EPS were

associated with the cells as shown by the strong SYPRO Ruby signal in Figure A.63, A-2. In contrast, little growth was seen in the microcosms containing GTL kerosene. Some sparse attachment of single cells could be seen in both phases, but there was little evidence of significant growth nor production of EPS. This pattern was repeated for the other microorganisms tested (data not shown).

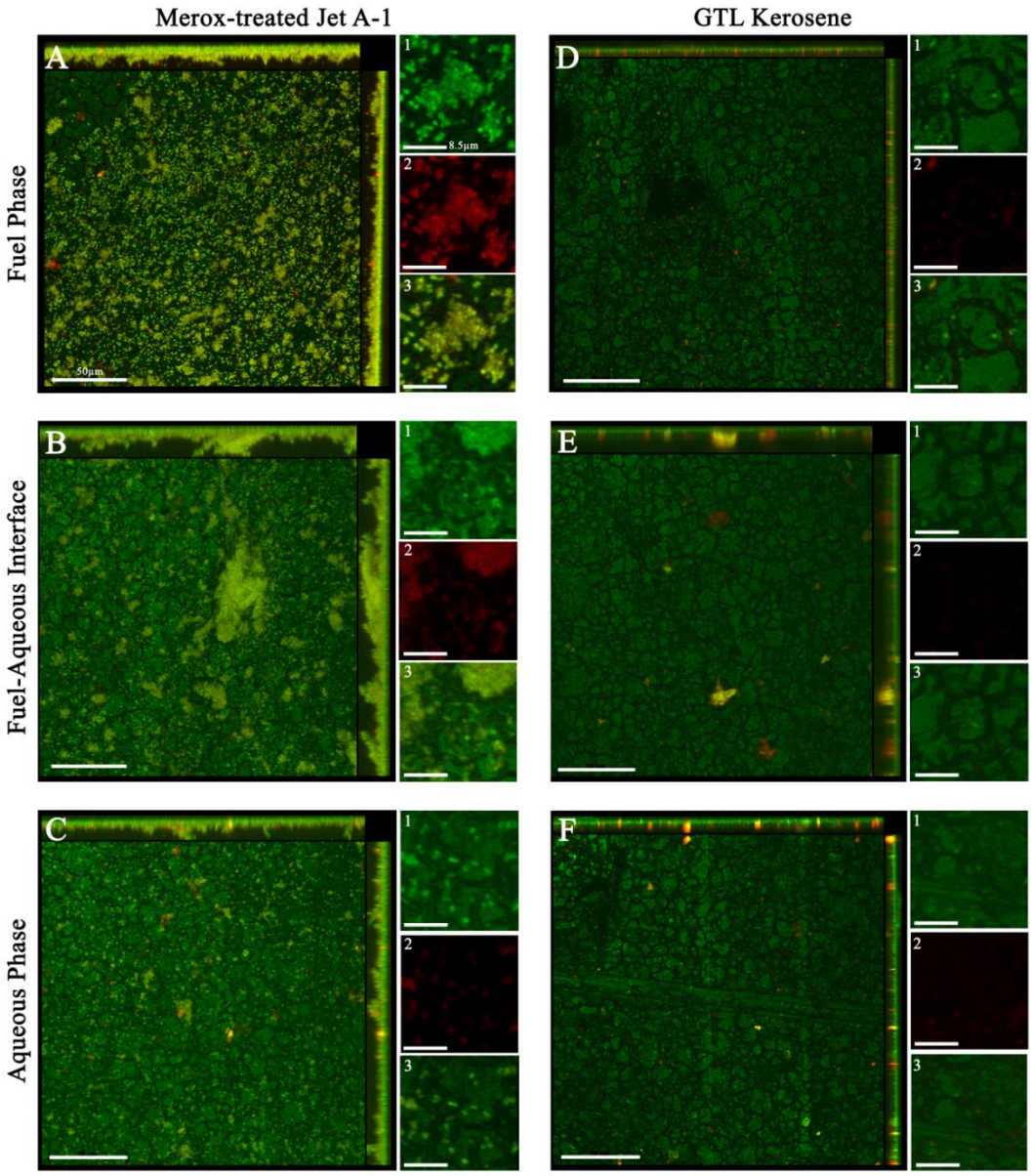

Figure A.63 – CLSM images of P. putida biofilms on stainless steel coupons incubated for 4 weeks in microcosms containing Merox-treated Jet A-1 (A-C) and GTL kerosene (D-F). Images were taken at different points along the coupon in the aqueous phase, at fuel/aqueous interface and in the fuel phase. The main image is a maximum intensity projection image in X, Y and Z dimensions of the DNA stain SYTO 9 (light green) and the EPS stain SYPRO Ruby (red). Non-specific staining shows as dark green and is of non-biological origin. Close up images are shown as inserts of the SYTO 9 (1), SYPRO Ruby (2) and combined signals (3). Scale bars are 50µm (main images) and 8.5µm (insets).

A.4.2 Chemical analysis of microcosms

To better understand the chemical differences in microcosms containing different fuel types and blends, chemical analysis was performed on the major ions in the aqueous phase (using

ion chromatography) and the hydrocarbon content of the fuel phase (using GC-MS). No major differences in the hydrocarbon content of the microcosms could be detected (data not shown), presumably as the amount of carbon used by the microbes was very low compared to the total available. However, significant changes in the ion content of the aqueous phase were detected. These were analysed by Partial Least Squares-Discriminant Analysis (PLS-DA) to identify differences in ions associated with the growth differences seen between microcosms (Figure A.64, A). The microcosms containing GTL kerosene alone clearly separated from the other fuel types and blends. The loading plot (Figure A.64, B) showed that this separation was driven by nitrate and ammonium, which was confirmed by analysis of the variable importance in projections (VIP). Nitrate was the most important factor in both component 1 and 2 with additional contributions from ammonium and sulphate. Figure A.64, C shows plots of selected ions.

There was little change in the phosphate concentration of the microcosms, but both nitrate and ammonium were utilised in those microcosms containing conventional jet fuels. In contrast, little nitrate or ammonium was consumed in the GTL kerosene systems with the exception of *C. tropicalis* where ammonium was consumed. This correlated with the slightly better growth of *C. tropicalis*, in the GTL kerosene systems, compared to other organisms. Figure A.64, D shows a plot of growth versus nitrate concentration, indicating a close correlation between nitrate consumption and growth.

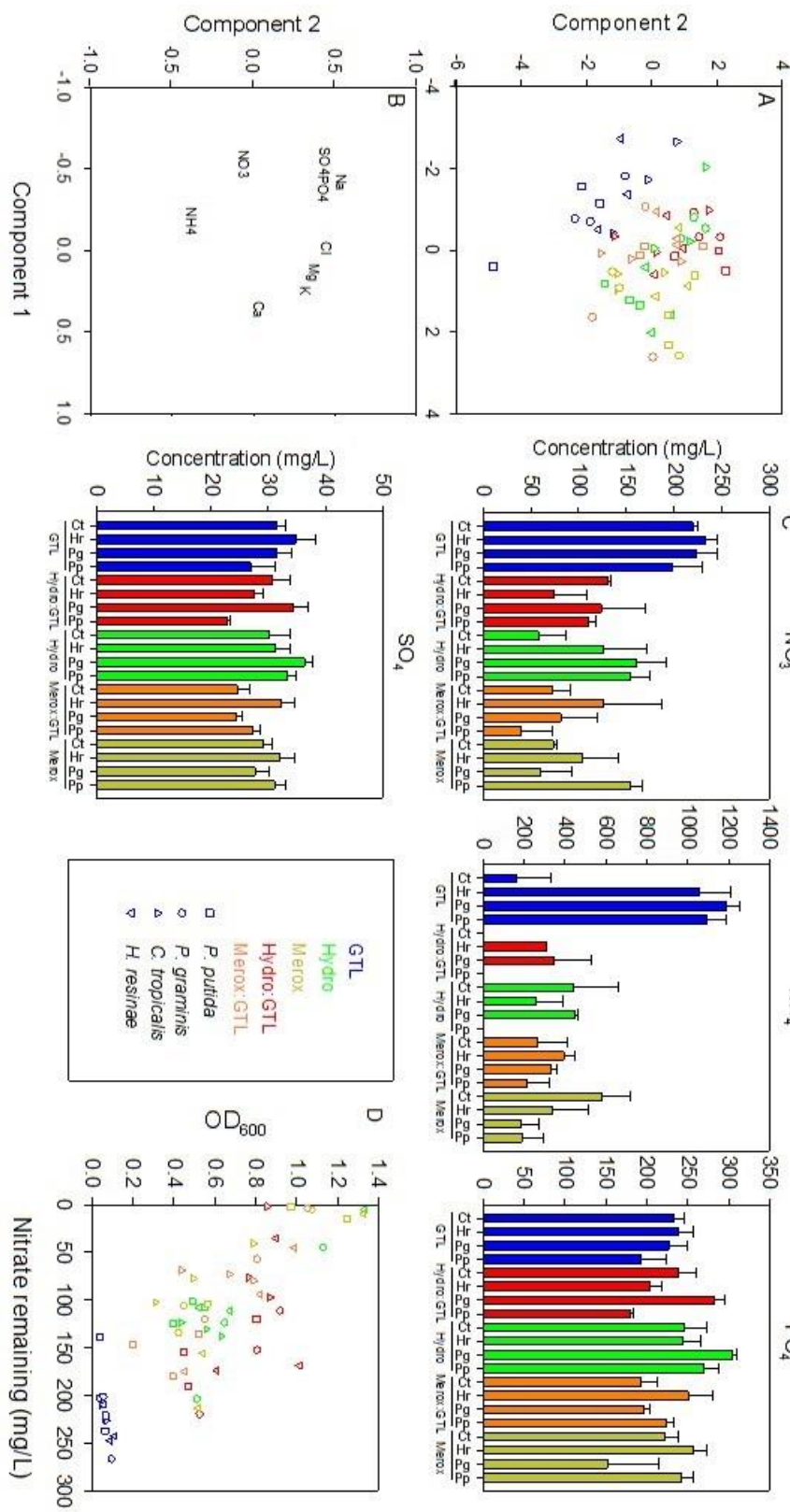

Figure A.64 – Analysis of ion content in the aqueous phase of the microcosms. A, PLS-DA plot of samples based on all major ions in solution (Cl, SO_4, NO_3, PO_4, Na, NH_4, K, Mg, Ca). B, Loading plots. C, Concentrations of selected ions (means +/- SE, n = 3). D, Nitrate remaining in the microcosm vs. growth.

A.4.3 The impact of fuel type on microbial community structure

Although the four isolates grew poorly on GTL kerosene compared to the other fuel types, we considered it unlikely that this was a general phenomenon, but rather a requirement in those specific isolates for compounds present in the more complex conventional fuels compared to the simpler GTL kerosene. We hypothesised that taking a mixed community from a Jet A-1 contaminated fuel tank and growing on different fuels would select communities of organisms better able to degrade specific fuel types. Therefore, we set up larger (200ml) microcosms with the different fuel types, inoculated with a mixed community and allowed microbial growth to occur for 2 weeks. An aliquot of the aqueous phase was then removed, used to inoculate new microcosms containing the same or different fuel types, and then incubated for a further 2 weeks. Experiments were performed in triplicate. Microbial cells were harvested from the aqueous phase/interface, DNA extracted and bacterial diversity assessed by T-RLFP of amplified 16S rRNA gene fragments. Future experiments will assess diversity in the eukaryotic population by analysis of Internal Transcribed Spacer (ITS) sequences and an in-depth analysis of the microbial populations by high through-put sequencing.

Between 10 and 51 terminal restriction fragments (T-RF) were produced per sample following digestion with *AluI*. There was considerable variation between samples, with a slight increase in species richness in the older microcosms compared to the starting inoculum. The average number of T-RFs and variation between microcosms is shown in Figure A.65, A. Of the 90 different T-RFs detected, 8 were common to all samples and included the most dominant bands. T-RFs of 78 and 258 bp were the most abundant and the shared T-RFs represented, on average, 92% of the total signal intensity in each lane.

Principle Component Analysis (PCA) was then used to identify factors that controlled variance in the samples (Figure A.65, B). The first two components explain 81% of the variation in the samples. The analysis was weighted for signal intensity identifying major T-RFs at 55, 75, 78 and 285 bp, as the major drivers of diversity within the microcosms (Figure A.65, C). Figure A.65, D-F show PCA analysis for microcosms containing GTL kerosene, Hydro-treated Jet A-1 and Merox-treated Jet A-1 separately. In each case only the first two components are shown as these explain the majority of the variation between the samples.

The PCAs show that the microbial communities from microcosms containing GTL kerosene and Hydro-treated Jet A-1 were relatively constant and did not deviate much from that seen in the initial inocula. However, as the incubation proceeded, variation tended to increase,

presumably as conditions became more favourable for a more diverse population of microorganisms. Variation in the Merox-treated Jet A-1 tended to be much greater after 2 weeks than with the other fuel types, a pattern which persisted after 4 weeks of incubation, most likely due to the higher sulphur content of this fuel. The biggest variation was seen when the fuel type was changed from GTL kerosene to a conventional jet fuel or vice versa. The data indicated a large population shift occurred in these samples.

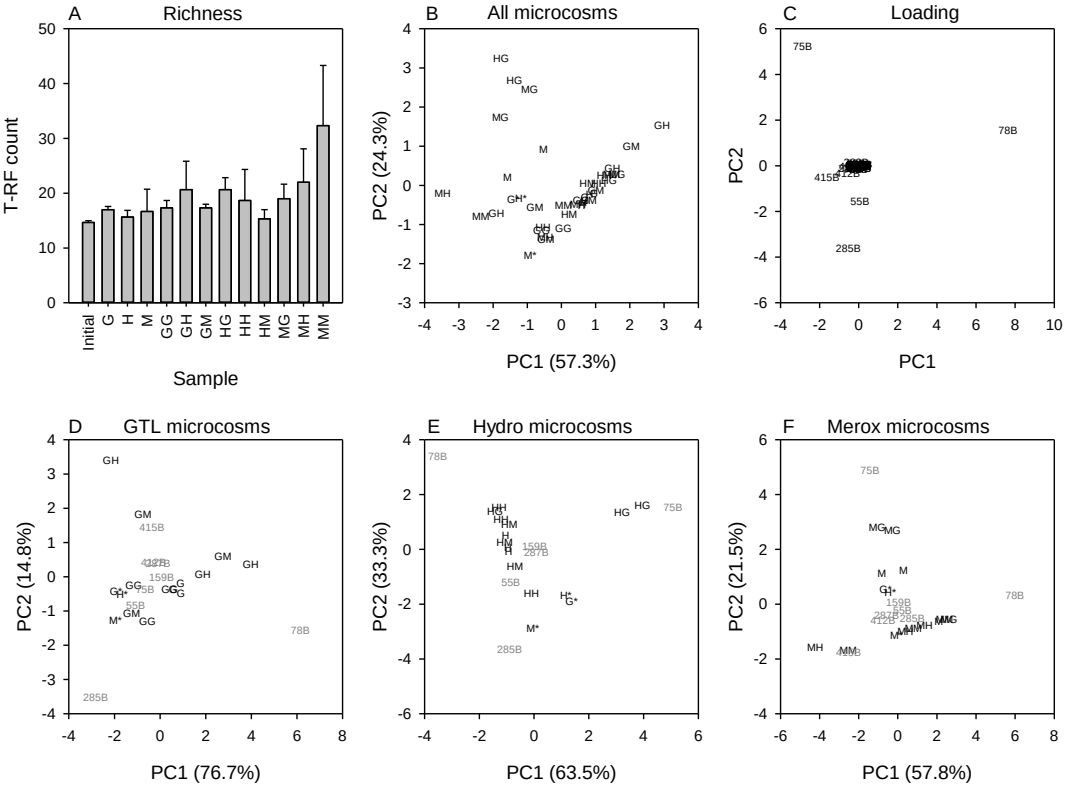

Figure A.65 – A, T-RF count in each microcosm. B and C, PCA of all samples and loading plots. D, E and F, PCA of microcosms containing each fuel type. T-RFs which account for 1% or more of the variation (weighted for signal intensity) are shown in grey. * indicates initial inoculum. G, H, M represent samples from microcosms are 2 weeks incubation with GTL kerosene, Hydro- and Merox-treated Jet A-1 respectively. Where two letters are shown (e.g. HG) the first two weeks incubation was in Hydro-treated Jet A-1 that was then used to inoculate a microcosm containing GTL kerosene.

A.5 Discussion

Jet fuels are a complex mixture of hydrocarbons, typically containing thousands compounds. These can be broadly categorised into aliphatic (≥80% including normal, iso- and cyclo-alkanes) and aromatic (≤25%) hydrocarbons, along with a variety of heteroatomic compounds (≥25%)[15,16,17]. These groups vary in their susceptibility to degradation by microorganisms, but in general aliphatic hydrocarbons show the highest degradation rates[18] and high molecular weight aromatics and polar compounds the lowest[19,20]. Many previous studies have looked at the microbial degradation of hydrocarbons[21,22], however most field studies focus on remediation of environmental contamination[23,24,25] and not degradation within fuel systems. In this study we have examined how microbial growth responds to changes in hydrocarbon composition with a view of understanding likely responses of microbial communities to the introduction of alternative fuels. Specifically we have looked at how industry-relevant single isolates and mixed communities responded to GTL kerosene.

We have found that when microcosms were inoculated with *P. putida*, *P. graminis*, *H. resinae* and *C. tropicalis* in monoculture, both planktonic growth and biofilm formation was significantly lower in pure GTL kerosene when compared to fuels containing conventional jet fuels. This was not due to a toxicity effect of GTL kerosene as this effect was not seen in 50:50 blends of GTL kerosene with conventional fuels. Therefore we hypothesise that these isolates, in monoculture, lacked the ability to metabolise paraffins/iso-paraffins and were therefore carbon limited in these systems[26]. At present, we do not know which hydrocarbons are responsible for these growth differences as the fuel was in massive excess in the microcosms and no overt differences in hydrocarbon use could be detected by GC-MS. To address this important point, we will create a range of model fuel blends from individual purified components and test the growth responses of single isolates. We have also isolated organisms from GTL kerosene and conventional fuel microcosms so that a comparative genomic analysis can be used to identify key degradative genes.

All of the microcosms in this study were designed as eutrophic systems with the aqueous phase providing all of the mineral nutrients required for microbial growth. Analysis of the aqueous phase showed that in most cases growth continued until nitrogen became limiting. This is to be expected as the typical C:N ratio of bacterial cells is in the range of 5-10 whilst C:P ratios are ~10-fold higher. A large amount of planktonic and biofilm biomass had developed at this point. We recognise that jet fuel systems will be oligotrophic (and other environmental factors such as low temperature and associated freeze/thaw cycles) are likely to strongly influence microbial communities. For example, low nutrients and the removal of

the water phase by routine tank drainage will favour biofilm formation[27,28]. Our future studies will explore biofilm communities in oligotrophic environments, building upon the baseline knowledge about hydrocarbon utilisation described in this report. Biofilms are of particular importance as they can lead to operational problems such as filter plugging and corrosion. In these systems the surfaces to which microorganisms attach will be of key importance, as both the physical and chemical properties of these surfaces will have an impact on biofilm formation[29]. Further work will study the effect of varying surface type on cell attachment and biofilm formation in representative oligotrophic systems.

Our results have demonstrated that the selected industry-relevant isolates that we tested use GTL kerosene much less efficiently than conventional fuels. However, the impact of altering fuel types on mixed communities was much less marked. T-RFLP analysis showed that the dominant bacteria in the microcosms were present irrespective of fuel type. We will attempt to isolate these organisms and characterise their ability to degrade diverse fuels. During the course of the microcosm incubations there tended to be an increase in microbial diversity due to the appearance of numerous, small T-RFs. Similar results have been seen in other xenobiotic degrading microcosms – initially the systems are dominated by a few, highly competitive organisms but as the systems mature, a wider diversity of microbes becomes apparent[13]. We will use high-throughput sequencing to characterise these in the future. We will also explore the eukaryotic fungal and yeast communities as these are important contaminants of many jet fuel systems.

A.6 Conclusion

In conclusion, our results have demonstrated that the introduction of GTL kerosene into the jet fuel supply system is likely to impact the microbial communities present with implications for current operating procedures and test methods. This impact will be less marked in systems where GTL kerosene is used in mixtures with conventional fuels. Many questions remain to be addressed including the identity of genes able to degrade GTL kerosene, how these may be transferred between organisms in the fuel system environment, the role of biofilms and the impact of new surfaces on biofilm formation and the complex physical and metabolic interactions between members of microbial consortia. By using microcosms to disassemble these systems and drawing comparisons with research on the environmental impacts of fuel release we aim to provide a greater understanding of the problem of microbial contamination in jet fuel systems of the future.

A.7 Acknowledgements

This work was funded by Shell Research Ltd., Shell supervisors Paul Bogers and Dr. Joanna Bauldreay. The authors wish to thank Despina Berdeni, James P. Berry, Paul Blackbourn, Dr. Anne Cotton, Andrew Fairburn, Petra Hedbavna, Dr. Gabriella Kakonyi, Dr. Katherine Fish, Sarah Sommer and Nichola White for providing invaluable advice and assistance with many of the technical aspects of this paper.

A.8 References

1. Balster, L. M., Chelgren, S. K., Strobel, E. M., Vangsness, M. D. & Bowen, L. L. Characterization of the bio-burden in United States aviation fuel: A comparison of FTA paper and other methods for obtaining genetic material from aviation fuel microbes. *Prepr. Pap.-Am. Chem. Soc., Div. Petr. Chem.* **51,** 558–560 (2006).
2. Raikos, V., Vamvakas, S. S., Kapolos, J., Koliadima, A. & Karaiskakis, G. Identification and characterization of microbial contaminants isolated from stored aviation fuels by DNA sequencing and restriction fragment length analysis of a PCR-amplified region of the 16S rRNA gene. *Fuel* **90,** 695–700 (2011).
3. Mara, D. & Horan, N. *The handbook of water and wastewater microbiology*. (Elsevier Ltd, 2003).
4. Anon. *Guidance material on microbiological contamination in aircraft fuel tanks*. (International Air Transport Association, 2009).
5. White, J. *et al.* Culture-Independent Analysis of Bacterial Fual Contamination Provides Insight into the Level of Concordance with the Standard Industry Practice of Aerobic Cultivation. *Appl. Environ. Microbiol.* 4527–4538 (2011).
6. Brown, L. M. *et al.* Community dynamics and phylogenetics of bacteria fouling Jet A and JP-8 aviation fuel. *Int. Biodeterior. Biodegradation* **64,** 253–261 (2010).
7. Denaro, T. R. *et al. DNA isolation of microbial contaminants in aviation turbine fuels via traditional polymerase chain reaction (PCR) and direct PCR (preliminary results)*. (2005).
8. Rauch, M. E. *et al.* Characterization of microbial contamination in United States Air Force aviation fuel tanks. *J. Ind. Microbiol. Biotechnol.* **33,** 29–36 (2006).
9. Stratton, R. W., Wolfe, P. J. & Hileman, J. I. Impact of aviation non-CO_2 combustion effects on the environmental feasibility of alternative jet fuels. *Environ. Sci. Technol.* **45,** 10736–43 (2011).
10. Xia, J. & Wishart, D. S. Web-based inference of biological patterns, functions and pathways from metabolomic data using MetaboAnalyst. *Nat. Protoc.* **6,** 743–760 (2011).
11. Chelius, M. K. & Triplett, E. W. The Diversity of Archaea and Bacteria in Association with the Roots of *Zea mays* L. *Microb. Ecol.* **41,** 252–263 (2001).
12. Bodenhausen, N., Horton, M. W. & Bergelson, J. Bacterial Communities Associated with the Leaves and the Roots of Arabidopsis thaliana. *PLoS One* **8,** (2013).

13. Elliott, D. R. *et al.* Dynamic changes in microbial community structure and function in phenol-degrading microcosms inoculated with cells from a contaminated aquifer. *FEMS Microbiol. Ecol.* **71,** 247–259 (2010).
14. Culman, S. W., Bukowski, R., Gauch, H. G., Cadillo-Quiroz, H. & Buckley, D. H. T-REX: software for the processing and analysis of T-RFLP data. *BMC Bioinformatics* **10,** 171 (2009).
15. Mbadinga, S. M. *et al.* Microbial communities involved in anaerobic degradation of alkanes. *Int. Biodeterior. Biodegradation* **65,** 1–13 (2011).
16. Passman, F. J. Microbial contamination and its control in fuels and fuel systems since 1980 – a review. *Int. Biodeterior. Biodegradation* (2013).
17. Gaylarde, C. C., Bento, F. M. & Kelley, J. Microbial contamination of stored hydrocarbon fuels and its control. *Rev. Microbiol.* 1–10 (1999).
18. Atlas, R. M. Microbial degradation of petroleum hydrocarbons: an environmental perspective. *Microbiol. Rev.* **45,** 180–209 (1981).
19. Fuchs, G. Anaerobic metabolism of aromatic compounds. *Ann. N. Y. Acad. Sci.* **1125,** 82–99 (2008).
20. Leahy, J. G. & Colwell, R. R. Microbial degradation of hydrocarbons in the environment. *Microbiol. Rev.* **54,** 305–15 (1990).
21. Fuchs, G., Boll, M. & Heider, J. Microbial degradation of aromatic compounds - from one strategy to four. *Nat. Rev. Microbiol.* **9,** 803–16 (2011).
22. Xia, W. *et al.* Biosurfactant produced by novel Pseudomonas sp. WJ6 with biodegradation of n-alkanes and polycyclic aromatic hydrocarbons. *J. Hazard. Mater.* **276,** 489–98 (2014).
23. Chandankere, R. *et al.* Properties and characterization of biosurfactant in crude oil biodegradation by bacterium Bacillus methylotrophicus USTBa. *Fuel* **122,** 140–148 (2014).
24. Lisiecki, P. *et al.* Biodegradation of diesel/biodiesel blends in saturated sand microcosms. *Fuel* **116,** 321–327 (2014).
25. Yanto, D. H. Y. & Tachibana, S. Potential of fungal co-culturing for accelerated biodegradation of petroleum hydrocarbons in soil. *J. Hazard. Mater.* **278,** 454–63 (2014).
26. Susan S. Mueller, Loryn L. Bowen, Lisa M. Brown, Nicholas A. Brown, Oscar N. Ruiz, Marlin Vangsness, Lori Balster, Steven Zabarnick, Linda Shafer, Rhonda Cook, E. M. S.

A Comparision Study of the Effects of Bacterial Contamination on Alternative Fuels Versus Petroleum-Derived. in 1–23 (IASH, 2011).

27. Garrett, T. R., Bhakoo, M. & Zhang, Z. Bacterial adhesion and biofilms on surfaces. *Prog. Nat. Sci.* **18,** 1049–1056 (2008).

28. Koch, B., Worm, J., Jensen, L. E., Hojberg, O. & Nybroe, O. Carbon limitation induces σ^S-dependent gene expression in Pseudomonas fluorescens in soil . *Appl. Environ. Microbiol.* **67,** 3363–3370 (2001).

29. Percival, S. L., Knapp, J. S., Wales, D. S. & Edyvean, R. G. J. The effect of turbulent flow and surface roughness on biofilm formation in drinking water. *J. Ind. Microbiol. Biotechnol.* **22,** 152–159 (1999).

Appendix B

Field and microcosm samples analysed in Chapter 2

Appendix B – Field and microcosm samples analysed in Chapter 2

Table B.31 – List of field samples analysed by direct sequencing in Chapter 2

Sample number	Site	Source type	Source phase	Nutrient medium	Fuel
52	Germany1	Aircraft	Water	N/A	N/A
53	Germany1	Aircraft	Water	N/A	N/A
55	Germany1	Aircraft	Water	N/A	N/A
54	Germany1	Aircraft	Water	N/A	N/A
49	Germany1	Aircraft	Water	N/A	N/A
56	Germany1	Aircraft	Water	N/A	N/A
57	Germany1	Aircraft	Water	N/A	N/A
50	Germany1	Aircraft	Water	N/A	N/A
51	Germany1	Aircraft	Water	N/A	N/A
43	UK2	Tank	Water	N/A	N/A
44	UK2	Tank	Water	N/A	N/A
45	UK2	Tank	Water	N/A	N/A
46	UK2	Tank	Water	N/A	N/A
48	UK2	Tank	Water	N/A	N/A

Table B.32 – List of microcosm sample analysed by direct sequencing in Chapter 2

Sample number	Site	Source type	Inoculum	Nutrient medium	Fuel
3	Germany1	Aircraft	Water	Bushnell-Haas	Merox-treated Jet A-1
28	Germany1	Aircraft	Fuel	Water	Fuel from the field
12	Germany1	Aircraft	Fuel	Bushnell-Haas	Fuel from the field
17	Germany1	Aircraft	Water	Bushnell-Haas	Merox-treated Jet A-1
1	Germany1	Aircraft	Fuel	Bushnell-Haas	Fuel from the field
2	Germany1	Aircraft	Fuel	Bushnell-Haas	Fuel from the field
38	Germany1	Aircraft	Fuel	Water	Fuel from the field
42	Germany1	Aircraft	Fuel	Water	Fuel from the field
15	Germany1	Aircraft	Water	Bushnell-Haas	Merox-treated Jet A-1
18	Germany1	Aircraft	Water	Bushnell-Haas	Merox-treated Jet A-1
16	Germany1	Aircraft	Water	Bushnell-Haas	Merox-treated Jet A-1
13	Germany1	Aircraft	Fuel	Bushnell-Haas	Fuel from the field
36	Germany1	Aircraft	Fuel	Water	Fuel from the field
4	Germany1	Aircraft	Water	Bushnell-Haas	Merox-treated Jet A-1
5	Germany1	Aircraft	Water	Bushnell-Haas	Merox-treated Jet A-1
6	Germany1	Aircraft	Fuel	Bushnell-Haas	Fuel from the field
32	Germany1	Aircraft	Fuel	Water	Fuel from the field
7	Germany1	Aircraft	Fuel	Bushnell-Haas	Fuel from the field
34	Germany1	Aircraft	Fuel	Water	Fuel from the field
8	Germany1	Aircraft	Fuel	Bushnell-Haas	Fuel from the field
9	Germany1	Aircraft	Fuel	Bushnell-Haas	Fuel from the field
30	Germany1	Aircraft	Fuel	Water	Fuel from the field
40	Germany1	Aircraft	Fuel	Water	Fuel from the field
10	Germany1	Aircraft	Water	Bushnell-Haas	Merox-treated Jet A-1

Sample number	Site	Source type	Inoculum	Nutrient medium	Fuel
11	Germany1	Aircraft	Fuel	Bushnell-Haas	Fuel from the field
25	Germany1	Aircraft	Fuel	Water	Fuel from the field
14	Germany1	Aircraft	Water	Bushnell-Haas	Merox-treated Jet A-1
58	Greece1	Tank	Fuel	Bushnell-Haas	Fuel from the field
63	Greece1	Tank	Fuel	Water	Fuel from the field
68	Greece1	Tank	Water	Bushnell-Haas	Merox-treated Jet A-1
59	Greece1	Tank	Fuel	Bushnell-Haas	Fuel from the field
64	Greece1	Tank	Fuel	Water	Fuel from the field
60	Greece1	Tank	Fuel	Bushnell-Haas	Fuel from the field
65	Greece1	Tank	Fuel	Water	Fuel from the field
61	Greece1	Tank	Fuel	Bushnell-Haas	Fuel from the field
66	Greece1	Tank	Fuel	Water	Fuel from the field
62	Greece1	Tank	Fuel	Bushnell-Haas	Fuel from the field
67	Greece1	Tank	Fuel	Water	Fuel from the field
19	Holland1	Tank	Fuel	Bushnell-Haas	Fuel from the field
21	Holland2	Tank	Fuel	Bushnell-Haas	Fuel from the field
41	Holland3	Tank	Fuel	Bushnell-Haas	Fuel from the field
23	Qatar1	Tank	Fuel	Bushnell-Haas	Fuel from the field
47	Qatar1	Tank	Fuel	Bushnell-Haas	Fuel from the field
37	Qatar1	Tank	Fuel	Water	Fuel from the field
77	UK1	Aircraft	Fuel	Bushnell-Haas	Fuel from the field
78	UK1	Aircraft	Fuel	Water	Fuel from the field
73	UK1	Tank	Fuel	Bushnell-Haas	Fuel from the field
74	UK1	Tank	Fuel	Water	Fuel from the field
75	UK1	Tank	Fuel	Bushnell-Haas	Fuel from the field

Sample number	Site	Source type	Inoculum	Nutrient medium	Fuel
33	UK2	Tank	Fuel	Water	Fuel from the field
22	UK2	Tank	Fuel	Bushnell-Haas	Fuel from the field
24	UK2	Tank	Fuel	Bushnell-Haas	Fuel from the field
35	UK2	Tank	Fuel	Water	Fuel from the field
31	UK2	Tank	Fuel	Water	Fuel from the field
29	UK2	Tank	Fuel	Bushnell-Haas	Fuel from the field
27	UK2	Tank	Fuel	Bushnell-Haas	Fuel from the field
26	UK2	Tank	Fuel	Water	Fuel from the field
71	UK3	Tank	Fuel	Bushnell-Haas	Fuel from the field
72	UK3	Tank	Fuel	Water	Fuel from the field
69	UK3	Tank	Fuel	Bushnell-Haas	Fuel from the field
70	UK3	Tank	Fuel	Water	Fuel from the field

Appendix C

QIIME scripts

Appendix C – QIIME scripts

C.1 Demultiplexing samples (fastqsplit)

The first time fastqsplit is run it requires, biopython, numpy and egglib to be installed. To do this:

```
sudo pip install numpy
sudo pip install biopython
```

Download egglib-3.0.0b6, to install this copy the gz file to your Shared_Folder, then:

```
tar -xvzf *.gz
cd egglib-3.0.0b6/
python setup.py build
sudo python setup.py install
```

This unpacks the zip file and installs the python module. You can check it has worked with:

```
python
import egglib
exit()
```

To run fastqsplit, copy fastqsplit.py into your working directory and use the following command line. It requires a mapping file to be set up (see below), and an output directory to be created:

```
./fastqsplit.py -a <forward sequence file> -b <reverse sequence
file> -f <forward barcode file> -r <reverse barcode file> -m
<map file> -o <output directory>
```

An example of the mapping file looks like this, and is <tab> separated and included the primers and barcodes (forward and reverse):

```
Sample    PrimerF    BarcodeF    PrimerR    BarcodeR
AlexMcF_Bacteria_MA1_FF      AACMGGATTAGATACCCKG      ACTCGCTA
ACGTCATCCCCACCTTCC    TTATGCGA
AlexMcF_Bacteria_MA2_FF      AACMGGATTAGATACCCKG      ACTCGCTA
ACGTCATCCCCACCTTCC    GAGCCTTA
AlexMcF_Bacteria_MA3_FF      AACMGGATTAGATACCCKG      ACTCGCTA
ACGTCATCCCCACCTTCC    AAGGCTAT
AlexMcF_Bacteria_MA4_FF      AACMGGATTAGATACCCKG      ACTCGCTA
ACGTCATCCCCACCTTCC    CTATTAAG
AlexMcF_Bacteria_MA1_WF      AACMGGATTAGATACCCKG      ACTCGCTA
ACGTCATCCCCACCTTCC    GCGTAAGA
AlexMcF_Bacteria_MA2_WF      AACMGGATTAGATACCCKG      ACTCGCTA
ACGTCATCCCCACCTTCC    CCTAGAGT
AlexMcF_Bacteria_MA3_WF      AACMGGATTAGATACCCKG      ACTCGCTA
ACGTCATCCCCACCTTCC    TTCTAGCT
```

```
AlexMcF_Bacteria_MA4_WF      AACMGGATTAGATACCCKG      ACTCGCTA
ACGTCATCCCCACCTTCC    TCGACTAG
```

The content of fastqsplit is:

```
import sys,getopt,os.path,csv,json
from Bio import SeqUtils

import egglib

def main(argv):
     seqafile=""
     seqbfile=""
     primffile=""
     primrfile=""
     mfile=""
     odir=""
     nlimit=0
     verbose=False
     allow_mismatch=1
     print  "Allow",  allow_mismatch,"mismatches  in  primer
sequence"
     try:

     opts,args=getopt.getopt(argv,"hm:a:b:f:r:o:n:v",["mfile=
","afile=","bfile=","ffile=","rfile=","odir=","nlimit="])
     except getopt.GetOptError:
          print "fastqsplit.py -a <forward seq inputfile> -b
<reverse seq inputfile> -f <forward barcode file> -r <reverse
barcode file> -m <map file> -o <output dir> -n <limit reads> -
v verbose"
          sys.exit(2)
     for opt , arg in opts:
          if opt=="-h":
               print   "fastqsplit.py   -a   <forward   seq
inputfile> -b <reverse seq inputfile> -f <forward barcode file>
-r <reverse barcode file> -m <map file> -o <output dir>"
               sys.exit()
          elif opt in ("-a","--afile"):
               seqafile=arg
          elif opt in ("-b","--bfile"):
               seqbfile=arg
          elif opt in ("-m","--mfile"):
               mfile=arg
          elif opt in ("-f","--ffile"):
               primffile=arg
          elif opt in ("-r","--rfile"):
               primrfile=arg
          elif opt in ("-o","--odir"):
               odir=arg
          elif opt in ("-v","--verbose"):
               verbose=True
          elif opt in ("-n","--nlimit"):
               nlimit=int(arg)
```

```
if os.path.isfile(seqafile)==False:
     print "Cannot find forward seq input file",seqafile
     sys.exit()
if os.path.isfile(seqbfile)==False:
     print "Cannot find reverse seq input file",seqbfile
     sys.exit()
if os.path.isfile(primffile)==False:
     print "Cannot find forward barcode file",primffile
     sys.exit()
if os.path.isfile(primrfile)==False:
     print "Cannot find reverse barcode file",primrfile
     sys.exit()
if os.path.isfile(mfile)==False:
     print "Cannot find map file",mfile
     sys.exit()
```

Read the map file in using csv reader.

```
print "Reading map file:",mfile
with open(mfile,"r") as csvfile:
     #set up some empty lists
     s,a,b,f,r=[],[],[],[],[]

mreader=csv.DictReader(csvfile,dialect=csv.excel_tab)
     for row in mreader:
          s.append(row['Sample'])
          a.append(row['PrimerF'])
          f.append(row['BarcodeF'])
          b.append(row['PrimerR'])
          r.append(row['BarcodeR'])
```

Now write a log file - open it now in case there's a problem.

```
lfile=open(odir+"log.txt","w")

print "opening lots of output files"
print "Output directory is",odir
```

To open multiple output files and store their handles - for the forward and reverse sequences:

```
     ahandles=[open(odir+"%s_Pair_Forward.fastq" %
sfile,"w",10000) for sfile in s]
     bhandles=[open(odir+"%s_Pair_Reverse.fastq" %sfile
,"w",10000) for sfile in s]
     afhandles=[open(odir+"%s_Unpaired_Forward.fastq" %
sfile,"w",10000) for sfile in s]
     brhandles=[open(odir+"%s_Unpaired_Reverse.fastq" %sfile
,"w",10000) for sfile in s]

     nomatchA=open(odir+"nomatchA.fastq","w",10000)
     nomatchB=open(odir+"nomatchB.fastq","w",10000)
     nomatchF=open(odir+"nomatchF.fastq","w",10000)
```

```
nomatchR=open(odir+"nomatchR.fastq","w",10000)

#create an empty list to hold the counts
c=[0]*len(s)
cf=[0]*len(s)
cr=[0]*len(s)

myreadcount=0
myalloccount=0
print "Reading the sequences"
```

Open the forward sequence file with open(seqafile,"r",1000000) as afile (all other files must have the same number of entries - if it doesn't then this is going to fail):

```
bfile=open(seqbfile,"r",1000000)
ffile=open(primffile,"r",1000000)
rfile=open(primrfile,"r",1000000)
```

Read in the input file 4 lines at a time:

```
while True:

     if (nlimit<>0) & (myreadcount>=nlimit):
          break
     aline1=afile.readline()
     #break is it's an empty line as that's EOF
     if aline1.strip()=="":
          break
     aline2=afile.readline()
     aline3=afile.readline()
     aline4=afile.readline()

     bline1=bfile.readline()
     bline2=bfile.readline()
     bline3=bfile.readline()
     bline4=bfile.readline()

     fline1=ffile.readline()
     fline2=ffile.readline()
     fline3=ffile.readline()
     fline4=ffile.readline()

     rline1=rfile.readline()
     rline2=rfile.readline()
     rline3=rfile.readline()
     rline4=rfile.readline()
```

Line 1 contains a header
Line 2 contains the sequence
Line 3 is a +
Line 4 is the quality

The barcodes won't have IUPAC codes so just match. The primer must be in the first part of the sequence so only sample that:

```
                myreadcount=myreadcount+1
                matched=False
```

Search on the barcodes:

```
                if verbose:
                     print "Readcount",myreadcount
                for index,item in enumerate(f):
```

Do a simple match for the input file - compare line 2 with the primer. Strip out the end of line:

```
                          if (fline2[:-1]==f[index]):
                               matchF=True
                          else:
                               matchF=False

                          if(rline2[:-1]==r[index]):
                               matchR=True
                          else:
                               matchR=False

                          if (matchF==True)&(matchR==True):
```

Get the match with a mismatch allowed:

```
     mismatcha=egglib.tools.motif_iter(aline2[0:len(a[index])
],a[index],mismatches=allow_mismatch)
```

Use the enumerate object to get the length of the list of matches:

```
     lmismatcha=list(enumerate(mismatcha))

                          if len(lmismatcha)>0:
                               matchA=True
                          else:
                               matchA=False


     matchb=SeqUtils.nt_search(bline2[0:len(b[index])],b[inde
x])

     mismatchb=egglib.tools.motif_iter(bline2[0:len(b[index])
],b[index],mismatches=allow_mismatch)
```

Use the enumerate object to get the length of the list of matches:

```
     lmismatchb=list(enumerate(mismatchb))
                          if len(lmismatchb)>0:
                               matchB=True
                          else:
```

```
                                    matchB=False

                               if          (matchA==True)          &
(matchB==False):
```

Only the forward matches:

```
      tmp=afhandles[index].write(aline1)

      tmp=afhandles[index].write(aline2)

      tmp=afhandles[index].write(aline3)

      tmp=afhandles[index].write(aline4)
                                    cf[index]=cf[index]+1
                                    myalloccount=myalloccount+1
                                    matched="match A only"
                                    if verbose:
                                          print s[index]
                                          print matched
                                          print aline2.strip()
                                          print lmismatcha,matchA
                                          print bline2.strip()
                                          print lmismatchb,matchB
                                          print fline2.strip()
                                          print f[index],matchF
                                          print rline2.strip()
                                          print r[index],matchR


                               elif        (matchA==False)        &
(matchB==True):
```

Only the reverse matches:

```
      tmp=brhandles[index].write(aline1)

      tmp=brhandles[index].write(aline2)

      tmp=brhandles[index].write(aline3)

      tmp=brhandles[index].write(aline4)
                                    cr[index]=cr[index]+1
                                    myalloccount=myalloccount+1

                                    matched="match B only"
                                    if verbose:
                                          print s[index]
                                          print matched
                                          print aline2.strip()
                                          print lmismatcha,matchA
                                          print bline2.strip()
                                          print lismatchb,matchB
                                          print fline2.strip()
                                          print f[index],matchF
```

```
                                        print rline2.strip()
                                        print r[index],matchR

                                elif (matchA==True) &
(matchB==True):
```

Print out the forward reads:

```
      tmp=ahandles[index].write(aline1)

      tmp=ahandles[index].write(aline2)

      tmp=ahandles[index].write(aline3)

      tmp=ahandles[index].write(aline4)
```

Print out the reverse reads:

```
      tmp=bhandles[index].write(bline1)

      tmp=bhandles[index].write(bline2)

      tmp=bhandles[index].write(bline3)

      tmp=bhandles[index].write(bline4)
                                #update the count
                                c[index]=c[index]+1
                                myalloccount=myalloccount+1
                                matched="match A and B"
                                if verbose:
                                      print s[index]
                                      print matched
                                      print aline2.strip()
                                      print lmismatcha,matchA
                                      print bline2.strip()
                                      print lmismatchb,matchB
                                      print fline2.strip()
                                      print f[index],matchF
                                      print rline2.strip()
                                      print r[index],matchR

                  if (matched==False):
                        nomatchA.write(aline1)
                        nomatchA.write(aline2)
                        nomatchA.write(aline3)
                        nomatchA.write(aline4)
                        nomatchB.write(bline1)
                        nomatchB.write(bline2)
                        nomatchB.write(bline3)
                        nomatchB.write(bline4)
                        nomatchF.write(fline1)
                        nomatchF.write(fline2)
                        nomatchF.write(fline3)
                        nomatchF.write(fline4)
                        nomatchR.write(rline1)
```

```
                    nomatchR.write(rline2)
                    nomatchR.write(rline3)
                    nomatchR.write(rline4)
                    if verbose:
                         print "No match in list"
                         print aline2.strip()
                         print bline2.strip()
                         print fline2.strip()
                         print rline2.strip()

          matched=False
     print "Closing things down"
     print "Read in ",myreadcount,"sequences"
     print "Allocated",myalloccount,"sequences"
```

Close all of the files:

```
     afile.close()
     bfile.close()
     ffile.close()
     rfile.close()
     nomatchA.close()
     nomatchB.close()
     nomatchF.close()
     nomatchR.close()

     temp=[f.close() for f in ahandles]
     temp=[f.close() for f in bhandles]
     temp=[f.close() for f in afhandles]
     temp=[f.close() for f in brhandles]

     print "Writing log file:",odir+"log.txt"

     lfile.write("Sample,Forward,Reverse,Paired"+"\n")
     for index,item in enumerate(s):

     lfile.write(s[index]+","+str(cf[index])+","+str(cr[index
])+","+str(c[index])+"\n")
     lfile.write("Read in "+str(myreadcount)+"
sequences"+"\n")
     lfile.write("Allocated "+str(myalloccount)+"
sequences"+"\n")
     lfile.close()

if __name__ == "__main__":
     main(sys.argv[1:])
```

C.2 Concatenating files

If the reverse (or potentially forward) reads are of poor quality, it may be necessary to discard them and only use the forward reads. If that is the case pair.sh will combine the forward

paired and forward unpaired to maximise the amount of reads per sample. Change to reverse if the reverse reads are required. To run, copy pair.sh into your working directory:

```
./pair.sh
```

Pair.sh contains:

```
#!/bin/bash

for i in $(ls *Pair_Forward*); do
      #that's the Pair_Forward file
      #create a new file based on this file name
      NEWNAME=$(echo "$i" |sed 's/Pair_Forward/All_Forward/')
      echo $NEWNAME
      OTHERNAME=$(echo "$i" |sed
's/Pair_Forward/Unpaired_Forward/')
      cp $i $NEWNAME
      cat $OTHERNAME >> $NEWNAME
      done
```

C.3 Processing the data in QIIME

C.3.1 Usearch quality checks

This pipeline makes use of usearch and QIIME.

Data as supplied by TGAC:

FASTQ data, demultiplexed into sub-folders. There are 5 files per folder:

```
ForwardPrimerX.fastq
ForwardPrimerX_paired.fastq
ReversePrimerX.fastq
ReversePrimerX_paired.fastq
PrimerX_unpaired.fastq
```

Data produced by pair.sh:

```
AlexMcF_Bacteria_G1_WF_All_Forward.fastq
AlexMcF_Bacteria_G1_WF_Pair_Forward.fastq
AlexMcF_Bacteria_G1_WF_Pair_Reverse.fastq
AlexMcF_Bacteria_G1_WF_Unpaired_Forward.fastq
AlexMcF_Bacteria_G1_WF_Unpaired_Reverse.fastq
```

Inspection of these files shows that Forward_PrimerX_paired is a subset of Forward_PrimerX (and the same is true for the ReversePrimer sequences). PrimerX_unpaired don't match and is a mixture of forward and reverse primer sequences. The reverse sequences need to be reverse complemented.

C.3.2 Quality checks

Visually check data with FastQC, in particular the Q values (Q30 means 1 in 1000 errors, Q20 means 1 in 100 errors). Typically values of Q20 and above are acceptable. Use this information to decide whether to just use the forward primers or whether to try and match up the forward and reverse.

For forwards reads only use the file:

```
AlexMcF_Bacteria_G1_WF_All_Forward.fastq
```

And, for paired reads use the ForwardPrimerX_paired and:

```
ReversePrimerX_paired
```

For paired files rename them:

```
sample_R1_001.fastq
sample_R2_001.fastq
```

For forward reads rename them:

```
sample.fastq
```

For forward reads, check the quality of each data file with:

```
usearch81 -fastq_eestats2 sample.fastq -output sample.txt
```

Display the information using:

```
cat sample.txt
```

This will produce an output like:

```
68465 reads, max len 251, avg 251.0

Length         MaxEE 0.50         MaxEE 1.00         MaxEE
2.00
------   ----------------   ----------------   ---------------
-
    50      68005( 99.3%)      68463(100.0%)
68464(100.0%)
   100      61853( 90.3%)      67284( 98.3%)      68313(
99.8%)
   150      56219( 82.1%)      62177( 90.8%)      66965(
97.8%)
   200      47450( 69.3%)      55120( 80.5%)      61908(
90.4%)
   250      36124( 52.8%)      44261( 64.6%)      50916(
74.4%)
```

The norm is to use a maxEE value of 1 (an error of 1 in 1000) and in this instance it can be seen that 64.6% of the full length sequences pass. Repeat this for every sample to be analysed.

For paired reads, merge the forward and reverse reads, and then quality check. The merging command is:

```
usearch81 -fastq_mergepairs sample_R1_*.fastq -fastqout
samplepair.fastq

usearch81 -fastq_eestats samplepair.fastq -output
samplestats.txt

cat samplestats.txt
```

Convert the .fastq files into .fasta files. Use a sensible default for this e.g. Set the minimum length to be 350 for paired and 200 for unpaired (this will depend on your primers)

Either:

```
usearch81 -fastq_filter samplepair.fastq -fastaout
samplepair.fasta -fastq_maxee 1.0 -fastq_minlen 350
```

Or:

```
usearch81 -fastq_filter samplepair.fastq -fastaout
samplepair.fasta -fastq_maxee 1.0 -fastq_minlen 200
```

The information outputted will look like:

```
37388  FASTQ recs (37.4k)
     10053  Low qual recs discarded (expected errs > 1.00)
     27319  Converted (27.3k, 73.1%)
```

Do this with all of the samples for analysis, then move all the fasta files to a subdirectory called fasta.

Create a mapping file.

An example of the mapping file looks like this, and is <tab> separated and includes two tabs between sample1 and the LinkerPrimer, because there are no barcodes. Call this map.txt.

```
#SampleID    BarcodeSequence    LinkerPrimerSequence
InputFilename    Description
sample1        AACCGGATTAGATACCCTG    sample1pair.fasta
descriptionX
sample2        AACCGGATTAGATACCCTG    sample2pair.fasta
descriptionX
```

```
sample3        AACCGGATTAGATACCCTG    sample3pair.fasta
descriptionX
sample4        AACCGGATTAGATACCCTG    sample4pair.fasta
descriptionY
sample5        AACCGGATTAGATACCCTG    sample5pair.fasta
descriptionY
sample6        AACCGGATTAGATACCCTG    sample6pair.fasta
descriptionY
sample7        AACCGGATTAGATACCCTG    sample7pair.fasta
descriptionZ
sample8        AACCGGATTAGATACCCTG    sample8pair.fasta
descriptionZ
sample9        AACCGGATTAGATACCCTG    sample9pair.fasta
descriptionZ
```

Convert the data into QIIME format, using:

```
add_qiime_labels.py -m map.txt -i fasta/ -c InputFilename -o
fout/
```

New sequences are in:

```
fout/combined_seqs.fna
```

C.3.3 Removing the primers

Remove the primers before processing the data. The set number will depend on how long the primers used are. For 799F and 1193R use 19. For ITS 3 and ITS4 use 22. Other primers will vary.

To removing primers from paired reads:

```
usearch81 -fastx_truncate fout/combined_seqs.fna -stripleft 19
-striptright 19 -fastaout fout/combined_np.fna
```

To remove primers from just the forward reads:

```
usearch81 -fastx_truncate fout/combined_seqs.fna -stripleft 19
-fastaout fout/combined_np.fna
```

C.3.4 Processing prokaryotic data

Remove chimeras (prokaryotes)

Remove chimeras by comparing with rdp_gold.fa by:

```
identify_chimeric_seqs.py -i fout/combined_np.fna -m usearch61
-o chimeras/ -r rdp_gold.fa
```

This will produce an identify_chimeric_seqs.log in the chimeras/ folder, which will contain data like:

```
ref_non_chimeras    534112
```

```
ref_chimeras    30481
denovo_chimeras    30314
denovo_non_chimeras    534279
```

About 10% chimeras are to be expected, and are listed in chimeras.txt.

Remove these from combined_np.fna. First check the amount of sequences in the file using:

```
count_seqs.py -i fout/combined_np.fna
```

Output will look like:

```
564593  : fout/combined_seqs.fna (Sequence lengths (mean +/-
std): 415.9552 +/- 0.5601)
564593  : Total
```

Then remove the chimeras using:

```
filter_fasta.py -f fout/combined_np.fna -o
fout/combined_seqs_nc.fna -s chimeras/chimeras.txt -n
```

Check the amount of sequences remaining using:

```
count_seqs.py -i fout/combined_seqs_nc.fna
```

Output will look like:

```
534339  : fout/combined_seqs_nc.fna (Sequence lengths (mean
+/- std): 415.9676 +/- 0.5170)
534339  : Total
```

C.3.5 Pick prokaryotic OTUs (Greengenes)

Create a parameter file, include:

```
pick_otus:similarity 0.97
pick_otus:refseqs /usr/local/lib/python2.7/dist-
packages/qiime_default_reference/gg_13_8_otus/rep_set/97_otus.
fasta
alpha_diversity:metrics observed_species,chao1,simpson
```

And save as param.txt in the working directory. Then to assign OTUs using the Greengenes database at 97% similarity:

```
pick_open_reference_otus.py -i $PWD/fout/combined_seqs_nc.fna
-o $PWD/usearch_otu_gg/ -m usearch61 -p param.txt
```

Get a summary of the table:

```
biom summarize-table -i
usearch_otu_gg/otu_table_mc2_w_tax_no_pynast_failures.biom
```

Output looks like:

```
Num samples: 9
Num observations: 111
Total count: 534245
Table density (fraction of non-zero values): 0.477

Counts/sample summary:
 Min: 9879.0
 Max: 160069.0
 Median: 44134.000
 Mean: 59360.556
 Std. dev.: 54456.984
 Sample Metadata Categories: None provided
 Observation Metadata Categories: taxonomy

Counts/sample detail:
 sample1: 9879.0
 sample2: 10694.0
 sample3: 25356.0
 sample4: 27227.0
 sample5: 44134.0
 sample6: 49023.0
 sample7: 52793.0
 sample8: 155070.0
 sample9: 160069.0
```

Summarising by taxa by rarefying the data to equal counts, before looking at the taxa. Note the minimum number of reads, in this case 9879 and rarefy to that depth, using:

```
single_rarefaction.py -i
usearch_otu_gg/otu_table_mc2_w_tax_no_pynast_failures.biom -o
otutab_rare.biom -d 9879
```

And check the summary to ensure it has worked using:

```
biom summarize-table -i otutab_rare.biom
```

Output looks like:

```
Num samples: 9
Num observations: 74
Total count: 88911
Table density (fraction of non-zero values): 0.455

Counts/sample summary:
 Min: 9879.0
 Max: 9879.0
 Median: 9879.000
 Mean: 9879.000
 Std. dev.: 0.000
 Sample Metadata Categories: None provided
 Observation Metadata Categories: taxonomy

Counts/sample detail:
 sample1: 9879.0
```

```
sample2: 9879.0
sample3: 9879.0
sample4: 9879.0
sample5: 9879.0
sample6: 9879.0
sample7: 9879.0
sample8: 9879.0
sample9: 9879.0
```

To display the taxonomy:

```
summarize_taxa_through_plots.py -i otutab_rare.biom -o tax/ -f
```

C.3.6 Pick prokaryotic OTUs (Silva)

Create a parameter file, include:

```
pick_otus:similarity 0.97
pick_otus:refseqs
~/Desktop/Shared_Folder/Silva119_release/rep_set/97/Silva_119_
rep_set97.fna
alpha_diversity:metrics observed_species,chao1,simpson
```

And save as param_silva.txt in the working directory. Then to assign OTUs using the Silva database at 97% similarity:

```
pick_open_reference_otus.py -i $PWD/fout/combined_seqs_nc.fna
-o $PWD/usearch_otu_silva/ -m usearch61 -p param_silva.txt
```

Get a summary of the table (note minimum depth):

```
biom summarize-table -i
usearch_otu_silva/otu_table_mc2_w_tax_no_pynast_failures.biom
```

Summarising by taxa by rarefying the data to equal counts as before:

```
single_rarefaction.py -i
usearch_otu_silva/otu_table_mc2_w_tax_no_pynast_failures.biom
-o otutab_rare_silva.biom -d 9879
```

And check the summary to ensure it has worked using:

```
biom summarize-table -i otutab_rare_silva.biom
```

To display the taxonomy:

```
summarize_taxa_through_plots.py -i otutab_rare_silva.biom -o
tax_silva/ -f
```

C.3.7 Pick prokaryotic OTUs above 99% (Greengenes)

Create a parameter file, include:

```
pick_otus:similarity 0.99
```

```
pick_otus:refseqs /usr/local/lib/python2.7/dist-
packages/qiime_default_reference/gg_13_8_otus/rep_set/99_otus.
fasta
alpha_diversity:metrics observed_species,chao1,simpson
```

And save as param_gg99.txt in the working directory. Then to assign OTUs using the Greengenes database at 99% similarity:

```
pick_open_reference_otus.py -i $PWD/fout/combined_seqs_nc.fna
-o $PWD/usearch_otu_gg99/ -m usearch61 -p param_gg99.txt
```

Get a summary of the table (note minimum depth):

```
biom summarize-table -i
usearch_otu_gg99/otu_table_mc2_w_tax_no_pynast_failures.biom
```

Summarising by taxa by rarefying the data to equal counts as before:

```
single_rarefaction.py -i
usearch_otu_gg99/otu_table_mc2_w_tax_no_pynast_failures.biom -
o otutab_rare_gg99.biom -d 9879
```

And check the summary to ensure it has worked using:

```
biom summarize-table -i otutab_rare_gg99.biom
```

To display the taxonomy:

```
summarize_taxa_through_plots.py -i otutab_rare_gg99.biom -o
tax_gg99/ -f
```

C.3.8 Remove chimeras (eukaryotes)

Remove chimeras by comparing with its_12_11_otus by:

```
identify_chimeric_seqs.py -i fout/combined_np.fna -m usearch61
-o chimeras/ -r
~/Desktop/Shared_Folder/its_12_11_otus/rep_set/97_otus.fasta
```

This will produce an identify_chimeric_seqs.log in the chimeras/ folder. Remove these from combined_np.fna. First check the amount of sequences in the file using:

```
count_seqs.py -i fout/combined_np.fna
```

Then remove the chimeras using:

```
filter_fasta.py -f fout/combined_np.fna -o
fout/combined_seqs_nc.fna -s chimeras/chimeras.txt -n
```

Check the amount of sequences remaining using:

```
count_seqs.py -i fout/combined_seqs_nc.fna
```

C.3.9 Pick eukaryotic OTUs (Unite)

Create a parameter file, include:

```
pick_otus:enable_rev_strand_match True
assign_taxonomy:assignment_method blast
assign_taxonomy:id_to_taxonomy_fp
/home/qiime/Desktop/Shared_Folder/its_12_11_otus/taxonomy/97_o
tu_taxonomy.txt
assign_taxonomy:reference_seqs_fp
/home/qiime/Desktop/Shared_Folder/its_12_11_otus/rep_set/97_ot
us.fasta
alpha_diversity:metrics observed_species,chao1,simpson
```

And save as param_its.txt in the working directory. Then to assign OTUs using the Unite database at 97% similarity:

```
pick_open_reference_otus.py -i $PWD/fout/combined_seqs_nc.fna
-o $PWD/usearch_its/ -m usearch61 -r
/home/qiime/Desktop/Shared_Folder/its_12_11_otus/rep_set/97_ot
us.fasta -p param_its.txt --suppress_align_and_tree -f
```

Get a summary of the table:

```
biom summarize-table -i usearch_its/otu_table_mc2_w_tax.biom
```

To display the taxonomy:

```
summarize_taxa_through_plots.py -i otu_table_mc2_w_tax.biom -o
tax/
```

C.3.10 Alpha diversity (prokaryotes)

To do alpha diversity measurements on the prokaryotic data, used the below command. Choose an appropriate sample depth, and ensure any measurements wanted are included in the parameter file (see above).

```
alpha_rarefaction.py -i
usearch_otu_gg/otu_table_mc2_w_tax_no_pynast_failures.biom -m
map.txt --min_rare_depth 1000 --max_rare_depth 5000 -o alpha/
-t usearch_otu_gg/rep_set.tre -p param.txt -f
```

Use the alpha diversity measurement to produce plots of interest, for example Simpson diversity and Chao1 index. Select the metadata category of interest.

```
compare_alpha_diversity.py -i
alpha/alpha_div_collated/simpson.txt -m map.txt -c <metadata
category> -o alpha_simpson/
```

```
compare_alpha_diversity.py -i
alpha/alpha_div_collated/chao1.txt -m map.txt -c <metadata
category> -o alpha_chao1/
```

C.3.11 Beta diversity (prokaryotes)

To do beta diversity measurements on the data, used the below command. Choose an appropriate sample depth.

```
jackknifed_beta_diversity.py -i otutab_rare.biom -o beta_gg97/
-m map.txt -t usearch_otu_gg/rep_set.tre -e 1000
```

C.3.12 Alpha and Beta diversity (eukaryotes)

To do alpha and beta diversity measurements on the eukaryotic data, used the below command. This differs from the prokaryotic measurements, because it is not phylogenetically relevant. Choose an appropriate sample depth, and ensure any measurements wanted are included in the parameter file (see above).

```
core_diversity_analyses.py -i
usearch_its/otu_table_mc2_w_tax.biom -o alpha/ -m map.txt -e
1000 --nonphylogenetic_diversity -p param_its.txt
```

Use the alpha diversity measurement to produce plots of interest (beta diversity is already generate with Bray Curtis distance), for example Simpson diversity and Chao1 index. Select the metadata category of interest.

```
compare_alpha_diversity.py -i
alpha_simpson/arare_max1000/alpha_div_collated/simpson.txt -m
map.txt -c <metadata category> -o alpha_simpson/

compare_alpha_diversity.py -i
alpha_simpson/arare_max1000/alpha_div_collated/chao1.txt -m
map.txt -c <metadata category> -o alpha_chao1/
```

Appendix D

Breakdown of sample read data for Chapters 2, 3 and 4

Appendix D – Breakdown of sample read data for Chapters 2, 3 and 4

Table D.33 – The number of reads obtained per sample before (A) and after (B) filtering through USEARCH8.1 and removing chimeras from the prokaryotic samples, as well as the percentage number of unfiltered reads with a MaxEE 1.0 (one error per one thousand base pairs) at 250 bp for the forward and reverse sequences for the prokaryotes in Chapter 2.

	Prokaryotes			
	Reads per sample		**MaxEE 1.0 (%) (250 bp)**	
Sample	**A**	**B**	**Forward primer**	**Reverse primer**
1	118,714	79,487	73.7	62.0
2	75,160	43,488	76.8	63.2
3	88,476	72,635	85.8	74.6
4	127,961	49,750	77.6	37.4
5	97,151	54,366	80.7	53.3
6	129,972	54,496	79.7	37.9
7	43,805	30,168	77.2	64.3
8	38,133	31,540	85.6	75.0
9	85,724	70,375	85.0	74.5
10	144,006	116,620	84.6	73.5
11	83,781	69,683	85.3	75.9
12	78,588	65,821	86.2	76.4
13	143,562	77,075	82.3	52.3
14	103,402	75,477	83.8	62.0
15	110,878	72,138	79.1	66.8
16	56,309	38,484	74.3	60.8
17	107,939	69,059	79.5	56.0
18	165,883	118,868	74.0	62.8
19	43,419	25,827	79.9	48.6
20	73,440	56,809	84.5	69.1
21	98,247	80,892	85.3	75.3
22	102,198	79,221	84.1	69.9
23	120,144	77,881	75.6	57.1
24	92,388	71,385	84.7	71.8
25	55,694	47,144	87.7	76.5
26	60,191	51,267	88.3	76.6
27	44,940	34,259	80.5	59.6
28	171,325	144,837	87.9	76.3
29	62,712	51,492	86.5	73.5
30	56,226	47,030	87.8	74.5
31	71,646	60,596	87.9	76.3
32	46,119	35,401	87.5	68.6
33	45,812	37,588	86.7	73.4
34	39,274	32,769	87.2	75.0
35	80,783	68,359	88.0	76.3
36	76,508	62,832	88.1	73.4

	Prokaryotes			
	Reads per sample		MaxEE 1.0 (%) (250 bp)	
Sample	A	B	Forward primer	Reverse primer
37	148,065	118,572	85.8	69.3
38	71,795	57,995	86.1	69.6
39	978	283	47.4	19.4
40	209,098	166,575	85.6	68.7
41	91,509	73,726	85.5	69.2
42	146,636	117,066	86.2	67.9
43	79,881	36,722	77.7	33.5
44	69,542	26,507	76.3	27.2
45	215,772	153,127	76.8	51.8
46	252,570	131,697	75.8	42.1
47	95,976	51,472	73.1	41.8
48	66,335	37,573	75.8	45.7
49	148,485	83,450	75.8	32.3
50	61,034	34,006	77.2	44.2
51	131,911	68,547	79.5	38.4
52	164,762	40,432	77.0	17.5
53	72,577	39,920	79.3	42.4
54	105,037	52,207	77.2	33.4
55	71,378	21,671	78.7	22.8
56	126,854	56,793	78.5	31.6
57	149,184	71,507	77.8	34.8
58	159,355	107,978	76.4	42.9
59	60,790	50,260	85.7	75.5
60	82,007	68,921	86.7	76.9
61	91,946	76,455	85.5	75.8
62	63,700	53,069	85.8	75.3
63	101,861	78,346	82.8	60.7
64	943,065	768,813	85.1	73.5
65	83,109	69,512	85.9	76.2
66	155,023	127,960	85.8	73.4
67	168,121	140,942	85.8	76.2
68	66,555	51,281	82.8	62.8
69	119,770	98,594	85.0	74.3
70	237,390	196,870	85.7	75.1
71	68,549	57,082	85.8	75.1
72	81,699	68,577	86.8	76.0
73	48,712	40,972	86.4	76.7
74	121,433	102,539	86.7	76.7
75	65,173	54,994	87.4	76.2
76	1,185	743	78.1	46.2
77	85,213	72,358	87.1	77.5
78	94,048	78,703	86.6	75.0
Total	8,518,593	6,059,936		

	Prokaryotes			
	Reads per sample		MaxEE 1.0 (%) (250 bp)	
Sample	**A**	**B**	**Forward primer**	**Reverse primer**
Average	109,213	77,691	82.1	61.6
Max	943,065	768,813	88.3	77.5
Min	978	283	47.4	17.5

Table D.34 – The number of reads obtained per sample before (A) and after (B) filtering through USEARCH8.1 and removing chimeras from the eukaryotic samples, as well as the percentage number of unfiltered reads with a MaxEE 1.0 (one error per one thousand base pairs) at 250 bp for the forward and reverse sequences for the eukaryotes in Chapter 2.

	Eukaryotes			
	Reads per sample		MaxEE 1.0 (%) (250 bp)	
Sample	A	B	Forward primer	Reverse primer
1	62,652	62,272	84.2	56.6
2	22,870	22,273	78.2	52.4
3				
4	58,826	38,099	51.4	53.0
5	54,371	47,566	65.7	18.3
6				
7				
8				
9	44	46	31.8	9.1
10	23,162	21,245	8.5	42.7
11				
12	26,286	23,673	6.9	48.1
13	32,055	24,179	30.3	47.3
14	42,176	40,099	54.5	17.2
15	61,762	52,837	66.0	57.8
16	47,112	45,673	81.3	58.7
17	31,237	31,515	87.0	50.4
18	21,600	21,711	86.3	57.0
19	36,966	31,607	67.8	37.4
20	37,946	35,175	4.4	45.7
21	29,466	30,354	87.1	38.9
22	22,743	20,421	2.8	37.0
23				
24	59,490	57,677	62.3	47.1
25	20	38	25.0	0.0
26	24,952	22,808	3.7	39.2
27				
28				
29	21,634	11,616	3.5	35.6
30	93	123	19.4	5.4
31	49,911	45,408	3.7	48.9
32				
33	43,774	39,674	3.7	48.0
34	80,578	80,180	87.5	71.8
35	9,387	8,631	4.5	48.8
36	54,645	49,975	4.3	44.2
37				

	Eukaryotes			
	Reads per sample		MaxEE 1.0 (%) (250 bp)	
Sample	A	B	Forward primer	Reverse primer
38				
39	45,782	42,281	3.3	46.7
40				
41	35	44	8.6	5.7
42	28,465	28,403	83.5	47.0
43	32,289	29,471	2.7	46.1
44	64,910	58,179	5.0	45.1
45				
46	21,299	11,783	1.9	43.4
47				
48	22,445	21,705	79.1	57.3
49	98	70	16.3	0.0
50	28,583	27,948	86.7	54.6
51				
52				
53	62,836	62,230	79.8	58.6
54				
55				
56				
57				
58	23,487	22,077	32.5	51.4
59	131	141	16.8	3.1
60				
61				
62				
63				
64				
65				
66				
67				
68	40,391	39,648	56.3	50.7
69				
70				
71				
72				
73				
74				
75	31,931	28,906	3.5	48.6
76				
77				
78				
Total	1,358,440	1,237,761		
Average	33,133	30,189	38.7	40.9

	Eukaryotes			
	Reads per sample		MaxEE 1.0 (%) (250 bp)	
Sample	A	B	Forward primer	Reverse primer
Max	80,578	80,180	87.5	71.8
Min	20	38	1.9	0.0

Table D.35 – The number of reads obtained per sample before (A) and after (B) filtering through USEARCH8.1 and removing chimeras from the prokaryotic samples, as well as the percentage number of unfiltered reads with a MaxEE 1.0 (one error per one thousand base pairs) at 150 bp and 250 bp for the forward sequences for the prokaryotes in Chapter 3.

	Prokaryotes (Forward primer)			
	Reads per sample		**MaxEE 1.0 (%)**	
Sample	**A**	**B**	**150 bp**	**250 bp**
Inoculum	115,557	65,182	85.1	61.2
	211,482	124,199	85.4	62.6
	545,191	309,978	85.7	60.9
G	24,047	14,513	88.6	64.0
	92,387	57,980	90.9	67.0
	53,805	30,989	87.0	62.0
GG	27,545	17,679	91.3	67.8
	58,435	35,107	89.6	64.4
	141,686	84,464	87.2	63.3
GH	78,791	46,216	87.9	62.7
	21,402	13,307	90.8	67.3
	27,887	17,359	88.9	66.5
GM	262,959	161,697	88.5	65.6
	56,217	34,303	89.3	65.4
	66,470	42,331	91.5	68.4
H	335,313	192,526	87.8	61.6
	320,779	163,827	86.2	56.0
	68,042	42,210	90.2	66.5
HG	472,675	273,083	86.1	62.4
	112,887	67,687	89.3	64.7
	251,587	152,338	88.7	65.1
HH	75,170	46,482	90.8	66.2
	73,031	44,830	87.6	65.4
	133,684	78,686	87.6	62.7
HM	13,769	8,030	87.8	62.1
	151	68	79.5	48.3
	311,152	189,451	89.2	64.7
M	19,979	12,181	85.2	64.2
	83,053	50,261	89.5	65.0
	62,147	37,579	90.1	65.5
MG	149,564	45,395	82.4	34.6
	48,853	28,535	87.7	62.8
	10,996	6,598	87.7	64.7
MH	13,700	8,176	85.7	63.8
	142,474	82,451	86.0	61.8
	38,693	23,381	88.8	64.5
MM	172,131	105,924	92.0	66.5

	Prokaryotes (Forward primer)			
	Reads per sample		MaxEE 1.0 (%)	
Sample	**A**	**B**	**150 bp**	**250 bp**
	25,679	14,985	85.9	62.0
	283,696	171,816	90.5	65.2
Total	5,003,066	2,901,804		
Average	128,283	74,405	87.9	63.0
Max	545,191	309,978	92.0	68.4
Min	151	68	79.5	34.6

Table D.36 – The number of reads obtained per sample before (A) and after (B) filtering through USEARCH8.1 and removing chimeras from the eukaryotic samples, as well as the percentage number of unfiltered reads with a MaxEE 1.0 (one error per one thousand base pairs) at 150 bp and 250 bp for the forward sequences for the eukaryotes in Chapter 3.

	Eukaryotes (Forward primer)			
	Reads per sample		MaxEE 1.0 (%)	
Sample	A	B	150 bp	250 bp
Inoculum	4,439	1,365	91.5	33.5
	5,762	701	93.1	14.4
	4,596	391	88.7	12.5
G	5,729	249	90.6	5.0
	138,901	5,234	91.4	4.5
	1,919	164	89.5	9.4
GG	117,141	1,621	90.1	1.8
	18,065	382	92.0	2.3
	52,514	2,164	92.9	4.8
GH	90,201	2,528	92.3	3.1
	167,428	3,470	92.8	2.3
	46,943	1,343	93.0	3.2
GM	84,032	2,314	90.8	3.5
	9,350	468	90.7	5.8
	46,428	1,408	92.2	3.5
H	65,210	2,278	92.5	4.3
	2,061	90	89.9	4.9
	1,469	32	85.2	2.6
HG	205,140	6,332	92.6	3.5
	37,001	1,629	93.2	5.2
	47,468	2,554	91.9	5.9
HH	61,662	1,466	92.9	2.8
	153,770	3,896	93.4	2.8
	43,747	865	92.2	2.2
HM	7,546	267	91.1	4.0
	7,254	82	91.0	1.3
	47,221	1,081	91.9	2.7
M	17,033	337	93.0	2.1
	73,875	1,605	90.3	2.8
	29,810	1,319	91.2	5.1
MG	81,564	3,231	92.8	4.9
	123,865	5,758	91.5	5.1
	52,438	1,468	91.7	3.5
MH	11,510	329	92.3	3.2
	25,700	328	91.3	1.4
	125,596	3,688	91.1	3.5
MM	191,020	3,117	90.9	2.0

	Eukaryotes (Forward primer)			
	Reads per sample		MaxEE 1.0 (%)	
Sample	**A**	**B**	**150 bp**	**250 bp**
	160,595	3,257	91.5	2.4
	38,376	1,014	92.8	3.1
Total	2,404,379	69,825		
Average	61,650	1,790	91.5	4.9
Max	205,140	6,332	93.4	33.5
Min	1,469	32	85.2	1.3

Table D.37 – The number of reads obtained per sample before (A) and after (B) filtering through USEARCH8.1 and removing chimeras for the prokaryotic samples, as well as the percentage number of unfiltered reads with a MaxEE 1.0 (one error per one thousand base pairs) at 250 bp for the forward sequences from the prokaryotes in Chapter 4.

	Prokaryotes		
	Reads per sample		MaxEE 1.0 (%) (250 bp)
Sample	A	B	Forward primer
G1WF	87,919	55,843	73.4
G2WF	71,349	44,305	75.8
G3WF	70,561	46,750	75.4
G4WF	60,378	39,153	73.0
G5WF	69,239	43,563	73.0
GE1FF	8,020	4,748	62.5
GE1FS	10,906	1,045	10.0
GE1WF	91,203	59,120	75.3
GE1WS	58,330	39,510	75.2
GE2FF	32,980	13,890	44.1
GE2FS	29,416	6,167	21.7
GE2WF	56,386	37,724	79.0
GE2WS	146,851	106,647	79.0
GE3FF	77,095	50,240	68.6
GE3FS	40,041	16,871	43.8
GE3WF	40,683	26,902	72.7
GE3WS	69,941	47,782	74.1
GE4FF	85,911	55,476	68.6
GE4FS	38,647	16,853	46.8
GE4WF	146,715	73,999	70.6
GE4WS	70,419	48,603	73.3
GN1FF	21,853	9,822	46.8
GN1WF	55,690	33,697	75.5
GN2FF	39,212	25,989	69.9
GN2WF	33,197	23,791	76.3
GN3FF	40,168	11,806	30.8
GN3WF	58,484	39,183	71.9
GN4FF	34,923	17,238	50.8
GN4WF	96,385	63,056	71.4
J1WF	68,137	46,448	75.3
J2WF	48,443	33,308	75.5
J3WF	51,556	35,711	75.4
J4WF	55,855	38,406	75.0
J5WF	71,236	49,784	76.8
MA1FF	34,238	638	2.0
MA1FS	32,783	1,227	4.0
MA1WF	76,152	55,915	78.3

	Prokaryotes		
	Reads per sample		MaxEE 1.0 (%) (250 bp)
Sample	A	B	Forward primer
MA1WS	61,220	46,305	78.6
MA2FF	28,107	4,805	18.0
MA2FS	35,063	1,107	3.4
MA2WF	355	185	56.9
MA2WS	50,846	39,138	79.7
MA3FF	51,022	7,457	15.1
MA3FS	94,458	6,172	6.9
MA3WF	79,728	57,900	77.7
MA3WS	31,638	22,122	73.0
MA4FF	35,777	2,871	8.3
MA4FS	29,177	4,055	15.0
MA4WF	173,580	121,028	76.2
MA4WS	33,636	24,629	76.9
MC1FF	23,048	4,646	21.3
MC1FS	38,653	21,527	57.5
MC1WF	432,957	260,742	65.7
MC1WS	61,628	45,303	77.1
MC2FF	61,692	36,026	62.9
MC2FS	14,408	739	5.4
MC2WF	114,757	81,135	77.1
MC2WS	48,877	35,986	77.9
MC3FF	50,174	24,428	51.9
MC3FS	42,496	3,897	9.6
MC3WF	95,824	66,386	74.6
MC3WS	18,815	8,835	49.4
MC4FF	52,422	16,173	33.9
MC4FS	141,643	11,062	8.3
MC4WF	40,389	12,379	32.4
MC4WS	38,348	15,349	41.9
ME1FF	33,136	17,700	55.8
ME1FS	20,435	4,026	21.5
ME1WF	30,495	20,422	70.5
ME1WS	68,134	51,995	79.8
ME2FF	25,062	1,779	7.3
ME2FS	20,554	917	4.7
ME2WF	92,454	70,578	81.4
ME2WS	91,840	71,830	82.2
ME3FF	34,373	1,288	3.9
ME3FS	49,125	7,723	16.7
ME3WF	73,123	52,541	77.1
ME3WS	94,444	70,449	77.6
ME4FF	36,682	13,106	37.0
ME4FS	25,029	3,214	13.3

	Prokaryotes		
	Reads per sample		MaxEE 1.0 (%) (250 bp)
Sample	**A**	**B**	**Forward primer**
ME4WF	80,883	58,564	77.2
ME4WS	85,077	62,221	77.5
MN1FF	40,123	15,356	40.4
MN1WF	49,246	37,608	79.4
MN2FF	48,837	28,203	62.8
MN2WF	74,525	54,458	75.7
MN3FF	41,655	8,955	22.5
MN3WF	43,473	26,119	62.6
MN4FF	59,610	12,969	23.0
MN4WF	177,339	62,335	36.8
Total	5,557,694	3,057,953	
Average	61,752	33,977	53.5
Max	432,957	260,742	82.2
Min	355	185	2.0

Table D.38 – The number of reads obtained per sample before (A) and after (B) filtering through USEARCH8.1 and removing chimeras from the eukaryotic samples, as well as the percentage number of unfiltered reads with a MaxEE 1.0 (one error per one thousand base pairs) at 250 bp for the forward sequences from the eukaryotes in Chapter 4.

	Eukaryotes		
	Reads per sample		MaxEE 1.0 (%) (250 bp)
Sample	A	B	Forward primer
G1WF	35,383	9,670	38.6
G2WF	36,648	10,692	41.3
G3WF	42,371	11,854	39.4
G4WF	81,099	21,446	37.6
G5WF	41,061	10,174	36.6
GE1FF	43	7	23.3
GE1FS	14,012	8,353	66.3
GE1WF	3,858	2,575	73.5
GE1WS	3,889	2,635	73.8
GE2FF	7,400	5,482	78.9
GE2FS	3,117	1,786	65.3
GE2WF	5,461	3,705	75.2
GE2WS	60	21	48.3
GE3FF	488	147	31.4
GE3FS	18,553	11,818	71.6
GE3WF	9,415	6,337	75.0
GE3WS	6,606	4,509	73.8
GE4FF	17,536	12,575	78.0
GE4FS	3,051	2,176	77.2
GE4WF	10,132	5,281	58.3
GE4WS	4,098	2,109	55.3
GN1FF	3,138	793	28.0
GN1WF	7,908	5,371	75.2
GN2FF	110	61	58.2
GN2WF	6,313	4,409	75.0
GN3FF	986	634	68.6
GN3WF	3,715	2,500	73.9
GN4FF	1,383	841	71.8
GN4WF	26,660	18,306	73.7
J1WF	20,660	3,540	22.4
J2WF	29,458	5,444	24.2
J3WF	20,046	3,181	20.6
J4WF	41,356	8,984	27.7
J5WF	9,507	1,490	21.4
MA1FF	8,777	280	3.6
MA1FS	6,086	981	21.4
MA1WF	3,522	1,490	60.5

	Eukaryotes		
	Reads per sample		MaxEE 1.0 (%) (250 bp)
Sample	A	B	Forward primer
MA1WS	4,099	1,852	64.9
MA2FF	27,391	5,839	29.9
MA2FS	4,580	2,297	61.6
MA2WF	2,608	655	41.0
MA2WS	3,838	1,799	62.9
MA3FF	4,183	1,083	29.5
MA3FS	11,767	6,881	66.7
MA3WF	8,632	1,335	24.3
MA3WS	7,196	2,615	52.3
MA4FF	5,891	1,967	45.4
MA4FS	203	117	62.1
MA4WF	5,418	917	24.7
MA4WS	3,726	670	25.7
MC1FF	17,040	1,288	10.0
MC1FS	2,956	2,256	77.8
MC1WF	2,378	806	54.4
MC1WS	2,917	1,590	61.2
MC2FF	1,868	755	55.0
MC2FS	577	355	70.5
MC2WF	47,517	20,732	57.7
MC2WS	3,369	1,884	62.5
MC3FF	16,793	9,790	70.5
MC3FS	1,573	855	61.5
MC3WF	29,606	9,773	51.7
MC3WS	3,463	1,316	55.9
MC4FF	4,717	2,612	68.9
MC4FS	5,049	2,953	64.6
MC4WF	8,907	485	7.2
MC4WS	6,961	2,975	58.2
ME1FF	4,299	414	13.8
ME1FS	6,264	928	16.7
ME1WF	3,454	1,378	60.2
ME1WS	5,879	2,578	63.5
ME2FF	2,399	900	53.3
ME2FS	111	9	9.0
ME2WF	4,744	2,162	63.9
ME2WS	7,201	3,366	64.5
ME3FF	2,346	764	52.8
ME3FS	6,217	4,083	75.1
ME3WF	17,199	7,711	63.2
ME3WS	9,931	4,286	61.6
ME4FF	2,885	1,271	60.8
ME4FS	4,749	3,207	77.2

	Eukaryotes		
	Reads per sample		MaxEE 1.0 (%) (250 bp)
Sample	**A**	**B**	**Forward primer**
ME4WF	4,528	1,552	47.2
ME4WS	6,670	2,763	55.6
MN1FF	3,291	657	23.7
MN1WF	8,068	3,580	65.4
MN2FF	1,573	1,010	75.3
MN2WF	9,286	4,380	65.0
MN3FF	2,999	1,834	74.7
MN3WF	4,709	2,006	63.9
MN4FF	1,901	1,426	83.8
MN4WF	9,361	3,285	48.4
Total	909,193	335,659	
Average	10,102	3,730	52.9
Max	81,099	21,446	83.8
Min	43	7	3.6

Appendix E

GC-MS analysis

Appendix E – GC-MS analysis

E.1 Analysis of GC-MS data using MassHunter, XCMS and Metaboanalyst

E.1.1 XCMS using R

The following script is used for processing .mzdata files in R (R Development Core Team 2008). Data has been converted from .D files to .mzdata files using the MassHunter Workstation Qualitative Analysis B.06.00 (Agilent Technologies, USA), and the data files moved into subdirectories containing a replicate set of each file. Any script highlighted in red can be adjusted for different data sets. The parameters below were used to analyse the Merox- and Hydro-treated Jet A-1 and GTL kerosene samples used in this thesis.

Install the following packages into R:

```
source("http://bioconductor.org/biocLite.R")
biocLite("xcms")
biocLite("mzR")
biocLite("multtest")
biocLite("CAMERA",dependencies=TRUE)
biocLite("RANN")
```

Then load the following libraries:

```
rm=list(ls()
library("mzR")
library(xcms)
library(RANN)
library("multtest")
library("CAMERA")
```

Set the working directory and read in the files. Each subdirectory should contain a replicate set of files, and load in the data.

```
mzdatapath<-("E:/GCMSmz/Merox")
setwd(mzdatapath)
mzdatafiles<-list.files(mzdatapath,recursive =
TRUE,full.names=TRUE,pattern="*.xml")
mzdatafiles
```

The scan range (scans), peak width (full width at half maximum (fwhm), which is 50% of the peak width in seconds), masses per peak and step sizes (bins) can then be defined. The data is grouped using the nearest peak as the grouping factor and the retCor parameter is used to stop a peak shifting more than 2 seconds.

For Merox- and Hydro-treated Jet A-1:

```
xset<-xcmsSet(mzdatafiles,scanrange =
c(900,9500),fwhm=6,max=200,profmethod="bin",step=.1)
```

For GTL kerosene:

```
xset<-xcmsSet(mzdatafiles,scanrange =
c(950,6500),fwhm=6,max=200,profmethod="bin",step=.1)
```

The 'nearest' algorithm groups the data and the parameter 'rtCheck' is used to control the distance the groups can move.

```
xset<-group(xset,method='nearest',rtCheck=2)
```

A new group is created to correct for retention time, and the smoothness of the line controlled with the span command.

```
xset2 <- retcor(xset,family="s",plottype="m",smooth="loess")
```

The span function can also be increase makes things smoother, if necessary.

```
xset2                                                    <-
retcor(xset,family="s",plottype="m",smooth="loess",span=.6)
```

Groups are now created using the corrected peaks, and any missing values fill in with a small number to prevent errors messages.

```
xset2<-group(xset2,method='nearest',rtCheck=2)
xset2<-fillPeaks(xset2)
```

A table of peaks, corrected for drift and with small values filled in has now been generated and can be exported as a .csv file for further analysis in Metaboanalyst v 3.0 (Xia & Wishart 2011).

```
dat<-groupval(xset2,"medret","into")
dat[1:10,]
phenoData(xset2)
```

```
dat<-rbind(group=as.character(phenoData(xset2)$class),dat)
write.csv(dat,file="peaktable.csv")
```

Check in Excel and upload peak_table.csv into Metaboanalyst.

E.1.2 Quality control checks

Open the peak_table.csv file in Excel and calculate the RSD for each treatment.

Samples are in columns B:E and F:I, calculate these separately and get the minimum.

In J3 enter

=STDEV(B3:E3)/AVERAGE(B3:E3)

K3

=STDEV(F3:I3)/AVERAGE(F3:I3)

L3

=MIN(J3:K3)

Drag these down to fill all the rows, sort all of the data on column L, select a cut-off value and remove all of the samples where this is exceeded. Delete all of the rows which have a minimum RSD of greater than 0.25 and re-save the CSV file.

E.1.3 Metaboanalyst

http://www.metaboanalyst.ca/

Press Start then Statistical Analysis. Under 1) upload your data. Select Peak Intensity Table, Samples in columns (unpaired) and then Choose File. Press Submit. Missing values were dealt with in R so press Skip. Then normalise the data using Interquartile Range. Normalize by median, log transformation, auto scale, and press Submit. Then undertake the desired downstream analysis.

Appendix F

Jet fuel certificates of quality (CofQ)

Appendix F – Jet fuel certificate of quality (C of Q)

Table F.39 – Jet fuel certificates of quality showing the standard specification tests for all jet fuel batched products and supplied by Shell Research Ltd. (analysis was not undertaken during this PhD).

	Method	Units	Merox-treated Jet A-1	Hydro-treated Jet A-1	GTL kerosene
Appearance					
Visual appearance	ASTM D4176		Clear and bright	Clear and bright	Clear and bright
Colour	ASTM D156		30	24	30
Particulates	IP 423	mg/L	0.08	0.10	0.14
Composition					
Total acidity	IP 354	mg KOH/g	0.008	0.006	0.001
Total aromatics	IP 436	% Vol	18.6	22.3	<5.0
Total sulphur	IP 336	mg/kg	325	<100	<100
Total sulphur	ASTM D2622	mg/kg		<5	<5
Mercaptan sulphur	IP 342	% m/m	0.0006	<0.0003	<0.0003
Total nitrogen	ASTM D4629	mg/kg	3.06	0.3	<0.05
Volatility					
Distillation	IP 123				
Initial boiling point		°C	147.8	153.7	156.4
10% recovery		°C	167.8	169.3	160.8
20% recovery		°C	174.9	176.6	162.2
50% recovery		°C	197.4	200.4	166.7
90% recovery		°C	239.2	238.5	182.2
Final boiling point		°C	258.6	257.9	197.1
Residue		% Vol	1.3	1.3	1.3
Loss		% Vol	0.5	0.5	0.1
Flash point	IP 170	°C	41.5	41.0	39.0
Density at 15°C	IP 365	kg/m^3	804.7	821.2	735.7
Fluidity					
Freeze point	ASTM D5972	°C	-54.0	-64.9	-55.1
Viscosity at -20°C	IP 71	mm^2/s	3.911	4.208	2.439
Combustion					
Smoke point	ASTM D1322	mm	21.0	20.0	>50.0

	Method	Units	Merox-treated Jet A-1	Hydro-treated Jet A-1	GTL kerosene
Naphthalene content	ASTM D1840	% Vol	2.01	0.66	0.22
Specific energy	ASTM D3338	MJ/kg	43.210	42.989	44.131
Corrosion					
Copper strip (3 hr)	IP 154		1A	1B	1A
Copper strip (2hr at 100 °C)	IP 154		1A	1B	1A
Thermal stability					
JFTOT	IP 323				
Test temperature	IP 323	°C	260	260	260
Tube rating visual	IP 323		1	1	1
Pressure differential	IP 323	mmHG	<1	<1	<1
Fuel returned	IP 323	ml	460	455	455
Contaminants					
Existent gum	IP 540	mg per 100 ml	<1	1	<1
MSEP	ASTM D3948		87	90	99
Conductivity					
Electrical conductivity	IP 274	pS/m	248	433	3
Conductivity temperature	IP 274	°C	20	23	22
Lubricity					
Wear scar diameter (1)		mm	0.647	0.750	1.021
Wear scar diameter (2)		mm	0.634	0.750	1.005
Wear scar diameter (3)		mm	0.640	0.750	1.013

Appendix G

Chapter four species richness

Appendix G – Chapter four species richness

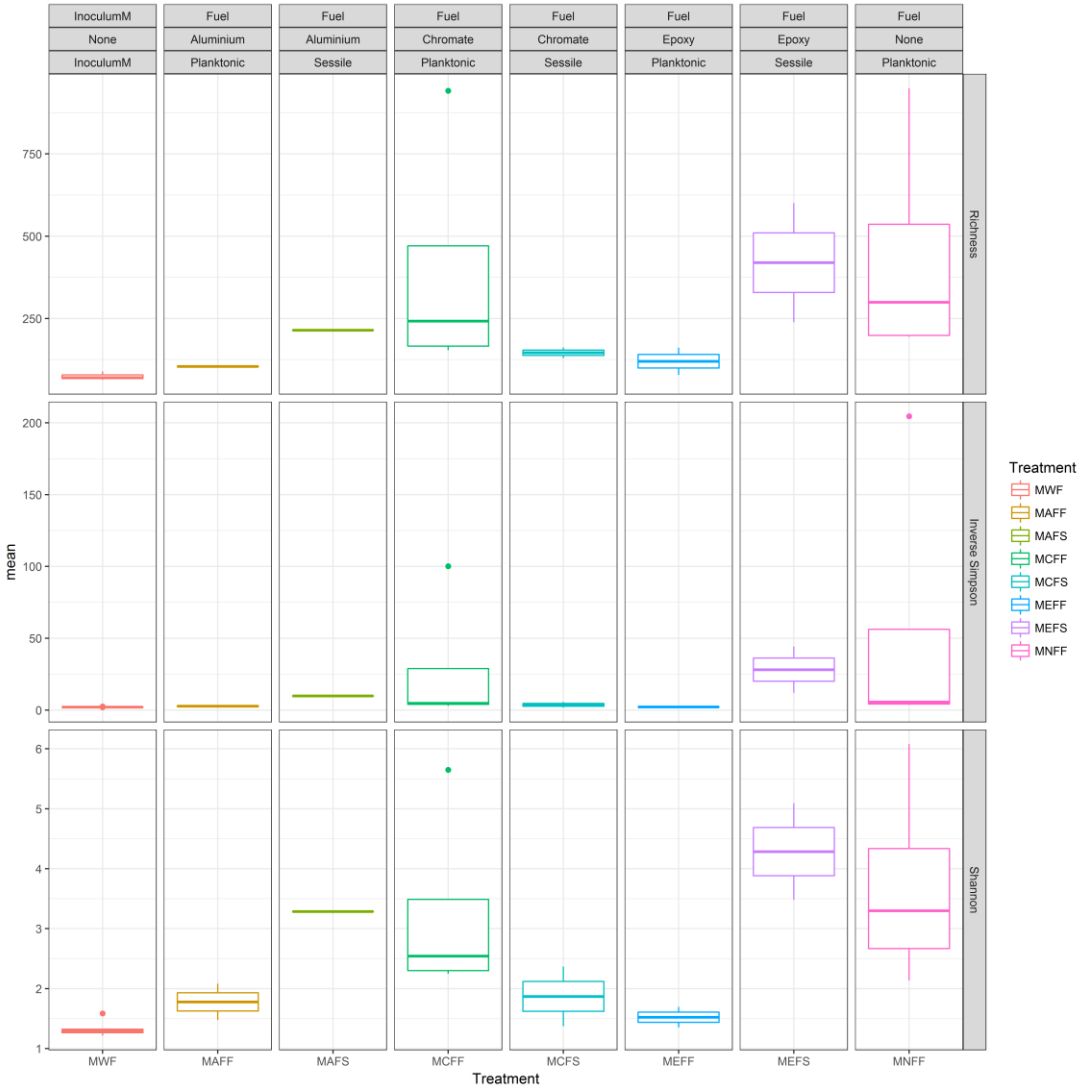

Figure G.66 – Box and Whisker plot showing the species richness and diversity using the inverse Simpson and Shannon diversity indices for the prokaryotic communities growing in the fuel phase of the Merox-treated Jet A-1. Boxes represent the upper and lower interquartile ranges, line in the middle of the box represents the mean (n = 4), whiskers show the lowest and highest values. Dots are outliers.

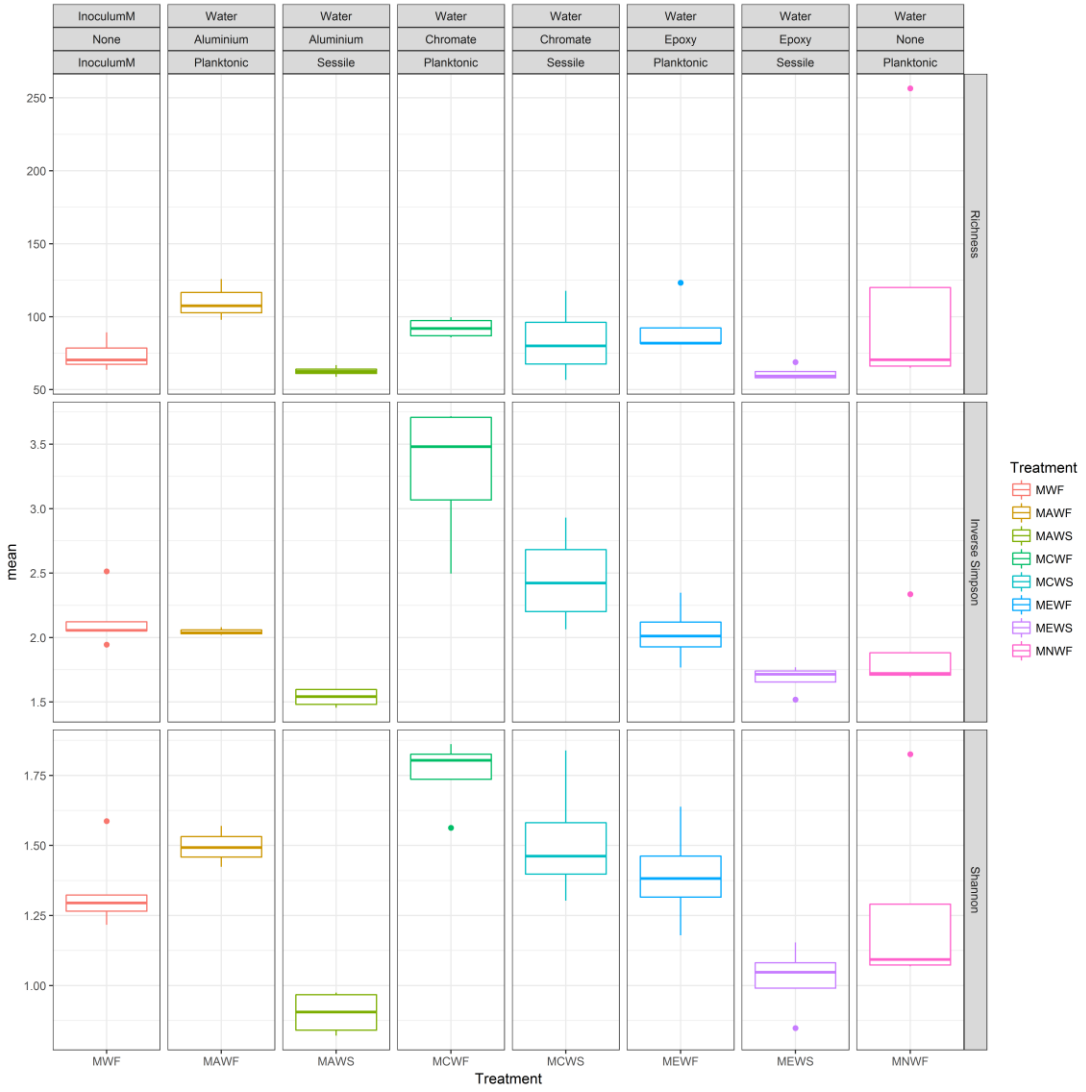

Figure G.67 – Box and Whisker plot showing the species richness and diversity using the inverse Simpson and Shannon diversity indices for the prokaryotic communities growing in the water phase of the Merox-treated Jet A-1. Boxes represent the upper and lower interquartile ranges, line in the middle of the box represents the mean (n = 4), whiskers show the lowest and highest values. Dots are outliers.

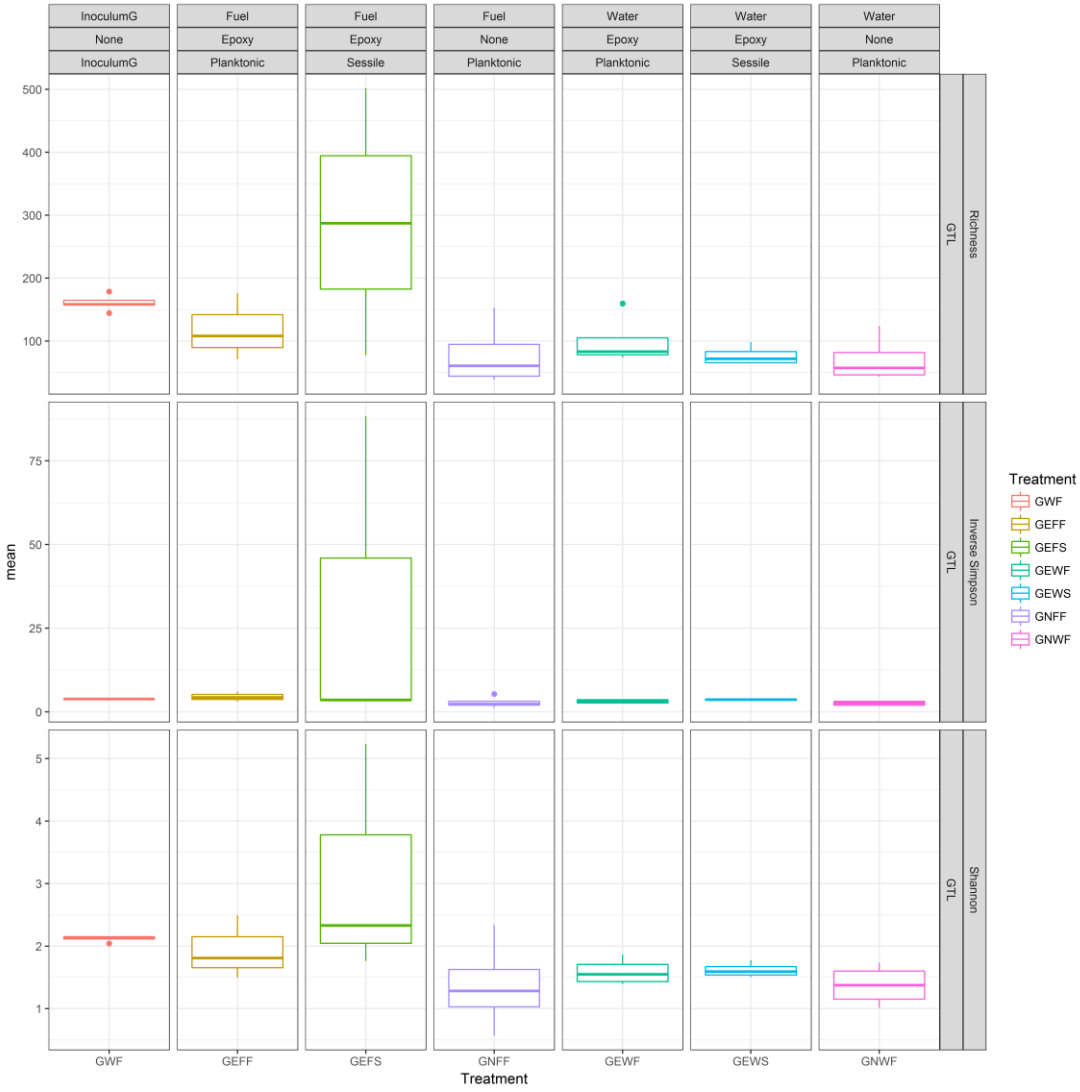

Figure G.68 – Box and Whisker plot showing the species richness and diversity using the inverse Simpson and Shannon diversity indices for the prokaryotic communities growing in both the fuel and water phases of the GTL kerosene. Boxes represent the upper and lower interquartile ranges, line in the middle of the box represents the mean (n = 4), whiskers show the lowest and highest values. Dots are outliers.

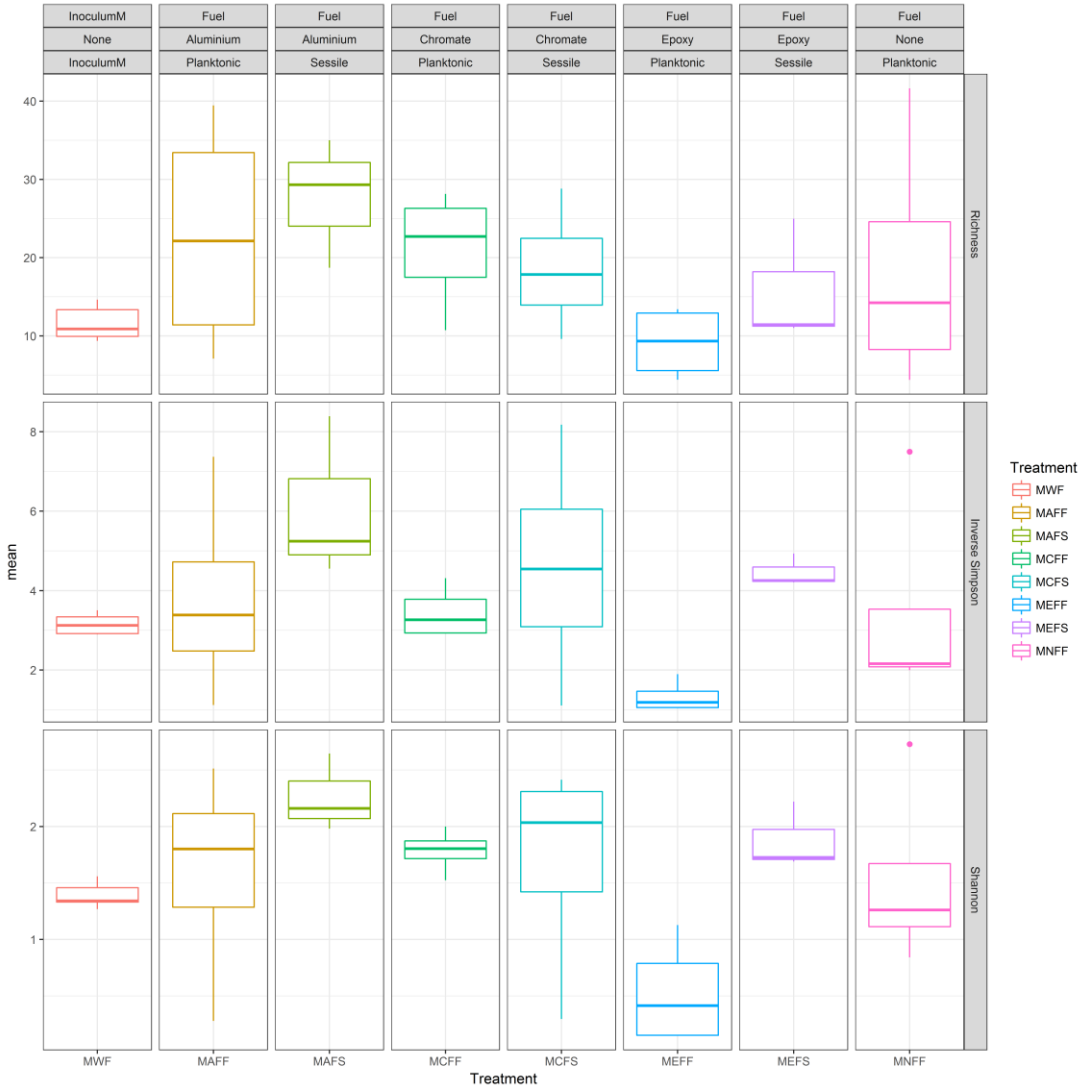

Figure G.69 – Box and Whisker plot showing the species richness and diversity using the inverse Simpson and Shannon diversity indices for the prokaryotic communities growing in the fuel phase of the GTL kerosene. Boxes represent the upper and lower interquartile ranges, line in the middle of the box represents the mean (n = 4), whiskers show the lowest and highest values. Dots are outliers.

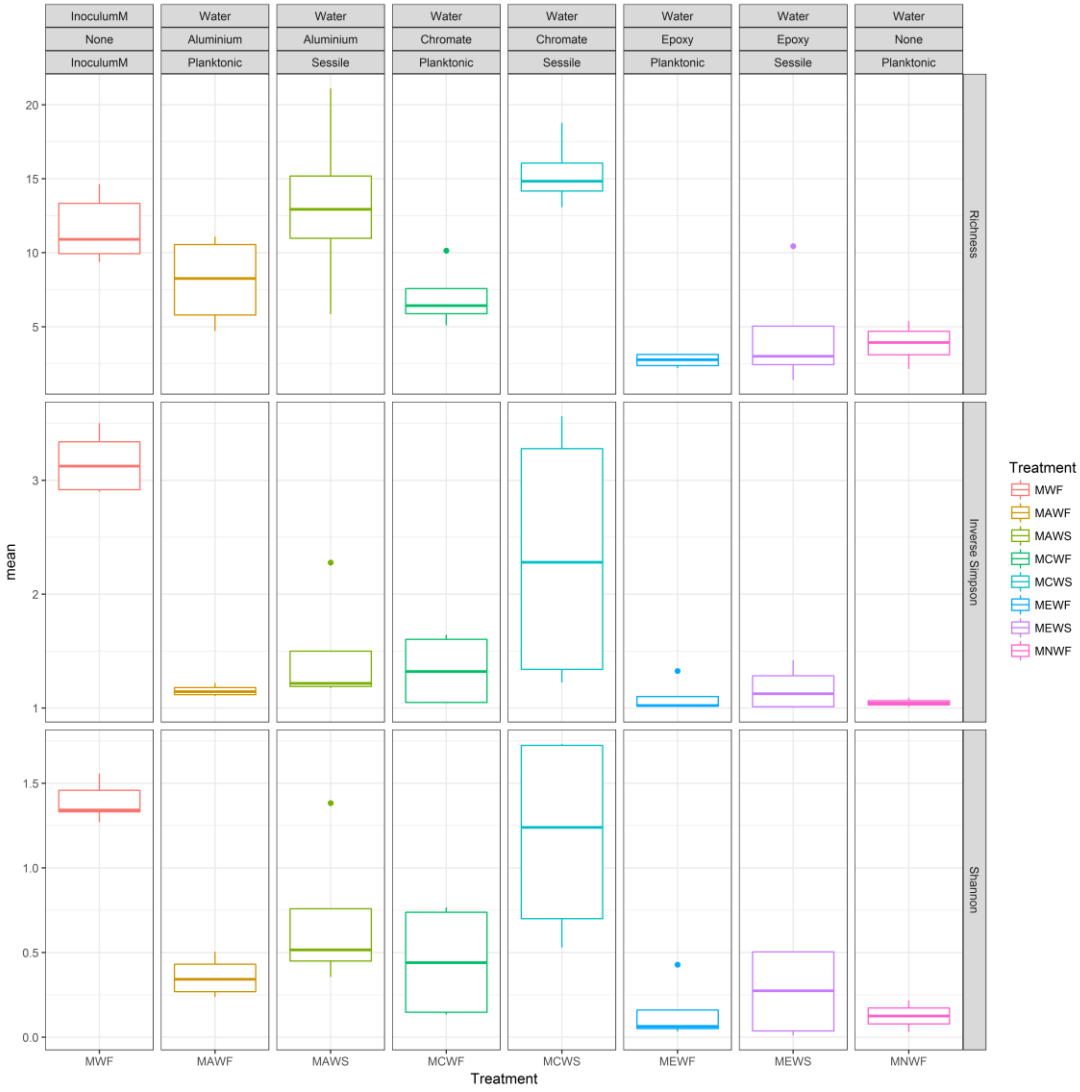

Figure G.70 – Box and Whisker plot showing the species richness and diversity using the inverse Simpson and Shannon diversity indices for the prokaryotic communities growing in the water phase of the Merox-treated Jet A-1. Boxes represent the upper and lower interquartile ranges, line in the middle of the box represents the mean (n = 4), whiskers show the lowest and highest values. Dots are outliers.

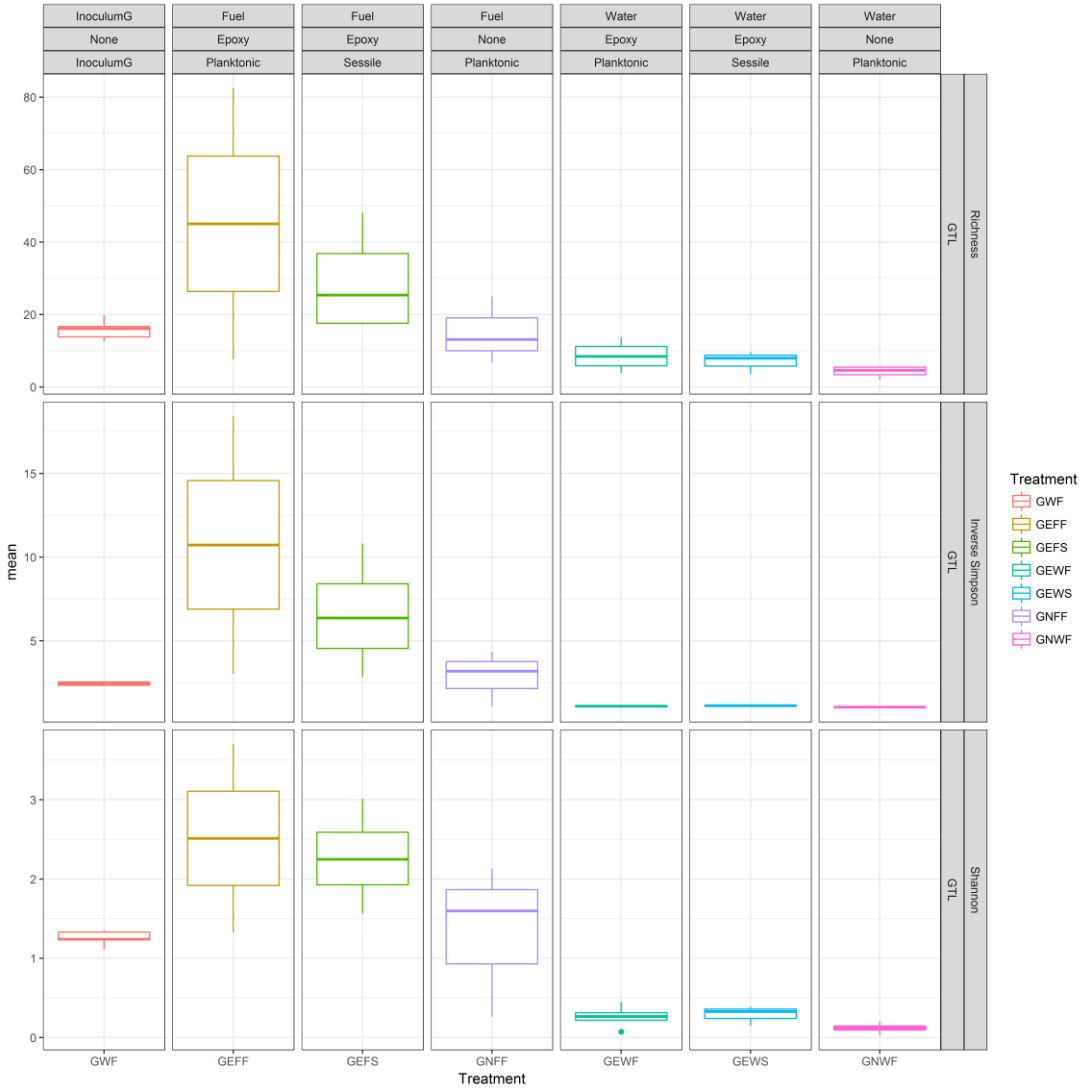

Figure G.71 – Box and Whisker plot showing the species richness and diversity using the inverse Simpson and Shannon diversity indices for the prokaryotic communities growing in both the fuel and water phases of the GTL kerosene. Boxes represent the upper and lower interquartile ranges, line in the middle of the box represents the mean (n = 4), whiskers show the lowest and highest values. Dots are outliers.

Appendix H

Environmental isolate sequences

Appendix H – Environmental isolate sequences

H.1 Prokaryotes

>Bacillus_simplex

GACGAACGCTGGCGGCGTGCCTAATACATGCAAGTCGAGCGAATCGATGGGAGCTTGCTCCC
AAAGATTAGCGGCGGACGGGTGAGTAACACGTGGGTAACCTGCCTGTAAGATTGGGATAACT
CCGGGAAACCGGAGCTAATACCGGATAACATTTCGAACCGCATGGTTCGAAATTGAAAGATG
GTTTCGGCTATCACTTACAGATGGACCCGCGGCGCATTAGCTAGTTGGTGAGGTAACGGCTC
ACCAAGGCAACGATGCGTAGCCGACCTGAGAGGGTGATCGGCCACACTGGGACTGAGACACG
GCCCAGACTCCTACGGGAGGCAGCAGTAGGGAATCTTCCGCAATGGACGAAAGTCTGACGGA
GCAACGCCGCGTGAACGAAGAAGGCCTTCGGGTCGTAAAGTTCTGTTGTTAGGGAAGAACAA
GTACCAGAGTAACTGCTGGTACCTTGACGGTACCTAACCAGAAAGCCACGGCTAACTACGTG
CCAGCAGCCGCGGTAATACGTAGGTGGCAAGCGTTGTCCGGAATTATTGGGCGTAAAGCGCG
CGCAGGTGGTTCCTTAAGTCTGATGTGAAAGCCCTCGGCTCAACCGTGGAGGGTCATTGGAA
ACTGGGGAACTTGAGTGCAGAAGAGGAAAGTGGAATTCCAAGTGTAGCGGTGAAATGCGTAG
AGATTTGGAGGAACACCAGTGGCGAAGGCGACTTTCTGGTCTGTAACTGACACTGAGGCGCG
AAAGCGTGGGGAGCAAACAGGATTAGATACCCTGGTAGTCCACGCCGTAAACGATGAGTGCT
AAGTGTTAGAGGGTTTCCGCCCTTTAGTGCTGCAGCTAACGCATTAAGCACTCCGCCTGGGG
AGTACGGCCGCAAGGCTGAAACTCAAAGGAATTGACGGGGGCCCGCACAAGCGGTGGAGCAT
GTGGTTTAATTCGAAGCAACGCGAAGAACCTTACCAGGTCTTGACATCCTCTGACAACCCTA
GAGATAGGGCTTTCCCCTTCGGGGGACAGAGTGACAGGTGGTGCATGGTTGTCGTCAGCTCG
TGTCGTGAGATGTTGGGTTAAGTCCCGCAACGAGCGCAACCCTTGATCTTAGTTGCCAGCAT
TCAGTTGGGCACTCTAAGGTGACTGCCGGTGACAAACCGGAGGAAGGTGGGGATGACGTCAA
ATCATCATGCCCCTTATGACCTGGGCTACACACGTGCTACAATGGATGGTACAAAGGGCTGC
AAACCTGCGAAGGTAAGCGAATCCCATAAAGCCATTCTCAGTTCGGATTGCAGGCTGCAACT
CGCCTGCATGAAGCCGGAATCGCTAGTAATCGCGGATCAGCATGCCGCGGTGAATACGTTCC
CGGGCCTTGTACACACCGCCCGTCACACCACGAGAGTTTGTAACACCCGAAGTCGGTGAGGT
AACCTTCATGGAGCCAGCCGCCTAAGGTGGGACAGATGATTGGGGTG

>Bacillus_sp.
GTAGTCCACGCCGTAAACGATGAGTGCTAAGTGTTAGAGGGTTTCCGCCCTTTAGTGCTGCA
GCTAACGCATTAAGCACTCCGCCTGGGGAGTACGGCCGCAAGGCTGAAACTCAAAGGAATTG
ACGGGGGCCCGCACAAGCGGTGGAGCATGTGGTTTAATTCGAAGCAACGCGAAGAACCTTAC
CAGGTCTTGACATCCTCTGACAACCCTAGAGATAGGGCTTTCCCCTTCGGGGGACAGAGTGA
CAGGTGGTGCATGGTTGTCGTCAGCTCGTGTCGTGAGATGTTGGGTTAAGTCCCGCAACGAG
CGCAACCCTTGATCTTAGTTGCCAGCATTCAGTTGGGCACTCTAAGGTGACTGCCGGTGACA
AACCGGA

>Cellulosimicrobium_sp.

GTAGTCCATGCCGTAAACGTTGGGCACTAGGTGTGGGGCTCATTCCACGAGTTCCGTGCCGC
AGCAAACGCATTAAGTGCCCCGCCTGGGGAGTACGGCCGCAAGGCTAAAACTCAAAGGAATT
GACGGGGGCCCGCACAAGCGGCGGAGCATGCGGATTAATTCGATGCAACGCGAAGAACCTTA
CCAAGGCTTGACATGCACGAGAAGCCACCAGAGTTGGTGGTCTCTTTGGACACTCGTGCACA
GGTGGTGCATGGTTGTCGTCAGCTCGTGTCGTGAGATGTTGGGTTAAGTCCCGCAACGAGCG
CAACCCTCGTCCCATGTTGCCAGCGGGTTATGCCGGGGACTCATGGGAGACTGCCGGGGTCA
ACTCGGAGGAAGGTGGGGATGACGTAAT

>Erwinia_billingiae

GTAGTCCACGCCGTAAACGATGTCGACTTGGAGGTTGTGCCCTTGAGGCGTGGCTTCCGGAG
CTAACGCGTTAAGTCGACCGCCTGGGGAGTACGGCCACAAGGTTAAAACTCAAATGAATTGA
CGGGGGCCCGCACAAGCGGTGGAGCATGTGGTTTAATTCGATGCAACGCGAAGAACCTTACC
TGGCCTTGACATCCACGGAATTCGGCAGAGATGCCTTAGTGCCTTCGGGAACCGTGAGACAG

GTGCTGCATGGCTGTCGTCAGCTCGTGTTGTGAAATGTTGGGTTAAGTCCCGCAACGAGCGC
AACCCTTATCCTTTGTTGCCAGCGAGTAATGTCGGGAACTCAAAGGAGACTGCCGGTGACAA
ACCGGAGGAAGGTGGGGATGACGTAAT

>Escherichia_coli

GTAGTCCACGCCGTAAACGATGTCGACTTGGAGGTTGTACCCTTGAGGCGTGGCTTCCGGAG
CTAACGCGTTAAGTCGACCGCCTGGGGAGTACGGCCGCAAGGTTAAAACTCAAACGAATTGA
CGGGGGCCCGCACAAGCGGTGGAGCATGTGGTTTAATTCGATGCAACGCGAAGAACCTTACC
TGGTCTTGACATCCACGGAAGTTTTCAGAGATGAGAATGTGCCTTCGGGAACCGTGAGACAG
GTGCTGCATGGCTGTCGTCAGCTCGTGTTGTGAAATGTTGGGTTAAGTCCCGCAACGAGCGC
AACCCCTATCCTTTGTTGCCAGCGGTCCGGCCGGGAACTCAAAGGAGACTGCCAGTGATAAA
CTGGA

>Exiguobacterium_arabatum

GACGAACGCTGGCGGCGTGCCTAATTCATGCAGTCGAGCGCAGGAAGCCGTCTGAACCCTTC
GGGGGGACGACGGTGGAATGAGCGGCGGACGGGTGAGTAACACGTAAAGAACCTGCCCATAG
GTCTGGGATAACCACGAGAAATCGGGGCTAATACCGGATGTGTCATCGGACCGCATGGTCCG
CTGATGAAAGGCGCTCCGGCGTCGCCCATGGATGGCTTTGCGGTGCATTAGCTAGTTGGTGG
GGTAACGGCCCACCAAGGCGACGATGCATAGCCGACCTGAGAGGGTGATCGGCCACACTGGG
ACTGAGACACGGCCCAGACTCCTACGGGAGGCAGCAGTAGGGAATCTTCCACAATGGACGAA
AGTCTGATGGAGCAACGCCGCGTGAACGATGAAGGCTTTCGGGTCGTAAAGTTCTGTTGTAA
GGGAAGAACAAGTGCCGCAGGCAATGGCGGCACCTTGACGGTACCTTGCGAGAAAGCCACGG
CTAACTACGTGCCAGCAGCCGCGGTAATACGTAGGTGGCAAGCGTTGTCCGGAATTATTGGG
CGTAAAGCGCGCGCAGGCGGCCTCTTAAGTCTGATGTGAAAGCCCCCGGCTCAACCGGGGAG
GGCCATTGGAAACTGGGAGGCTTGAGTATAGGAGAGAAGAGTGGAATTCCACGTGTAGCGGT
GAAATGCGTAGAGATGTGGAGGAACACCAGTGGCGAAGGCGACTCTTTGGCCTATAACTGAC
GCTGAGGCGCGAAAGCGTGGGGAGCAAACAGGATTAGATACCCTGGTAGTCCACGCCGTAAA
CGATGAGTGCTAGGTGTTGGAGGGTTTCCGCCCTTCAGTGCTGAAGCTAACGCATTAAGCAC
TCCGCCTGGGGAGTACGGTCGCAAGGCTGAAACTCAAAGGAATTGACGGGGACCCGCACAAG
CGGTGGAGCATGTGGTTTAATTCGAAGCAACGCGAAGAACCTTACCAACTCTTGACATCCCC
CTGACCGGTACAGAGATGTACCTTCCCCTTCGGGGGCAGGGGTGACAGGTGGTGCATGGTTG
TCGTCAGCTCGTGTCGTGAGATGTTGGGTTAAGTCCCGCAACGAGCGCAACCCTTGTCCTTA
GTTGCCAGCANNNNNNTGGGCACTCTAGGGAGACTGCCGGTGACAAACCGGAGGAAGGTGGG
GATGACGTCAAATCATCATGCCCCTTATGAGTTGGGCTACACACGTGCTACAATGGACGGTA
CAAAGGGCAGCGAAGCCGCGAGGTGGAGCCAATCCCAGAAAGCCGTTCTCAGTTCGGATTGC
AGGCTGCAACTCGCCTGCATGAAGTCGGAATCGCTAGTAATCGCAGGTCAGCATACTGCGGT
GAATACGTTCCCGGGTCTTGTACACACCGCCCGTCACACCACGAGAGTTTGCAACACCCGAA
GTCGGTGAGGTAACCGTAAGGAGCCAGCCGCCGAAGGTGGGGCAGATGATTGGGGTGAAGTC
GTA

>Flavobacterium_sp.

TTGGAAGGTGGGGATGACGTAACAGGATTAGATACCCGGTTGGAAGGTGGGGATGACGTAGA
AGGTGGGGATGACGTAGAAGGTGGGGATGACGTAACCGGATTAGATACCCGGTTGGAAGGTG
GGGATGACGTAACAGGATTAGATACCCGGAAGGTGGGGATGACGTAACAGGATTAGATACCC
GGTTGGAAGGTGGGGATGACGTGGAAGGTGGGGATGACGTAACAGGATTAGATACCCTGGTA
GTCCACGCCGTAAACGATGGATACTAGCTGTTGGAAGCAATTTCAGTGGCTAAGCGAAAGTG
ATAAGTATCCCACCTGGGGAGTACGTTCGCAAGAATGAAACTCAAAGGAATTGACGGGGGCC
CGCACAAGCGGTGGAGCATGTGGTTTAATTCGATGATACGCGAGGAACCTTACCAAGGCTTA
AATGTAGATTGACCGGTTTGGAAACAGATCTTTCGCAAGACAATTTACAAGGTGCTGCATGG
TTGTCGTCAGCTCGTGCCGTGAGGTGTCAGGTTAAGTCCTATAACGAGCGCAACCCCTGTTG
TTAGTTGCCAGCGAGTCATGTCGGGAACTCTAACAAGACTGCCAGTGCAAACTGTGAGGAAG
GTGGGGATGACGTAACAGGATTAGAAAT

>Kocuria_rhizophila

GACGAACGCCGGCGGCGTGCTTAACTCATGCAAGTCGAACGCTGAAGCTTGGTGCTTGCACT
GGGTGGATGAGTGGCGAACGGGTGAGTAATACGTGAGTAACCTGCCCTTGACTCTGGGATAA
GCCTGGGAAACTGGGTCTAATACTGGATATGACATGTCACCGCATGGTGGTGTGTGGAAAGG
GTTTTACTGGTTTTGGATGGGCTCACGGCCTATCAGCTTGTTGGTGGGGTAATGGCTCACCA
AGGCGACGACGGGTAGCCGGCCTGAGAGGGTGACCGGCCACACTGGGACTGAGACACGGCCC
AGACTCCTACGGGAGGCAGCAGTGGGGAATATTGCACAATGGGCGGAAGCCTGATGCAGCGA
CGCCGCGTGAGGGATGACGGCCTTCGGGTTGTAAACCTCTTTCAGCACGGAAGAAGCGAAAG
TGACGGTACGTGCAGAAGAAGCGCCGGCTAACTACGTGCCAGCAGCCGCGGTAATACGTAGG
GCGCAAGCGTTGTCCGGAATTATTGGGCGTAAAGAGCTCGTAGGCGGTTTGTCGCGTCTGCT
GTGAAAGCCCGGGGCTTAACCCCGGGTGTGCAGTGGGTACGGGCAGACTTGAGTGCAGTAGG
GGAGACTGGAATTCCTGGTGTAGCGGTGAAATGCGCAGATATCAGGAGGAACACCGATGGCG
AAGGCAGGTCTCTGGGCTGTTACTGACGCTGAGGAGCGAAAGCATGGGGAGCGAACAGGATT
AGATACCCTGGTAGTCCATGCCGTAAACGTTGGGCACTAGGTGTGGGGAACATTCCACGTTT
TCCGCGCCGTAGCTAACGCATTAAGTGCCCCGCCTGGGGAGTACGGCCGCAAGGCTAAAACT
CAAAGGAATTGACGGGGGCCCGCACAAGCGGCGGAGCATGCGGATTAATTCGATGCAACGCG
AAGAACCTTACCAAGGCTTGACATACACCGGACCGGGCCAGAGATGGTCTTTCCCCCTTGTG
GGGCTGGTGTACAGGTGGTGCATGGTTGTCGTCAGCTCGTGTCGTGAGATGTTGGGTTAAGT
CCCGCAACGAGCGCAACCCTCGTTCTATGTTGCCAGCACGTGATGGTGGGGACTCATAGGAG
ACTGCCGGGGTCAACTCGGAGGAAGGTGGGGATGACGTCAAATCATCATGCCCCTTATGTCT
TGGGCTTCACGCATGCTACAATGGCCAGTACAATGGGTTGCGATGCCGCGAGGTGGAGCTAA
TCCCAAAAAGCTGGTCTCAGTTCGGATCGTGGTCTGCAACTCGACCACGTGAAGTCGGAGTC
GCTAGTAATCGCAGATCAGCAACGCTGCGGTGAATACGTTCCCGGGCCTTGTACACACCGCC
CGTCAAGTCACGAAAGTTGGTAACACCCGAAGCCGGTGGCCTAACCCTTGTGGGGGGAGCCG
TCGAAGGTGGGACTGGCGATTGGGACT

>Novosphingobium_resinovorum

GTAGTCCACGCCGTAAACGATGATAACTAGCTGTCCGGTCACTTGGTGATTGGGTGGCGCAG
CTAACGCATTAAGTTATCCGCCTGGGGAGTACGGTCGCAAGATTAAAACTCAAAGGAATTGA
CGGGGGCCTGCACAAGCGGTGGAGCATGTGGTTTAATTCGAAGCAACGCGCAGAACCTTACC
AGCGTTTGACATCCTCATCGCGGATTAGAGAGATCTTTTCCTTCAGTTCGGCTGGATGAGTG
ACGGGTGCTGCATGGCTGTCGTCAGCTCGTGTCGTGAGATGTTGGGTTGAGTCCCGCAACGA
GCGCAACCCTCGTCCTTAGTTGCCATCATTTAGTTGGGCACTCTAAGGAAACTGCCGGTGAT
AAGCCGGA

>Paenibacillus_sp.

GACGAACGCTGGCGGCGTGCCTAATACATGCAAGTCGAGCGGACTTGATGGAGTGCTTGCAC
TCCTGATGGTTAGCGGCGGACGGGTGAGTAACACGTAGGCAACCTGCCCTTAAGACTGGGAT
AACTACCGGAAACGGTAGCTAATACCGGATAATTTATTACATAGCATTATGTGATAATGAAA
GACGGAGCAATCTGTCACTTGGGGATGGGCCTGCGGCGCATTAGCTAGTTGGTGGGGTAATG
GCCCACCAAGGCGACGATGCGTAGCCGACCTGAGAGGGTGAACGGCCACACTGGGACTGAGA
CACGGCCCAGACTCCTACGGGAGGCAGCAGTAGGGAATCTTCCGCAATGGGCGAAAGCCTGA
CGGAGCAACGCCGCGTGAGTGATGAAGGTTTTCGGATCGTAAAGCTCTGTTGCCAAGGAAGA
ACGTCTCATAGAGTAACTGCTATGAGAGTGACGGTACTTGAGAAGAAAGCCCCGGCTAACTA
CGTGCCAGCAGCCGCGGTAATACGTAGGGGGCAAGCGTTGTCCGGAATTATTGGGCGTAAAG
CGCGCGCAGGCGGTTCTTTAAGTCTGGTGTTTAAACCTGGGGCTCAACTTCAGGTCGCACTG
GAAACTGGGGAACTTGAGTGCAGAAGAGGAGAGTGGAATTCCACGTGTAGCGGTGAAATGCG
TAGATATGTGGAGGAACACCAGTGGCGAAGGCGACTCTCTGGGCTGTAACTGACGCTGAGGC
GCGAAAGCGTGGGGAGCAAACAGGATTAGATACCCTGGTAGTCCACGCCGTAAACGATGAAT
GCTAGGTGTTAGGGGTTTCGATACCCTTGGTGCCGAAGTTAACACATTAAGCATTCCGCCTG
GGGAGTACGGTCGCAAGACTGAAACTCAAAGGAATTGACGGGGACCCGCACAAGCAGTGGAG

TATGTGGTTTAATTCGAAGCAACGCGAAGAACCTTACCAAGTCTTGACATCCCTCTGAATCT
GCTAGAGATAGCAGCGGCCTTCGGGACAGAGGAGACAGGTGGTGCATGGTTGTCGTCAGCTC
GTGTCGTGAGATGTTGGGTTAAGTCCCGCAACGAGCGCAACCCTTGATTTTAGTTGCCAGCA
GGTAAGGCTGGGCACTCTAGAATGACTGCCGGTGACAAACCGGAGGAAGGCGGGGATGACGT
CAAATCATCATGCCCCTTATGACTTGGGCTACACACGTACTACAATGGCTGGTACAACGGGA
AGCGAAGCCGCGAGGTGGAGCCAATCCTATAAAAGCCAGTCTCAGTTCGGATTG

>Pantoea_eucalypti

GTAGTCCACNCCGTAAACGATGTCGACTTGGAGGTTGTTCCCTTGAGGAGTGGCTTCCGGAG
CTAACGCGTTAAGTCGACCGCCTGGGGAGTACGGCCGCAAGGTTAAAACTCAAATGAATTGA
CGGGGGCCCGCACAAGCGGTGGAGCATGTGGTTTAATTCGATGCAACGCGAAGAACCTTACC
TACTCTTGACATCCAGAGAACTTTCCAGAGATGGATTGGTGCCTTCGGGAACTCTGAGACAG
GTGCTGCATGGCTGTCGTCAGCTCGTGTTGTGAAATGTTGGGTTAAGTCCCGCAACGAGCGC
AACCCTTATCCTTTGTTGCCAGCGCGTGATGGCGGGAACTCAAAGGAGACTGCCGGTGATAA
ACCGGAGGAAGGTGGGGATGACGTAAT

>Pantoea_sp.

GTAGTCCACGCCGTAAACGATGTCGACTTGGAGGTTGTTCCCTTGAGGAGTGGCTTCCGGAG
CTAACGCGTTAAGTCGACCGCCTGGGGAGTACGGCCGCAAGGTTAAAACTCAAATGAATTGA
CGGGGGCCCGCACAAGCGGTGGAGCATGTGGTTTAATTCGATGCAACGCGAAGAACCTTACC
TACTCTTGACATCCAGAGAACTTTCCAGAGATGGATTGGTGCCTTCGGGAACTCTGAGACAG
GTGCTGCATGGCTGTCGTCAGCTCGTGTTGTGAAATGTTGGGTTAAGTCCCGCAACGAGCGC
AACCCTTATCCTTTGTTGCCAGCGCGTGATGGCGGGAACTCAAAGGAGACTGCCGGTGATGA
ACCGGA

>Paracoccus_yeei

TCAGAACGAACGCTGGCGGCAGGCCTAACACATGCAAGTCGAGCGAGGACTTCGGTTCTAGC
GGCGGACGGGTGAGTAACGCGTGGGAATGTGCCCTTCTCTACGGAATAGCCCTGGGAAACTG
GGAGTAATACCGTATACGCCCTTTTGGGGAAAGATTTATCGGAGAAGGATCAGCCCGCGTTG
GATTAGGTAGTTGGTGGGGTAATGGCCTACCAAGCCGACGATCCATAGCTGGTTTGAGAGGA
TGATCAGCCACACTGGGACTGAGACACGGCCCAGACTCCTACGGGAGGCAGCAGTGGGGAAT
CTTAGACAATGGGGGCAACCCTGATCTAGCCATGCCGCGTGAGTGATGAAGGCCTTAGGGTT
GTAAAGCTCTTTCAGCTGGGAAGATAATGACGGTACCAGCAGAAGAAGCCCCGGCTAACTCC
GTGCCAGCAGCCGCGGTAATACGGAGGGGGCTAGCGTTGTTCGGAATTACTGGGCGTAAAGC
GCACGTAGGCGGACCGGAAAGTCAGAGGTGAAATCCCAGGGCTCAACCTTGGAACTGCCTTT
GAAACTATCGGTCTGGAGTTCGAGAGAGGTGAGTGGAATTCCGAGTGTAGAGGTGAAATTCG
TAGATATTCGGAGGAACACCAGTGGCGAAGGCGGCTCACTGGCTCGATACTGACGCTGAGGT
GCGAAAGCGTGGGGAGCAAACAGGATTAGATACCCTGGTAGTCCACGCCGTAAACGATGAAT
GCCAGTCGTCGGGCAGCATGCTGTTCGGTGACACACCTAACGGATTAAGCATTCCGCCTGGG
GAGTACGGTCGCAAGATTAAAACTCAAAGGAATTGACGGGGGCCCGCACAAGCGGTGGAGCA
TGTGGTTTAATTCGAAGCAACGCGCAGAACCTTACCAACCCTTGACATCGCAGGACAGCCCG
AGAGATCGGGTCTTCTCGTAAGAGACCTGTGGACAGGTGCTGCATGGCTGTCGTCAGCTCGT
GTCGTGAGATGTTCGGTTAAGTCCGGCAACGAGCGCAACCCACGTCTTTAGTTGCCAGCATT
CAGTTGGGCACTCTAAAGAAACTGCCGATGATAAGTCGGAGGAAGGTGTGGATGACGTCAAG
TCCTCATGGCCCTTACGGGTTGGGCTACACACGTGCTACAATGGTGGTGACAGTGGGTTAAT
CCCCAAAAGCCATCTCAGTTCGGATTGGGGTCTGCAACTCGACCCCATGAAGTTGGAATCGC
TAGTAATCGCGGAACAGCATGCCGCGGTGAATACGTTCCCGGGCCTTGTACACACCGCCCGT
CACACCATGGGAGTTGGGTCTACCCGACGGCCGTGCGCCAACCAGCAATGGAGGCAGCGGAC
CACGGTAGGCTCAGCGACTGGGGTG

>Pseudomonas_fluorescens

GTAGTCCACGCCGTAAACGATGTCAACTAGCCGTTGGGAGCCTTGAGCTCTTAGTGGCGCAG
CTAACGCATTAAGTTGACCGCCTGGGGAGTACGGCCGCAAGGTTAAAACTCAAATGAATTGA
CGGGGGCCCGCACAAGCGGTGGAGCATGTGGTTTAATTCGAAGCAACGCGAAGAACCTTACC
AGGCCTTGACATCCAATGAACTTTCTAGAGATAGATTGGTGCCTTCGGGAACATTGAGACAG
GTGCTGCATGGCTGTCGTCAGCTCGTGTCGTGAGATGTTGGGTTAAGTCCCGTAACGAGCGC
AACCCTTGTCCTTAGTTACCAGCACGTAATGGTGGGCACTCTAAGGAGACTGCCGGTGACAA
ACCGGA

>Pseudomonas_graminis

ATTGAACGCTGGCGGCAGGCCTAACACATGCAAGTCGAGCGGATGAAGAGAGCTTGCTCTCT
GATTCAGCGGCGGACGGGTGAGTAATGCCTAGGAATCTGCCTGGTAGTGGGGGACAACGTCT
CGAAAGGGACGCTAATACCGCATACGTCCTACGGGAGAAAGCAGGGGACCTTCGGGCCTTGC
GCTATCAGATGAGCCTAGGTCGGATTAGCTAGTTGGTGAGGTAATGGCTCACCAAGGCGACG
ATCCGTAACTGGTCTGAGAGGATGATCAGTCACACTGGAACTGAGACACGGTCCAGACTCCT
ACGGGAGGCAGCAGTGGGGAATATTGGACAATGGGCGAAAGCCTGATCCAGCCATGCCGCGT
GTGTGAAGAAGGTCTTCGGATTGTAAAGCACTTTAAGTTGGGAGGAAGGGCAGTAAGCGAAT
ACCTTGCTGTTTTGACGTTACCGACAGAATAAGCACCGGCTAACTCTGTGCCAGCAGCCGCG
GTAATACAGAGGGTGCAAGCGTTAATCGGAATTACTGGGCGTAAAGCGCGCGTAGGTGGTTT
GTTAAGTTGAATGTGAAATCCCCGGGCTCAACCTGGGAACTGCATCCAAAACTGGCAAGCTA
GAGTAGGGCAGAGGGTGGTGGAATTTCCTGTGTAGCGGTGAAATGCGTAGATATAGGAAGGA
ACACCAGTGGCGAAGGCGACCACCTGGGCTCATACTGACACTGAGGTGCGAAAGCGTGGGGA
GCAAACAGGATTAGATACCCTGGTAGTCCACGCCGTAAACGATGTCAACTAGCCGTTGGAAG
CCTTGAGCTTTTAGTGGCGCAGCTAACGCATTAAGTTGACCGCCTGGGGAGTACGGCCGCAA
GGTTAAAACTCAAATGAATTGACGGGGGCCCGCACAAGCGGTGGAGCATGTGGTTTAATTCG
AAGCAACGCGAAGAACCTTACCAGGCCTTGACATCCAATGAACTTTCCAGAGATGGATTGGT
GCCTTCGGGAACATTGAGACAGGTGCTGCATGGCTGTCGTCAGCTCGTGTCGTGAGATGTTG
GGTTAAGTCCCGTAACGAGCGCAACCCTTGTCCTTAGTTACCAGCACGTTATGGTGGGCACT
CTAAGGAGACTGCCGGTGACAAACCGGAGGAAGGTGGGGATGACGTCAAGTCATCATGGCCC
TTACGGCCTGGGCTACACACGTGCTACAATGGTCGGTACAGAGGGTTGCCAAGCCGCGAGGT
GGAGCTAATCCCAGAAAACCGATCGTAGTCCGGATCGCAGTCTGCAACTCGACTGCGTGAAG
TCGGAATCGCTAGTAATCGCGAATCAGAATGTCGCGGTGAATACGTTCCCGGGCCTTGTACA
CACCGCCCGTCACACCATGGGAGTGGGTTGCACCAGAAGTAGCTAGTCTAACCTTCGGGAGG
ACGGTTACCACGGTGTGATTCATGACTGGGGTG

>Pseudomonas_sp.

GGAAGGTGGGGATGACGTAACCGGATTAGATACCCTGGTAGTCCACGCCGTAAACGATGTCA
ACTAGCCGTTGGAAGCCTTGAGCTTTTAGTGGCGCAGCTAACGCATTAAGTTGACCGCCTGG
GGAGTACGGCCGCAAGGTTAAAACTCAAATGAATTGACGGGGGCCCGCACAAGCGGTGGAGC
ATGTGGTTTAATTCGAGGCAACGCGAAGAACCTTACCAGGCCTTGACATCCAATGAACTTTC
TAGAGATAGATTGGTGCCTTCGGGAACATTGAGACAGGTGCTGCATGGCTGTCGTCAGCTCG
TGTCGTGAGATGTTGGGTTAAGTCCCGTAACGAGCGCAACCCTTGTCCTTAGTTACCAGCAC
GTTATGGTGGGCACTCTAAGGAGACTGCCGGTGACAAACCGGAAAT

>Pseudomonas_tolaasii

GTAGTCCACGCCGTAAACGATGTCAACTAGCCGTTGGAAGCCTTGAGCTTTTAGTGGCGCAG
CTAACGCATTAAGTTGACCGCCTGGGGAGTACGGCCGCAAGGTTAAAACTCAAATGAATTGA
CGGGGGCCCGCACAAGCGGTGGAGCATGTGGTTTAATTCGAAGCAACGCGAAGAACCTTACC
AGGCCTTGACATCCAATGAACTTTCCAGAGATGGATTGGTGCCTTCGGGAACATTGAGACAG
GTGCTGCATGGCTGTCGTCAGCTCGTGTCGTGAGATGTTGGGTTAAGTCCCGTAACGAGCGC
AACCCTTGTCCTTAGTTACCAGCACGTTATGGTGGGCACTCTAAGGAGACTGCCGGTGACAA
ACCGGA

>Roseomonas_sp.

TGGCTCAGAGCGAACGCTGGCGGCATGCTTAACACATGCAAGTCGCACGGGCAGCAATGTCA
GTGGCGGACGGGTGAGTAACGCGTAGGAACGTGTCCTGAGGTGGGGGACAACCCCGGGAAAC
TGGGGCTAATACCGCATATGGGCTGAGGCCCAAAGCCGAGAGGCGCCTTTGGAGCGGCCTGC
GTCCGATTAGGTAGTTGGTGGGGTAAAGGCCTACCAAGCCTGCGATCGGTAGCTGGTCTGAG
AGGACGACCAGCCACACTGGGACTGAGACACGGCCCAGACTCCTACGGGAGGCAGCAGTGGG
GAATATTGGACAATGGGCGAAAGCCTGATCCAGCAATGCCGCGTGGGTGAAGAAGGTCTTCG
GATCGTAAAGCCCTTTCGACGGGGACGATGATGACGGTACCCGTAGAAGAAGCCCCGGCTAA
CTTCGTGCCAGCAGCCGCGGTAATACGAAGGGGGCTAGCGTTGCTCGGAATTACTGGGCGTA
AAGGGCGCGTAGGCGGCGGCCCAAGTCAGGCGTGAAATTCCTGGGCTCAACCTGGGGACTGC
GCTTGATACTGGGTTGCTTGAGGATGGAAGAGGCTCGTGGAATTCCCAGTGTAGAGGTGAAA
TTCGTAGATATTGGGAAGAACACCGGTGGCGAAGGCGGCGAGCTGGTCCATTACTGACGCTG
AGGCGCGACAGCGTGGGGAGCAAACAGGATTAGATACCCTGGTAGTCCACGCCGTAAACGAT
GTGCGCTGGATGTTGGGGCCCATAGGGTCTCAGTGTCGTAGCCAACGCGGTAAGCGCACCGC
CTGGGGAGTACGGCCGCAAGGTTGAAACTCAAAGGAATTGACGGGGGCCCGCACAAGCGGTG
GAGCATGTGGTTTAATTCGAAGCAACGCGCAGAACCTTACCAGCCCTTGACATGGTCACGAC
CGGTCCAGAGATGGACTTTCCTAGCAATAGGCGTGATGCACAGGTGCTGCATGGCTGTCGTC
AGCTCGTGTCGTGAGATGTTGGGTTAAGTCCCGCAACGAGCGCAACCCTCGCCTCTAGTTGC
CAGCATGCTCCGGGTGGGCACTCTAGAGGAACTGCCGGTGACAAGCCGGAGGAAGGTGGGGA
TGACGTCAAGTCCTTCATGGCCCTTATGGGCTGGGCCTACACACGTGCTACAATGGCGGTGA
CAGAGGGAAGCCAGGTCGCGAGGCCGAGCCGATCCCGAAAAGCCGTCTCAGTTCGGATTGCA
CTCTGCAACTCGGGTGCATGAAGGTGGAATCGCTAGTAATCGCGGATCAGCACGCCGCGGTG
AATACGTTCCCGGGCCTTGTACACACCGCCCGTCACACCATGGGAGTTGGTTCTACCTTAAG
TCGTTGCGCTAACCAGCGATGGGGGCAGGCGACCACGGTAGGGTCAGCGACTGGGGTGAAGT
CGTAACAAGGTAACCGTAA

>Serratia_sp.

GTAGTCCACGCTGTAAACGATGTCGACTTGGAGGTTGTGCCCTTGAGGCGTGGCTTCCGGAG
CTAACGCGTTAAGTCGACCGCCTGGGGAGTACGGCCGCAAGGTTAAAACTCAAATGAATTGA
CGGGGGCCCGCACAAGCGGTGGAGCATGTGGTTTAATTCGATGCAACGCGAAGAACCTTACC
TACTCTTGACATCCAGAGAATTCGCTAGAGATAGCTTAGTGCCTTCGGGAACTCTGAGACAG
GTGCTGCATGGCTGTCGTCAGCTCGTGTTGTGAAATGTTGGGTTAAGTCCCGCAACGAGCGC
AACCCTTATCCTTTGTTGCCAGCACGTAATGGTGGGAACTCAAAGGAGACTGCCGGTGATAA
ACCGGAGGAAGGTGGGGATGACGTAAT

>Shigella_sp.

TCCAGTTTATCACTGGCAGTCTCCTTTGAGTTCCCGGCCGGACCGCTGGCAACAAAGGATAA
GGGTTGCGCTCGTTGCGGGACTTAACCCAACATTTCACAACACGAGCTGACGACAGCCATGC
AGCACCTGTCTCACGGTTCCCGAAGGCACATTCTCATCTCTGAAAACTTCCGTGGATGTCAA
GACCAGGTAAGGTTCTTCGCGTTGCATCGAATTAAACCACATGCTCCACCGCTTGTGCGGGC
CCCCGTCAATTCATTTGAGTTTTAACCTTGCGGCCGTACTCCCCAGGCGGTCGACTTAACGC
GTTAGCTCCGGAAGCCACGCCTCAAGGGCACAACCTCCAAGTCGACATCGTTTACGGCGTGG
ACT

>Staphylococcus_epidermidis

GTAGTCCACGCCGTAAACGATGAGTGCTAAGTGTTAGGGGGTTTCCGCCCCTTAGTGCTGCA
GCTAACGCATTAAGCACTCCGCCTGGGGAGTACGACCGCAAGGTTGAAACTCAAAGGAATTG
ACGGGGACCCGCACAAGCGGTGGAGCATGTGGTTTAATTCGAAGCAACGCGAAGAACCTTAC
CAAATCTTGACATCCTCTGACCCCTCTAGAGAAAGAGTTTTCCCCTTCGGGGGACAGAGTGA
CAGGTGGTGCATGGTTGTCGCCAGCTCGTGTCGTGAGATGTTGGGTTAAGTCCCGCAACGAG
CGCAACCCTTAAGCTTAGTTGCCATCATTAAGTTGGGCACTCTAAGTTGACTGCCGGTGACA
AACCGGA

>Staphylococcus_sp.

TCCGGTTTGTCACCGGCAGTCAACTTAGAGTGCCCAACTTAATGATGGCAACTAAGCTTAAG
GGTTGCGCTCGTTGCGGGACTTAACCCAACATCTCACGACACGAGCTGACGACAACCATGCA
CCACCTGTCACTCTGTCCCCCGAAGGGGAAAACTCTATCTCTAGAGGGGTCAGAGGATGTCA
AGATTTGGTAAGGTTCTTCGCGTTGCTTCGAATTAAACCACATGCTCCACCGCTTGTGCGGG
TCCCCGTCAATTCCTTTGAGTTTCAACCTTGCGGTCGTACTCCCCAGGCGGAGTGCTTAATG
CGTTAGCTGCAGCACTAAGGGACGGAAACCCCCTAACACTTAGCACTCATCGTTTACGGCGT
GGACT

>Stenotrophomonas_maltophilia

AGTGAACGCTGGCGGTAGGCCTAACACATGCAAGTCGAACGGCAGCACAGTAAGAGCTTGCT
CTTATGGGTGGCGAGTGGCGGACGGGTGAGGAATACATCGGAATCTACTTTTTCGTGGGGGA
TAACGTAGGGAAACTTACGCTAATACCGCATACGACCTACGGGTGAAAGCAGGGGATCTTCG
GACCTTGCGCGATTGAATGAGCCGATGTCGGATTAGCTAGTTGGCGGGGTAAAGGCCCACCA
AGGCGACGATCCGTAGCTGGTCTGAGAGGATGATCAGCCACACTGGAACTGAGACACGGTCC
AGACTCCTACGGGAGGCAGCAGTGGGGAATATTGGACAATGGGCGCAAGCCTGATCCAGCCA
TACCGCGTGGGTGAAGAAGGCCTTCGGGTTGTAAAGCCCTTTTGTTGGGAAAGAAATCCAGC
CGGCTGATACCTGGTTGGGATGACGGTACCCAAAGAATAAGCACCGGCTAACTTCGTGCCAG
CAGCCGCGGTAATACGAAGGGTGCAAGCGTTACTCGGAATTACTGGGCGTAAAGCGTGCGTA
GGTGGTTGTTTAAGTCTGTTGTGAAAGCCCTGGGCTCAACCTGGGAACTGCAGTGGAAACTG
GACAACTAGAGTGTGGTAGAGGGTAGCGGAATTCCTGGTGTAGCAGTGAAATGCGTAGAGAT
CAGGAGGAACATCCATGGCGAAGGCAGCTACCTGGACCAACACTGACACTGAGGCACGAGAG
CGTGGGGAGCAAACAGGATTAGATACCCTGGTAGTCCACGCCCTAAACGATGCGAACTGGAT
GTTGGGTGCAATTTGGCACGCAGTATCGAAGCTAACGCGTTAAGTTCGCCGCCTGGGGAGTA
CGGTCGCAAGACTGAAACTCAAAGGAATTGACGGGGGCCCGCACAAGCGGTGGAGTATGTGG
TTTAATTCGATGCAACGCGAAGAACCTTACCTGGCCTTGACATGTCGAGAACTTTCCAGAGA
TGGATGGGTGCCTTCGGGAACTCGAACACAGGTGCTGCATGGCTGTCGTCAGCTCGTGTCGT
GAGATGTTGGGTTAAGTCCCGCAACGAGCGCAACCCTTGTCCTTAGTTGCCAGCACGTAATA
GTGGGAACTCTAAGGAGACCGCCGGTGACAAACCGGAGGAAGGTGGGGATGACGTCAAGTCA
TCATGGCCCTTACGGCCAGGGCTACACACGTACTACAATGGTAGGGACAGAGGGCTGCAAGC
CGGCGACGGTAAGCCAATCCCAGAAACCCTATCTCAGTCCGGATTGGAGTCTGCAACTCGAC
TCCATGAAGTCGGAATCGCTAGTAATCGCAGATCAGCATTGCTGCGGTGAATACGTTCCCGG
GCCTTGTACACACCGCCCGTCACACCATGGGAGTTTGTTGCACCAGAAGCAGGTAGCTTAAC
CTTCGGGAGGGCGCTTGCCACGGTGTGGCCGATGACTGGGGTG

>Variovorax_paradoxus

GAACGCTGGCGGCATGCCTTACACATGCAAGTCGAACGGCCAGCGCGGGAGCAATCCTGGCG
GCGAGTGGCGAACGGGTGAGTAATACATCGGAACGTGCCCAATCGTGGGGGATAACGCAGCG
AAAGCTGTGCTAATACCGCATACGATCTACGGATGAAAGCAGGGGATCGCAAGACCTTGCGC
GAATGGAGCGGCCGATGGCAGATTAGGTAGTTGGTGAGGTAAAGGCTCACCAAGCCTTCGAT
CTGTAGCTGGTCTGAGAGGACGACCAGCCACACTGGGACTGAGACACGGCCCAGACTCCTAC
GGGAGGCAGCAGTGGGGAATTTTGGACAATGGGCGCAAGCCTGATCCAGCCATGCCGCGTGC
AGGATGAAGGCCTTCGGGTTGTAAACTGCTTTTGTACGGAACGAAACGGCCTTTTCTAATAA
AGAAGGGCTAATGACGGTACCGTAAGAATAAGCACCGGGCTAACTACGTGCCAGCAGCCGCG
GTAATACGTAGGGTGCAAGCGTTAATCGGAATTACTGGGCGTAAAGCGTGCGCAGGCGGTAA
TGTAAGACAGTTGTGAAATCCCCGGGCTCAACCTGGGAACTGCATCTGTGACTGCATTGCTG
GAGTACGGCAGAGGGGGATGGAATTCCGCGTGTAGCAGTGAAATGCGTAGATATGCGGAGGA
ACACCGATGGCGAAGGCAATCCCCTGGGCCTGTACTGACGCTCATGCACGAAAGCGTGGGGA
GCAAACAGGATTAGATACCCTGGTAGTCCACGCCCTAAACGATGTCAACTGGTTGTTGGGAA
TTCACTTTCTCAGTAACGAAGCTAACGCGTGAAGTTGACCGCCTGGGGAGTACGGCCGCAAG
GTTGAAACTCAAAGGAATTGACGGGGACCCGCACAAGCGGTGGATGATGTGGTTTAATTCGA
TGCAACGCGAAAAACCTTACCCACCTTTGACATGTACGGAATTCGCCAGAGATGGCTTAGTG
CTCGAAAGAGAACCGTAACACAGGTGCTGCATGGCTGTCGTCAGCTCGTGTCGTGAGATGTT

GGGTTAAGTCCCGCAACGAGCGCAACCCTTGTCATTAGTTGCTACATTCAGTTGGGCACTCT
AATGAGACTGCCGGTGACAAACCGGAGGAAGGTGGGGATGACGTCAAGTCCTCATGGCCCTT
ATAGGTGGGGCTACACACGTCATACAATGGCTGGTACAAAGGGTTGCCAACCCGCGAGGGGG
AGCTAATCCCATAAAACCAGTCGTAGTCCGGATCGCAGTCTGCAACTCGACTGCGTGAAGTC
GGAATCGCTAGTAATCGTGGATCAGAATGTCACGGTGAATACGTTCCCGGGTCTTGTACACA
CCGCCCGTCACACCATGGGAGCGGGTTCTGCCAGAAGTAGTTAGCTTAACCGCAAGGAGGGC
GAT

H.2 Eukaryotes

>Amorphotheca_resinae

GAAATGCGATAAGTAATGCGAATTGCAGAATTCAGTGAGTCATCGAATCTTTGAACGCACAT
TGCGCCCTGTGGTATTCCGCAGGGCATGCCTGTTCGAGCGTCATTTCAACCCTCAAGCTCTG
CTTGGTGTTGGGCCCTGCCCGTCGCGGCCGGCCCTAAAATCAGTGGCGGTGCCGCTGGGCTC
TGAGCGTAGTACATCTCTCGCTCCAGCGCCCCGCGGTGGCTTGCCAGAACCCCAACTTCTGT
GGTTGACCTCGGATCAGGTAGGGATACCCGCTGAACTTAAGCATATCAATAAGCGGAGGA

>Candida_krusei

TTAAGTTCAGCGGGTAGTCCTGTCTGATCTGAGGTTGAATAATAAAGGTCAAACGTGTTTGT
AAATCTATTTCAAGGAAGGAGTACAACCTCATAGAGAAACAACGCTCAAACAGACATGCCTA
GCGGAATACCACTAGGCGCAATGTGCGTTCAAAAATTGATGATTCACTTCTGCAATTCACAA
AACATATCGCGTTTCGCTGCGTTCTTCATCGATGC

>Candida_sp.

TTAAGTTCAGCGGGTAGTCCTGTCTGATCTGAGGTTGAATAATAAAGGTCAAACGTGTTTGT
AAATCTATTTCAAGGAAGGAGTACAACCTCATAGAGAAACAACGCTCAAACAGACATGCCTA
GCGGAATACCACTAGGCGCAATGTGCGTTCAAAAATTGATGATTCACTTCTGCAATTCACAA
AACATATCGCGTTTCGCTGCGTTCTTCATCGATGC

>Entrophospora_sp.

TTAAGTTCAGCGGGTATCCCTACCTGATCCGAGGTCAAAAGTTAAAAAAGGCTTATGGACGC
AAGTATTATCGGCTAGAATCGCAAAATGTGCTGCGCTTCAATACCAAAACACTGGCTGCCAA
TTGCTTTAAGGCGAGTCCAAACGCAAAGGAGAGGACAAACACCCAACACCAAGCAGAGCTTG
AGGGTACAAATGACGCTCGAACAGGCATGCCCTGCGGAATACCACAGGGCGCAATGTGCGTT
CAAAGATTCGATGACTCACTGAATTCTGCAATTCGCATTACTTATCGCATTTC

>Epicoccum_nigrum

TTAAGTTCAGCGGGTATCCCTACCTGATCCGAGGTCAAAAGTTAAAAAAGGCTTATGGACGC
AAGTATTATCGGCTAGAATCGCAAAATGTGCTGCGCTTCAATACCAAAACACTGGCTGCCAA
TTGCTTTAAGGCGAGTCCAAACGCAAAGGAGAGGACAAACACCCAACACCAAGCAGAGCTTG
AGGGTACAAATGACGCTCGAACAGGCATGCCCCATGGAATACCAAGGGGCGCAATGTGCGTT
CAAAGATTCGATGATTCACTGAATTCTGCAATTCACACTACTTATCGCATTTCGCTGCGTTC
TTCATCGATGCA

>Meyerozyma_caribbica

TTAAGTTCGGCGGGTATTCCTACCTGATTTGAGGTCAAGCTTGTTTGGTTGTTGTAAGGCCG
GGCCAACAATACCAGAAATATCCCGCCACACCATTCAACGAGTTGGATAAACCTAATACATT
GAGAGGTCGACAGCACTATCCAGTACTACCCATGCCAATACTTTTCAAGCAAACGCCTAGTC
CGACTAAGAGTATCACTCAATACCAAACCCGGGGGTTTGAGAGAGAAATGACGCTCAAACAG
GCATGCCCTCTGGAATACCAGAGGGCGCAATGTGCGTTCAAAGATTCGATGATTCACGAAAA
TCTGCAATTCATATTACTTATCGCATTTC

>Peniophora_sp.

TTAAGTTCAGCGGGTAGTCCCGCCTGATTTGAGGTCAAGTTTGTAGTAGTTGTCCCTTTCGA
GACGGTTGGAAGCAAGTCCCCTATATTCGCTAAGCCGAGGCGTAGATGACTATCACACCAAG
GCCGCAAGGGCTTCGCTAATGTATTCAAGGAGAGCGGATCGGCCAGGGACCCGCAAGCTCCC
AAATCCCAGCCCAACACCTTCCGAAAAAGGTGGAGGGTGGAGGAGTTCACGACACTCAAACA

GGCGTGCCCTTCGGAATGCCAAAGGGCGCAAGGTGCGTTCAAAGATTCGATGATTCACTGAA
TTCTGCAATTCACATTACTTATCGCATTTCGCTGCGTTCTTCATCGATGC

>Pseudallescheria_boydii

TTAAGTTCAGCGGGTAACCCTACCTGATCCGAGGTCAAACCATCTGGAGTTATAGGTGGTTT
GACGGCAGGCCTCCGCCGGGACCCAATGCGAGCTTGCAAAAGAGACTTACTACGCAGAAGGC
AACCGCGGCGGGACCGCCACTGTATTTCAGGGCCTACGGAGGGTCGCGAAGACTCGCCGTAG
CGCCCCAACACCGACCCTGAGCTTCCCTGAGGAAACGGAGGTTCGAGGGTTGAAATGACGCT
CGGACAGGCATGCCCGGCAGATTACTGCCGGGCGCAATGTGCGTTCAAAGATTCGATGATTC
ACTGAATTCTGCAATTCACATTACTTATCGCATTTCGCTGCGTTCTTCATCGATGC

>Sclerostagonospora_sp.

TTAAGTTCAGCGGGTATCCCTACCTGATCCGAGGTCAAAAGTTAAAAAAGGCTTATGGACGC
AAGTATTATCGGCTAGAATCGCAAAATGTGCTGCGCTTCAATACCAAAACACTGGCTGCCAA
TTGCTTTAAGGCGAGTCCAAACGCAAAGGAGAGGACAAACACCCAACACCAAGCAGAGCTTG
AGGGTACAAATGACGCTCGAACAGGCATGCCCCATGGAATACCAAGGGGCGCAATGTGCGTT
CAAAGATTCGATGATTCACTGAATTCTGCAATTCACACTACTTATCGCATTTCGCTGCGTTC
TTCATCGATGCA

>Trametes_sp.

GAAATGCGATAAGAAATGTGAATTGCAGAATTCAGTGAATCATCGAATCTTTGAACGCACCT
TGCGCTCCTTGGTATTCCGAGGAGCATGCCTGTTTGAGTGTCATGGAATTCTCAACTTATAA
ATCCTTGTGATCTATAAGCTTGGACTTGGAGGCTTGCTGGCCCTCGTTGGTCGGCTCCTCTT
GAATGCATTAGCTCGATTCCGTACGGATCGGCTCTCAGTGTGATAATCGTCTACGCTGTGAC
CGTGAAGTGTTTTGGCGAGCTTCTAACCGTCCATTAGGACAACTTTTTAACATCTGACCTCA
AATCAGGTAGGACTACCCGCTGAACTTAAGCATATCAATAAGCGGAGGAGCATATCAATAAG
CGGAGGGGCATATCAATAAGCGGAGGA

>Yarrowia_lipolytica

TTAAGTTCAGCGGGTAATCTCGGATGAAGGAGGTGAAATGACGTAATAATTGAGAGTTTAAA
AAATCCATTTCAAGAAAGCAATGCGATCCCAGAGGGAACACGCTCCTCCATCCGTGCGGTAC
GGAATGCCATACCGCGCAATGTGCGTTCAAAAATTGATGATTCACATCTGCAAGTCACAAAA
AATATCGCGGTTC

Appendix I

Identified microorganisms

Appendix I – Identified microorganisms

Table I.40 – Prokaryotic and eukaryotic microorganisms isolated from jet fuel samples in the experiments undertaken in this thesis.

Archaea	*Gordonia sp.*
Candidatus Nitrososphaera sp.	Intrasporangiaceae (Other)
	Janibacter sp.
Acidobacteria	Kineosporiaceae (Other)
[Bryobacteraceae] (Other)	*Kocuria sp.*
Acidobacteriaceae (Other)	*Kribbella sp.*
Candidatus Koribacter sp.	*Kytococcus sp.*
Candidatus Solibacter sp.	*Lamia sp.*
	Lentzea sp.
Actinobacteria	*Leucobacter sp.*
Acidimicrobiales (Other)	Microbacteriaceae (Other)
Actinocorallia sp.	*Microbacterium sp.*
Actinokineospora sp.	Micrococcaceae (Other)
Actinomyces sp.	*Micrococcus sp.*
Actinomycetales (Other)	*Microlunatus sp.*
Actinomycetospora sp.	Micromonosporaceae (Other)
Actinotalea sp.	*Mycetocola sp.*
Aeromicrobium sp.	*Mycobacterium sp.*
Agromyces sp.	Nakamurellaceae (Other)
Arsenicicoccus sp.	*Nesterenkonia sp.*
Arthrobacter sp.	*Nocardia sp.*
Bifidobacteriaceae (Other)	Nocardiaceae (Other)
Bifidobacterium sp.	*Nocardioides sp.*
Brachybacterium sp.	*Nonomuraea sp.*
Brevibacterium sp.	*Patulibacter sp.*
Catellatospora sp.	Patulibacteraceae (Other)
Cellulomonadaceae (Other)	*Phycicoccus sp.*
Cellulomonas sp.	*Promicromonospora sp.*
Cellulosimicrobium sp.	Promicromonosporaceae (Other)
Corynebacterium sp.	Propionibacteriaceae (Other)
Curtobacterium sp.	*Propionibacterium sp.*
Demequina sp.	*Pseudoclavibacter sp.*
Dermabacteraceae (Other)	*Pseudonocardia sp.*
Dermacoccus sp.	Pseudonocardiaceae (Other)
Dietzia sp.	*Rathayibacter sp.*
Dietziaceae (Other)	*Rhodococcus sp.*
Frankiaceae (Other)	*Rothia sp.*
Friedmanniella sp.	*Rubrobacter sp.*
Frigoribacterium sp.	Rubrobacteraceae (Other)
Gaiellaceae (Other)	*Saccharopolyspora sp.*
Geodermatophilaceae (Other)	*Salana sp.*
Geodermatophilus sp.	*Salinibacterium sp.*
Georgenia sp.	*Sanguibacter sp.*
Glycomyces sp.	Sanguibacteraceae (Other)

Solirubrobacteraceae (Other)
Sporichthyaceae (Other)
Streptomyces sp.
Streptomycetaceae (Other)
Streptosporangiaceae (Other)
Streptosporangium sp.
Terracoccus sp.
Thermomonosporaceae (Other)
Williamsia sp.
Xylanimicrobium sp.

Bacteroidetes
[Prevotella] sp.
[Weeksellaceae] (Other)
Adhaeribacter sp.
Bacteroides sp.
Capnocytophaga sp.
Chitinophagaceae (Other)
Chryseobacterium sp.
Cloacibacterium sp.
Crocinitomix sp.
Cryomorphaceae (Other)
Cytophagaceae (Other)
Dyadobacter sp.
Flavisolibacter sp.
Flavobacteriaceae (Other)
Flavobacterium sp.
Gillisia sp.
Myroides sp.
Paludibacter sp.
Pedobacter sp.
Porphyromonadaceae (Other)
Porphyromonas sp.
Prevotella sp.
Rubricoccus sp.
Saprospiraceae (Other)
Solitalea sp.
Sphingobacterium sp.

Chlamydiae
Candidatus Protochlamydia sp.
Parachlamydiaceae (Other)

Chlorobi
OPB56
PK329
SJA-28

Chloroflexi
[Roseiflexales] (Other)
5B-12
A4b
[Kouleothrixaceae] (Other)
C0119
Dehalococcoidaceae (Other)
Dolo_23
Herpetosiphonales (Other)
mle1-48
S085
SHA-26
TK10

Cyanobacteria
ML635J-21
Streptophyta sp.

Elusimicrobia
Elusimicrobiales (Other)
FAC88
IIb

Fibrobacteres
258ds10
TSCOR003-O20
Ucp1540

Firmicutes
[Exiguobacteraceae] (Other)
[Mogibacteriaceae] (Other)
[Tissierellaceae] (Other)
Aerococcaceae (Other)
Aerococcus sp.
Alicyclobacillus sp.
Alloiococcus sp.
Anaerococcus sp.
Anoxybacillus sp.
Bacillaceae (Other)
Bacillales (Other)
Bacillus sp.
Caldicoprobacter sp.
Caloramator sp.
Carnobacteriaceae (Other)
Carnobacterium sp.
Clostridiisalibacter sp.
Clostridium sp.
Cohnella sp.
Dorea sp.

Enterococcaceae (Other)
Enterococcus sp.
Epulopiscium sp.
Ethanoligenens sp.
Exiguobacterium sp.
Facklamia sp.
Faecalibacterium sp.
Finegoldia sp.
Gemellaceae (Other)
Geobacillus sp.
Granulicatella sp.
Jeotgalicoccus sp.
Lachnospiraceae (Other)
Lactobacillus sp.
Lactococcus sp.
Leuconostocaceae (Other)
Listeriaceae (Other)
Lysinibacillus sp.
Marinibacillus sp.
Oscillospira sp.
Paenibacillaceae (Other)
Paenibacillus sp.
Paenisporosarcina sp.
Peptoniphilus sp.
Peptostreptococcaceae (Other)
Peptostreptococcus sp.
Planifilum sp.
Planococcaceae (Other)
Planomicrobium sp.
Proteiniclasticum sp.
Ruminococcaceae (Other)
Ruminococcus sp.
Rummeliibacillus sp.
Solibacillus sp.
Sporosarcina sp.
Staphylococcaceae (Other)
Staphylococcus sp.
Streptococcaceae (Other)
Streptococcus sp.
Tepidimicrobium sp.
Thermicanus sp.
Thermoactinomycetaceae (Other)
Veillonella sp.
Weissella sp.

Fusobacteria
Sneathia sp.

Gemmatimonadetes
Ellin5290
Ellin5301
Gemm-1
Gemm-2
Gemm-3
Gemmatimonadetes (Other)
Gemmatimonas sp.
KD8-87
N1423WL

Nitrospirae
Nitrospira sp.
Nitrospiraceae (Other)

Planctomycetes
d113
DH61
Gemmata sp.
Gemmataceae (Other)
p04_C01
Phycisphaerales (Other)
Pirellula sp.
Pirellulaceae (Other)
Pla4

Proteobacteria
[Chromatiaceae (Other)]
[Entotheonellaceae (Other)]
[Marinicellaceae (Other)]
0319-6G20
211ds20
Acetobacteraceae (Other)
Achromobacter sp.
Acinetobacter sp.
Aeromonadaceae (Other)
Afifella sp.
Agrobacterium sp.
Alcaligenaceae (Other)
Alcaligenes sp.
Alcanivorax sp.
Alteromonadales (Other)
Amaricoccus sp.
Anaeromyxobacter sp.
Arenimonas sp.
Asticcacaulis sp.
Aurantimonadaceae (Other)
Azoarcus sp.
Azorhizobium sp.

Azospirillum sp.	*Hydrogenophaga sp.*
Bacteriovoracaceae (Other)	*Hylemonella sp.*
Balneimonas sp.	Hyphomicrobiaceae (Other)
BD7-3	*Hyphomicrobium sp.*
Bdellovibrio sp.	Hyphomonadaceae (Other)
Beijerinckiaceae (Other)	IS-44
Bosea sp.	*Janthinobacterium sp.*
Bradyrhizobiaceae (Other)	*Kaistia sp.*
Bradyrhizobium sp.	*Kaistobacter sp.*
Brevundimonas sp.	*Kingella sp.*
Brucellaceae (Other)	*Klebsiella sp.*
Burkholderia sp.	*Labrys sp.*
Burkholderiaceae (Other)	*Lampropedia sp.*
Candidatus Portiera sp.	*Lautropia sp.*
Caulobacter sp.	*Legionella sp.*
Caulobacteraceae (Other)	Legionellales (Other)
Cellvibrio sp.	*Limnohabitans sp.*
Chromatiales (Other)	*Luteimonas sp.*
Collimonas sp.	*Lutibacterium sp.*
Colwelliaceae (Other)	*Lysobacter sp.*
Comamonadaceae (Other)	*Marinobacter sp.*
Comamonas sp.	*Marinomonas sp.*
Corallococcus sp.	*Mesorhizobium sp.*
Coxiellaceae (Other)	*Methylibium sp.*
Crenothrix sp.	Methylobacteriaceae (Other)
Cupriavidus sp.	*Methylobacterium sp.*
Cystobacterineae sp.	Methylococcaceae (Other)
Dechloromonas sp.	Methylocystaceae (Other)
Delftia sp.	*Methylophaga sp.*
Desulfovibrio sp.	Methylophilaceae (Other)
Desulfuromonadales (Other)	Methylophilales (Other)
Devosia sp.	*Methylosinus sp.*
Dokdonella sp.	*Methylotenera sp.*
EB1003	MIZ46
Ellin329	MND1
Ellin6067	Moraxellaceae (Other)
Enterobacteriaceae (Other)	*Morganella sp.*
Erwinia sp.	*Mycoplana sp.*
Erythrobacteraceae (Other)	Myxococcaceae (Other)
Ewingella sp.	Myxococcales (Other)
FAC87	*Myxococcus sp.*
Gallionella sp.	*Nannocystis sp.*
Geobacter sp.	NB1-j
Geobacteraceae (Other)	*Neisseria sp.*
Gluconacetobacter sp.	Neisseriaceae (Other)
Haemophilus sp.	*Nevskia sp.*
Haliangiaceae (Other)	Nitrosomonadaceae (Other)
Halomonadaceae (Other)	*Nitrosovibrio sp.*
HTCC2089	*Novosphingobium sp.*

Oceanospirillaceae (Other)
Ochrobactrum sp.
OM27
OM60
Oxalobacteraceae (Other)
Pandoraea sp.
Pantoea sp.
Paracoccus sp.
Parvibaculum sp.
Pedomicrobium sp.
Pelobacteraceae (Other)
Phenylobacterium sp.
PHOS-HD29
Photobacterium sp.
Phyllobacteriaceae (Other)
Phyllobacterium sp.
Pigmentiphaga sp.
Piscirickettsiaceae (Other)
Plantago sp.
Pleomorphomonas sp.
Plesiocystis sp.
Polaromonas sp.
Polyangiaceae (Other)
Procabacteriaceae (Other)
Pseudochrobactrum sp.
Pseudomonadaceae (Other)
Pseudomonas sp.
Pseudoxanthomonas sp.
Ralstonia sp.
Ramlibacter sp.
Rhizobiaceae (Other)
Rhizobium sp.
Rhodobacter sp.
Rhodobacteraceae (Other)
Rhodocyclaceae (Other)
Rhodoplanes sp.
Rhodospirillaceae (Other)
Rickettsiaceae (Other)
Rickettsiella sp.
Roseococcus sp.
Roseomonas sp.
Rubrivivax sp.
SBla14
SC-I-84
Serratia sp.
Shewanella sp.
Simplicispira sp.
Sinobacteraceae (Other)
Sphingomonas sp.
Sorangium sp.
Sphingobium sp.
Sphingomonadaceae (Other)
Sphingopyxis sp.
Spirobacillales (Other)
Stenotrophomonas sp.
Steroidobacter sp.
Syntrophobacteraceae (Other)
TA18
Tepidimonas sp.
Thauera sp.
Thermomonas sp.
Thiobacillus sp.
Thiothrix sp.
UD5
Vogesella sp.
Xanthobacter sp.
Xanthobacteraceae (Other)
Xanthomonadaceae (Other)
Yersinia sp.
Zoogloea sp.

Spirochaetes
Mycoplasma sp.
Spirochaeta sp.
Turneriella sp.

TM6
SBRH58
TM6

TM7
EW055
I025
MJK10
SC3
TM7-1
TM7-3

Verrucomicrobia
[Pedosphaerales] (Other)
auto67_4W
Chthoniobacter sp.
DA101
Ellin515
Ellin517
Pedosphaera sp.
Prosthecobacter sp.

Ascomycota
Ajellomyces sp.
Alternaria sp.
Amorphotheca sp.
Ampelomyces sp.
Annulohypoxylon sp.
Arthrobotrys sp.
Aspergillus sp.
Aureobasidium sp.
Bacidina sp.
Beauveria sp.
Blumeria sp.
Cadophora sp.
Candida sp.
Capnobotryella sp.
Cephalotheca sp.
Cladonia sp.
Cladosporium sp.
Claviceps sp.
Coniosporium sp.
Cordyceps sp.
Crocicreas sp.
Curvularia sp.
Cyphellophora sp.
Cytospora sp.
Debaryomyces sp.
Dermateaceae (Other)
Diaporthe sp.
Dictyosporium sp.
Dipodascaceae (Other)
Dipodascus sp.
Endoconidioma sp.
Erysiphe sp.
Eupenicillium sp.
Eutypa sp.
Eutypella sp.
Exophiala sp.
Galactomyces sp.
Geopora sp.
Geotrichum sp.
Gibberella sp.
Glomerella sp.
Helotiales (Other)
Hirsutella sp.
Kendrickiella sp.
Khuskia sp.
Kluyveromyces sp.
Lachnum sp.
Lasiosphaeriaceae (Other)
Lecanicillium sp.
Lepraria sp.
Leptospora sp.
Meyerozyma sp.
Mollisia sp.
Monilinia sp.
Monographella sp.
Mycosphaerella sp.
Myrmecridium sp.
Myxotrichaceae (Other)
Nemania sp.
Nephromopsis sp.
Oidiodendron sp.
Ophiocordyceps sp.
Paecilomyces sp.
Penicillium sp.
Peyronellaea sp.
Pezizaceae (Other)
Phaeosphaeriaceae (Other)
Phialophora sp.
Phoma sp.
Phyllosticta sp.
Physcia sp.
Pichia sp.
Platismatia sp.
Pleosporaceae (Other)
Protoparmeliopsis sp.
Protoventuria sp.
Pseudallescheria sp.
Pyrenochaeta sp.
Ramichloridium sp.
Ramularia sp.
Rhinocladiella sp.
Saccharomyces sp.
Saccharomycetaceae (Other)
Satchmopsis sp.
Sclerotinia sp.
Sclerotiniaceae (Other)
Septoria sp.
Simplicillium sp.
Taphrinales (Other)
Valsa sp.
Vanderwaltozyma sp.
Verrucaria sp.
Verrucocladosporium sp.
Xylaria sp.
Xylariales (Other)
Yamadazyma sp.
Yarrowia sp.

Zygosaccharomyces sp.
Zygowilliopsis sp.

Basidiomycota
Abortiporus sp.
Agrocybe sp.
Anomoloma sp.
Antrodia sp.
Armillaria sp.
Atractiellales (Other)
Auriculariales (Other)
Baeospora sp.
Bannoa sp.
Bensingtonia sp.
Bjerkandera sp.
Calvatia sp.
Calyptella sp.
Camarophyllopsis sp.
Ceratobasidiaceae (Other)
Ceriporia sp.
Ceriporiopsis sp.
Chondrostereum sp.
Clavicorona sp.
Clavulina sp.
Clitopilus sp.
Conocybe sp.
Coprinellus sp.
Coprinopsis sp.
Corticiaceae (Other)
Cortinariaceae (Other)
Cortinarius sp.
Crepidotus sp.
Cristinia sp.
Cryptococcus sp.
Cystofilobasidiales (Other)
Daedaleopsis sp.
Datronia sp.
Dioszegia sp.
Entoloma sp.
Entomocorticium sp.
Entyloma sp.
Exidia sp.
Exobasidium sp.
Fibulobasidium sp.
Fibulomyces sp.
Filobasidium sp.
Flammulina sp.
Fomes sp.
Ganoderma sp.
Globulicium sp.
Gloeocystidiellum sp.
Gloiothele sp.
Grammothele sp.
Grifola sp.
Hemimycena sp.
Holtermanniella sp.
Hydnum sp.
Hymenochaetales (Other)
Hymenochaete sp.
Hyphoderma sp.
Hyphodontia sp.
Hypholoma sp.
Inocybe sp.
Kondoa sp.
Laetiporus sp.
Lepiota sp.
Lepista sp.
Leucosporidiales (Other)
Limonomyces sp.
Macrotyphula sp.
Malassezia sp.
Malasseziales (Other)
Morganella sp.
Mycena sp.
Panellus sp.
Paxillus sp.
Peniophora sp.
Peniophorella sp.
Phanerochaete sp.
Phlebia sp.
Phlebiella sp.
Phlebiopsis sp.
Pholiota sp.
Piptoporus sp.
Polyporales (Other)
Polyporus sp.
Postia sp.
Psathyrella sp.
Pseudoclitocybe sp.
Pseudozyma sp.
Resupinatus sp.
Rhodocollybia sp.
Rhodosporidium sp.
Rhodotorula sp.
Schizophyllum sp.
Scopuloides sp.
Sebacinaceae (Other)
Sistotrema sp.

Sistotremastrum sp.	*Typhula sp.*
Sporidiobolales (Other)	*Ustilago sp.*
Sporobolomyces sp.	*Wallemia sp.*
Stereum sp.	
Strophariaceae (Other)	**Chytridiomycota**
Suillus sp.	Rhizophydiales (Other)
Termitomyces sp.	*Rhizophydium sp.*
Tilletia sp.	
Tilletiaria sp.	**Glomeromycota**
Tilletiopsis sp.	Diversisporales (Other)
Trametes sp.	Glomeraceae (Other)
Trametopsis sp.	
Trechisporales (Other)	**Zygomycota**
Tremella sp.	*Lichtheimia sp.*
Tricholoma sp.	*Mucor sp.*
Tricholomataceae (Other)	*Rhizomucor sp.*
Trichosporon sp.	*Umbelopsis sp.*
Tulasnellaceae (Other)	